Co-funded by the
Erasmus+ Programme
of the European Union

Assessment and adaption of urban cultural heritage assets as touristic destination towards the impact of UHI

Case study: City of Edinburgh

Nerxhana TALLUSHI

A thesis submitted for the Joint programme of
Master in Urban Climate & Sustainability

September 2022

Author	Publication type	Completion year
TALLUSHI, Nerxhana	Thesis	2022
	Number of pages: 99	
Supervisor I	**Supervisor II**	
Dr. Eeva Aarrevara	Prof. Agnieszka Kelm	

Title

Assessment and adaption of urban cultural heritage assets as touristic destination towards the impact of UHI. Case study: City of Edinburgh

Degree: Master in Urban Climate & Sustainability

Abstract

Preserving cultural heritage sites has always faced many challenges in a rapidly growing and changing world, mainly in urban areas [Dastgerdi et al., 2019]. Overall, the urban environment faces imminent risks due to climate change, which are amplified due to extensive anthropogenic activities, development, and land-use changes [IPCC, 2014a]. In development strategies, urban planners consider not only the differences in UHI magnitude between urban and rural but also the different levels within the city [Wicki and Parlow, 2017]. Historic towns retain unique urban forms, which are hard to analyse compared to modern and contemporary development and despite that there is a lack of studies in this aspect.

A local climate zone (LCZ) can display the scale of UHI impact in various parts of the city depending on the build-up types, and these LCZ classes depend on morphological parameters [Steward and Oke, 2012]. This scheme works well in cases of homogenous development types in the U.S but is less effective in the case of European cities, whose old core consists of organic development patterns with narrow streets and irregular urban forms. Therefore, in the case of Edinburgh, the morphological parameters were calculated in the high-resolution grid (15m) from different sources. Land use / Land cover was introduced as a parameter needed to classify the LCZ classes. The combination between LULC and morphological parameters was not completed fully as the thresholds of different LCZ classes overlap, so the mean values were used. LULC representing the characteristics of cultural heritage assets of Edinburgh are recommended for future combination.

UHI can affect different sectors in a city due to the direct relation to outdoor thermal comfort. Tourism is a crucial sector for income in Edinburgh, with the world's fourth-highest tourist-to-local ratio in 2019. The thermal comfort at New Town, an important World Heritage tourist destination, is overcoming improvements by the City of Edinburgh, which will affect the tourist's experience. This study measures the implications that new improvements, such as materials with a high albedo, can bring to thermal comfort. In case of a heat wave, the new implementations will lower the air temperature, but apart from new shaded areas, the thermal comfort (PET) can worsen compared to the actual state. The improvement of thermal comfort and adaptation of climate-sensitive solutions in cases of World Heritage properties are burdened by guidelines to preserve the integrity and the authenticity of the cultural asset.

Keywords

Edinburgh, Local Climate Zone, Tourists Outdoor Thermal Comfort

Originality statement. I hereby declare that this Master's dissertation is my own original work, does not contain other people's work without this being stated, cited and referenced, has not been submitted elsewhere in fulfilment of the requirements of this or any other award.	**Signature**

TABLE OF CONTENT

ACKNOWLEDGEMENTS 5
ABBREVIATIONS 6
LIST OF FIGURES 7
LIST OF GRAPHS 10
LIST OF TABLES 13
Chapter 1: Introduction
1.1. Rationale 15
1.2. Aims & Objective 16
1.3. Outlines 17
1.3.1. Outline the Methodology 18
1.3.2. Outline of Dissertation 18
Chapter 2: Literature review
2.1. Climate change in the build environment focused on cultural heritage context 20
2.1.1. Vulnerability and impacts of climate change on cultural heritage 20
2.1.2. Deterioration of building materials 22
2.2. UHI effects based on historical sites 23
2.2.1. Local Climate Zones (LCZ) 23
2.3. Outdoor thermal comfort 26
2.3.1. Simulation approaches 27
2.4. Implementing Sustainable Development Goals in historical sites 29
Chapter 3: Edinburgh study area profile
3.1. Climate conditions overview 31
3.1.1. Current climate 31
3.1.2. Observed climate trends 31
3.1.3. Anticipated climate change 32
3.1.3.1. Global climate change and the Paris Agreement 32
3.1.3.2. Climate projections for Edinburgh 33
3.2. Cultural Landscape of Edinburgh 35
3.2.1. World Heritage Property 35
3.2.2. Management of World Heritage property 37

3.3. Urban development and climate adaptation actions 37
3.3.1. City planning 37
3.3.2. Climate strategy and Adaptation plan 38
3.4. Study case at neighbourhood scale 39
Chapter 4: Methodology
4.1. Research Framework 41
4.1.1. Research philosophy 41
4.1.2. Research approach 42
4.1.3. Research strategy 42
4.1.4. Data collection and analysis 42
4.2. Local Climate Zoning 43
4.2.1. Data 45
4.2.2. Morphological Parameters 46
4.2.3. Combination of Land Use / Land Cover and Morphological Parameters 57
4.3. Traverse survey and ENVI-met® model 49
4.3.1. Filed data collection and method 50
4.3.2. Initial simulation 52
4.3.3. Proposal 54
4.3.4. Thermal comfort evaluation 55
Chapter 5: Results
5.1. Local Climate Zoning 57
5.1.1. Land Use / Land Cover 57
5.1.2. Morphological Parameters 58
5.1.3. Combination of Land Use / Land Cover and Morphological Parameters 63
5.2. Traverse survey and ENVI-met® model 66
5.2.1. Accuracy 66
5.2.2. Scenarios 69
5.2.2.1. Potential Air Temperature - T_{Air} 70
5.2.2.2. Relative humidity - Rh 73
5.2.2.3. Mean Radiant Temperature - T_{mrt} 76
5.2.2.4. Physiological Equivalent Temperature – PET 79
Chapter 6: Discussion
6.1. LCZ 83

6.1.1. Morphological parameters 83
6.1.2. Combination of LULC and morphological parameters 83
6.1.3. Potential aggregations in the future 84
6.1.4. Limitations 85
6.2. Outdoor thermal comfort 86
6.2.1. Thermal sensation 86
6.2.2. Recommendations for improvements 93
6.2.3. Limitations 95
Chapter 7: Conclusion
7.1. Conclusions 97
7.2. Recommendations for future studies 98

REFERENCES 99
APPENDIX 1: Principal climate change risks and impacts on cultural heritage 114
APPENDIX 2: Summarises of indices used in urban areas evaluating the thermal impact on tourists 116
APPENDIX 3: George Street - New Town project, full study area 117
APPENDIX 4: Land Use classes and their codes 119
APPENDIX 5: Meteorological data on 07.07.2020 126
APPENDIX 6: Material assignment of pavements for the simulation 128
APPENDIX 7: Meteorological data on 07.07.2020 130
APPENDIX 8: Replacement of new pavement materials 132
APPENDIX 9: ENVI-met simulation setting 133
APPENDIX 10: Distribution of morphological parameters for each LULC class 134

ACKNOWLEDGMENT

Firstly, I would like to thank the entire MUrCS consortium, which gave me the possibility to experience this one-lifetime journey in three different countries.

I am really grateful to my supervisors, Dr Eeva Aarrevara and Prof. Agnieszka Kelm guiding me through this process and supporting me in overcoming any obstacle.

Special thanks to Prof. Rohinton Emmanuel for always sharing his knowledge, motivating and inspiring us.

I express my deep consideration to Carsten Hermann from Historic Environment Scotland (HES) for introducing me to Edinburgh's cultural heritage environment and characteristics.

Always blest by my family unconditional support.

Thank you to all the MUrCS family for exchanging all their experience, and in particular to the special people I have connected with, for always being there.

Lastly, I dedicate this thesis to my future self, hoping to use this experience in the future at best.

Till the next journey,

Faleminderit! - Thank you! – Kiitos! – ¡Gracias!

.

ABREVIATIONS

AR5 - Fifth Assement Report

BSF - Building Surface Fraction

DEM – Digital Elevation Model

DSM - Digital Surface Model

DTM - Digital Terrain Model

GIS - Geographic Information System

HES – Historic Environmental Scotland

OUV – Outstanding Universal Values

ICOMOS - International Council on Monuments and Sites

IPCC - Intergovernmental Panel on Climate Change

LCZ - Local climate zones

LULC - Land Use/Land Cover

MBH - Mean Building Height

PSF - Pervious Surface Fraction

PET - Physiological Equivalent Temperature

SAR - Street Aspect Ratio

SVF - Sky View Factor

T_{mrt} – Mean Radiant Temperature

UCL – Urban Canopy Layer

UBL – Urban Baoundary Layer

UHI – Urban Heat Island

UNESCO - The United Nations Educational, Scientific and Cultural Organization

WH – World Heritage

WHC - World Heritage Center

LIST OF FIGURES

Figure 1 General outline of the research 17

Figure 2 Spatial distribution of the proportion of pre-1919 dwellings in total dwellings, 2011 19

Figure 3 Steps to determine scope and problem definition based on IPCC outline.....20

Figure 4 General vulnerability framework based on IPCC definition 21

Figure 5 Schematic 2D representation of UHI urban canopy layer during day and night. The comparison is made between surface temperature (T0) and air temperature (Ta) in a traverse along the line A-B. The values of temperature follow the silhouette of the build-up area (suburban and urban), while in areas with green elements the temperature is lower 23

Figure 6 The 17 standard LCZs. Modified from Stewart & Oke.....24

Figure 7 WUDAPT workflow.....25

Figure 8 General LCZ mapping process in the GIS stream 25

Figure 9 Study case of Teramo UHI analysis showing ENVI-met® results of atmospheric temperature profile horizontal at 1.2 m height in July 22nd at 2 pm in three scenarios: (a) "base case": current conditions.; (b) the "cool case": all the roofs have been covered with high-reflectance material; (c) "green case": all roofs have been replaced with green roof; and on the left the main parameters for modelling 28

Figure 10 Study case of Venice UHI analysis showing the master plan of (a) "base case": current conditions; (b) the "cool case": cool pavements and roofs (white) replace the usual surfaces; (c) "green case": a park replaces the wholesale fruit and vegetable market and ENVI-met® results urban air temperature profile horizontal at 1.2 m height (lower limit 26,75 °C, higher limit 34,35 °C) in August 2nd at 3 pm in three scenarios.....28

Figure 11 Schematic representation of agendas for development, disaster risk reduction, and climate change and variability 30

Figure 12 Overview of Eastern Scotland's Changing Climate, comparison between 1961 and 2021.....31

Figure 13 Aerial view of Edinburgh with the New Town in the foreground.....35

Figure 14 Map showing the boundaries of the World Heritage Site of Old and New Towns of Edinburgh and its conservation areas 36

Figure 15 Location of neighbourhood scale site 39

Figure 16 Traffic and cycling lanes 40

Figure 17 Materials renders for one section of George Street 40

Figure 18 Research onion 41

Figure 19 The general framework for creating LCZ of the City of Edinburgh 44

Figure 20 Edinburgh's Land use / Land cover map (LULC) 45

Figure 21 Detailed methodology for the simulation part.....50

Figure 22 Location of site for the traverse survey, fixed and meteorological station.....50

Figure 23 Routes and 19 locations for the traverse study (field measurements), orange - urban canyons and brown – intersections 51

Figure 24 Aluminium foil funnel used to avoid direct solar radiation.....51

Figure 25 3D model in ENVI-met® software.....53

Figure 26 Pavements materials 54

Figure 27 Schematic representation of vegetation height in George Street.....55

Figure 28 LULC in 15m resolution.....57

Figure 29 Morphological parameters the City of Edinburgh: a) Mean building height b) Sky view factor c) Aspect ratio d) Building surface fraction e) Pervious surface fraction f) Impervious surface fraction of the city of Edinburgh in 15 m resolution and National British projection 59

Figure 30 Final conceptual LCZ map of the City of Edinburgh in 15 m resolution.....65

Figure 31 Points selected for further analysis.....69

Figure 32 Base Case masterplan 69

Figure 33 Cool Case masterplan 70

Figure 34 Green case masterplan.....70

Figure 35 Simulated Potential Air Temperature during 18th July at 1.5m height.....71

Figure 36 Simulated Relative Humidity during 18th July at 1.5m height 74

Figure 37 Simulated Mean Radiant Temperature during 18th July at 1.5m height.....77

Figure 38 Simulated Physiological Equivalent Temperature during 18th July at 1.5m height80

Figure 39 Close up of conceptual LCZ map in the area of the World Heritage property - New Town and Old Town 84

Figure 40 Example of simple classification of culture heritage assets proposed from Climate for Culture project. a) architectural and building structure; b) climatic condition and building structure energy performance 85

Figure 41 Possible aggregation in for natural neighbourhood scale (source: Own elaboration, 2022) 85

Figure 42 T_{Air} absolute difference between Base Case and Cool Case at 4pm 18th of July ...86

Figure 43 T_{mrt} absolute difference between Base Case and Cool Case at 4pm 18th of July ...89

Figure 44 PET absolute difference between Base Case and Cool Case at 4pm 18th of July ..90

Figure 45 Thermal comfort range of PET in different studies.....91

Figure 46 Pavement materials in one of alleys inside the blocks 94

Figure 47 Actual temporal structures by business owners used in George Street 94

Figure 48 Photo of tourists and locals spending time in St Andrew Square Garden.....94

Figure 49 George Street - New Town project.....117

Figure 50 3D renders of George Street - New Town project.....118

Figure 51 Actual pavement surfaces along George street and their replacement after proposal 132

LIST OF GRAPHS

Graph 1 Hourly temperatures on August 2nd 2012: measured (solid red line), simulated (solid black line), cool case (long dash line), cool and green case (long dash dot line) at 11 m height above ground.....28

Graph 2 Global surface temperature change based on different scenarios and relative comparison to the period 1850 – 1900: 1.5°C temperature incensement relative to 1850–1900 is expected to be exceeded in the near term (2021–2040) under the intermediate, high, and very high greenhouse gas emissions scenarios (SSP2-4.5, SSP3-7.0, SSP5-8.5); more likely than not to be exceeded under the low greenhouse gas emissions scenario (SSP1-2.6) and more likely than not to be reached under the very low greenhouse gas emissions scenario (SSP1-1.9).....32

Graph 3 The latest estimates of global average sea-level rise, combining IPCC scenarios & more recent data on rates of Antarctic and Greenland ice loss.....32

Graph 4 UKCP18 climate projections for the city of Edinburgh showing change in mean of annual temperature from 1961 to 2100. These are probabilistic projections: the dashed line is 50% central estimate; inner shading 25-75%; middle shading 10-90%; outer shading outer shading 5-95%. All values are compared to a 1981-2000 baseline average.....33

Graph 5 UKCP18 climate projections for the city of Edinburgh showing change in mean of winter precipitations from 1961 to 2100. These are probabilistic projections: the dashed line is 50% central estimate; inner shading 25-75%; middle shading 10-90%; outer shading 5-95%. All values are compared to a 1981-2000 baseline average 34

Graph 6 UKCP18 climate projections for the city of Edinburgh showing change in mean of summer precipitations from 1961 to 2100. These are probabilistic projections: the dashed line is 50% central estimate; inner shading 25-75%; middle shading 10-90%; outer shading 5-95%. All values are compared to a 1981-2000 baseline average 34

Graph 7 Change in sea level (m above 1981–2000 mean sea level) based on two scenarios: red – RCP 8.5/high emission and blue – RCP 2.6 low emission.....35

Graph 8 Mean building height distribution for: D1, D2, D3, D4, D5 and I1 classes.....60

Graph 9 Sky view factor values distribution for: D1, D2, D3, D4, D5 and I1 classes.....61

Graph 10 Road aspect ratio values distribution for: D1, D2, D3, D4, D5 and I1 classes 62

Graph 11 Meteorological parameters for 7th and 9th of July 2020: a) Air temperature, b) Relative humidity, c) Wind speed, d) Cloud coverage 66

Graph 12 Air temperature and relative humidity measured with TinyTag on 7th of July 67

Graph 13 Difference between measured and simulated temperature 67

Graph 14 Difference between measured and simulated results of air temperature and relative humidity 67

Graph 15 Potential air temperature variance during 18th of July for 5 points – Base case 72

Graph 16 Potential air temperature variance during 18th of July for 5 points – Cool case ...72

Graph 17 Potential air temperature variance during 18th of July for 5 points–Green case 72

Graph 18 Potential air temperature comparison during 18th of July between scenarios at 1.5m height – R1 73

Graph 19 Potential air temperature comparison during 18th of July between scenarios at 1.5m heigh – R2 73

Graph 20 Potential air temperature comparison during 18th of July between scenarios at 1.5m height – R3 73

Graph 21 Potential air temperature comparison during 18th of July between scenarios at 1.5m height – R4 73

Graph 22 Relative humidity variance during 18th of July for 5 points at 1.5m height – Base case 75

Graph 23 Relative humidity variance during 18th of July for 5 points at 1.5m height – Cool case 75

Graph 24 Relative humidity variance during 18th of July for 5 points at 1.5m height – Green case 75

Graph 25 Relative humidity comparison during 18th of July between scenarios at 1.5m height – R3 76

Graph 26 Relative humidity comparison during 18th of July between scenarios at 1.5m height – R3 76

Graph 27 Relative humidity comparison during 18th of July between scenarios at 1.5m height – R3 76

Graph 28 Relative humidity comparison during 18th of July between scenarios at 1.5m height – R3 76

Graph 29 T_{mrt} variance during 18th of July for 5 points at 1.5m height – Base case 78

Graph 30 T_{mrt} variance during 18th of July for 5 points at 1.5m height – Cool case 78

Graph 31 T_{mrt} variance during 18th of July for 5 points at 1.5m height – Green case 78

Graph 32 T_{mrt} comparison during 18th of July between scenarios – R1 79

Graph 33 T_{mrt} comparison during 18th of July between scenarios – R2 79

Graph 34 T_{mrt} comparison during 18th of July between scenarios at 1.5m height – R3 79

Graph 35 T_{mrt} comparison during 18th of July between scenarios at 1.5m height – R4 79

Graph 36 PET variance during 18th of July for 5 points – Base case 81

Graph 37 PET variance during 18th of July for 5 points at 1.5m height – Cool case 81

Graph 38 PET variance during 18th of July for 5 points at 1.5m height– Green case 81

Graph 39 PET comparison during 18th of July between scenarios – R1 82

Graph 40 PET comparison during 18th of July between scenarios – R2 82

Graph 41 PET comparison at 1.5m height during 18th of July between scenarios – R3 82

Graph 42 PET comparison at1.5m height during 18th of July between scenarios – R4 82

Graph 43 Change of T_{Air} between *Base Case* and *Cool Case* for 5 points of interest in % ...87

Graph 44 Change of T_{Air} between *Base Case* and *Cool Case* for 5 points of interest in % ...87

Graph 45 Change of Rh between *Base Case* and *Cool Case* for 5 points of interest in %) ...88

Graph 46 Change of Rh between *Base Case* and *Green Case* for 5 points of interest in % ..88

Graph 47 Change of T_{mrt} between *Base Case* and *Cool Case* for 5 points of interest in % ...89

Graph 48 Change of PET between *Base Case* and *Cool Case* for 5 points of interest in % ..91

Graph 49 Change of PET between *Base Case* and *Green Case* for 5 points of interest in %91

Graph 50 Comparison between PET and comfort range - *Base Case* for 5 points of interest92

Graph 51 Comparison between PET and comfort range - *Cool Case* for 5 points of interest92

Graph 52 Comparison between PET and comfort range – *Green Case* for 5 points of interest 92

Graph 53 PET frequency in comfort range – Base *Case* for 5 points of interest 93

Graph 54 PET frequency in comfort range – *Green Case* for 5 points of interest 93

Graph 55 PET frequency in comfort range – *Cool Case* for 5 points of interest 93

LIST OF TABLES

Table 1 Data used for the Climate Change Risk Assessment 22

Table 2 Ranges of thermal indexes 26

Table 3 Listed buildings and designated assets.....37

Table 4 Proportion of visitors to Edinburgh by season in 2019.....38

Table 5 Comparison of visitors to Edinburgh by season in 2019 38

Table 6 Main actions undertaken in LCLIP 2012 38

Table 7 Morphological parameters definitions 43

Table 8 Land use classes 45

Table 9 Data and sources used for accessing LCZ of Edinburgh 46

Table 10 Classes used for PSF estimation 47

Table 11 LCZ morphological parameters thresholds by Stewart and Oke [2012] and the criteria of terrain roughness class criteria omitted.....48

Table 12 Data and sources used for simulation in ENVI-met® 49

Table 13 Dates of field data collection.....49

Table 14 Parameters and instruments used during the field measurements.....51

Table 15 Technical specification of facade and roof materials.....53

Table 16 Technical specification of pavements materials 54

Table 17 Ranges of PET compared to different grades of thermal perception by human beings and physiological stress on human beings.....55

Table 18 Spatial extent (km^2 and %) of each LULC class from polygon to 15m grid size 58

Table 19 Morphological parameters average for each LULC class including the standard deviation 62

Table 20 Combination of each LULC class and LCZ classification (LCZ 1-10) through each morphological parameter mean ± standard deviation value range. Each number represents the LCZ type. LCZ 1-7 value ranges considered all 6 parameters, while LCZ 8-10 Aspect Ratio was omitted as the calculation is only building height - road width, not building height - space.....63

Table 21 Affiliation of LULC classes according to the LCZ thresholds by Stewart and Oke [2012]. All matches are summed up (maximum 6, dark red) and the individual boxes are coloured according to the number of matches 64

Table 22 LCZ class A-G affiliation to the non-build LULC classes 64

Table 23 Evaluation of the difference between the measured and simulation values of temperature and relative humidity for each control point for 7th of July 68

Table 24 Definition and classification of culture heritage based on the Paris Convention of 1972.....84

Table 25 Summary of T_{Air} parameter change for 5 points 87

Table 26 Summary of Rh parameter change for 5 points 88

Table 27 Summary of T_{mrt} parameter change for 5 points 89

Table 28 Summary of PET parameter change for 5 points 90

CHAPTER 1: INTRODUCTION

1.1. Rationale

Preserving the existence of cultural heritage sites has always faced many challenges in a rapidly growing and changing world, mainly those located inside urban areas [Dastgerdi *et al.*, 2019]. Among the actual existing pressure, researchers and authorities have now raised concerns about how climate change impacts the conservation of cultural heritage sites in the long term [Dastgerdi & Sargolini, 2019]. Due to the extensive anthropogenic activities, development, and land-use changes [IPCC, 2014a], the vulnerability of cultural heritage sites is not only defined by weather patterns [UNESCO, 2015] or by the existence of the physical characteristics of heritage assets to preserve cultural values [Pendlebury *et al.*, 2009] but can lead to other socio-economic problematics, such as loss of intangible values [Urdaniz, 2018], declining in tourists numbers and loss of community identity [Markham *et al.*, 2016; Scott *et al.*, 2016]. Cultural heritage values cannot be reversible, so once they lose their integrity or are destroyed, they cannot be recovered back. Even though UNESCO sites have a set of guidelines and regulations to protect and prevent the loss of these values, they are mainly focused on the conservation of the structures or constraints to new development dynamics, leaving out an important topic: "***Climate change effects on cultural heritage***". *How are cultural assets vulnerable? How could cultural heritage enhance the urban climate? Can adaption solutions within the UNESCO framework and guidelines improve the local climate conditions? How can we adapt these assets to improve the comfort in touristic destination?*

Starting to address these issues must lead to developing our understanding of the benefits and wider role of the historic environment for society [HES, 2019a]. World Heritage Committee brought for the first time into consideration the impact of climate change on World Heritage properties only at the 29th Session in Durban in 2005; awareness considered raised relatively late compared to other sectors; and based on the an overall review of the potential risks to WH properties posed due to climate change, the 30th Session in Vilnius in 2006, World Heritage Committee as all state parties to implement strategies in order to protect the outstanding universal values, integrity and authenticity towards the impacts of climate change [Sabbioni *et al.*, 2008]. As we respond to the reality of climate change in new ways, we can take the opportunity to highlight how the historic environment demonstrates resilience and adaptability as a lesson for the future. In 2008, the European Commission, the results from the Noah's Ark project suggested that more future studies are necessary to find how climate change is affecting the cultural heritage, mainly in the areas:

a) understanding the vulnerability of materials to climate, to reliably assess the future impact;

b) monitoring change, especially on decadal and even century-long time scales;

c) modelling and projecting changes in heritage climate at high spatial and temporal resolution, with an estimate of reliability;

d) developing tools to manage cultural heritage in a changing climate;

e) preventing damage by developing long term strategies [Sabbioni *et al.*, 2008].

Nowadays, after more than a decade, there are still a limited number of studies and practices related to the areas mentioned earlier, and these studies mainly focus on accessing the vulnerability of natural heritage, the archaeological sites to natural hazards (flooding, erosion, fire, etc.) or the indoor environmental conditions of historical buildings, leaving not much explored the cases of urban heritage sites:

> *"From the perspective of urban planning, it is essential to comprehend that preservation needs to be considered from the viewpoint of larger areas, and not only separate buildings. The concept of preservation is dynamic and changes over time."* - Carroll and Aarrevaara, 2021.

Cultural heritage sites in urban areas face various hazards like natural hazards, urban development dynamics, climate change, unsustainable exploitation for tourism purposes, etc. In these cases, the proposed solutions to prevent the historic site degradation should not be only climate-sensitive but, at the same time, should be in line with the UNESCO guidelines for conservation and preservation, making it more challenging to implement them.

The study will focus on the city of Edinburgh, which, apart from being the capital of Scotland, has a very dynamic cultural scene and has the most extensive collection in the country of historic buildings in Georgian and Victorian architectural styles and an urban morphology of winding medieval streets [University of Edinburgh, 2019]. The city has two UNESCO World Heritage Sites; the Old and New Towns of Edinburgh and the Forth Bridge. Due to this status Edinburgh has turned into an attractive destination for tourists [Halfpenny, 2021], becoming the fourth city in the world with the highest tourist-to-local ratio. This overwhelming with tourists is considered profitable when it comes to income and damaging to the cultural heritage assets.

1.2. Aim and Objectives

This study will aim to experiment with sustainable and climate-sensitive solutions to adapt urban cultural heritage sites in Edinburgh, which are vulnerable to climate change and urban dynamics while considering UNESCO conservation and preservation guidelines to provide a better comfort experience for tourists.

The objectives of this dissertation are to:

1. Exploring the urban culture heritage sensitivities, thresholds, and vulnerabilities in the city of Edinburgh to likely climatic scenarios in the future;

2. Develop a Local Climate Zone classification for the city of Edinburgh focusing on cultural heritage;

3. Evaluate the specific effects of Urban Heat Island in the actual conditions in cultural assets as touristic destination;

4. Introduce climate-sensitive solutions for different scenarios to analyse the impact of the outdoor thermal comfort for tourists.

1.3. Outlines

The general outline of the dissertation starts from identifying the impacts of climate change, focusing on cultural heritage at a city level (macro-scale) and trying to find concrete solutions at a site level (micro-scale). This range starts in the objectives set, which are co-depended between them and address the questions set for the dissertation theme and fill the research gaps found regarding "***Climate change effects on cultural heritage***". The general outline of the research is shown in *Figure 1*.

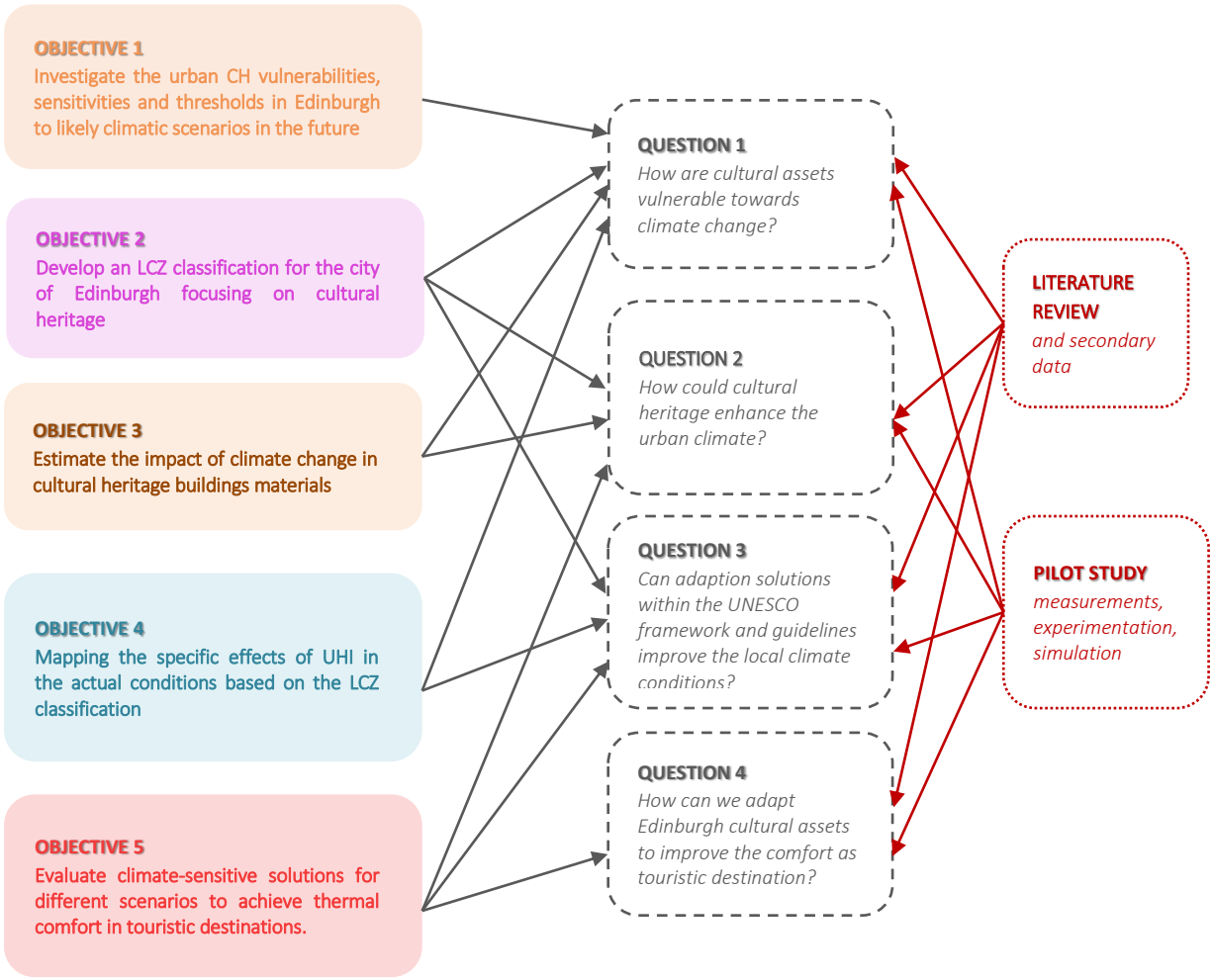

Figure 1 General outline of the research (source: Own elaboration)

1.3.1. Outline the Methodology

Climate change can affect culture heritage in different ways and its consequences can deteriorate existing problems in cases of urban historic cores. The study analyses these consequences considering the state of conservation, but also mapping the magnitude of Urban Heat Island affecting the local climate of Edinburgh. All the conditions created, where used to estimate the outdoor thermal comfort as a touristic destination. The research starts with literature review due to the importance of past conditions and declaration of authenticity and integrity, adding the recommendations and guidelines in case of World Heritage property in Edinburgh. The analysis begins from city scale, mainly with qualitative data and follows to neighbourhood scale with field data and simulation method. As in case of Edinburgh, there were no previous related studies, the outcomes can be considered as conceptual stage, serving as basis for future studies.

1.3.2. Outline of the Dissertation

The dissertation is structured into six chapters as follows:

Chapter 1 introduces the research topic and its foundation. It establishes the problem, specifies the goals and objectives, and characterises the study's scope.

Chapter 2 presents the key findings regarding previous research works and study cases related to the effects and impact of climate change on cultural heritage assets, UHI effects in historic urban towns, deterioration of building materials and challenges due to urban dynamics. Additionally, it defines the possible sustainable and climate-sensitive interventions. Last a summary of knowledge gaps identified regarding the topic.

Chapter 3 gives an overview of the city of Edinburgh regarding the climate conditions and projections, the cultural heritage assets, focusing in detail on the Old and New town - World Heritage property; and explains the urban dynamics happening in the city and its strategic development plan in adapting to climate change.

Chapter 4 explains the entire methodological approach and framework to reaching the thesis's goal and objectives. It summarises the research design, the datasets used, and the data collection process.

Chapter 5 shows the results processed from the collected data at each analysis step based on the methodology. After evaluating the current state, interventions are applied to improve tourist comfort at the site.

Chapter 6 concludes the research topic based on the results and discussion and answers the aim and objectives, followed by limitations that were perceived throughout the dissertation. Finally, some recommendations for future research on historic urban towns and Edinburgh's local authority, culture heritage site managers, urban planners, and designers are presented to preserve and adapt the cultural assets for today's multi-hazards.

CHAPTER 2: LITERATURE REVIEW

Today, cities and their built environments characterise the critical focus of scientific debate and global management of the effects of climate change. The impact of these changes is extensive and wide-reaching; including physical, environmental, social and economic aspects, ranging from monuments to historic towns and cultural landscapes [Jigyasu, 2019]. Climate change does not respect boundaries or borders, social classes or cultures, age or location [HES, 2019a]. Cultural heritage defines the identity of a community or a place, passed through generations in different shapes like customs, values, objects, and landscapes by determining a specific collective memory of an event not to be forgotten, including archaeological remains, cultural environments, infrastructure, buildings, interiors, and details [UNESCO, 1972]. Various factors are constantly jeopardising the existence of cultural heritage values, including the dynamic of urbanisation and climate change.

Regarding the characteristics of built environments in the old continent (*Figure 2*), Europe (including the United Kingdom), surveys from the Eurostat Census in 2011 revealed that there is a considerable percentage of dwellings pre-1919 [ESPON, 2020], and most of them are part "historical centre" of cities which define the urban landscape value of cities [UNESCO, 1976]. Some aspects of the environment must be regarded as non-renewable and thus irreplaceable, and cultural heritage is one example [Haugen & Mattson, 2011]. Climate change is likely to hasten or alter the degradation of cultural heritage [Cassar, 2005; Sabbioni *et al.*, 2008; Smith, 2014; Sesana *et al.*, 2021].

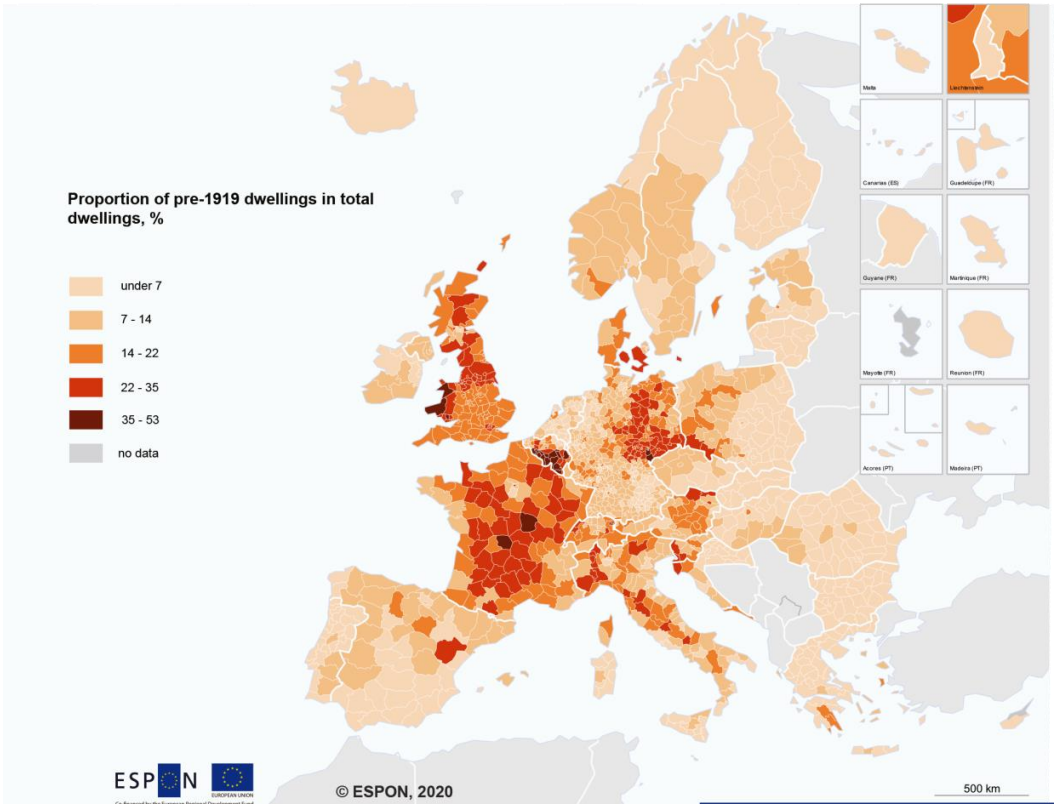

Figure 2 Spatial distribution of the proportion of pre-1919 dwellings in total dwellings, 2011 (source: ESPON, 2020)

2.1. Climate change in the build environment focused on cultural heritage context

A literature review was conducted to understand the impact of climate change on cultural heritage, how this impact has been accessed so far, and the solutions proposed to prepare or adapt for future climate variations. The link between climate change and cultural heritage was first brought up in the 1990s in Australia by Rowland [1992; 1999], followed by a publication by Viles [2002] on climate change and stone degradation. Still, these days, one of the most significant attempts to assess the impact of climate change focusing on cultural heritage is the Noah's Ark project, commissioned by the European Commission under its 6th Framework Programme for Research [Sabbioni *et al.*, 2008] and the results were in continental scale. M. Cassar and Pender conducted the first region-specific studies for UK cases in 2005. Nevertheless, it was only in the AR5 report from IPCC in 2014 that the impact was specifically treated [Sesana *et al.*, 2021]. From that moment, climate-change threats to cultural heritage sites are increasingly recognised as a threat to society on a large scale [Cassar, 2005; Erlandson, 2008; Fitzpatrick et al., 2015; Harvey and Perry, 2015; Markham and Wiser, 2015; Marzeion and Levermann, 2014; Rockman 2015]. So, publications increased enormously after the early 2000s, especially after 2007 [Sesana *et al.*, 2021]. The studies mainly focus on accessing the vulnerability of natural heritage, the archaeological sites towards natural hazards (flooding, erosion, fire, etc.), or historical buildings' indoor conditions.

2.1.1. Impacts of climate change on cultural heritage

Historic urban areas have a distinctive morphology, urban fabric, architecture, community structure and boundaries; and have evolved over generations through keen understanding among local communities reaching towards harmoniously co-existence, sustainable inter-relationships and built environment [Jigyasu, 2019]. It is essential to have a clearer view while proposing an effective risk reduction plan by having a good perception of the possible hazards, thus identifying the level of vulnerability [Dastgerdi & Sargolini, 2019] and knowing how the system would respond in the case of these hazards. The vulnerability assessment includes an analysis of the potential impacts of climate change due to foreseen changes in parameters [Carroll and Aarrevaara, 2018; Dastgerdi & Sargolini, 2019], and the first action to assess the vulnerability starts with defining the scope and the problem. Intergovernmental Panel of Climate Change (IPCC) [1992] established a general outline approach to defining the scoping, which can be summarised in the following steps:

Figure 3 Steps to determine scope and problem definition based on IPCC outline (source: IPCC, 1992; Carter and Blantran de Rozan, 1993)

Vulnerability is not only a final product, but as a function of the character, magnitude, and rate of climate variation to which a system is exposed, its sensitivity, and its adaptive capacity [IPCC, 2001] (*Figure 4*) accessed at a specific time but involves an entire process [Jigyasu, 2019]. UNESCO recommends assessing WH site sensitivity and exposure to climate hazards using a long-term perspective of 20, 25, or 30 years and medium-term objectives of 5 to 10 years [Collette and Cassar, 2007]. The assessment must identify if the vulnerability has increased, decreased, or reinforced over time. Investigating climate change vulnerability at historic sites and especially quantifying the level is essential in proposing long-term adaptation policies and solutions and can impact their effectiveness.

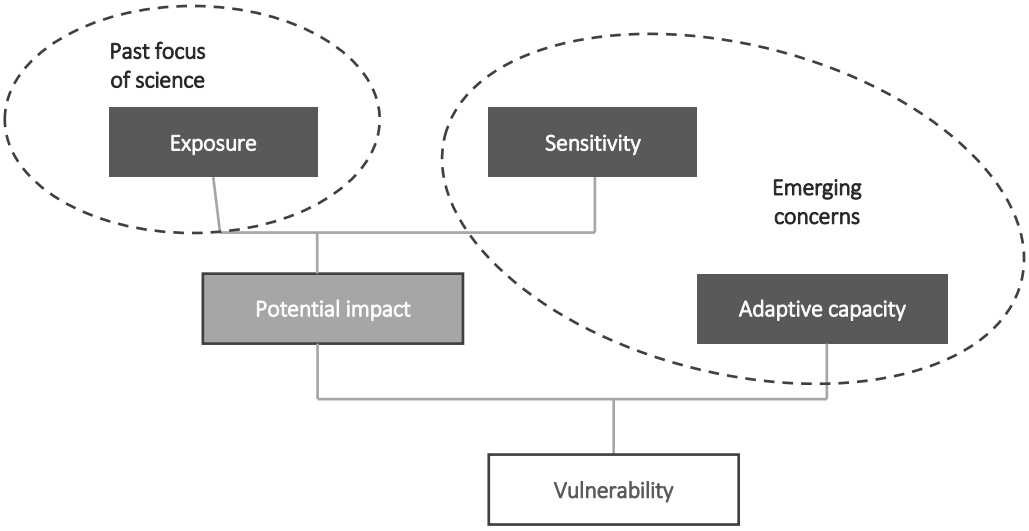

Figure 4 General vulnerability framework based on IPCC definition (source: Own elaboration)

Climate change's physical, social, and cultural effects on cultural heritage are intertwined. Cultural heritage may be structurally, non-structurally, or materially vulnerable to climate change-related dangers. [Jigyasu, 2019]. In the report *"Climate change and world heritage: report on predicting and managing the impacts of climate change on world heritage, and strategy to assist states parties to implement appropriate management responses",* UNESCO [Collette and Cassar, 2007] identified the significant impact of climate change on culture heritage assets, like:

- As the archaeological site typology depends on on-ground conservation, soil processes and cycles such as hydrological, chemical, and biological changes may threaten some sensitive material classes.
- Historic buildings have more interdependence with the ground than the contemporary ones due to their porosity, leading to high surface evaporation of the water from the soil. This reaction can happen from different structural parts (wall surfaces and floors), so if the soil moisture increases, there is more opportunity for salt mobilisation, leading to crystallisation on decorated surfaces.
- In the case of the materials used in cultural sites, organic materials like timber may be infested by biological components due to the migration of pests in latitudes and altitudes.

Britain was a pioneer in assessing the first report on climate change and the historic environment [Cassar, 2005], but this report was based on on-site managers and policy questionnaires. Historic Environment Scotland [2018] conducted a study called *"A Climate Change Risk Assessment of the Properties in Care of Historic Environment Scotland"*, targeting the first step to understanding, quantifying, monitoring, and managing environmental risk by identifying the impact of climate changes on cultural heritage assets. The product of this study was a climate change risk register for the Properties under Historic Environment Scotland Care, using Geographic Information System (GIS). As the study focused on the potential risk to cultural heritage from natural hazards, they used data from different sources for the research (*Table 1*), so they did not need to produce empirical data. The authors mapped the hazard probability of occurring by calculating the return period and also considered how much a hazard is unlikely to happen.

Table 1 Data used for the Climate Change Risk Assessment (source: HES, 2018)

Fluvial Flooding	Coastal Erosion obtained from Scottish Environment Protection Agency
Coastal Flooding	
Pluvial Flooding	Slope Instability, developed by the British Geological Survey
Groundwater Flooding Potential	Base mapping was created by the Ordnance Survey.

2.1.2. Deterioration of building materials

All cultural heritage is naturally subjected to physical, chemical, and biological effects to varying degrees [Collette and Cassar, 2007; Haugen & Mattson, 2011] and due to the increment of severe weather events and exposure, in addition to the ageing of materials and the existence of previous conservative interventions [Bertolin, 2019], the degradation progress continues to accelerate. As a result, various tangible and intangible cultural heritage attributes would be affected, leading to the loss of the values, because they exist as physical or spatial manifestations in the form of systems individual components such as buildings, trees, etc., which might be part of the systems. Natural hazards are not the only risk to cultural heritage, as gradual and progressive processes play a significant role [Jigyasu, 2019]. UNESCO report [Collette and Cassar, 2007, 25] shows an overall impact that different meteorological and climatic variables can cause on heritage structures (*Annex 1*). Degradation of building materials due to climate change is not a new topic in the research environment, but unfortunately, they are more focused on contemporary structures [Bertolin, 2019]. The geographical position is crucial because exposure to local climatic conditions provides a critical understanding of the overall risk of degradation, as it is related to the specific condition of materials *in situ*. [Gobakken *et al.*, 2008; Haglund *et al.*, 2010]. Regarding the heritage buildings in the UK, the factors putting in risk include [Cassar, 2005]: temperature/humidity variation directly affect the structure of materials, leading to their decay; increased seasonal rainfall and storms can lead to extra pressure to the existing drainage system, designed for lower capacity; soil moisture content alteration can could result in the retraction of soil away from the foundations of a building , sea level rise can put in danger coastal buildings due to intensified coastal erosion.

2.2. UHI effects based on historical sites

The Urban Heat Island (UHI) is a thermal anomaly with horizontal, vertical, and temporal dimensions [Oke, 1982], with the leading causes consisting of differences in thermal structures between urban and rural environments, such as thermal characteristics of the urban fabric and geometry, urban pollution, and anthropogenic activities [Park, 1986; Oke, 1991]. Due to the significant impact of UHI on urban sustainability, researchers have made a considerable effort to understand UHI [Steward and Oke, 2012]. It is proven that even though the UHI phenomenon is not generated by global climate change, it can magnify the magnitude of the presence of rising [Santamouris, 2014a] or lower [Santamouris, 2014b] temperatures at the local scale; however, effects of local warming are excluded while calculating projections of future climates [IPCC, 2014b]. The two main UHI produced by urbanization are Urban Boundary Layer (UBL) and Urban Canopy Layer (UCL) [Oke, 1976].

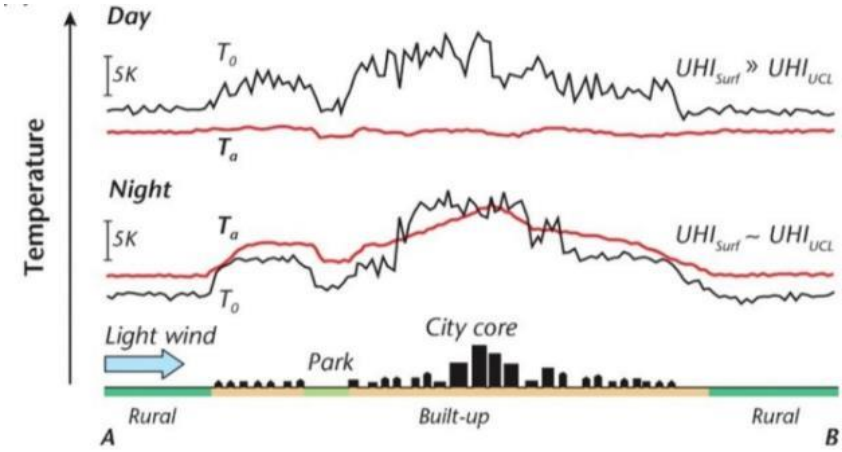

Figure 5 Schematic 2D representation of UHI urban canopy layer during day and night. The comparison is made between surface temperature (T0) and air temperature (Ta) in a traverse along the line A-B. The values of temperature follow the silhouette of the build-up area (suburban and urban), while in areas with green elements the temperature is lower (source: Health Canada, 2020)

The evaluation of UHI magnitude depends on the combination of four characteristics: technological (albedo, heat capacity), morphological (orientation, Height/Width ratio) and anthropogenic (traffic, industry activities) and weather/climatic parameters [Parsaee *et al*., 2019]. These characteristics causing the effect of UHI are controllable such as technological, urban morphology, and anthropogenic, and uncontrollable such as climatic, weather parameters and geographical features [Levermore *et al*. 2018]. However, some controllable characteristics in historic towns are limited to be modified. Historic areas are defined by their distinct morphology, urban fabric, architecture, community structure, and boundaries, which have carefully evolved through a keen understanding of local communities about their environment in which they have co-existed harmoniously, sustaining various inter-relationships and built environment over generations [Jigyasu, 2019].

2.3.1. Local Climate Zone (LCZ)

It is not easy to provide an objective protocol for measuring the strength of an urban heat island and facilitating controlled inter- and intra-UHI comparisons. According to the causal processes and measurement methods, the air temperature under investigation for UHI studies

is generally divided into two broad categories: UCL UHI [Oke, 1995] at the microscale and UBL UHI at the mesoscale [Barlow, 2014]. Local climate zones (LCZ) provide a research framework [Steward and Oke, 2012] of the UHI compared to the rural areas, and as such, the classification of 17 zone types at the local scale; 10 built types labelled as LCZ 1~10, and 7 land cover types labelled as LCZ A~G (*Figure 6*); helps to standardise the urban temperature observations on a global scale. Each class represents a specific urban thermal environment pattern, providing a microclimate conditions estimation tool for urban planning and policy makers [Quan and Bansal, 2021]. It is considered that UHI is related to structural and land cover, which is different between urban and rural areas. The LCZ system has been widely applied in research fields related to urban climate and urban planning [Jianga *et al.*, 2021]. Each settlement is unique as a combination of surface structure, cover, and human activity. Sites' classification into appropriate LCZs requires basic metadata and surface characterisation [Oke *et al.*, 2004].

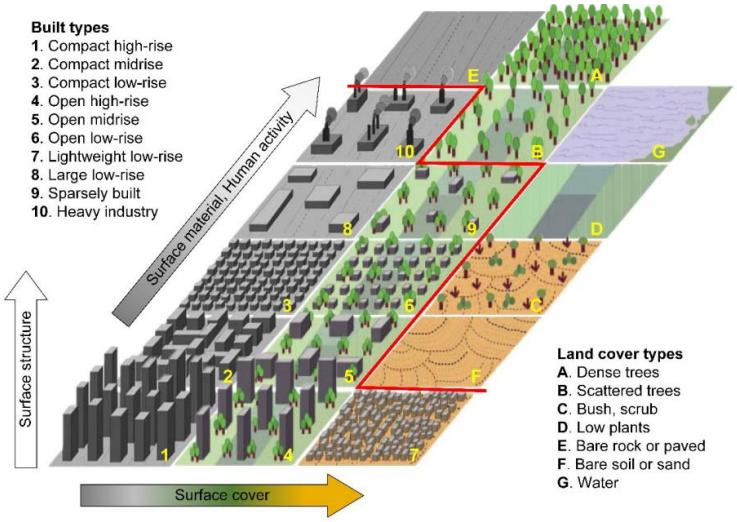

Figure 6 The 17 standard LCZs. Modified from Stewart & Oke (source: Jianga *et al.*, 2021)

The experience in mapping the LCZs division for cities is mainly conducted through remote sensing (RS) and GIS, as field surveys are not cost- and time- effective on a city-scale [Kotharkar & Bagade, 2018; Quan and Bansal, 2021]. RS approach is considered less data-intensive [Zheng *et al.*, 2018, Jianga *et al.*, 2021], as the division is based on supervised pixel-based classification of satellite images, contrary to the GIS approach, where primary and secondary data sources are required. The data required include urban morphology, planning and building information. Remote sensing approach is adopted in the World Urban Database and Access Portal Tools (WUDAPT) [Ching *et al.*, 2018] based on the workflow shown in *Figure 7*. However, GIS approach allows more diversity methods in implementing the original LCZ framework. The original LCZ scheme often has considerable problems when adapted to European cities with historical city centres, including narrow streets and irregular patterns, requiring the integration of different approaches and adapt the standardisation classification, to minimise the limitations. Nonetheless, this method remains a valuable tool for comparing different parts of cities, representing heterogeneous thermal behaviour within an urban environment [Wicki and Parlow, 2017].

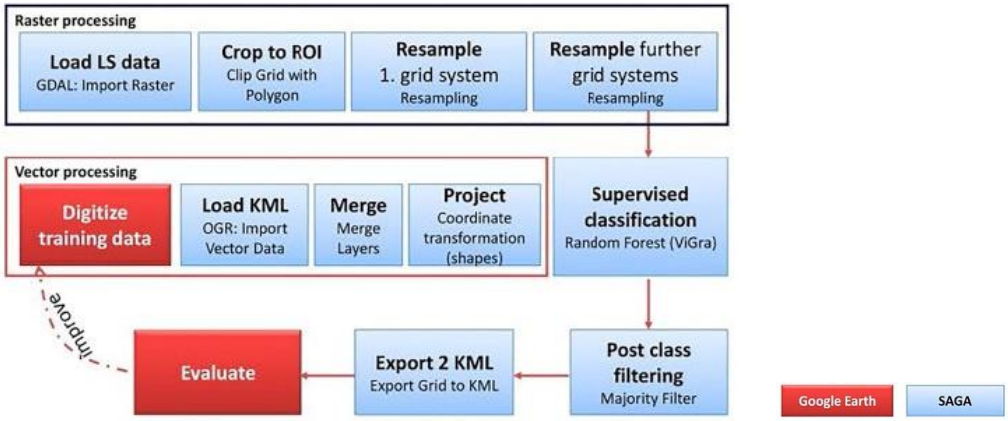

Figure 7 WUDAPT workflow (source: Quan and Bansal, 2021)

In GIS approach the LCZ classification is based on the value ranges of 10 parameters, which have proven to impact the local climate [Steward and Oke, 2012], 7 define the urban morphology: sky view factor, aspect ratio, building surface fraction, impervious surface fraction, pervious surface fraction, height of roughness elements, terrain roughness class and 3 define thermal, radiative, and metabolic parameters: surface admittance, surface albedo and anthropogenic heat output. Additional stages can be implemented to improve the optimisation while mapping a larger urban environment in order to optimise the findings of LCZ [Quan and Bansal, 2021]. Each spatial unit's LCZ type is determined through a classification on the basis of the calculated parameters. Then the spatial units undergo post-processing. Finally, the quality of the produced LCZ map is evaluated *(Figure 8).*

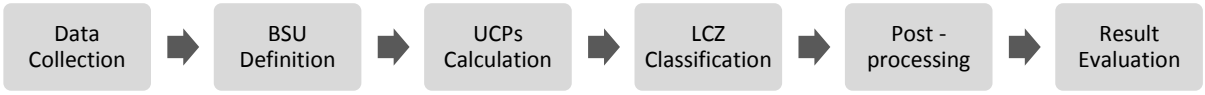

Figure 8 General LCZ mapping process in the GIS stream (source: Quan and Bansal, 2021)

There are three assigning the LCZ classes: removal, combination, and addition, depending to the actual cases. There are cases when some land cover has been combined into one [Quan, 2019], or one LCZ class has been removed [Chen *et al.*, 2020]. In case of LCZ classification researchers have used:

1. Standard rule-based classifier,
2. Modified standard rule-based classifier
3. Fuzzy rule-based classifier

The first one comes from the original LCZ framework and uses an "if–then" rule to assign each LCZ class, while taking into account the range values of morphological parameters. All the parameters must fall inside a certain LCZ class's range. The second method allows for a reduction of morphological parameters number from 10 to 3-7, but some researchers have also modified the range of the threshold [Zheng *el al.*, 2018]. The final one employs the membership degrees as soft labels to establish the LCZ class for each grid and uses a multi-dimensional linear interpolation.

2.3.Outdoor thermal comfort

The urban forms strongly influence microclimates [Oke, 1988] and different thermal conditions. Many studies regarding the evaluation of thermal comfort conditions in urban microclimates [Liu et al., 2015; Chen et al., 2004] revealed a strong relationship between micro-climates and the use of outdoor spaces and environments [Zacharias *et al*., 2001]. Cultural heritage creates the conditions for tourism development, and in some cases, this industry contributes in large part to the income of the economy and employment opportunities [Nasrollahi *et al.,* 2017]. Scotland has substantial economic and social benefits from a healthy and resilient historic environment. In 2017 alone, the historic environment generated £4.2bn for Scotland's economy, supported 66,000 full-time-equivalent jobs and attracted 18 million visitors [HES, 2018]. Globally, evidence show that visiting historical sites and places can be beneficial to health and wellbeing, reducing social vulnerability and increasing resilience. Tourists are likely to be affected by climate variability more than the local people [Lu *et al.*, 2016], making climate and weather conditions the main natural factor affecting tourism [De Freitas *et al.*, 2007; Matzarakis, A., 2006; Lecha and Shackleford, 1997; Shackleford and Olsson, 1995].

Many indices have been developed over the years to evaluate the tourist climate appropriateness [Nasrollahi *et al.,* 2017]. Mieczkowski [1985] proposed Tourism Climate Comfort Index (TCCI), which takes into consideration 7 climatic factors; three of which are independent and two are combined with bioclimatic ones [Anđelković, 2016]: *maximum daily air temperature; mean daily air temperature; minimum daily relative humidity; average daily relative humidity; the amount of precipitation; daily insolation;* and *average wind speed.* Meanwhile, Scott *et al.* [2008] supported that optimal climate conditions are related to four climate parameters (temperature, precipitation, insolation and wind) regarding three kinds of tourism: coastal, city and mountains. However, TCCI establishes a universal tourism climate index, leaving out the specific touristic site characteristics; therefore, integrating the neglected effects is needed during the evaluation process [De Freitas *et al.,* 2007]. Moreover, *Annex 2* summarises other indices used in urban areas evaluating the thermal impact on tourists.

Table 2 Ranges of thermal indexes (source: Oke *et al.* 2017)

PMV	PET	Thermal perceptions	Grade of physiological stress	Universal Thermal Climate Index UTCI
-3.5	4	Very cold	Extreme cold stress	< -40 -27 to -40
-2.5	8	Cold	Strong cold stress	-13 to -27
		Cool	Moderate cold stress	0 to -13
-1.5	13	Slightly cool	Slight cold stress	+9 to 0
-0.5	18	Comfortable	No thermal stress	+9 to +26
0.5	23			
1.5	29	Slightly warm	Slight heat stress	+26 to + 32
		Warm	Moderate heat stress	+32 to +38
2.5	35	Hot	Strong heat stress	+32 to +38
3.5	41	Very hot	Extreme heat stress	+ 38 to +46 >46

2.3.1. Simulation Approaches

Researchers have created various computer-based outdoor microclimatic simulation tools to investigate how the built environment influences a variety of thermodynamic phenomena, but these tools have limitations due to the complexity of urban forms [Albdour & Baranyai, 2019]. ENVI-met® is estimated to be the most efficient software [Bruse, 1999; Emmanuel *et al.*, 2007; Albdour & Baranyai, 2019] in predicting and simulating thermal comfort indices and meteorological parameters and the majority of outdoor design strategies. ENVI-met® is a 3d non- hydrostatic model for simulating surface-plant-air interactions, detailing the urban canopy layer, with a time-space resolution of 10 s/0.5–10 m and a time frame of 24 to 48 hours. Different cases have evaluated the UHI magnitude in a cultural heritage environment that mainly using ENVI-met® software. One case study refers to the Teramo, Abruzzo region in Italy, a small city with a population of 60.000, so the input parameters consist of a typical Italian summer. Different case studies were developed during the analysis, such as Base Case, Cool Case and Green Case of a site densely built with vegetation and surrounded by rural areas. The parameters used are shown in *Figure 9*. The results from the software simulation showed that the urban microclimate is quite altered even though the area selected was small, which leads to thinking that in a simulation at a larger scale, the magnitude of UHI might be even more significant [Ambrosini *et al.*, 2014].

The same approach was used in a similar case in Venice, Italy, by analysing the local climate condition in the mainland of Venice under different conditions of urbanisation. The researchers used data from weather stations distributed in the city centre and nearby rural areas. The climatic differences were found mainly at night during the summer, with an average difference of 4 °C between the surrounding and the actual urban area. They analysed different scenarios (*Figure 10 and Graph 1*), such as using "cool materials" and green porous surfaces as solutions to existing pavements and roofs, which lowered the temperature by 4 °C [Peron *et al.*, 2015].

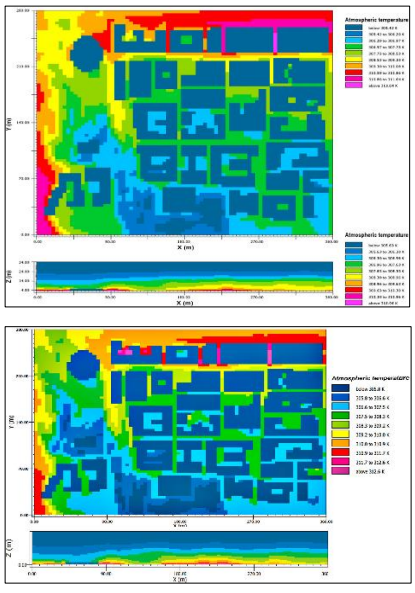

a

b

Time-space resolution of the model	10 s/0.5–10 m
Seasonal temperatures	5.5 °C (winter) and 25 °C (summer)
Simulation day	hottest summer days, assuming uniform temperature and humidity
Grid	width 385 m and length 285 m
Model	40 buildings
Building height	3 till 15 m

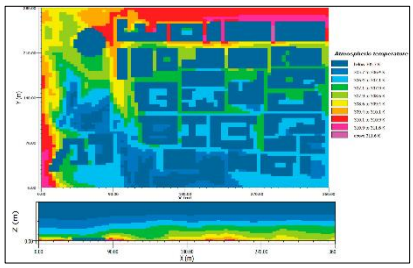

c

Vegetation types	"T1": tree 10 m tall, dense foliage, leafless base; "H2": thick bush, 2 m tall; "xx": grass, average density, 50 cm tall.

Figure 9 Study case of Teramo UHI analysis showing ENVI-met® results of atmospheric temperature profile horizontal at 1.2 m height in July 22nd at 2 pm in three scenarios: (a) "base case": current conditions.; (b) the "cool case": all the roofs have been covered with high-reflectance material; (c) "green case": all roofs have been replaced with green roof; and on the left the main parameters for modelling. (source: Ambrosini *et al.*, 2014307)

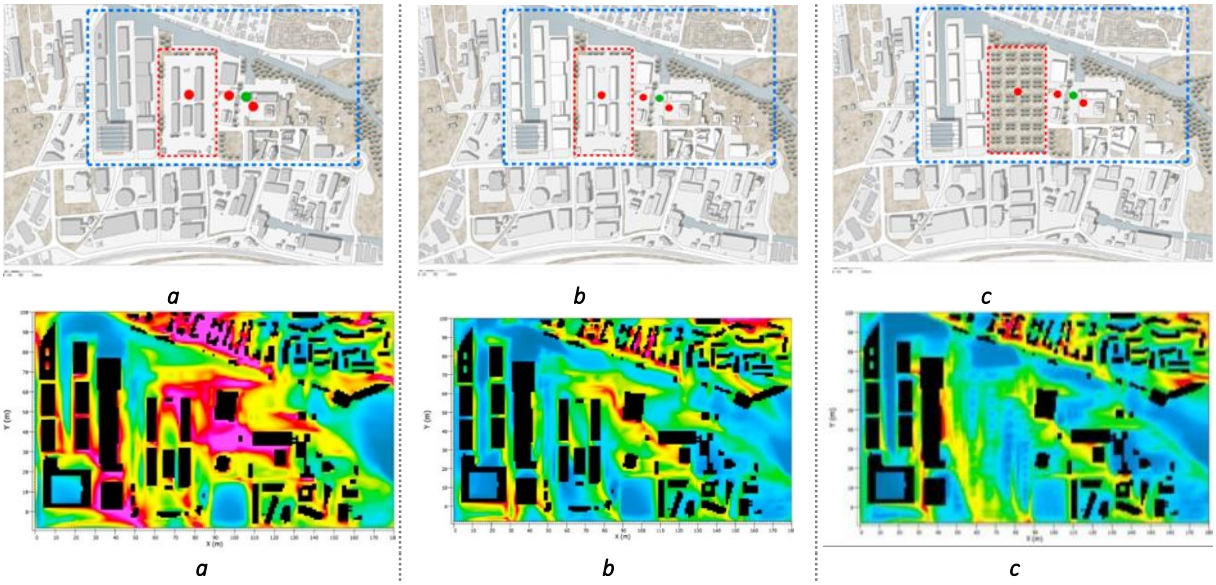

Figure 10 Study case of Venice UHI analysis showing the master plan of (a) "base case": current conditions; (b) the "cool case": cool pavements and roofs (white) replace the usual surfaces; (c) "green case": a park replaces the wholesale fruit and vegetable market and ENVI-met® results urban air temperature profile horizontal at 1.2 m height (lower limit 26,75 °C, higher limit 34,35 °C) in August 2nd at 3 pm in three scenarios. (source: Peron *et al.*, 2015, 307)

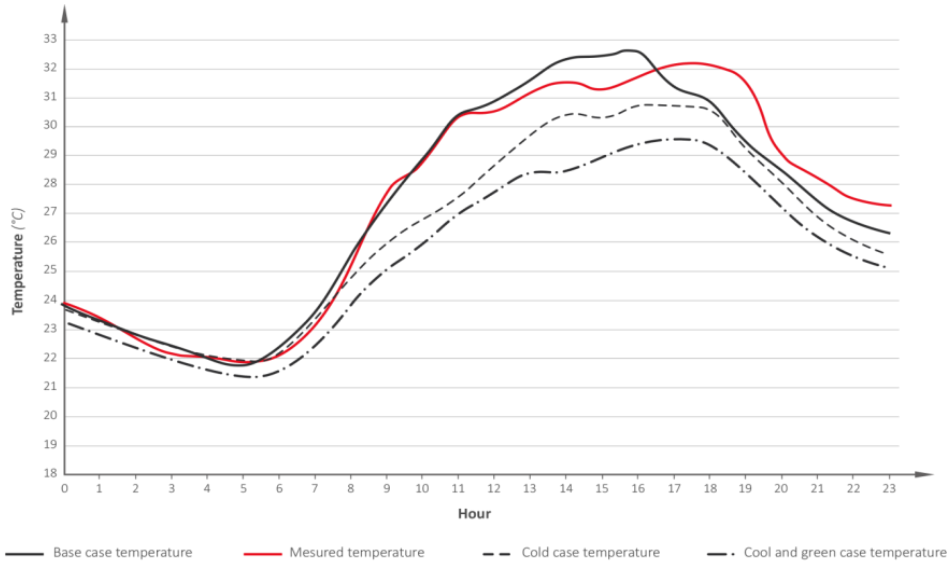

Graph 1 Hourly temperatures on August 2nd 2012: measured (solid red line), simulated (solid black line), cool case (long dash line), cool and green case (long dash dot line) at 11 m height above ground. (source: Peron *et al.*, 2015, 308)

2.4. Implementing Sustainable Development Goals in historical sites

There is a strong relationship between micro- climates and the use of outdoor spaces and environments [Nikolopoulou and Lykoudis, 2007], so nowadays, climate change has started to become an essential factor to consider in city planning. Several cities have become advocates for broad-scale efficiency and sustainability, supporting cross-sectoral initiatives (transportation, public buildings, etc.) to influence new city planning (i.e., Covenant of Major). Most of the adaptive solutions for buildings were derived from an assessment of microclimate alteration studies in cities. However, as far as there is an intention to adapt the new structures for the foreseen future, it is vital to consider factors that contribute to the degradation of cultural heritage buildings in the urban setting, as these values are not reversible. A study conducted by Carroll and Aarrevaara [2021] found that there is a lack of connection between urban planning tools and the impact of possible changes due to urbanisation climate change towards urban culture heritage assets.

Strategies resulted effective in response to the challenges presented by climate change to cultural heritage preservation include: planning timescales, enhance monitoring systems, management, maintenance, loss and obsolescence [Cassar, 2005; Hall *et al*., 2016; Jigyasu, 2019]. Rediscovery and adaptation of management approaches and traditional knowledge can address the effects of climate change on cultural heritage and aid in resource management and society's adaptation to modern climate change [HES, 2019a; Jigyasu, 2019]. The integration of sustainability with the protection of cultural landscapes is also a focus in many landscapes ecological approach [Pearson and Gorman, 2010; Hall *et al*., 2016] by identifying the needs of various stakeholders and promoting planning through an adaptive process that is both holistic and continuous. By using this approach, land use development can be dynamic and create a functional heritage landscape (opposite to “frozen” heritage), making adaptation is as valuable as mitigation [Loulanski, 2006; Head, 2010].

Intergovernmental Panel on Climate Change [2014b] considers adaptation as “adjustments in natural or human systems in response to actual or expected climatic stimuli or their effects, which moderates harm or exploits beneficial opportunities”, so the solutions should rely on interventions to adapt the historic ecosystem to climate change. Historic Environment Scotland [2019a] supports that Adaptation can be divided into 'Resistance' and 'Acceptance'. Both are direct answers to climate change, but they are approached differently:

Resistance
strategy for actively halting/reversing the impact and/or increasing the asset's capacity to cope with the effect (s). This could be accomplished by making physical changes to historic assets, such as strengthening drainage systems to allow sites to tolerate higher levels of rainfall.
Acceptance
mindset that recognises that change will occur but that it will be planned for before any significant damage or loss occurs. This could include creating a plan to properly record and/or excavate a site before it is damaged or lost or adopting a long-term strategy to manage a site's gradual loss.

The science pillar's impacts section focuses on methods and data that characterise interactions of climate change phenomena with cultural heritage components. Due to the variety of potential threats forms and the different ways affecting, the heritage sites in an integrated manner, including landscapes, buildings, and objects and collections [Dastgerdi & Sargolini, 2019]. The potential of consolidating synergies across different thematic areas of human development, disaster risk reduction, and climate change adaptation is by focusing on the three nodes of risk, vulnerability, and resilience [Jigyasu, 2019] and by bring together each theme agendas together *Figure 11*.

Sustainable Development Agenda

- Economic development: Growth & Equity
- Human Development
- Ecological Sustainability

Disaster Risk Reduction Agenda

- Vulnerability reduction
- Exposure reduction
- Risk modification
- Adaptation and Resilience

Climate Variability & Change Agenda

- Climate Adaptation
- Climate Mitigation
- Climate Co-benefits (added benefits of acting on climate change control and beyond the direct benefits of more stable climate).

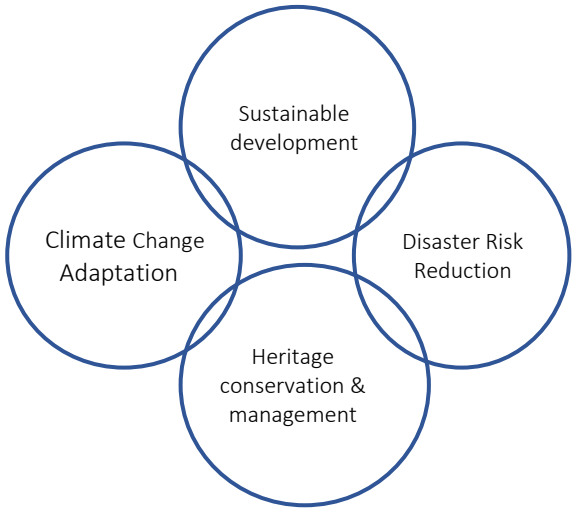

Figure 11 Schematic representation of agendas for development, disaster risk reduction, and climate change and variability. (source: Jigyasu, 2019)

CHAPTER 3: EDINBURGH STUDY AREA PROFILE

3.1. Climate conditions overview

3.1.1. Current climate

Edinburgh has a temperate climate, and extremes in temperature are uncommon due to its proximity to the sea, on steep lowlands on the banks of the Firth of Forth and the North Sea [Macdonald *et al.*, 2008]. Summers are fairly cool, while winters are rather mild, with average daily minimum temperatures hovering above freezing. Rain is common in the warmer south-westerly winds that come off the North Atlantic Current; the prevailing easterly winds are typically cold but primarily dry [Met Office, 2016]. The average yearly temperature in Edinburgh is 9°C. The warmest month (July) has an average temperature of 19°C, while the coldest month (January) has an average temperature of 3°C. The average annual rainfall is 685 mm, distributed equally throughout the year. October is the wettest month, receiving 54 mm of rain on average. March is usually the driest month, with an average of 27 mm of rain. The typical monthly relative humidity ranges from 77% in April to 86% in December, with an annual average of 81%. Edinburgh receives less than one-third of the possible sunshine for its latitude on an annual basis, with an average of 1406 hours per year [Met Office, 2022a].

3.1.2. Observed climate trends

Scotland has experienced rapid climate change during the last century. Records reveal that temperatures have risen over the last few decades, with the last decade being the warmest. Rainfall patterns have also shifted, with more solid downpours and more significant rainfall. Sea levels are rising faster, and there are fewer days with frost or snow cover.

Edinburgh is included within the Eastern Scotland region as defined by the UK Met Office. Trends over 1961-2021 show significant changes in many climate indicators, including:

- An increase in the average temperature of 0.57°C.
- Average precipitation has increased by 11.8%, with a 27% increase in winter and a 29.3% increase in summer. However, rainfall does not show a consistent trendline from year to year.
- Air frost has increased by 16.8%, but the trendline is not consistent from year to year.
- Days of heavy rain have increased by 7.8%.

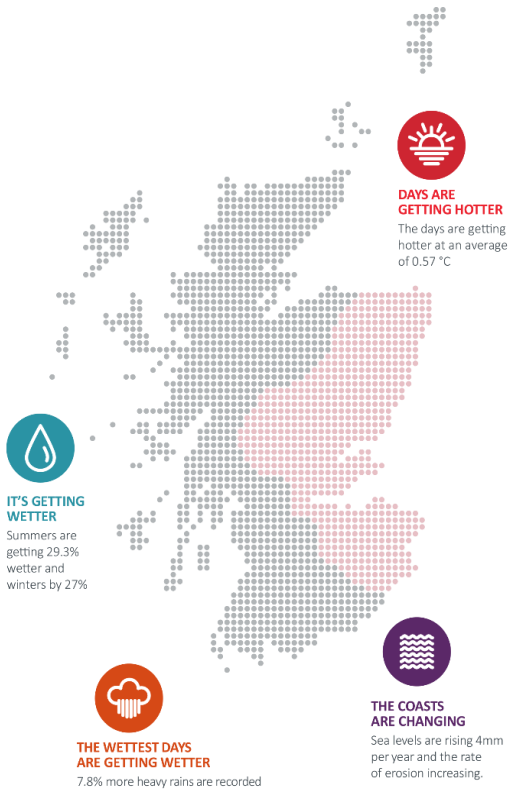

Figure 12 Overview of Eastern Scotland's Changing Climate, comparison between 1961 and 2021 (source: Met Office, 2022b; HES, 2019a)

3.1.3. Anticipated climate change

3.1.3.1. Global climate change and the Paris Agreement

The 2015 Paris Agreement, signed by 195 countries under the auspices of the UN Framework Convention on Climate Change (UNFCCC), aims to keep global temperature rise below 2°C compared to pre-industrial levels and limit the rise to 1.5°C in the near term (2021-2040) would result in unavoidable increases in multiple climate hazards and pose multiple risks to ecosystems and humans *(Graph 2)* [IPCC, 2022, 13]. According to World Meteorological Organization [WMO, 2020], the average temperatures have already become 1.2°C warmer since pre-industrial times. If emissions continue unabated, warming will likely reach 1.5°C in 2040 and 2°C by 2065.

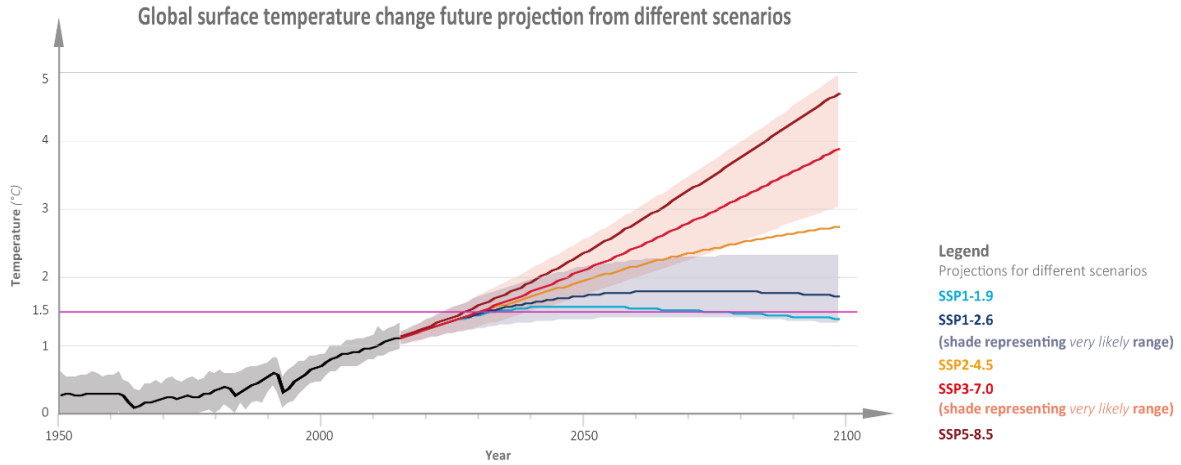

Graph 2 Global surface temperature change based on different scenarios and relative comparison to the period 1850 – 1900: 1.5°C temperature incensement relative to 1850–1900 is expected to be exceeded in the near term (2021–2040) under the intermediate, high, and very high greenhouse gas emissions scenarios (SSP2-4.5, SSP3-7.0, SSP5-8.5); more likely than not to be exceeded under the low greenhouse gas emissions scenario (SSP1-2.6) and more likely than not to be reached under the very low greenhouse gas emissions scenario (SSP1-1.9). (source: IPCC, 2022, 18)

Rising temperatures are hastening the sea level rise on a global scale, and according to NOAA [2017], the rate loss of the Greenland and Antarctic ice sheets in six scenarios projected a range between 0.5 metres and 2.4 metres higher by 2100 compared to 2000 *(Graph 3).* Warming oceans are also affecting marine biota, causing changes in the range and populations of fish species that provide food and income to hundreds of millions of people.

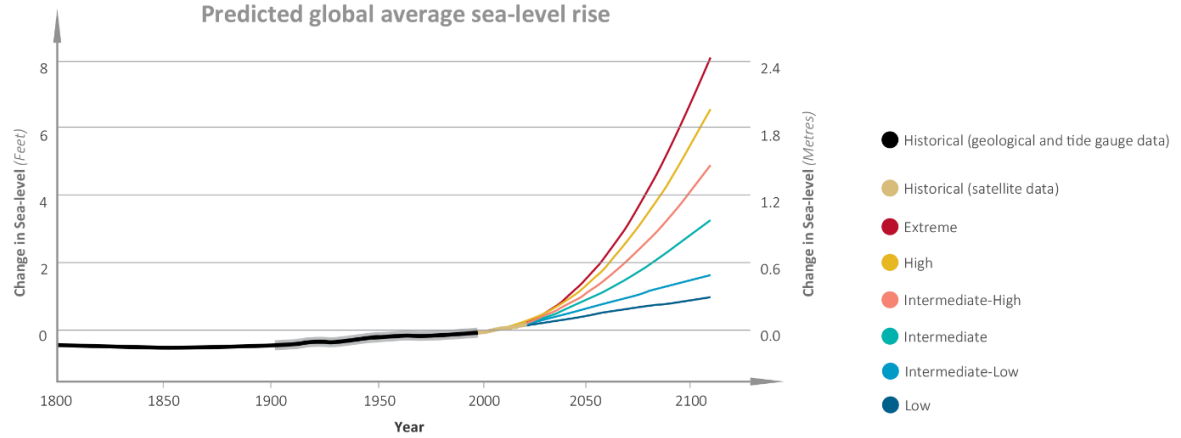

Graph 3 The latest estimates of global average sea-level rise, combining IPCC scenarios & more recent data on rates of Antarctic and Greenland ice loss (source: NOAA, 2017, 22)

3.1.3.2. Climate projections for Edinburgh

Edinburgh's climate is expected to become warmer and drier in the summer and milder and wetter in the winter in the coming years [Met Office, 2018], leading to a similar climate as London South East. According to the UKCP18, Edinburgh will face sea-level rise (H[1]), increased flooding, and coastal erosion, as well as experiencing more severe weather conditions such as heavy rainfall during winter, spring, and autumn (M); and more frequent winter storms (L), disrupting business activity and causing damage to housing, city's public and commercial buildings, including Edinburgh's UNESCO World Heritage Site [City of Edinburgh Council, 2021a, 9; HES, 2019a]. Due to geographical specifics, proximity to the sea, topography and urban dynamics, some indicators differ from the average projections for Scotland. Under a future high-emissions scenario (RCP 8.5), by the 2050s[2], Edinburgh is predicted to experience [Met Office, 2018b]:

- An increase in mean annual temperature of between 0.3 °C to 3.2 °C
- A change in mean winter temperature of between 0.6 °C cooler and 3.9 °C warmer
- A change in the mean summer temperature of between 0.4 °C cooler and 4.2 °C warmer
- A change in mean winter precipitation of between -39% drier to 55% wetter
- A change in mean summer precipitation of between -56% drier and 43% wetter.

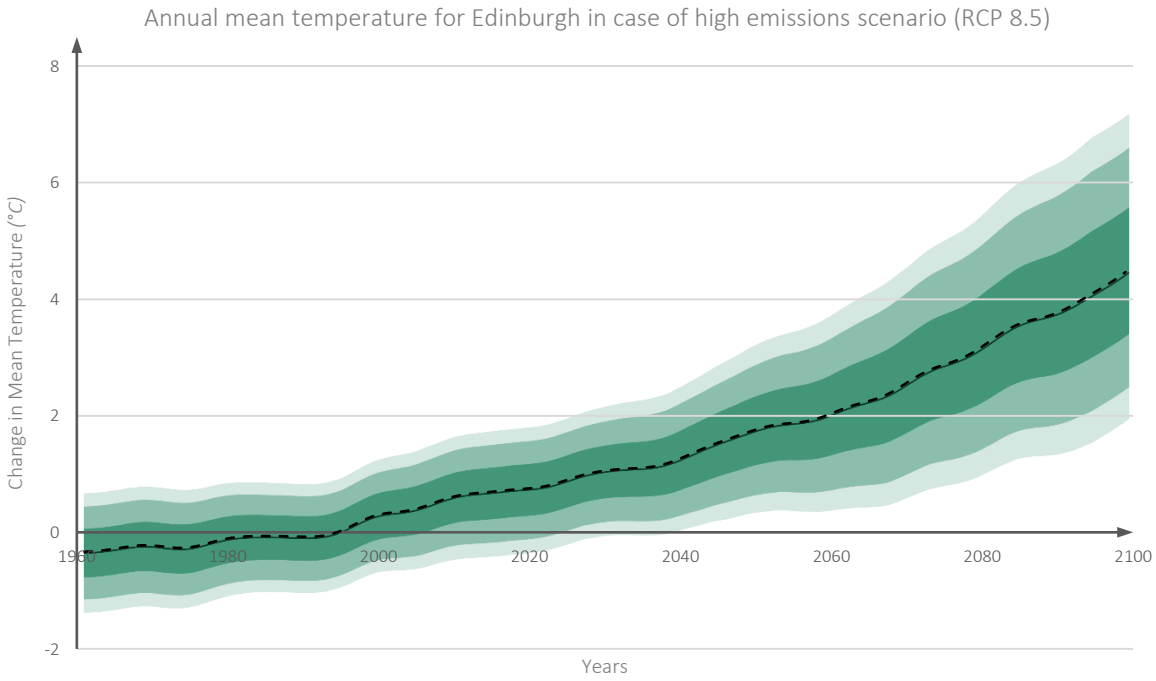

Graph 4 UKCP18 climate projections for the city of Edinburgh showing change in mean of annual temperature from 1961 to 2100. These are probabilistic projections: the dashed line is 50% central estimate; inner shading 25-75%; middle shading 10-90%; outer shading outer shading 5-95%. All values are compared to a 1981-2000 baseline average. (source: Met Office, 2018b; software: Excel)

[1] Probability of occurrence: High (H), Medium (M) and Low (L).

[2] The ranges given above are the 5th to 95th percentile ranges relative to a 1981 to 2000 baseline under a future high-emissions scenario and are specific to Edinburgh spatial dataset.

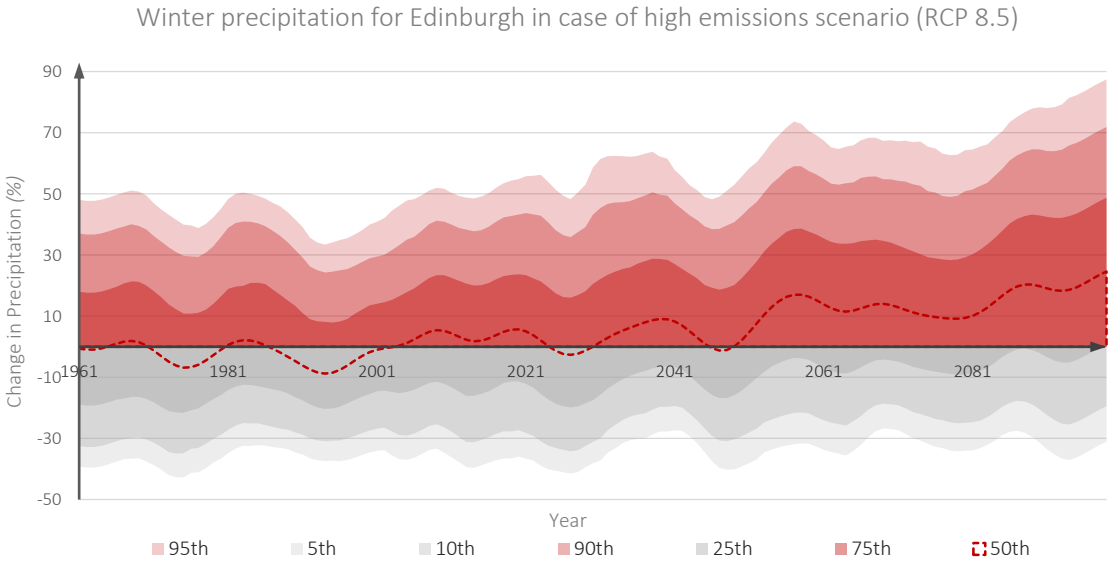

Graph 5 UKCP18 climate projections for the city of Edinburgh showing change in mean of winter precipitations from 1961 to 2100. These are probabilistic projections: the dashed line is 50% central estimate; inner shading 25-75%; middle shading 10-90%; outer shading 5-95%. All values are compared to a 1981-2000 baseline average. (source: Met Office, 2018; software: Excel)

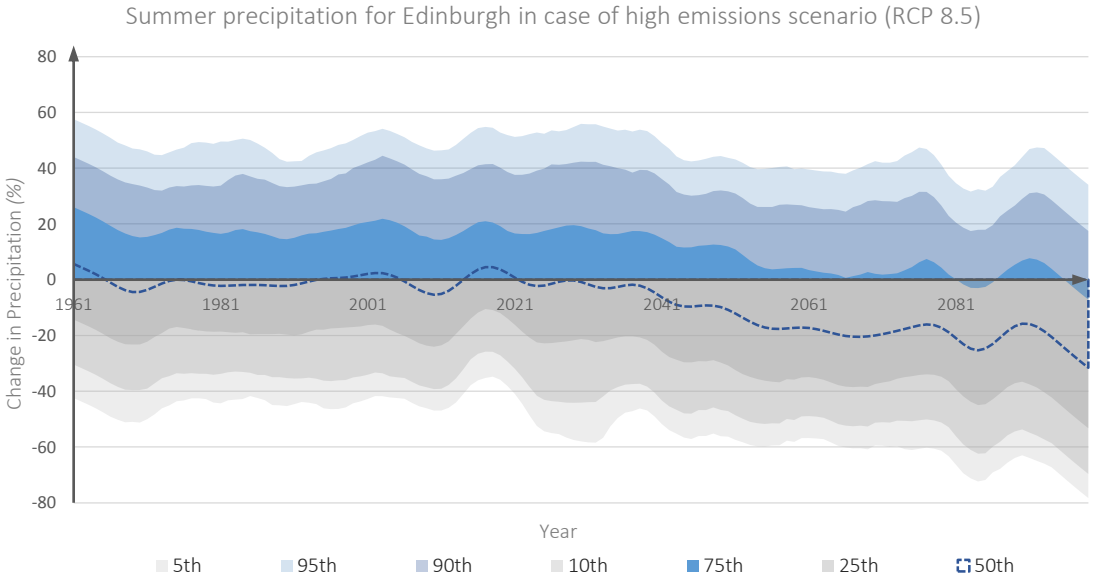

Graph 6 UKCP18 climate projections for the city of Edinburgh showing change in mean of summer precipitations from 1961 to 2100. These are probabilistic projections: the dashed line is 50% central estimate; inner shading 25-75%; middle shading 10-90%; outer shading 5-95%. All values are compared to a 1981-2000 baseline average. (source: Met Office, 2018; software: Excel)

Compared to South West Scotland, Edinburgh's projections regarding the mean and minimum sea-level rise values are lower but still considerable. Current projections for the Edinburgh coastline show that sea-level rise is predicted to be 0.09 m to 0.029 m by 2050, relative to the 1981 to 2000 baseline, and 0.3 m to 0.9 m by 2100, under a future high-emissions scenario (RCP 8.5). The ranges given above are the 5th to 95th percentile ranges for the Edinburgh coastline *(Graph 7).* There is currently uncertainty about changes in wind direction and strength, storm frequency and intensity, and wave energy; although when storms do occur, it is likely that their impact will be increased by other factors such as the sea-level rise and related changes in coastal dynamics [Met Office, 2018c, 11].

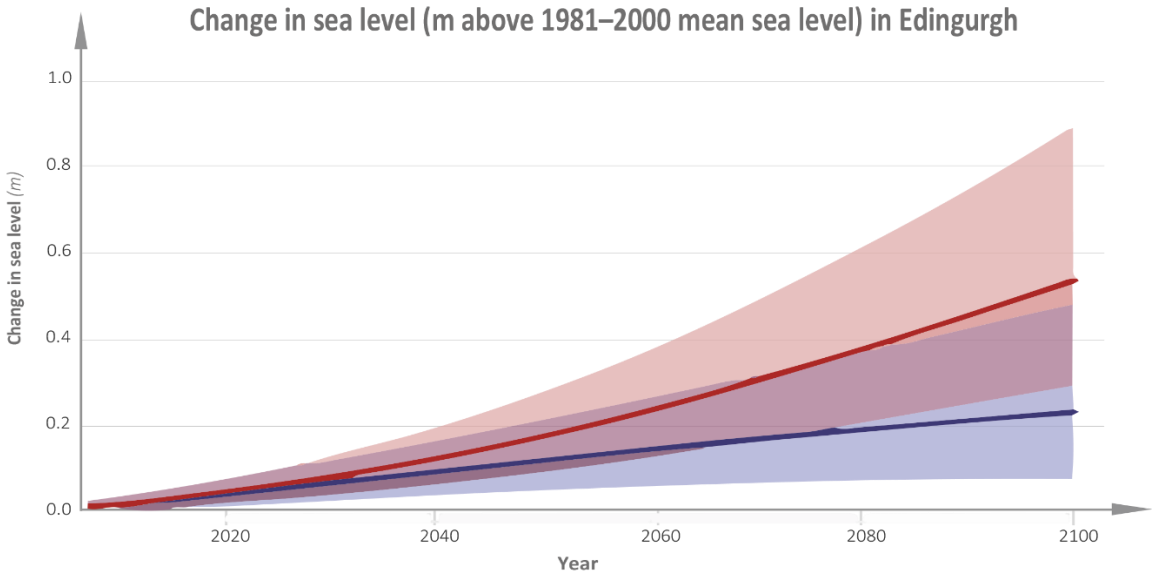

Graph 7 Change in sea level (m above 1981–2000 mean sea level) based on two scenarios: red – RCP 8.5/high emission and blue – RCP 2.6 low emission. (source: The Adaptation Scotland, 2021, 9)

3.2. Cultural Landscape of Edinburgh

3.2.1. World heritage Property

Edinburgh has been the Scottish capital since the 15th century, a status which has contributed to the significant cultural development of the city. "The Old and the New Towns of Edinburgh" was inscribed as a World Heritage property in 1995 by Decision CONF 203 VIII.C.1 [UNESCO, 1995], criteria (ii) and (iv). The asset is inscribed as a group of buildings, but with all its characteristics, the property is more complex. It has two different urban planning landscapes, medieval Old Town and neoclassical New Town, also constituting the property's name.

Figure 13 Aerial view of Edinburgh with the New Town in the foreground (source: HES, 2019b, 14)

Integrity – The two different urban planning landscapes provide a striking contrast in architecture and cityscape, representing two distinct periods of development, mediaeval and neoclassical, and encompassing a total surface area of 4.5 km^2 within the WH site. Over 75% of the building stock in this region has architectural or historical significance, laying the groundwork for evaluating the site's integrity. At the same time, the stunning urban landscape is defined by the combination of urban morphology and topography, which is punctuated by church spires, steeples, and monuments [ICOMOS, 1995]. However, the property's integrity is in jeopardy because it relies on the skyline's intelligibility [The City of Edinburgh Council *et al.*, 2016, 67]. The cumulative effect of a proposed development's mass, height, form, design, and materials could potentially harm the skyline and surrounding townscape, affecting landmark buildings, urban features, and the city's landscape setting, causing irreversible change and jeopardising the integrity of the city [HES, 2016].

Authenticity – The site still serves as Scotland's administrative and cultural capital, also remaining the core of the economic activities. Restoration projects have included high-quality workmanship to keep property's authenticity, but in the case of Edinburgh, material authenticity extends beyond building fabric to patterns of urban form and the qualities of urban areas [The City of Edinburgh Council *et al.*, 2016, 67]. Edinburgh's setting plays a crucial part with elements like the view out to Arthur's Seat or the Firth of Forth.

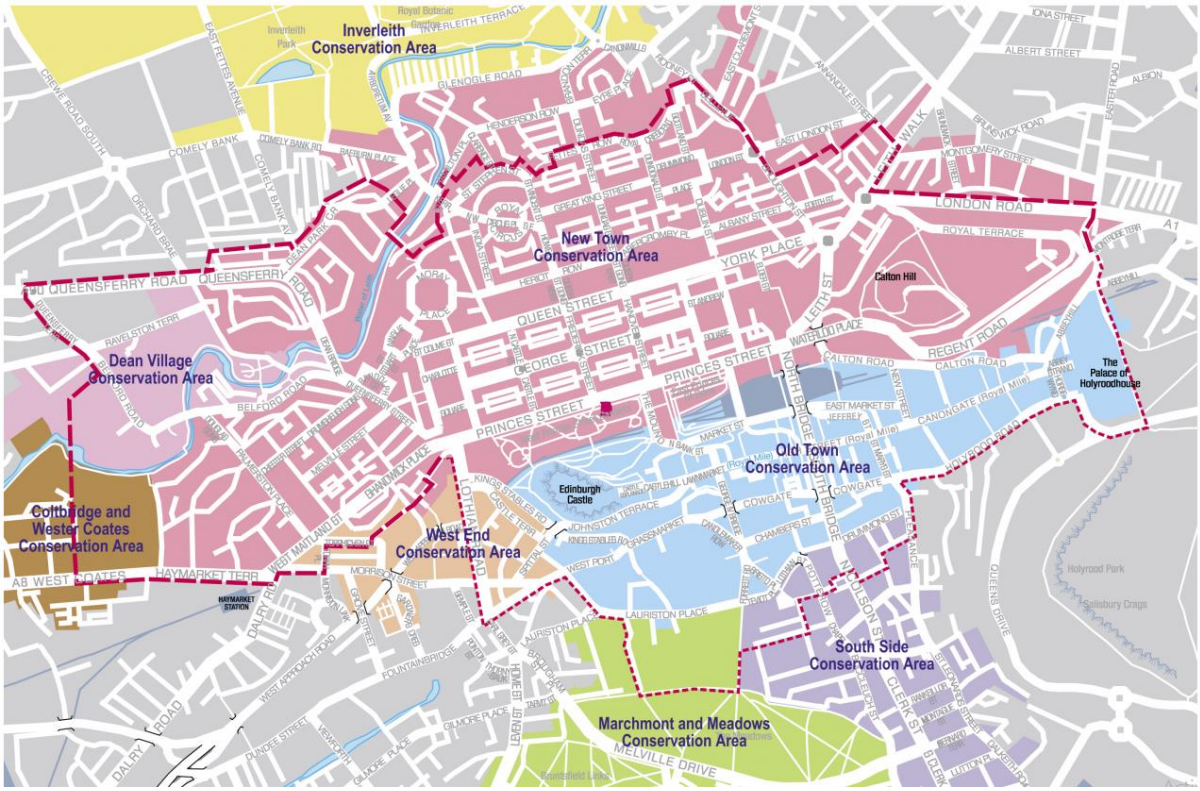

Figure 14 Map showing the boundaries of the World Heritage Site of Old and New Towns of Edinburgh and its conservation areas. (source: UNESCO – World Heritage Centre, 2005)

Table 3 Listed buildings and designated assets (source: The City of Edinburgh Council et al., 2016, 14)

	2005	2006	2007	2008	2011	2012	2013	2014	2015
A listed building[3]	656	864	656	656	655	655	654	653	654
B listed building[4]	863	864	863	863	864	863	864	867	865
C listed building[5]	157	156	157	157	157	156	157	156	156
Total for the World Heritage Site	**1676**	**1676**	**1676**	**1676**	**1676**	**1674**	**1675**	**1676**	**1675**

3.2.2. Management of World Heritage property

Management of the WHS is the site owner's responsibility, which includes private residents, businesses, institutions, and other user groups active in the city centre [The City of Edinburgh Council *et al.*, 2016,]. All the process is overseen by a Steering Group composed of representatives from Historic Environment Scotland (HES), the City of Edinburgh Council, and Edinburgh World Heritage, an independent charity focused on Edinburgh's World Heritage environmental dynamic. At the national level, the overall manager of the site is Department for Culture, Media & Sport (DCMS), complying with the World Heritage Convention. This Department does not play the role of the Scottish Government, as the responsibilities are not devolved, and the Scottish Government ensures DCMS meets the Convention. The lead public body for the historic environment, representative of the Scottish Governance, is Historic Environment Scotland (HES).

3.3. Urban development and climate adaptation actions

3.3.1. City planning

Urban dynamics put in constant pressure historic assets in many different ways [Dastgerdi and De Luca, 2019]. Due to human activities the WH property has been jeopardised many times. Recalling here the blaze of 2002 caused from a night club which damaged seriously a part of the Old Town, Cowgate part [ICOMOS, 2003]. The revitalisation process to recover from these damages was long and there have been examples when ICOMOS and UNESCO have expressed disapproval on the development of areas inside the WHO property such as development of the Caltongate, Haymarket, Leith Docks site as the project did not respect the historic landscape of WHO property [UNESCO, 2008].

"*The Old and New Towns of Edinburgh World Heritage Site: Management Plan 2017–2022*" [2016] establishes long-term goals and short-term activities for the development and conservation of WH property, as well as a framework for the state of the built environment.

[3] Buildings of national or international importance, either architectural or historic, or fine little altered examples of some particular period or style [Scottish Borders Council, 2022]

[4] Buildings of regional or more than local importance, or major examples of some particular period, style or building type which may have been altered [Scottish Borders Council 2022]

[5] Buildings of local importance, lesser examples of any period, style or building type, as originally constructed or moderately altered; and simple traditional buildings which group well with others in Categories A and B [Scottish Borders Council 2022]

This document is taken into consideration during the planning process. One of the tools developed to protect is heritage assets and preserve its authenticity and evaluating future development is the "*Guidance on the Protection of Key Views"* and the policy on tall buildings included since in the Local Plan in 2010. These concepts have been also included in "*Edinburgh Design Guidance*" [2020] which determined design requirements for interventions inside WH property. One of the key challenges affecting the WH property is the management of tourism, especially the concentration and volume of visitors on the Royal Mile [The City of Edinburgh Council *et al.*, 2016, 41]. In 2020, a study compiled by the Electronic System for Travel Authorization (ESTA) based on UN population numbers and UK visitor statistics for the case of the UK revealed that Edinburgh has the world's fourth-highest tourist-to-local ratio, welcoming 445 visitors for every 100 residents, trailing only Miami, Las Vegas, and Dubai [Matchett, 2020]. These figures show that tourists should be an essential part of the proposed solution to improve their experience while visiting the cultural assets in the city of Edinburgh.

Table 4 Proportion of visitors to Edinburgh by season in 2019 (source: Edinburgh by Numbers, 2021, 69)

Period	Overseas visitors	Domestic visitors
Jan-Mar	289,000	583,900
Apr-Jun	594,000	648,000
Jul-Sept	804,000	829,800
Oct-Dec	520,000	635,500

Table 5 Comparison of visitors to Edinburgh by season in 2019 (source: Edinburgh by Numbers, 2021, 70)

Period	Overseas visitors 2013	Domestic visitors	Difference 2013–019 (%)
Jan-Mar	136,000	289,000	113%
Apr-Jun	374,000	594,000	59%
Jul-Sept	568,000	804,000	42%
Oct-Dec	214,000	520,000	143%

3.3.2. Climate strategy and Adaptation plan

During the years Edinburgh have had different tools to tackle climate change. In 2012, the City of Edinburgh Council and three other cities in Scotland prepared the Local Climate Impacts Profile (LCLIP), assessing the impacts of climate change and extreme weather events on the delivery of local authority services [The City of Edinburgh Council, 2013b].

Table 6 Main actions undertaken in LCLIP 2012 (source: The City of Edinburgh, 2013b)

emergency planning	building control	transport infrastructure and fleet services
waste collection and disposal	estates management	provision and management of leisure facilities and open spaces
strategic and land-use planning	events management	protection and management of biodiversity and greenspaces

The Adaptation Action Plan for 2016 - 2020 [The City of Edinburgh Council, 2016] included some initiatives regarding the five main sector of Governance, Natural Environment and Green Spaces, Build Environment and Infrastructure, Flood prevention, Society and Economy, to capture the entire city of Edinburgh approach to adaptation towards climate change. As 2021 saw world leaders gathering in Scotland for the 26th Conference of Parties (COP26) to agree on actions to limit global temperature rise. Following up on the target set, one of the 12 actions recommended to the Scottish Government by the Climate Emergency Response Group [2021] was alignment with adaptation plans to ensure the choice and design of projects will help adapt to climate impacts in the future. The 2030 Climate Strategy, although aims adapting the city to be resilient to climate change [The City of Edinburgh Council, 2021a, 4], the actions are more towards energy emissions and consumption, to achieve a net zero emission target, which brings the interventions in the cultural sector at building scale, rather than adaption solutions in urban scale.

3.4. Study case at neighbourhood scale

The site selected for the evaluation of the UHI at local scale is part of the New Town WH property. It consists of 8 blocks arranged in a symmetrical grid within an area of 350 meters and 800 m (*Figure 15*). On both west and east, the site is bordered by open green space, Charlotte Square Private Garden and St. Andrew Square Garden. Meanwhile, in the north and south, the area is bordered by the Queen Street Gardens Edinburgh and the Princes Street Gardens plus the Historic Train Station.

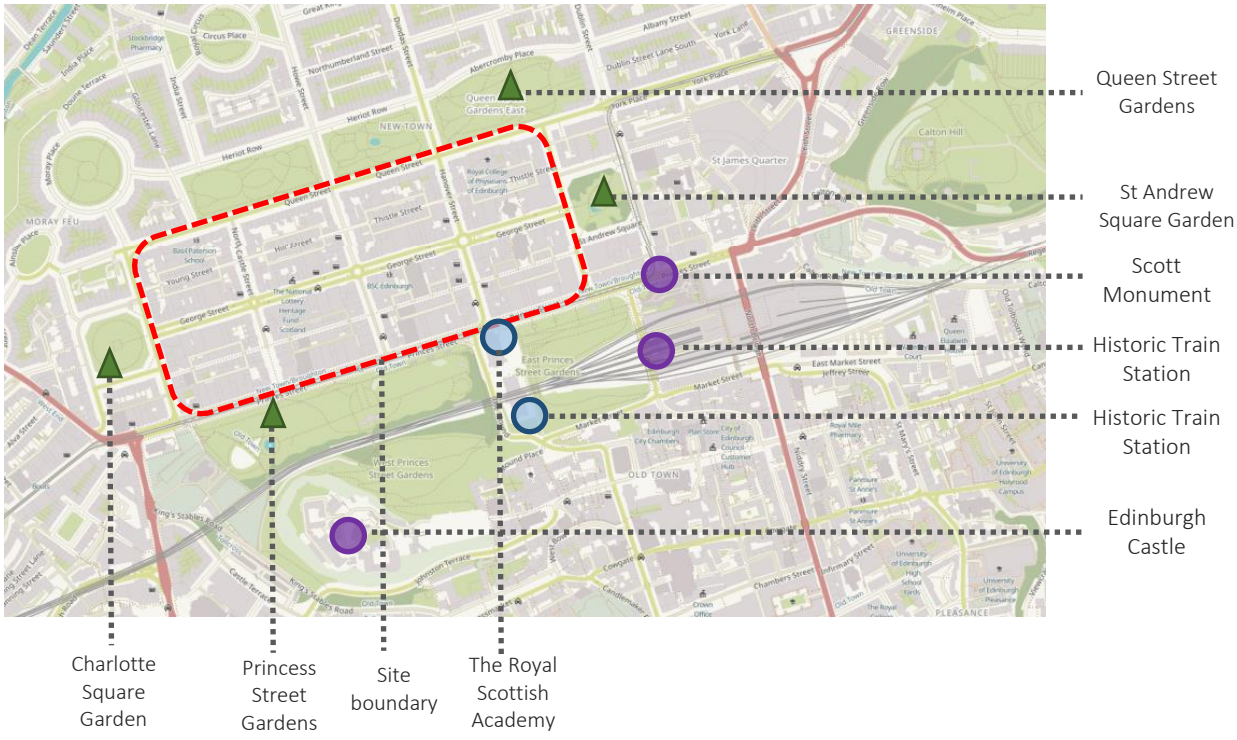

Figure 15 Location of neighbourhood scale site (source: Own elaboration, 2022, Background: Open Street Map, 2022)

The biggest issue at the historic site is that during regular hours, traffic can get quite congested with motorists looking for on-street parking spaces. Other problems relate to the degradation of the area, mainly the pavement surfaces. The site is very frequented by tourists

and also locals, due to the presence of retail shops, bars and restaurants. There are several development projects planned to occur in the following years in the area, derived from different policies such as: City Centre Transformation [JACOBS and the City of Edinburgh Council, 2019] planned to start construction in 2024, City Plan 2030 [The City of Edinburgh Council, 2021b], City Mobility Plan 2021-2030 [The City of Edinburgh Council, 2021c], Public and Accessible Transport Action Plan 2013 – 2020 [The City of Edinburgh Council, 2013b], etc. "George Street and First New Town Public Realm Improvements" [The City of Edinburgh Council *et al.*, 2021], proposes the first renewal project for the area since its construction, where the main vision is creating a walkable space through:

- adaptable and landscaped areas with seating,
- space for play and opportunities for events;
- space for outdoor seating for cafes and restaurants;
- better lighting to animate the streets after dark;
- level access crossings at street junctions for unimpeded crossing;
- disabled parking bays on George Street and interconnected streets (*Annex 3*).

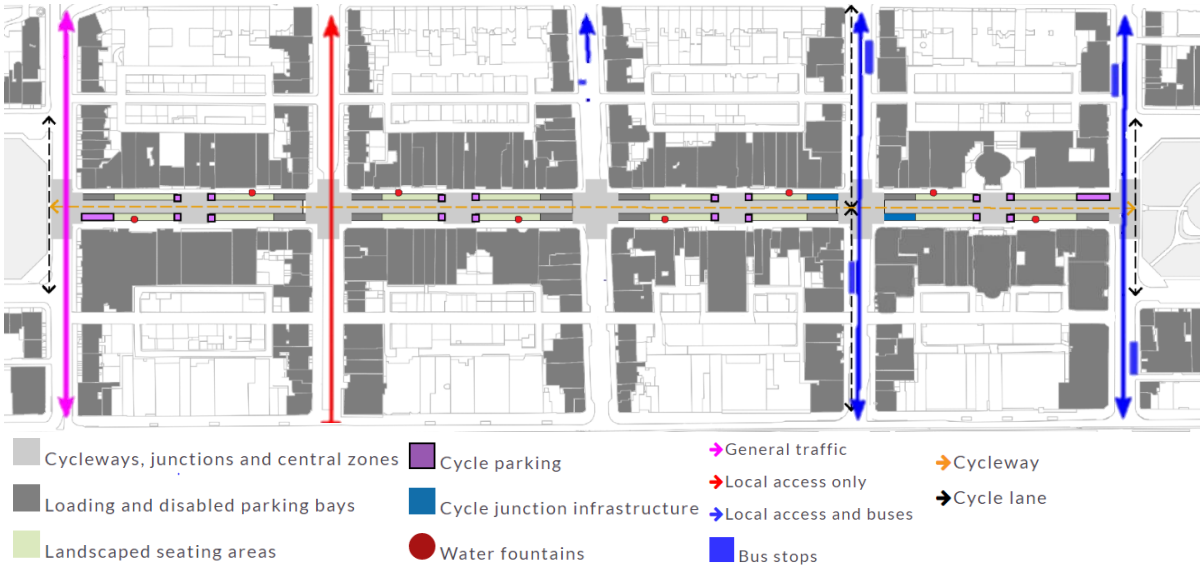

Figure 16 Traffic and cycling lanes (source: The City of Edinburgh Council *et al.*, 2021)

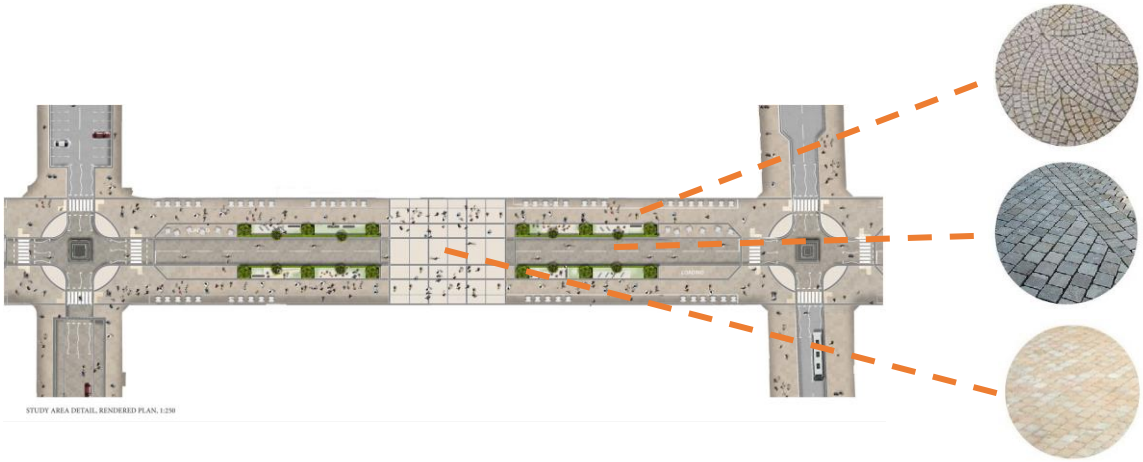

Figure 17 Materials renders for one section of George Street (source: The City of Edinburgh Council *et al.*, 2021)

CHAPTER 4: METHODOLOGY

Each of the goals outlined in Chapter 1's methodology is presented in this chapter. A multidisciplinary approach was used for the city of Edinburgh and the WH property to complete a thorough investigation of the cultural heritage assets connected to climate change, UHI, and outdoor thermal comfort.

4.1. Research Framework

In order to construct and analyse the UHI and outdoor thermal comfort issue in the context of Edinburgh's cultural assets, a multi-approach methodology was adopted, considering various approaches and data sources. Three main sections compose this dissertation are:

- The first section consists of a literature review of the effects of UHI detected in Edinburgh and potential impacts on cultural heritage assets facing climate change and urban sprawl threats
- The second section includes the LCZ map able to capture historic towns' heterogeneity and UHI's magnitude
- The third section estimates the outdoor thermal comfort as a tourist destination in New Town, part of WH property, through a comparison between PET and thermal sensations, based on ENVI-met® simulation and literature review.

The full methodology followed for each of the above sections is detailed in this chapter.

4.1.1. Research philosophy

The Research onion developed by Saunders *et al.* [2018] was followed at the beginning of the study to facilitate the entire process and develop a practical methodology to achieve the objectives. Overall the study combines positivism and interpretivism because of the multidisciplinary methodology adopted. According to Patel [2015], the positivist component of knowledge is created by empirical research, such as traverse studies and weather observation. Interpretivism was required to highlight the social and cultural impacts of the study area as a touristic destination [Crossley and Jansen, 2021; Zala, 2020].

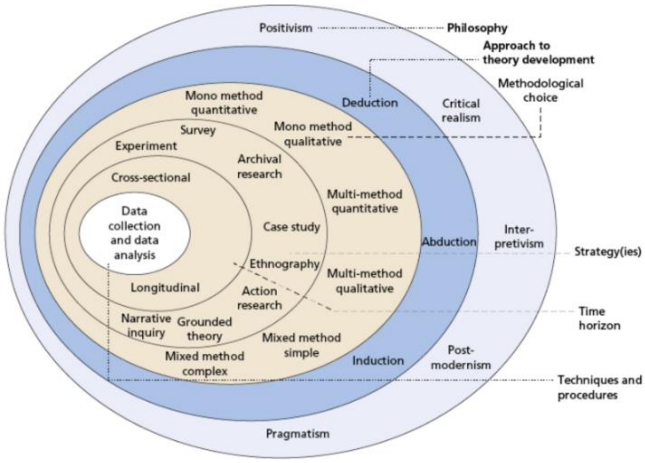

Figure 18 Research onion (source: Saunders et al. 2019)

4.1.2. Research approach

The literature study that precedes this thesis's main deductive argument identifies the analysis and theories created for other sectors and can be applied to the case of cultural resources. However, the study can generate fresh insights that adhere to an inductive method thanks to the gap research discovered in the context of cultural heritage and specifically to the city in question [DeCarlo, 2018]. This combination of methodologies may better suit the nature of the work. This combination of approaches is also reflected in the mixed method conducted during each section by combining qualitative and quantitative methods.

4.1.3. Research strategy

The fundamentals of each analysis of cultural heritage are based on literature review, as the past conditions and evaluations through time are essential to preserving their authenticity and integrity. Therefore, thorough research on official documents and reports was conducted to analyse the specifics of the case, the state of conservation and risks from a long perspective. The literature review also allowed the review of publications, recommendations and guidelines to foresee relevant steps in the case of Edinburgh.

The analysis starts with spatial analysis a city scale, but with a focus in the culture heritage assets to define the relationship between morphological parameters and potential threads. The strategy continued in focusing in a smaller case study and mainly on quantitative data such as traverse field study, meteorological data records and computer-based simulations.

LCZ present the UHI magnitude at the actual state of the city even though the dataset used come were produced at different period, while the outdoor thermal comfort is evaluated for the worst condition (hottest) day during the touristic season in Edinburgh in the last section.

4.1.4. Data collection and analysis

Given that the final products require various sorts of inputs, the data gathering procedures for each section were unique. While mainly the geospatial data for LCZ was required to estimate the morphological characteristics, the data required for the traverse investigation was gathered in-situ. The datasets come from a variety of sources, including articles, books, images, geographical data, census data, and transversal surveys. A thorough summary in tabular style is provided for each part. In order to aid the research and provide a larger volume that could be examined, secondary data were provided.

Each task was completed using different software, depending on the best fit for the process. In the case of LCZ, even though the map was created using the GIS approach, apart from Arc-GIS Pro, different extensions and plug-ins such as UMEP and ADMS-Urban were needed for complex parameter calculations. With the help of ENVI-met® software (version 5.0.3), the microclimate and outdoor thermal conditions were measured for the neighbourhood scale and compared with potential interventions.

4.2. Local Climate Zoning

The primary method will mainly be ArcGIS-based, specifically ArcGIS Pro 2.8 software, as the GIS approach allows more diversity in implementing the LCZ scheme, allowing fully supervised classification, in contrast to the RS approach, which WUDAPT does not allow. An essential step in the GIS approach is the definition of morphological parameters [Quan and Bansal, 2021], which will determine the method of discretization of the data and influence the final results. Between the five different definitions used: lot area polygon, urban block, regular grid, neighbourhood and sensor unit area, this study uses the regular grid. The different historic urban layers of the City of Edinburgh [Rowland et al., 2020, 36] make LCZ's actual scheme not efficient in covering the heterogeneity of the city [Wicki and Parlow, 2017]. Therefore, in contrast to the classical scheme based on a grid of 300 m size, the LCZ mapping and calculations of morphological parameters will be based on a much smaller grid, 15m grid cell size. Sky View Factor will be estimated through QGIS 3.24 with Urban Multiscale Environmental Predictor (UMEP) extension. *Table 7* shows each morphological parameter's definition, and the entire workflow of the whole steps of LCZ mapping is summarized in *Figure 19*.

Table 7 Morphological parameters definitions

Parameter	Definition
Mean Height of roughness elements	The geometric mean of building heights for LCZs 1–10 and the tree/plant heights for LCZs A–G [Steward and Oke, 2012; Quan and Bansal, 2021].
Building surface fraction (BSF)	The total area of building footprint divided by the area of the selected zone [Steward and Oke, 2012; Abougendia *et al.,* 2020].
Sky view factor (SVF)	Ratio of the amount of sky hemisphere visible from ground level to that of an unobstructed hemisphere [Steward and Oke, 2012].
Pervious surface fraction (PSF)	Combination of all land covers of vegetation, waterbody and bare soil [Steward and Oke, 2012]. PSF is calculated as the total coverage area divided by the zone area from the selected samples.
Impervious surface fraction (ISF)	The impervious surface fraction is defined as the fraction of paved areas on the ground area [Steward and Oke, 2012]. ISF is estimated in indirect area through the formula: ISF = 1 (BSF+PSF) [Abougendia *et al.,* 2020]
Aspect ratio (H/W)	Aspect ratio is defined as the street canyon H/W ratio for LCZs 1–7, the building height–spacing ratio for LCZs 8–10, and the tree height–spacing ratio for LCZs A–G [Quan and Bansal, 2021] Consecutively, the aspect ratio of the street canyon (H/W) is calculated by two sides of the street canyon by the following equation: H/W = (Hr/W + Hl/W) / 2 where Hr/W is the aspect ratio of the right side of the street, and Hl/W is the aspect ratio of the left side of the street [Abougendia *et al.,* 2020]

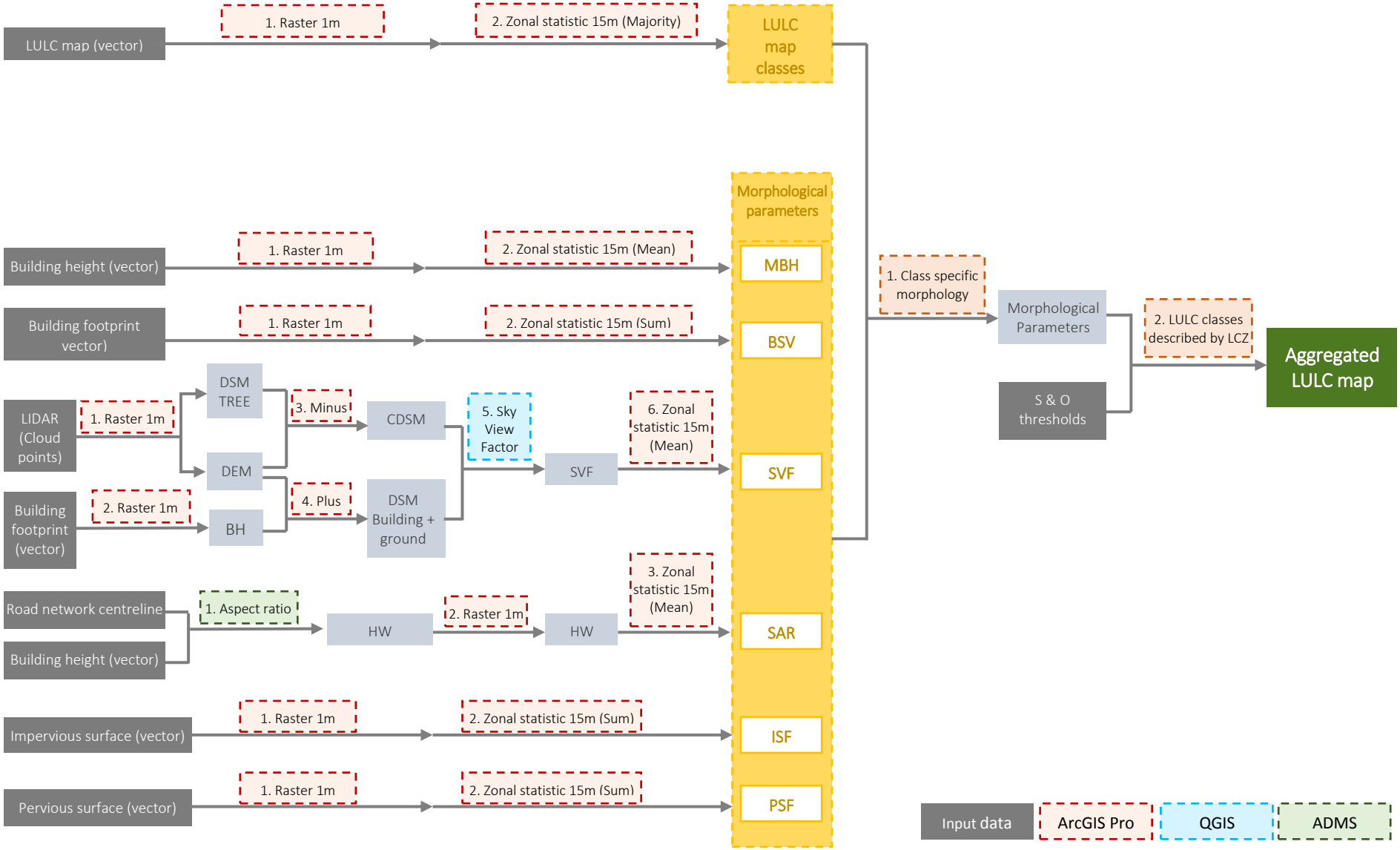

Figure 19 The general framework for creating LCZ of the City of Edinburgh (source: Own elaboration, 2022)

4.2.1. Data

For this section, the data used came from two primary sources. Due to limited time, Edinburgh's Land use / Land cover map (LULC) was retrieved from Urban Atlas for the reference year of 2018 and revised in 2020, with an accuracy of 90.7% for urban classes and 82.8% for rural classes [Copernicus Land Monitoring Service at the European Environment Agency, 2018]. The map covers the entire city and FUA (cities and their commuting zones), leaving no area of the City of Edinburgh without classification. The total number of classes is 25 (*Figure 20 and Table 8*), showing the city's heterogeneity. Each land use class are described and coded to facilitate data usage (*Annex 4).*

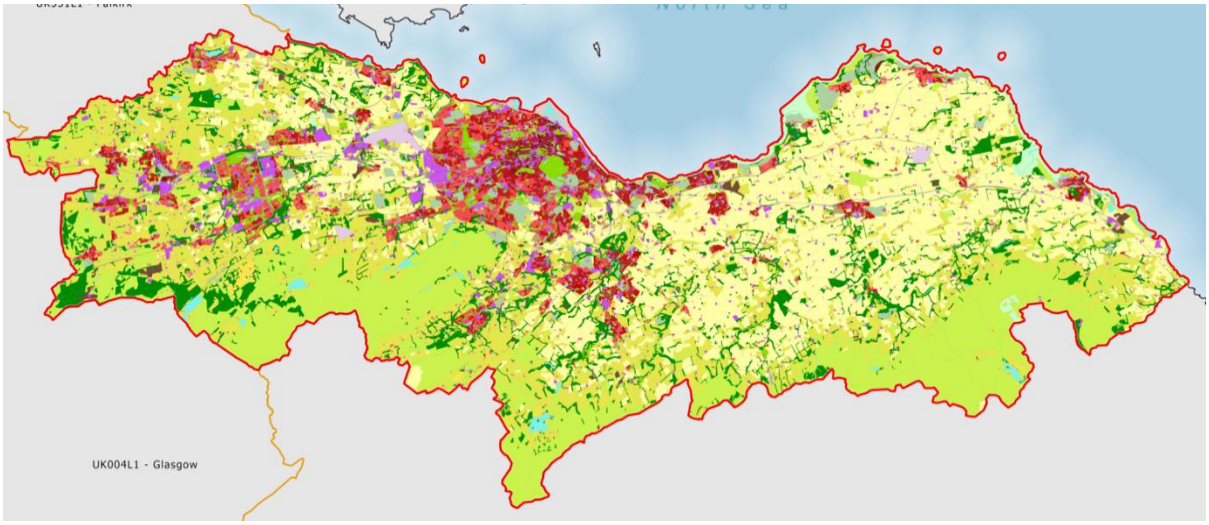

Figure 20 Edinburgh's Land use / Land cover map (LULC) (source: Copernicus Land Monitoring Service at the European Environment Agency, 2018)

Table 8 Land use classes (source: Copernicus Land Monitoring Service at the European Environment Agency, 2018)

Green urban areas	Pastures	Arable land (annual crops)	Other roads and associated land
Construction sites	Forests	Railways and associated land	Sports and leisure facilities
Isolated structures	Water	Mineral extraction and dump sites	Continuous urban fabric (S.L.: > 80%)
Port areas	Wetlands	Discontinuous medium density urban fabric (S.L.: 30% -50%)	Discontinuous dense urban fabric (S.L.: 50% - 80%)
Land without current use	Airports	Discontinuous low-density urban fabric (S.L.: 10% -30%)	Complex and mixed cultivation patterns
Fast transit roads and associated land		Discontinuous very low-density urban fabric (S.L.: < 10%)	Industrial, commercial, public, military and private units
		Herbaceous vegetation associations (natural grassland, moors...)	Open spaces with little or no vegetation (beaches, dunes, bare rocks, glaciers)

The morphological parameters; mean building height (MBH), building surface fraction (BSF), sky view factor (SVF), street aspect ratio (SAR), the impervious surface fraction (ISF) and the pervious surface fraction (PSF); were estimated by rasterizing the LIDAR data, including point cloud and DSM, DTM at a resolution of 50 cm, provided by Scottish Remote Sensing Portal (governmental portal). The building footprint and height were collected from polygons provided by Edina Digimap, Verisk Service. *Table 9* shows in detail all the data used and the sources.

Table 9 Data and sources used for accessing LCZ of Edinburgh (source: Own elaboration, 2022)

Layer	Format	Version	Data Acquired	Details	Source
Edinburgh city boundary-line	Vector	May 2022	1 July 2022	Scale 1:10000	EDINA Digimap, Ordnance Survey Service, <https://digimap.edina.ac.uk>
Edinburgh LULC	Vector	(2018) Revised 2020	1 July 2022	Urban classes accuracy – 90.2%	Copernicus Land Monitoring Service at the European Environment Agency, <https://land.copernicus.eu/local/urban-atlas/urban-atlas-2018/fetch-land-file?hash=1b53c0f7c9b9db08842bc6c8e68f4979d00f85f2>
LIDAR points	Cloud point (laz)	Phase 5	1 July 2022	Scale 1:1000 Grid Size: 1 km by 1 km tiles	EDINA Digimap, Lidar Scotland Service, <https://digimap.edina.ac.uk>
Building	Vector	March 2022	1 July 2022	Scale 1:5000	EDINA Verisk Digimap Service, <https://digimap.edina.ac.uk>
Digital Elevation Model (DEM)	Raster	2010	4 July 2022	90m	https://datashare.ed.ac.uk/handle/10283/2578?show=full
Digital Surface Model (DSM)	Raster	Phase 5	1 July 2022	Scale 1:2000 Resolution: 50cm Grid Size: 5 km by 5 km tiles	EDINA Digimap, Lidar Scotland Service, <https://digimap.edina.ac.uk>
Digital Terrain Model (DTM)	Raster	Phase 5	1 July 2022	Scale 1:2000 Resolution: 50cm Grid Size: 5 km by 5 km tiles	EDINA Digimap, Lidar Scotland Service, <https://digimap.edina.ac.uk>

4.2.2. Morphological Parameters

Mean building is computed in ArcGIS Pro using the vector data from Verisk service, which contains information only for buildings and is rasterized to 1-m cell and as cell value the height of the building. Then the average height is calculated on a 15m grid. The same vector data is used to calculate the building surface fraction, but in the case, while rasterizing to a 1-m cell, the value is 1, representing a surface of $1m^2$. Then the sum surface is calculated on a 15m grid and divided by the cell's surface (15m x15m).

The sky view factor (SVF) is calculated based on Lindberg *et al.* [2015] approach, with the urban multiscale environmental predictor (UMEP), an extension of QGIS. The vegetation data were retrieved from the LIDAR cloud point data and checked the accuracy of urban trees with the open data provided by the City of Edinburgh. As the software has some limitations in the number of pixels computing at one time, the Digital Surface Model of Building and

Ground (DSM building + ground) and Canopy Digital Surface Model (CDSM) were resampled to 4m and were divided into eight tiles. After the calculations of each tile, they were merged into one in ArcGIS Pro. The values of the roof and the vegetation pixels were masked to obtain the ground-level sky view factor product [Wicki and Parlow, 2017], and then the average SVF was calculated on a 15m grid.

Due to limited time and the heterogeneity of the City of Edinburgh [Rowland et al., 2020, 36], the street aspect ratio was estimated by first calculating the left and right average width of roads and their respective height in ArcMap with the Street Canyon tool. Then for each side, the respective buildings' height was divided by the width, added and divided by 2. In the case of LCZs A–G, the average tree height–spacing ratio is required to be estimated, but due to the lack of data, could not be estimated. Pervious surface fraction (PSF) was calculated using vector data containing the surface coverage information. The categories considered as non-sealed surfaces are shown in *Table 10*. The data was rasterized to 1-m cell, with a value of 1, representing a surface of $1m^2$. Then the sum surface is calculated on a 15m grid and divided by the surface of the cell (15m x15m). Impervious surface fraction (ISF) was calculated in the indirect method with the formula:

$$ISF = 1\ (BSF+PSF) \quad (1)$$

Table 10 Classes used for PSF estimation (source: Own elaboration, 2022)

Classes included for PSF			
Green urban areas	Pastures	Water	Forests
Herbaceous vegetation associations (natural grassland, moors…)	Open spaces with little or no vegetation (beaches, dunes, bare rocks, glaciers)	Land without current use	Complex and mixed cultivation patterns
Wetlands	Arable land (annual crops)		

4.2.3. Combination of Land Use / Land Cover and Morphological Parameters

LCZ have specific morphological characteristics, which parameters value can be summarised in corresponding thresholds. With the combination of the morphological behaviour with each of the LULC classes, each of these land cover classifications can be affiliated to each LZC using the defined LCZ thresholds by Steward and Oke [2012] (*Table 11*). The aggregation between LULC and morphological parameters and combination with LCZ was computed within a 15m resolution.

For this study, first, the Modified Standard rule-based classifier is adopted to assign each LCZ class. The clustering process was conducted through ArcGIS PRO software. As the calculated morphological parameters can define only from LCZ 1 to 8, the Standard rule-based classifier based on equation *(2)* and LCZ 8 to 10 based on equation *(3).* In equation (3) the parameter of SAR is omitted, as it does not represent the building – space aspect ratio. The classification of land cover cases LCZ A to G was made based on the land use/cover class and similar studies [Sigler, 2022], just as a conceptual reference. In this case, the morphological parameter values will be the mean value within the LULC class. If the criteria are not fulfilled for all the parameters, then the assignment will be based on the following highest number of best fit.

If ([MBH] > a and [BSF] >b and [ISF] >c and [PSF] > d and [SVF] > e and [SAR] > f)
Then Classify = "LCZ x" *(2)*

where: a, b, c, d, e, f - value ranges from *Table 11* and x LCZ class from 1 to 7

If ([MBH] > a and [BSF] >b and [ISF] >c and [PSF] > d and [SVF] > e)
Then Classify = "LCZ y" *(3)*

where: a, b, c, d, e, f - value ranges from *Table 11* and y LCZ class from 8 to 10

Table 11 LCZ morphological parameters thresholds by Stewart and Oke [2012] and the criteria of terrain roughness class criteria omitted

Local climate zone	Sky View factor [a]	Mean Building height [b]	Building Surface Fraction [c]	Aspect Ratio [d]	Impervious Surface Fraction [e]	Pervious Surface Fraction [f]
LCZ 1	0.2 to 0.4	> 25	40 to 60	> 2	40 to 60	< 10
LCZ 2	0.3 to 0.6	10 to 25	40 to 70	0.75 to 2	30 to 50	< 20
LCZ 3	0.2 to 0.6	3 to 10	40 to 60	0.75 to 1.5	20 to 50	< 30
LCZ 4	0.5 to 0.7	> 25	20 to 40	0.75 to 1.25	30 to 40	30 to 40
LCZ 5	0.5 to 0.8	10 to 25	20 to 40	0.3 to 0.75	30 to 50	20 to 40
LCZ 6	0.6 to 0.9	1 to 10	20 to 40	0.3 to 0.75	20 to 50	30 to 60
LCZ 7	0.2 to 0.5	2 to 4	60 to 90	1 to 2	< 20	< 30
LCZ 8	> 0.7	3 to 10	30 to 50	0.1 to 0.3	40 to 50	< 20
LCZ 9	> 0.8	3 to 10	10 to 20	0.1 to 0.25	< 20	60 to 80
LCZ 10	0.6 to 0.9	5 to 15	20 to 30	0.2 to 0.5	20 to 40	40 to 50
LCZ A	< 0.4	3 to 30	< 10	> 1	< 10	> 90
LCZ B	0.5 to 0.8	3 to 15	< 10	0.25 to 0.75	< 10	> 90
LCZ C	0.7 to 0.9	< 2	< 10	0.25 to 1	< 10	> 90
LCZ D	> 0.9	< 1	< 10	< 0.1	< 10	> 90
LCZ E	> 0.9	< 0.25	> 90	< 0.1	< 10	< 10
LCZ F	> 0.9	< 0.25	< 10	< 0.1	< 10	> 90
LCZ G	> 0.9	-	< 10	< 0.1	< 10	> 90

a - Ratio of the amount of sky hemisphere visible from ground level to that of an unobstructed hemisphere
b - Geometric average of building heights (LCZs 1-10) and tree / plant height (LCZs A-F) *m*
c - Ratio of building plan area to total plan area *%*
d - Mean height – to width ratio of street canyons (LCZs 1-7), building spacing (LCZs 8-10), and tree spacing (LCZs A-G)
e - Ratio of impervious plan area (paved, rock) to total plan area *%*
f – Ratio of pervious plan area (bare soil, vegetation, water) to total plan are *%*

4.3. Traverse survey and ENVI-met® model

The data used to simulate the thermal comfort parameters in the study case site was derived from field data measurements and other open sources. *Table 12* summarises all data sources for each specific parameter used. The field measurements were conducted in two days (*Table 13*) and will help understand the spatial distribution of air temperature during summertime conditions in the case of pedestrians and calibrate/validate the numerical model in the ENVI-met® software. The detailed framework for the site simulation is shown in *Figure 21*. Due to the size of the site, the observation time from the first point to the last is not synchronous, so the comparison to find the hottest point was made after temporal correcting them through linear regression. The air parameters were collected trying to avoid the UHI effect, so it came through the fixed station near Edinburgh Castle and Bannerman Way Weather Station, located at a higher altitude from the build-up area (*Figure 22*).

Table 12 Data and sources used for simulation in ENVI-met® (source: Own elaboration, 2022)

Layer	Format	Version	Data Acquired	Details	Source
Listed building	Vector	26 April 2022	3 July 2022	Building material	https://data.edinburghcouncilmaps.info/datasets/cityofedinburgh::listed-buildings/explore
Building	Vector	March 2022	1 July 2022	Building height	EDINA Verisk Digimap Service, <https://digimap.edina.ac.uk>
Tree	Vector	25 May 2021	3 July 2022	Vegetation	https://data.edinburghcouncilmaps.info/datasets/trees/explore
Meteorological data for model calibration	xlsx	2010	4 July 2022		https://datashare.ed.ac.uk/handle/10283/2578?show=full
Meteorological data in extreme weather conditions	cvs	18 July 2022	19 July 2022	Bannerman Way Weather Station	https://www.wunderground.com/dashboard/pws/IEDINB59/table/2022-07-18/2022-07-18/daily
Road surface parameters	Vector	3 May 2022	3 July 2022		https://data.edinburghcouncilmaps.info/datasets/adopted-roads-1/explore

Table 13 Dates of field data collection (source: Own elaboration, 2022)

Date	Day of week
7 July 2022	Thursday
9 July 2022	Saturday

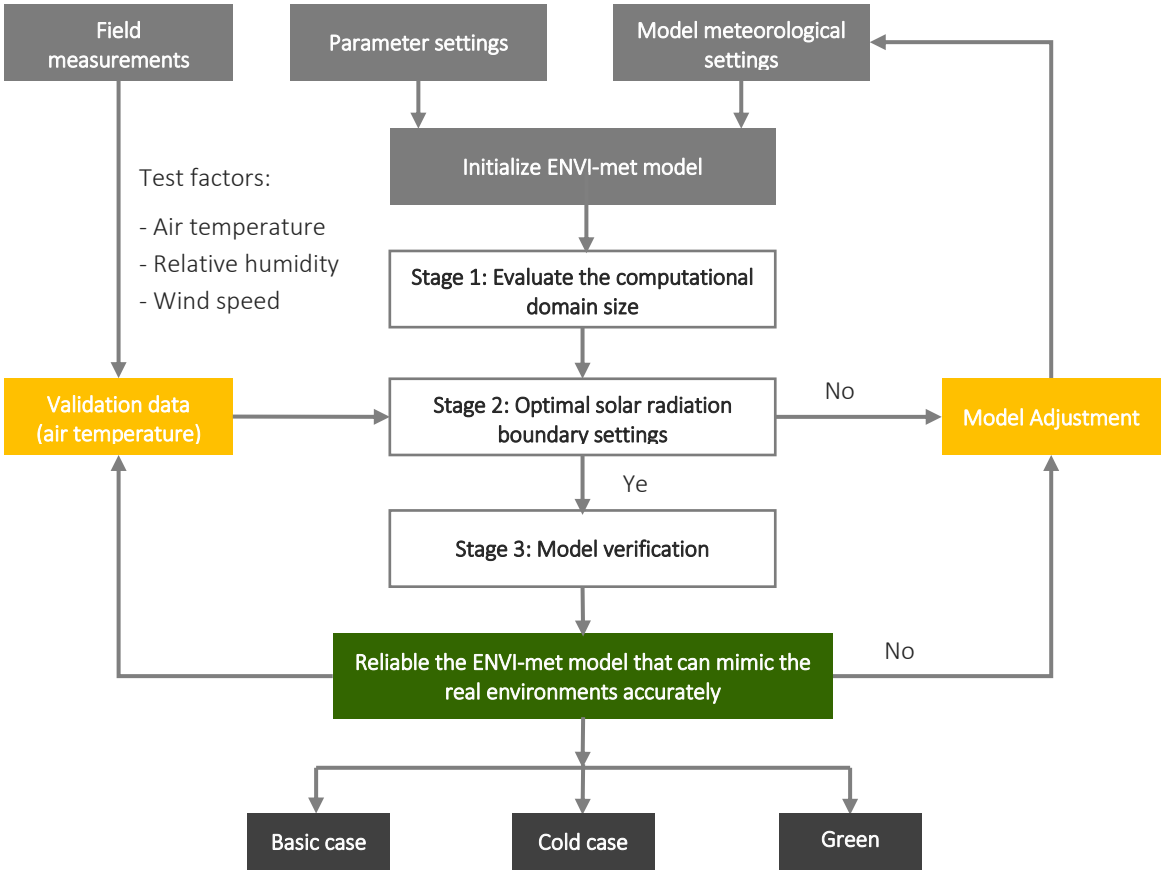

Figure 21 Detailed methodology for the simulation part (source: Own elaboration)

Figure 22 Location of site for the traverse survey, fixed and meteorological station (source: Own elaboration, 2022, Background: Open Street Map, 2022)

4.3.1. Filed data collection and method

Field measurements were carried out around the site boundary following a route of 2.2 km, measuring 19 points with different characteristics (*Figure 23*). For each point of the site, the parameters of temperature, relative humidity, wind direction and wind speed were collected

with the instruments shown in *Table 14*. The Tiny Tag TGP-4020 was covered with an aluminium foil funnel to avoid direct solar radiation (*Figure 24*) and ensured to capture the parameters 1.5 m over the ground level [Maharoof *et al.*, 2020]. The data of the wind direction and speed was handwritten. Inside the site, there are no green areas or urban trees. Determining the field measurement date was a challenge, as the optimal conditions to conduct the traverse study should include steady weather, with a clear sky, no rainfall and low cloud coverage [Yan *et al.*, 2019], and usually, March is the driest month in Edinburgh [Met Office, 2022a]. Moreover, the availability of the equipment was only after April. Therefore, the field data measurements were conducted in July on two different weekdays, one during the week (07.07.2022) and one at the weekend (09.07.2022), to measure the conditions when the frequency of the tourists is different.

Figure 23 Routes and 19 locations for the traverse study (field measurements), orange - urban canyons and brown – intersections (source: Own elaboration, Background: Aerial Imagery 2020, Edina – Digimap)

Table 14 Parameters and instruments used during the field measurements. (source: Own elaboration)

Instrument	Parameter	Resolution/Range	Frequency
Tiny Tag TGP-4020	Air temperature	±0.4 ℃ (-40 to +125 ℃)	10 sec
Tiny Tag TGP-4020	Relative humidity	(0 to 100%)	10 sec
Kestrel 3000	Wind speed / Air speed	±3% (0.4 to 60.0 m/s)	1 sec

Figure 24 Aluminium foil funnel used to avoid direct solar radiation (source: Own elaboration, 2020)

Bannerman Way Weather Station is located in the north part of Holyrood Park, and it is 1.76 km (aerial distance) from the New Town. This station records every 5 minutes and produces the following information: temperature, dew point, relative humidity, wind direction, wind speed, wind gust, pressure and precipitation [Weather Underground, 2022]. The fixed station, the Tiny Tag TGP-4020 model, was placed near the entrance of Edinburgh castle. The place is located at a relatively higher altitude than the New Town, in ample open space, making it favourable to measure air temperature without the UHI effect.

4.3.2. Initial simulation

Settings and the Calibration of ENVI-met® Model

The microclimates under different scenarios in the case study area were estimated with ENVI-met® software (version 5.0.3). The total amount of simulation was 30 hours, adding extra 6 hours (18:00 to 00:00 h) from the previous day. The software uses these first six hours to achieve microclimate stabilisation [Zhang *et al.*, 2019]. The 3D model was created using the Sketch-up INUX plug-in to make it more accurate. In the numerical model, the distribution of grids in the domain model area (222 m × 171 m × 31 m) was 4 m and 3 m in horizontal (Δx and Δy) and vertical 3m in (Δz) directions, respectively. As the tallest building in the model is 45m, and the z direction of the grid includes twice this height, telescoping was not considered in this simulation, but to calculate the thermal comfort parameters more accurate at pedestrian level, the option to split in 5 sub-cells the lowest Δz grid box was chosen [ENVI-met®, 2021]. The grid was rotated 16 clockwise from the north. Five nested grids were adopted to discretize the numerical model [Zhang *et al.*, 2019]. 19 receptors were put on the model, corresponding to the exact location of field measurement points, and the simulation outputs were calculated every 4 minutes. Therefore, there was no need for any temporal corrections through a linear equation to find the air temperature for the 19 points simultaneously.

Meteorological parameters

The meteorological parameters such as wind speed, air temperature and relative humidity were mainly obtained from field measurements and from the fixed station (*Annex 5*). The data used were the one collected on 07.07.2022 as the weather conditions were more stable, and the cloud coverage was almost 0. As Full Forcing is used, the data needed is every 30 minutes. Model roughness length z0 was determined to be 0.03m [Watson *et al.*, 2015], while air moisture content at 2500.0 m was set as default.

Building and materials parameters

The area's building footprint and height data were derived from Edina Digimap, Verisk Service. The materials of the buildings were retrieved from the "Listed Buildings" description of HES and compared with field observation. The 3D model of the buildings (*Figure 25*) was created as a volume from the footprint, with horizontal roof surfaces and no detailed façade elements, discarding their actual shape due to lack of information and time. The main

building material used in the New Town comes from a traditional Scottish material, the Craigleith sandstone. The Craigleith sandstone technical properties were introduced in the ENVI-met® database. Some specifications were adapted from Hazeldean sandstone as the best fit substituent. For the roofing material in the WH properties case, it is essential to take into consideration the age of the building and its periodical maintenance. As the solar absorbance of the surface changes with time due to dust and ageing [Berdahl and Bretz, 1997], studies have proven that the reflectivity properties can change even during one year. Due to the lack of possibilities for experimental and lab tests, the material's properties have been modified from the default properties of ENVI-met®; mainly the reflection was decreased by 20% (*Table 15*).

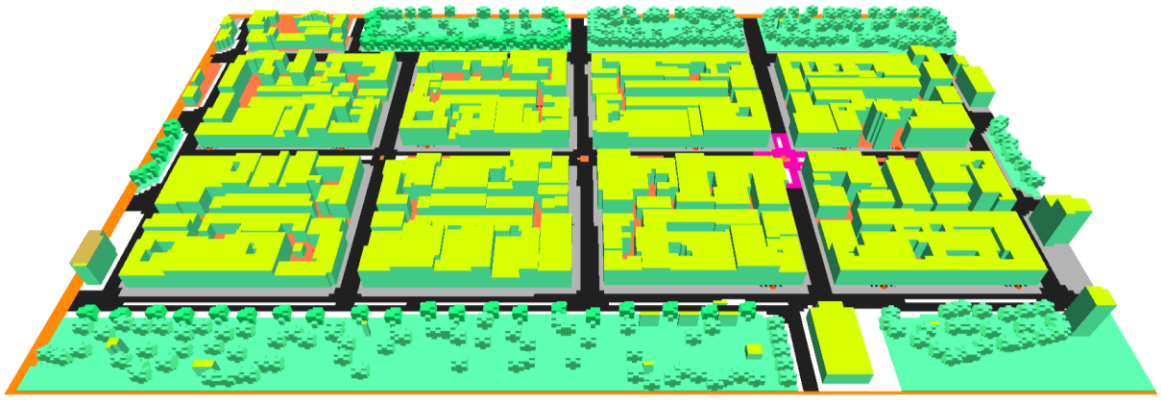

Figure 25 3D model in ENVI-met® software (source: Own elaboration, 2022)

Table 15 Technical specification of facade and roof materials

Facades		Roof	
Name	White sandstone	Name	Roof Tile
Thickness	0.2	Thickness	0.05
Absorption	0.5	Absorption	0.6
Transmission	0.18	Transmission	0
Reflection	0.32	Reflection	0.4
Emissivity	0.59	Emissivity	0.9
Specific Heat	920	Specific Heat	800
Thermal conductivity	1.71	Thermal conductivity	0.84
Density	2453	Density	1900

Soil parameters

The New Town's footpaths were constructed from various materials, from the Hailes flagstone pavements of Dundas Street to the horonized walks of Drummond Place formed from fragments of stone working waste [The City of Edinburgh Council *et al.*, 2016, 60]. The impervious pavement features were adapted based on the data provided under the layer "Adopted roads" [The City of Edinburgh, 2022] available in GIS format. Also, in the case of the pavement, due to the ageing of the material, properties have been modified from the default the ENVI-met® contains and the albedo was increased by 20%. A summary of the features of the materials is represented in *Annex 6* and each assignment in ENVI-met®. The classification of surfaces with unidentified data, was made through site field survey. The specifications of used pavements materials are shown in *Table 16.*

Table 16 Technical specification of pavements materials

Pavements				
Name	Asphalt	Red flags	Concrete Pavement grey	Asphalt road with red coating
Z0 Roughness Length	0.01	0.01	0.1	0.05
Albedo	0.24	0.24	0.7	0.5
Emissivity	0.9	0.9	0.9	0.9

Simulation

After the calibration, the model was simulated under extreme weather conditions. From research, the hottest day in Edinburgh was 25 July 2019, with temperatures reaching around 31.2°C [Mitchell, 2019], but due to lack of hourly data, the Base Case (the actual state of the site without changes) was simulated under the weather conditions on 18 July 2022, with a maximum temperature was 31°C. The hourly data was retrieved from Bannerman Way Weather Station (*Annex 7*).

4.3.3. Proposal

As explained in section 3.4, the City of Edinburgh Council has approved a new project transforming George Street. The following proposal considers the majority of the interventions of street design approved, but it is also expanded to the entire site.

The *Cold Case* was an integration of the proposed project but expanded in the entire site. Regarding the facades and roofs, the materials specifications were modified to represent the improvement due to maintenance [Salata *et al.*, 2015]. The pavements along George street are replaced with the materials proposed in the project in section 3.4. For the other streets, the technical specifications were modified to represent the conditions after maintenance (*Annex 8)*. Other interventions include temporary shades along the coffees and restaurants for outdoor sittings, also based on the strategies of the City of Edinburgh Council.

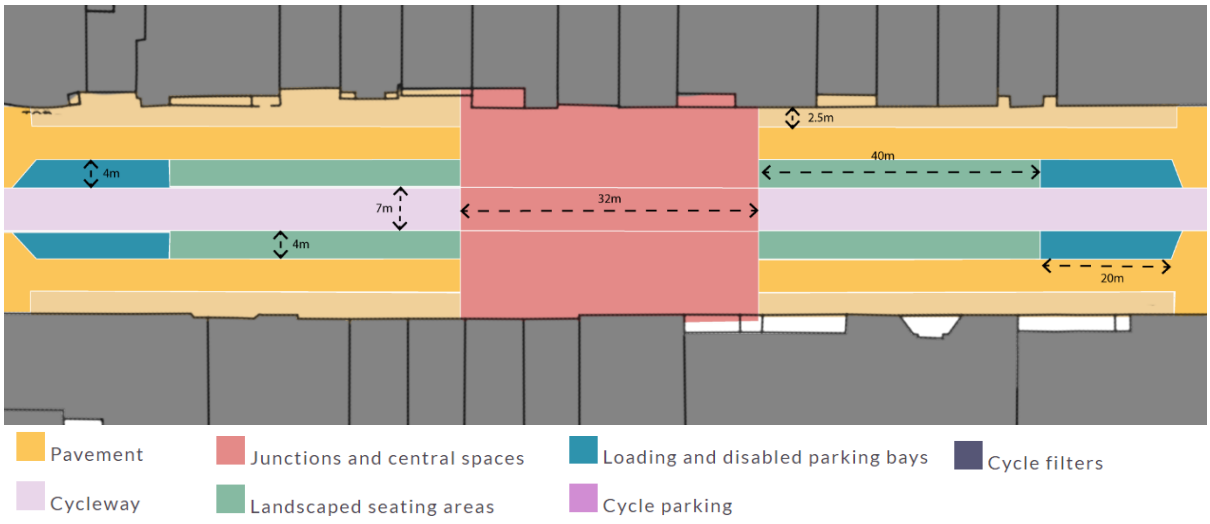

Figure 26 Pavements materials (source: Modified from The City of Edinburgh Council et al., 2021)

The *Green Case* the proposal was a bit limited; as we are in a WH site, the historic landscape must be considered. Therefore, green facades and green roofs would not compromise the authenticity of the WH property. The same issue comes with introducing tall trees in George Street, a strong axis from Charlotte Square to St Andrew's Square, where intervisibility is a unique characteristic of the urban form [The Cockburn Association, 2021]. Moreover, considering the other sides of the streets' space limitation, mainly in the inner space of the block, where pathways' widths make it impossible to introduce green spaces. The main green spaces introduced in the area are hedges, shrubs along George Street and various pot trees. The overall ENVI-met® setting for each of the cases is shown in *Annex 9.*

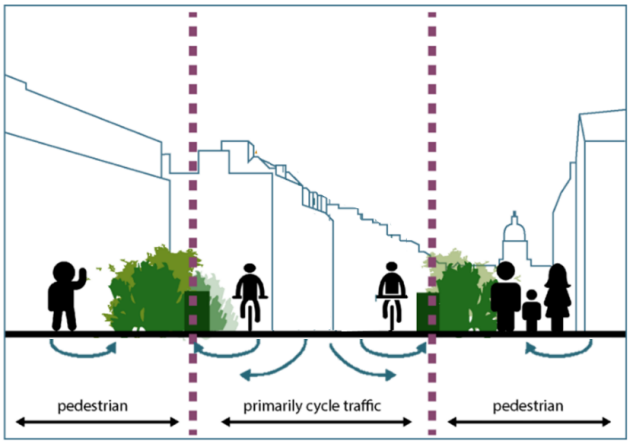

Figure 27 Schematic representation of vegetation height in George Street (source: Modified from The City of Edinburgh Council et al., 2021)

4.3.4. Thermal comfort evaluation

All three cases, Base Case, Green Case and Cool Case, will be evaluated using the PET index, approved by Germany's VDI standard and is used as the outdoor thermal comfort index [Nasrollahi *et al.*, 2017]. This index has been used for study cases with different climates, making it eligible to compare the results with the accepted comfort ranges in different areas, which foreign tourists can use with different climates. PET is calculated with BIO-met, which is a post-processor tool, using the parameters of temperature, relative humidity, wind speed, and mean radiant temperature, which was calculated on ENVI-met® based on RayMan [Lin *et al.*, 2010; Gal and Kantor, 2020]; and human's clothing, and activity. RayMan approach to estimating T_{mrt} is based on Matzarakis *et al.* [2010]. The ranges of PET values have been tested and verified for the climate of North and West Europe following:

Table 17 Ranges of PET compared to different grades of thermal perception by human beings and physiological stress on human beings. (source: Matzarakis *et al.*, 1999)

PET (°C)	4	8	13	18	23	29	35	41	
Thermal Perception	Very cold	Cold	Cool	Slight cool	Comfort -able	Slightly warm	Warm	Hot	Very hot
Grade of physiological stress	Extreme cold stress	Strong cold stress	Moderate cold stress	Slight cold stress	No thermal stress	Slight heat stress	Moderate stress	Strong heat stress	Extreme heat stress

CHAPTER 5: **RESULTS**

5.1. Local Climate Zoning

5.1.1. Land Use/ Land Cover

Land Use / Land Cover attribution for each grid cell size was made using the majority concept for each class. *Figure 28* shows the final LULC map within a resolution of 15m grid. *Table 18* shows each class's spatial extent before and after the discrimination process to quantify each class change. There are changes within the total balance, mainly in classes related to streets, roads and motorways, due to their linear spatial extend compared to other classes. The spatial distribution is dominated by two rural classes, CR1 - *Arable crops* and CR3 - *Pastures*. These classes are located in the rural area of Edinburgh, mainly concentrated in the west part and more fragmented in the south and east part. The classes covering the central historic town, including WHS, include D3 - *Discontinuous medium density urban fabric (S.L.: 30%-50%)*, D4 - *Discontinuous medium density urban fabric (S.L.: 50%-80%)*, D5 - *Continuous urban fabric (S.L.: > 80%)*, GU – *Green urban areas*, R1 – *Railways and associated land*, R3 – *Other roads and associated land*, I1 – *Industrial, commercial, public, military and private units* and these classes cover approximately 35, 87% of the total. Furthermore, each class was classified into two categories: build – up and non-build up. The first one will be used for classifying LCZ 1-10 and the second category for classifying LCZ A-G.

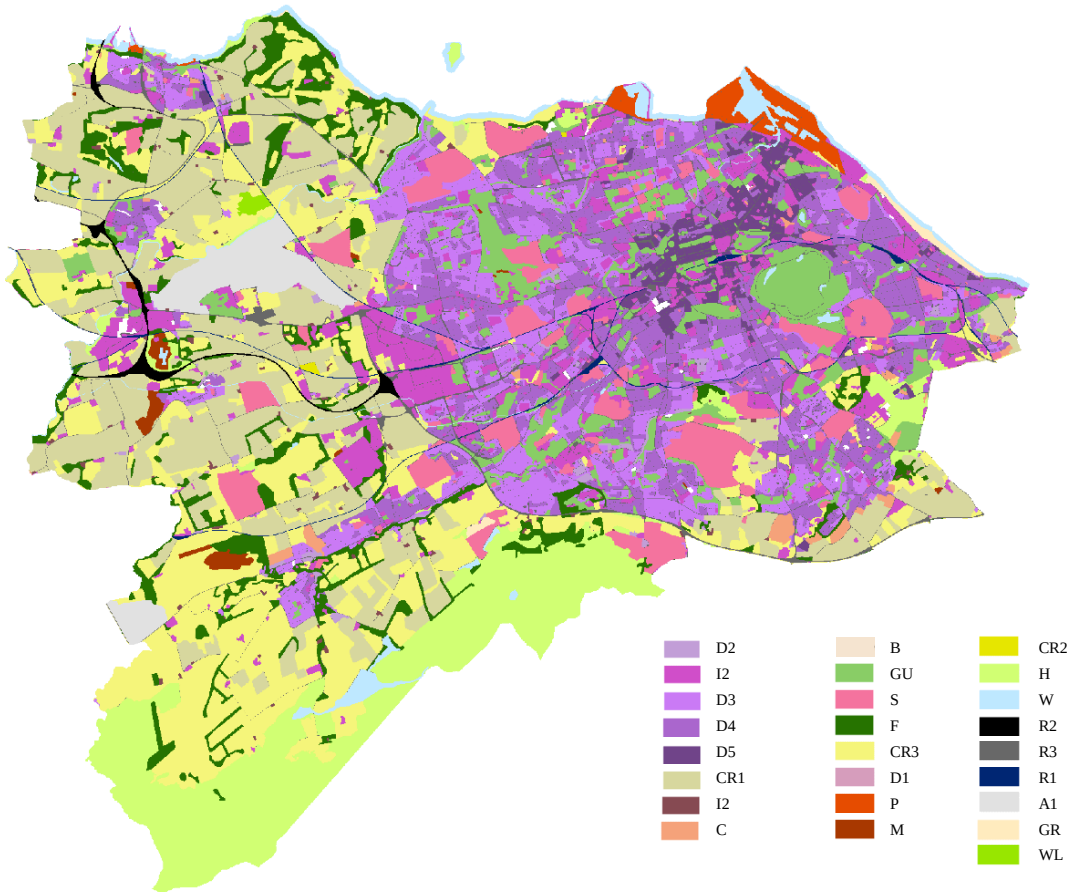

Figure 28 LULC in 15m resolution (source: Copernicus Land Monitoring Service at the European Environment Agency, 2018; software: ArcGIS Pro)

Table 18 Spatial extent (km^2 and %) of each LULC class from polygon to 15m grid size (source: Own elaboration, 2022)

LULC Class	Category	Before process total area		After process total area	
		Km^2	%	Km^2	%
D2	Build-up	1.37	0.36	1.38	0.51
I1	Build-up	20.70	5.42	20.61	7.69
D3	Build-up	23.80	6.24	25.09	9.36
D4	Build-up	26.30	6.89	27.92	10.41
D5	Build-up	4.51	1.18	4.8	1.79
CR1	Non-build-up	49.15	12.88	44.9	16.75
I2	Build-up	0.71	0.19	0.69	0.26
C	Build-up	1.45	0.38	1.38	0.51
B	Non-build-up	0.45	0.12	0.45	0.17
GU	Non-build-up	16.28	4.27	16.46	6.14
S	Build-up	14.77	3.87	14.8	5.52
F	Build-up	14.91	3.91	13.9	5.18
CR3	Non-build-up	47.82	12.53	42.56	15.87
D1	Build-up	0.05	0.01	0.05	0.02
P	Build-up	2.22	0.58	2.29	0.85
M	Build-up	1.10	0.29	1.1	0.41
CR2	Non-build-up	0.09	0.02	0.09	0.03
H	Non-build-up	89.47	23.44	26.6	9.92
W	Non-build-up	15.39	4.03	5.31	1.98
R2	Build-up	1.37	0.36	1.12	0.42
R3	Build-up	41.31	10.82	9.05	3.38
R1	Build-up	2.25	0.59	1.3	0.48
A1	Build-up	5.30	1.39	5.29	1.97
GR	Non-build-up	0.68	0.18	0.68	0.25
WL	Non-build-up	0.28	0.07	0.28	0.10

5.1.2. Morphological Parameters

An overview of each of the six morphological parameters results are shown in the *Figure 29* in city scale. Analysing closely, the histograms (*Graphs 8, 9 and 10*) show the frequency distribution of means building height, SVF and road aspect ratio values for the main urban classes. The other classes are shown in *Annex 10*.

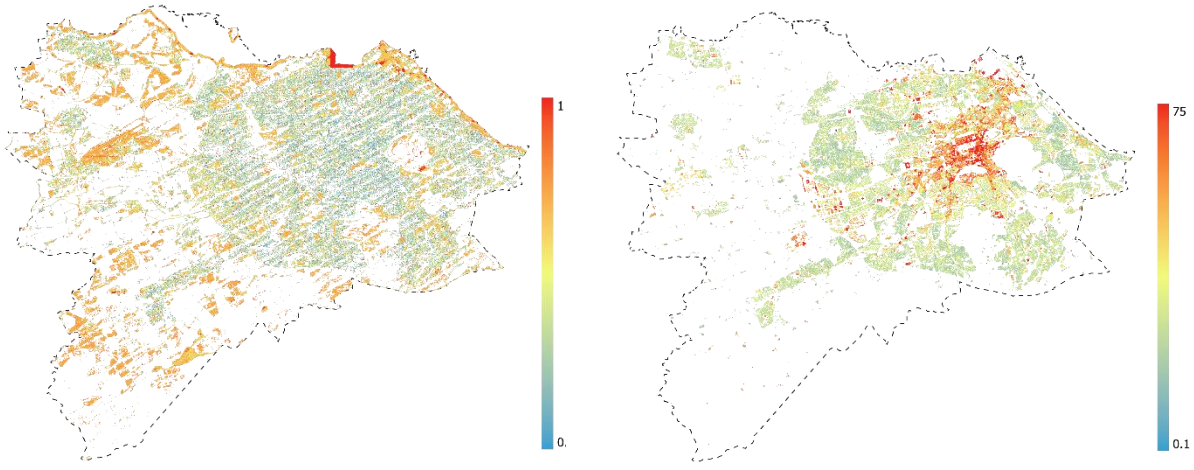

a ***b***

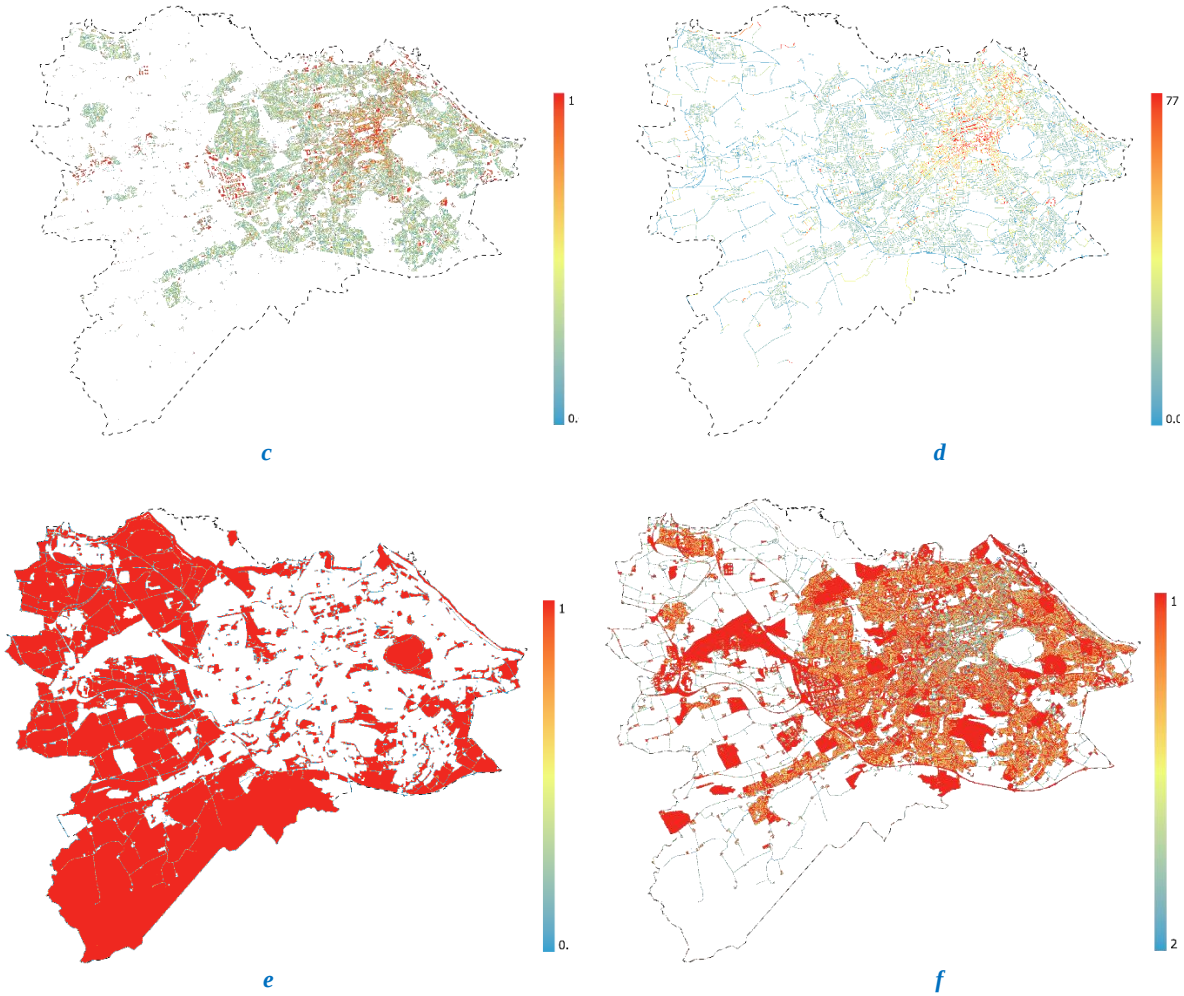

c *d*

e *f*

Figure 29 Morphological parameters the City of Edinburgh: a) Mean building height b) Sky view factor c) Aspect ratio d) Building surface fraction e) Pervious surface fraction f) Impervious surface fraction of the city of Edinburgh in 15 m resolution and National British projection (source: Own elaboration, 2022, software: ArcGIS Pro)

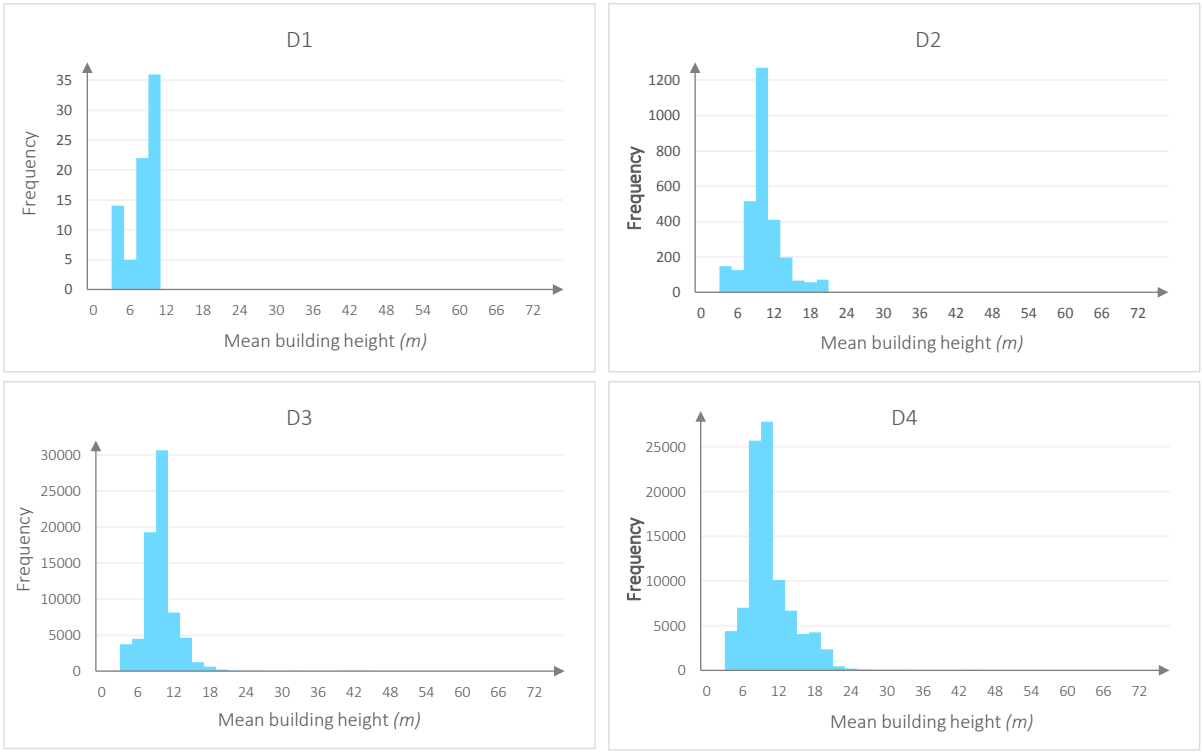

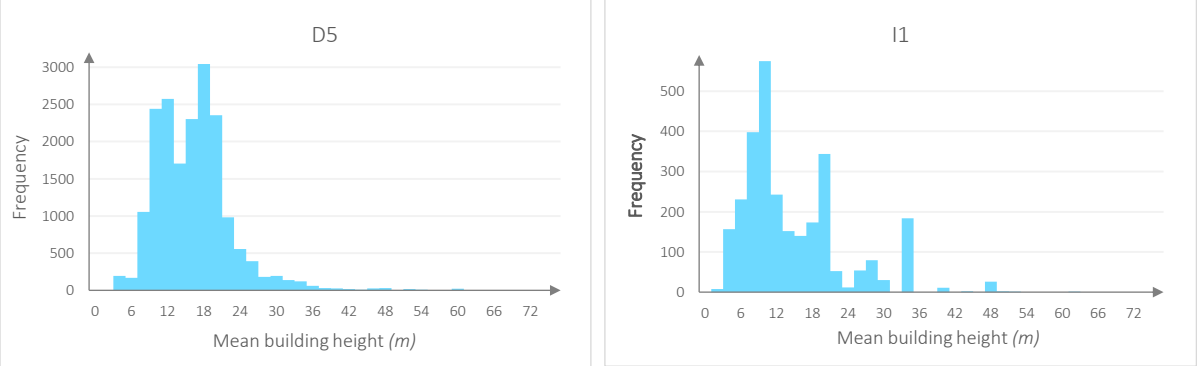

Graph 8 Mean building height distribution for: D1, D2, D3, D4, D5 and I1 classes (source: Own elaboration, 2022)

The mean building height histograms (*Graph 8*) represent the urban structures with a medium height range between 6-18 meters, close to a binomial distribution for classes D2, D3 and D4, while in the case of class D5, the range is higher (12-24m) due to the fact this is a more compact and dense class. Regarding the other classes, the distributions do not follow any specific pattern, which is understandable due to the classes' characteristics, function and period of the build. It is essential to point out that the histograms show only the distribution of mean building height for all classes and do not include the vegetation height in the case of rural classes.

A deeper understanding of the class's morphological class's is shown through the histograms of the sky view factor (*Graph 9*). As predicted, class D1 has a wide range of SVF values compared to the total spatial extension, varying from 0.05 to 0.7. Meanwhile, as predicted the values of SVF tend to go closer to 0 for classes D2, D3 and D4. However, even between these classes, the frequency is higher, closer to SVF values of 0 from the less dense urban area to the higher dense one. In the case of class I1 and other classes (*Annex 10*), the distribution of SVF values is closer to the binomial distribution, showing the relation to the location of the classes, where for example, the road class will have a lower value near the urban area and will increase while passing the suburban and rural area. In this case, the SVF values and the spatial distribution will be affected, decreasing the frequency distribution in rural areas.

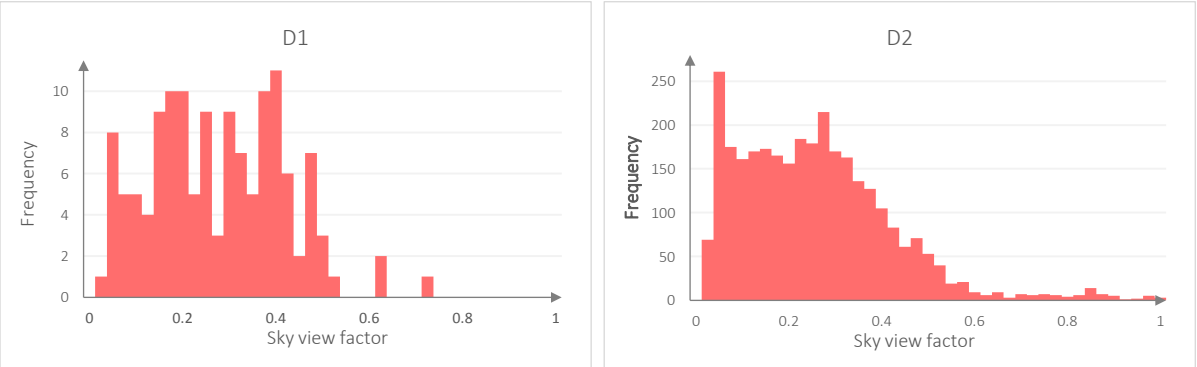

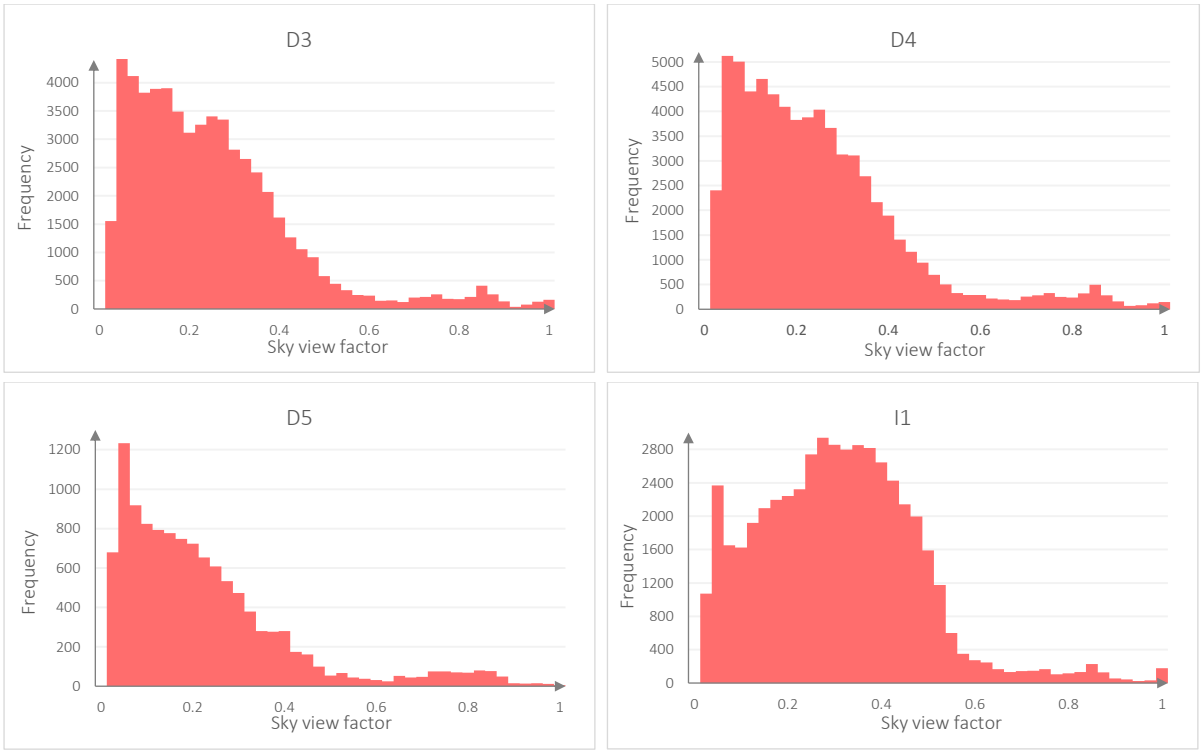

Graph 9 Sky view factor values distribution for: D1, D2, D3, D4, D5 and I1 classes (source: Own elaboration, 2022)

The aspect ratio histogram shows only the road aspect ratio, as due to the limitation of the software and the data available, it was not possible to calculate the building height–spacing ratio useful for LCZs 8–10 and the tree height–spacing ratio for LCZs A–G. The range of the road aspect ratio is between 0 to 2, except in cases in the city centre near the high rise and dense classes in the narrow one-way streets.

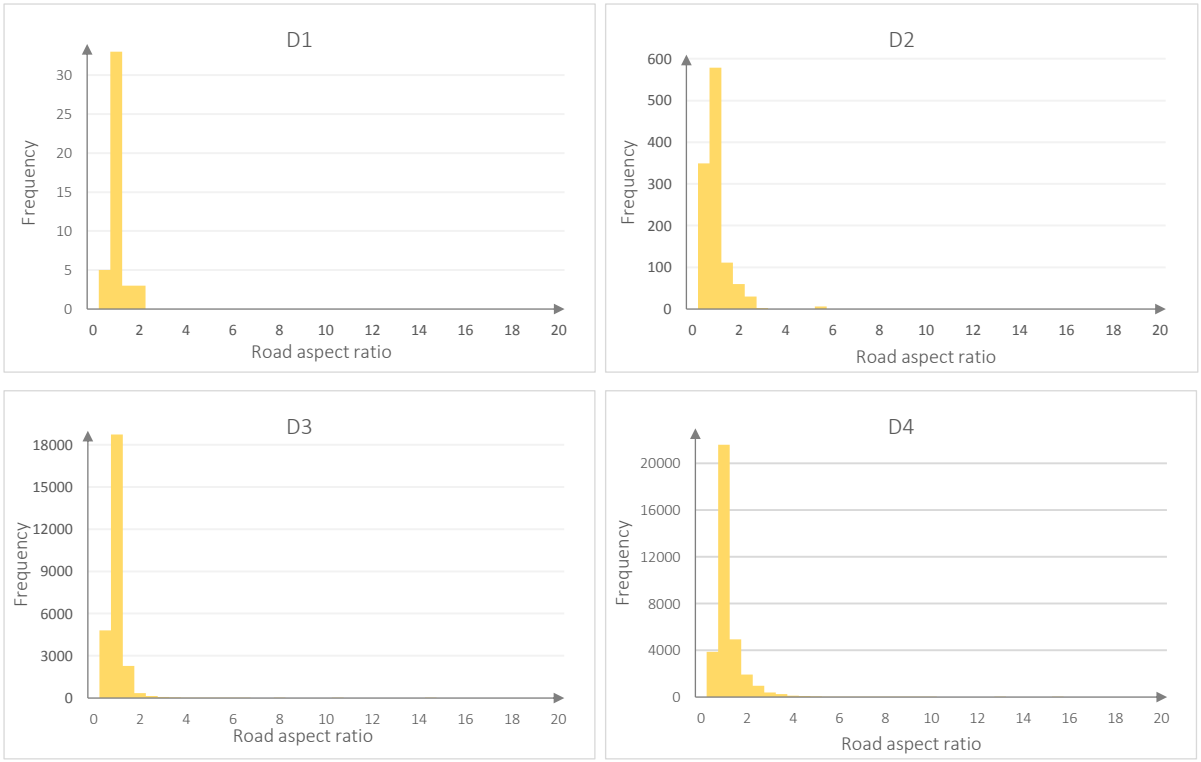

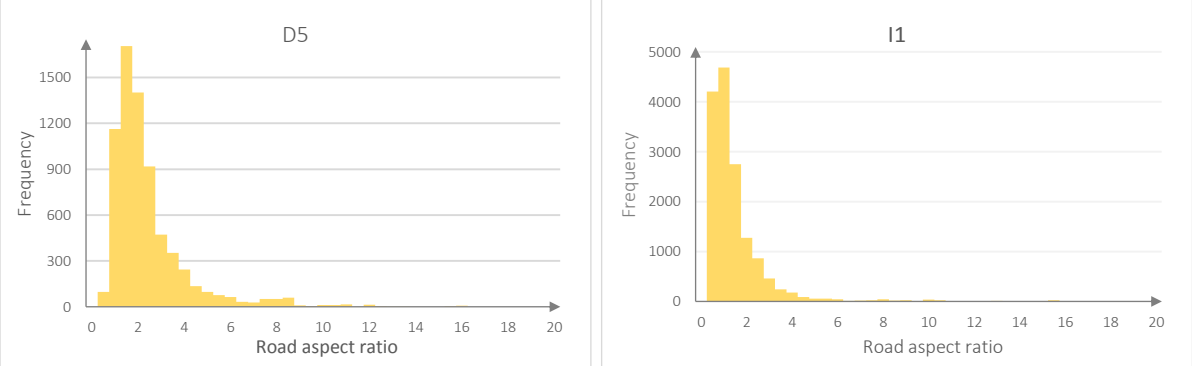

Graph 10 Road aspect ratio values distribution for: D1, D2, D3, D4, D5 and I1 classes (source: Own elaboration, 2022)

The mean value and the standard deviation of the morphological parameters for build-up classes are shown in *Table 19,* estimating the range values of each morphological parameter. The mean is used to estimate the fitting LCZ class based on Oke and Steward's [2012] thresholds.

Table 19 Morphological parameters average for each LULC class including the standard deviation (source: Own elaboration, 2022)

LULC Class	Sky View factor	Mean Building height	Building Surface Fraction	Aspect Ratio	Impervious Surface Fraction0.26	Pervious Surface Fraction
D2	[0.24 ± 0.17]	[9.3 ± 3]	[0.26 ± 0.21]	[0.76 ± 0.56]	[0.86 ± 0.14]	[0.02 ± 0.02]
I1	[0.29 ± 0.17]	[13.8 ± 7.9]	[0.48 ± 0.34]	[1.6 ± 1.23]	[0.75 ± 0.34]	[0.01 ± 0.06]
D3	[0.24 ± 0.18]	[8.6 ± 2.65]	[0.28 ± 0.21]	[0.73 ± 0.42]	[0.81 ± 0.22]	[0.01 ± 0.04]
D4	[0.24 ± 0.18]	[9.5 ± 4.16]	[0.31 ± 0.23]	[0.95 ± 0.34]	[0.76 ± 0.24]	[0.04 ± 0.03]
D5	[0.22 ± 0.19]	[15.4 ± 6.4]	[0.44 ± 0.29]	[2.4 ± 2.24]	[0.62 ± 0.3]	[0.12 ± 0.12]
I2	[0.28 ± 0.17]	[10.1 ± 4.25]	[0.28 ± 0.23]	[0.77 ± 0.7]	[0.83 ± 0.17]	[0.19 ± 0.15]
C	[0.32 ± 0.17]	[11.2 ± 3.3]	[0.26 ± 0.2]	[0.88 ± 0.61]	[0.88 ± 0.12]	[0.19 ± 0.16]
S	[0.42 ± 0.13]	[13.7 ± 8.8]	[0.29 ± 0.27]	[0.74 ± 0.73]	[0.98 ± 0.02]	[0.19 ± 0.15]
D1	[0.26 ± 0.14]	[7 ± 1.96]	[0.2 ± 0.17]	[0.66 ± 0.38]	[0.9 ± 0.1]	[0.15 ± 0.14]
P	[0.26 ± 0.14]	[16.5 ± 10.9]	[0.39 ± 32]	[1.18 ± 1.34]	[0.9 ± 0.1]	[0.18 ± 0.15]
M	[0.43 ± 0.16]	[9.1 ± 4.6]	[0.21 ± 0.2]	[0.83 ± 0.43]	[0.97 ± 0.03]	[0.21 ± 0.16]
R2	[0.41 ± 0.12]	[9.6 ± 9.3]	[0.24 ± 0.11]	[0.13 ± 0.09]	[0.96 ± 0.04]	[0.2 ± 0.15]
R3	[0.3 ± 0.14]	[12.3 ± 6.3]	[0.17 ± 0.14]	[0.77 ± 0.1]	[0.88 ± 0.12]	[0.29 ± 0.16]
R1	[0.29 ± 0.19]	[14.9 ± 8.9]	[0.29 ± 0.29]	[0.93 ± 0.84]	[0.9 ± 0.1]	[0.22 ± 0.14]
A1	[0.46 ± 0.14]	[9.4 ± 5.3]	[0.32 ± 0.29]	[0.46 ± 0.44]	[0.98 ± 0.02]	[0.02 ± 0.02]

5.1.3. Combination of Land Use / Land Cover and Morphological Parameters

The overview of the combination with each LCZ classification (*Table 20*) was done using the range from the average of morphological parameters (*Table 19)* and the threshold values ranges by Oke and Steward [2012] from *Table 11*. One LULC class resulted in fitting in more than one LCZ class as the threshold values between different LCZ classes overlap. Building Surface Fraction (BSF), Impervious Surface Fraction (ISF) and Pervious Surface Fraction (PSF) for some classes were out of the value range due to the small grid size, which can lead to reaching the minimum (0) and maximum (1) in cell size. However, only one value can reach the maximum as the ISF is calculated from BSF and PSF.

Table 20 Combination of each LULC class and LCZ classification (LCZ 1-10) through each morphological parameter mean ± standard deviation value range. Each number represents the LCZ type. LCZ 1-7 value ranges considered all 6 parameters, while LCZ 8-10 Aspect Ratio was omitted as the calculation is only building height - road width, not building height - space. (source: Own elaboration, 2022)

LULC class	Sky View factor	Mean Building height	Building Surface Fraction	Aspect Ratio	Pervious Surface Fraction
D2	1, 3, 7	3, 6, 8 to 10	4 to 6, 10	2 to 4,	1 to 3, 7, 8
I1	1, 3, 7	2, 5, 10	1 to 3	2, 7	1 to 3, 7, 8
D3	1, 3, 7	3, 6, 8 to 10	4 to 6, 10	5, 6	1 to 3, 7, 8
D4	1, 3, 7	3, 6, 8 to 10	4 to 6, 8	2, 3, 7	1 to 3, 7, 8
D5	1, 3, 7	2, 5	1 to 3	1	2 ,3, 7, 8
I2	1, 3, 7	2, 5, 10	4 to 6, 10	2 to 4	2 ,3, 7, 8
C	1 to 3, 7	2, 5, 10	4 to 6, 10	2 to 4	2 ,3, 7, 8
S	2, 3, 7	2, 5, 10	4 to 6, 10	5, 6	2 ,3, 7, 8
D1	1, 3, 7	3, 6, 8 to 10	4 to 6, 9, 10	5, 6	2 ,3, 7, 8
P	1, 3, 7	2, 5	4 to 6, 8	2 to 4, 7	2 ,3, 7, 8
M	2, 3, 7	3, 6, 8 to 10	4 to 6, 10	2 to 4	3, 7
R2	2, 3, 7	3, 6, 8 to 10	4 to 6, 10	5, 6	2 ,3, 7, 8
R3	1 to 3, 7	2, 5, 10	9	2 to 4	3, 7
R1	1, 3, 7	2, 5, 10	4 to 6, 10	2 to 4	3, 7
A1	2, 3, 7	3, 6, 8 to 10	4 to 6, 8	5, 6	1 to 3, 7, 8

Table 20 results are summarised in *Table 21* by evaluating the fitting scale of the criteria from 0 - no matches to 5 - fitting to all criteria for LCZ 1-7 and from 0 - no matches to 4 - fitting to all criteria for LCZ 8-10. No LULC class could reach the maximum combination. Only five classes could best fit in only one class: D2 - *Discontinuous low-density urban fabric (S.L.: 10% -30%)*, I1 – *Industrial, commercial, public, military and private units*; C – *Construction sites*; M – *Mineral extraction and dump sites* and A1 – *Airports*. The other classes resulted in fitting in more than one class.

Table 21 Affiliation of LULC classes according to the LCZ thresholds by Stewart and Oke [2012]. All matches are summed up (maximum 6, dark red) and the individual boxes are coloured according to the number of matches. (source: Own elaboration, 2022)

LULC Class	LCZ 1	LCZ 2	LCZ 3	LCZ 4	LCZ 5	LCZ 6	LCZ 7	LCZ 8	LCZ 9	LCZ 10
D2	2	2	4	2	1	2	2	2	2	2
I1	3	4	3	0	1	0	3	1	0	1
D3	2	1	3	1	2	3	2	2	1	2
D4	2	2	4	1	1	2	3	3	1	1
D5	3	3	3	0	1	0	2	1	0	0
I2	1	3	3	2	2	1	2	1	0	2
C	1	4	3	2	2	1	2	1	0	2
S	0	3	2	1	3	2	2	1	0	2
D1	1	1	3	1	2	3	2	2	2	2
P	1	3	3	2	2	1	3	2	0	0
M	0	2	4	2	1	2	2	1	1	2
R2	0	2	3	1	2	3	2	2	1	2
R3	1	3	3	1	1	0	2	0	1	1
R1	1	2	3	2	2	1	2	0	0	2
A1	1	2	3	1	2	3	2	3	1	1

Regarding the assignment of non-build classes to LCZ A-G, which was based on land cover and the description of each class (*Annex 4*), the affiliation is shown in *Table 22,* based on results from a study in Oslo, Norway, using the same LULC classes [Sigler, 2022]. After the entire the combinations explained above, the final conceptual LCZ is shown in *Figure 30*.

Table 22 LCZ class A-G affiliation to the non-build LULC classes (source: Own elaboration, 2022)

LULC class	LCZ class
CR1	LCZ D
CR2	LCZ D
CR3	LCZ D
F	LCZ A
H	LCZ B
W	LCZ G
GR	LCZ C
GU	LCZ B/D
B	LCZ F
WL	LCZ B/D

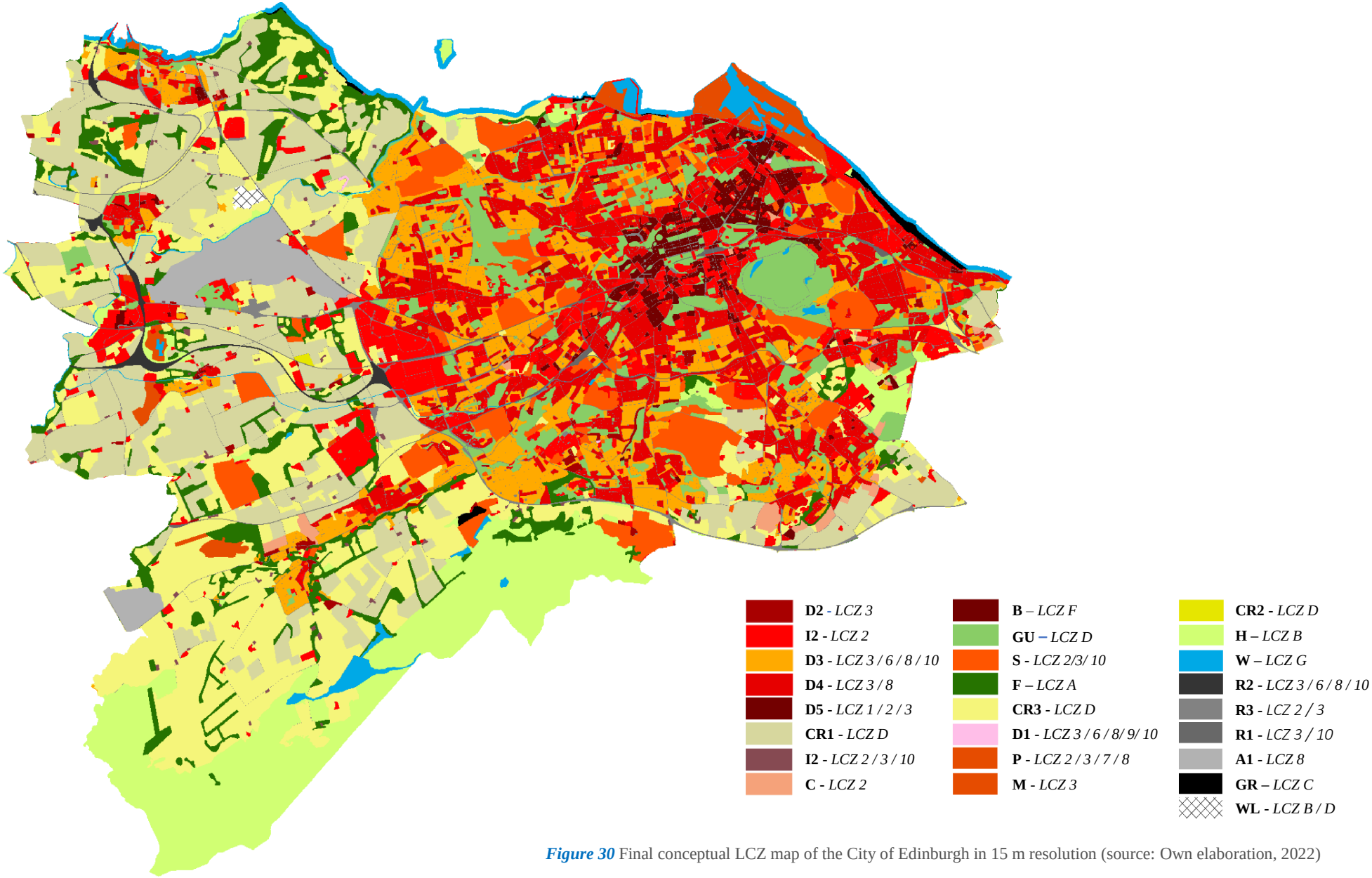

Figure 30 Final conceptual LCZ map of the City of Edinburgh in 15 m resolution (source: Own elaboration, 2022)

5.2. Traverse survey and ENVI-met® model

5.2.1. Accuracy

Field measurement

The weather on both days that the traverse study was conducted, respectively 7th and 9th of July 2022 was mostly sunny, without any precipitation. Bannerman Way Weather Station recorded the maximum temperature at 15:20 (22.1℃) and the minimum at 5:10 (12.6℃) on 7th of July, while on 9th of July; the maximum temperature recorded was 22.1℃ at 16:50 and the minimum 11.6℃ at 5:20. During these days the average relative humidity was 72% on 7th of July and 65% on 9th of July. *Graph 11* summarises the meteorological parameters for both dates of the traverse study. Even though most parameters were the same, the cloud coverage and the change of wind speed direction more frequently on the 9th led to more stable conditions on the 7th of July for the simulation. A temporal correction was conducted based on linear regression to calculate the temperature value of all 19 points at 14:00 with an air temperature of 21.3℃ (*Graph 12*) and to identify the hottest points in the area. The hottest points are the ones along George Street, understandable as the location of measured points faces direct sunlight during 12–5pm, without any shade available. These points also have the lowest relative humidity.

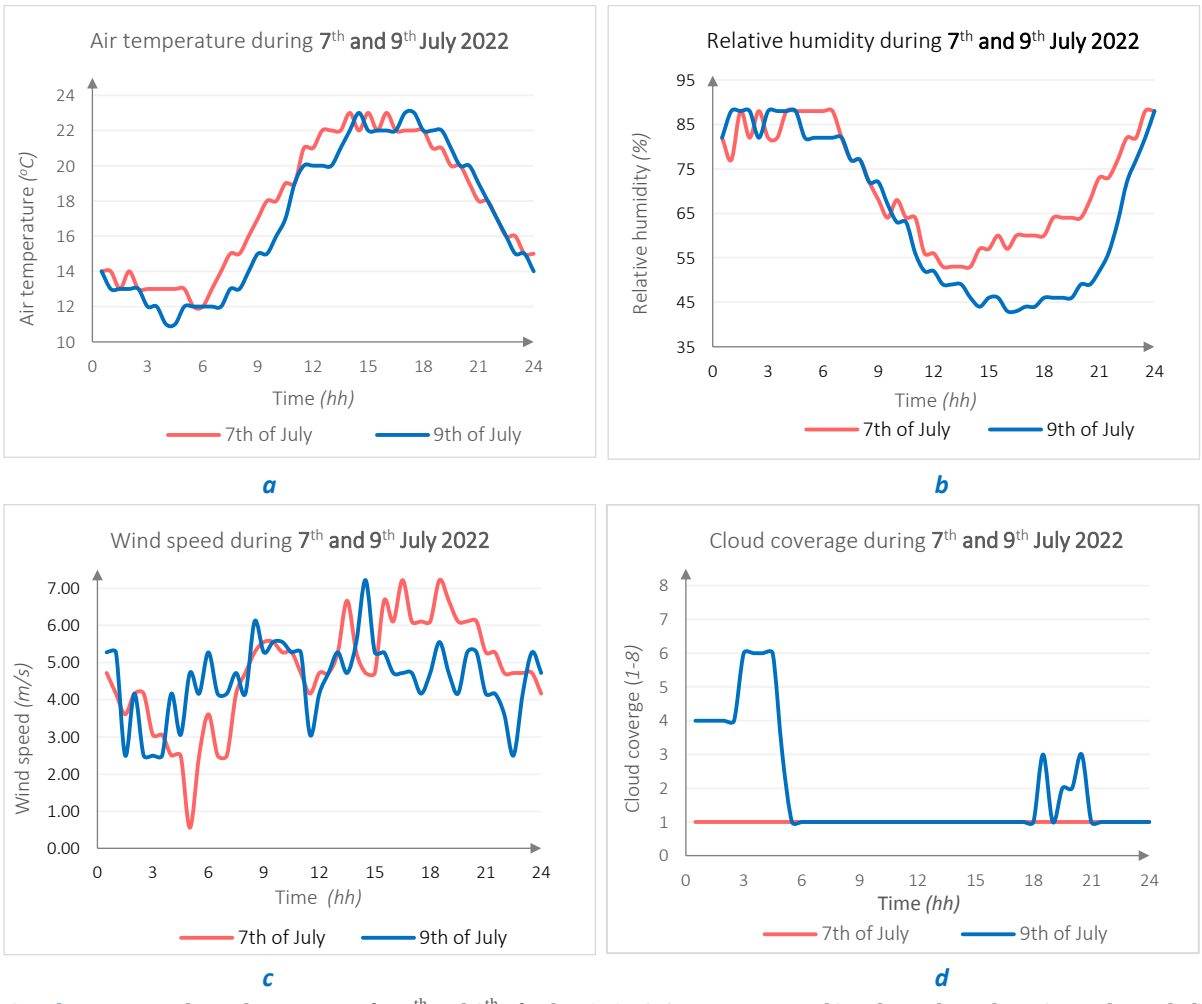

Graph 11 Meteorological parameters for 7th and 9th of July 2020: a) Air temperature, b) Relative humidity, c) Wind speed, d) Cloud coverage (source: Own elaboration, 2022, data retrieved from Weather Underground, 2022; software: Excel)

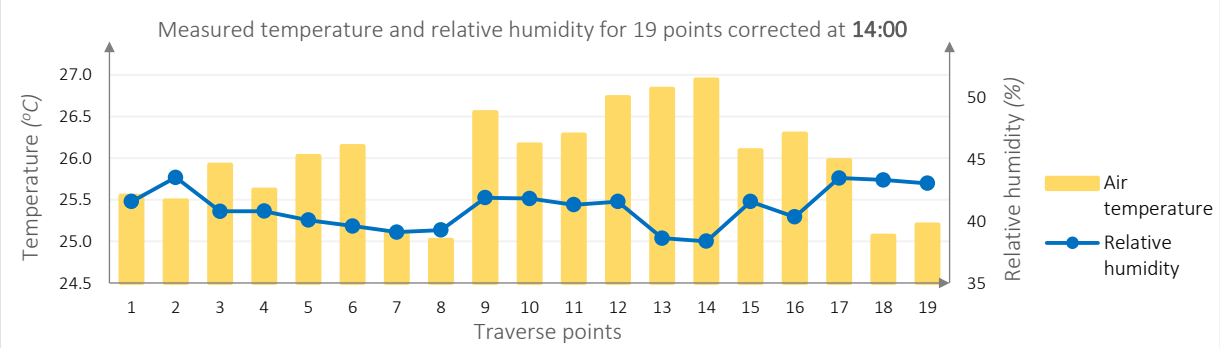

Graph 12 Air temperature and relative humidity measured with TinyTag on 7th of July (source: Own elaboration, 2022, data retrieved from Weather Underground, 2022; software: Excel)

Model calibration

As explained in the previous section, the validation of the model is based on the 7th of July traverse study. The input parameters are adjusted to reach the most favourable Root Mean Square Error (RMSE). The adjustment is needed as the software calculates the Potential Air Temperature (θ) at sea level pressure, 1013hPA *(4)*. *Graph 13* compares the simulation's values obtained before and after the adjustment. These adjustments were considered even in the Base, Green and Cool Case. The point that best fit the air temperature value between the measured and simulated is point 8, and the one with the worst fitting is point 14 (*Table 23*). This difference can be neglected as this point is near the site's border; therefore, it is affected by the surrounding area, which was not detailed in the model and is outside the study case.

$$\theta = T\left(\frac{1000}{p_i}\right)^{\frac{R}{c_p}} \qquad (4)$$

- θ is the potential temperature [K];
- T is the absolute air temperature [K];
- p_i is the pressure. T will be determined according to p1 [hPa];
- $k = R/c_p = 0.286$

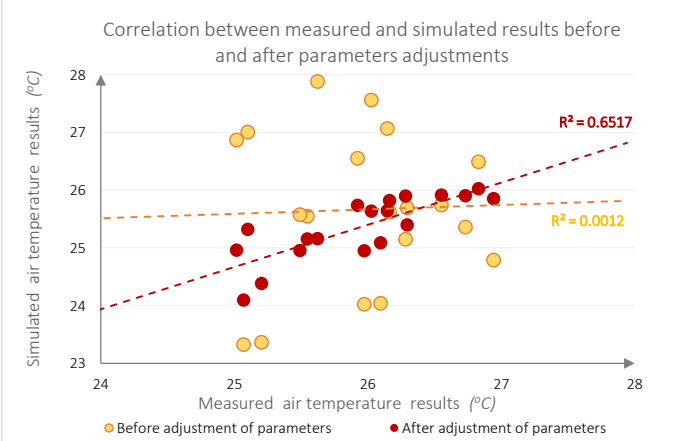

Graph 13 Difference between measured and simulated temperature (source: Own elaboration, 2022; software: Excel)

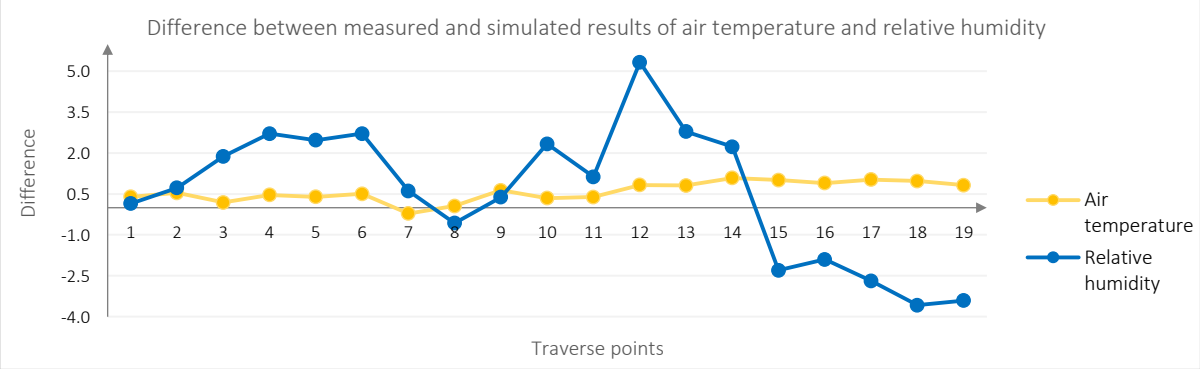

Graph 14 Difference between measured and simulated results of air temperature and relative humidity

Table 23 Evaluation of the difference between the measured and simulation values of temperature and relative humidity for each control point for 7th of July (source: Own elaboration, 2022)

Time	Point	Measured		Simulation		Difference ΔT	Difference Square ΔT	Difference ΔRh	Difference Square ΔRh
		Air temperature *(°C)*	Relative humidity *(%)*	Air temperature *(°C)*	Relative humidity *(%)*				
14:04	1	25.549	41.57	25.153	41.42	0.396	0.156816	0.15	0.0225
14:16	2	25.494	43.53	24.955	42.81	0.539	0.290521	0.72	0.5184
14:20	3	25.924	40.79	25.735	38.91	0.189	0.035721	1.88	3.5344
14:28	4	25.624	40.8	25.159	38.09	0.465	0.216225	2.71	7.3441
14:36	5	26.027	40.08	25.635	37.61	0.392	0.153664	2.47	6.1009
14:44	6	26.147	39.59	25.642	36.88	0.505	0.255025	2.71	7.3441
14:52	7	25.101	39.1	25.318	38.49	-0.217	0.047089	0.61	0.3721
14:56	8	25.019	39.27	24.958	39.84	0.061	0.003721	-0.57	0.3249
15:04	9	26.552	41.89	25.916	41.51	0.636	0.404496	0.38	0.1444
15:12	10	26.164	41.82	25.817	39.48	0.347	0.120409	2.34	5.4756
15:20	11	26.285	41.32	25.899	40.19	0.386	0.148996	1.13	1.2769
15:24	12	26.733	41.57	25.904	36.24	0.829	0.687241	5.33	28.4089
15:36	13	26.832	38.61	26.022	35.82	0.81	0.6561	2.79	7.7841
15:44	14	26.943	38.37	25.854	36.14	1.089	1.185921	2.23	4.9729
15:52	15	26.097	41.57	25.088	43.87	1.009	1.018081	-2.3	5.29
16:00	16	26.295	40.33	25.395	42.23	0.9	0.81	-1.9	3.61
16:08	17	25.975	43.47	24.946	46.16	1.029	1.058841	-2.69	7.2361
16:16	18	25.071	43.32	24.094	46.9	0.977	0.954529	-3.58	12.8164
16:20	19	25.204	43.05	24.381	46.46	0.823	0.677329	-3.41	11.6281
						Average	0.46741		6.01
						RMSE	0.68		2.45

Considering the optimal RMSE, four points were selected for further analysis of the air temperature, relative humidity, mean radiant temperature and physiological equivalent temperature for the hottest day in the three case scenarios *(Figure 31).* R1 will show tourists' thermal comfort in an area designated for activities, while R2 and R3 will show the difference in this comfort in areas with identic characteristics, but R2 is most of the time exposed to direct sunlight, while P3 is mainly in the shadow during the day. At last, R4 will show the vegetation's effect in thermal comfort in the green case scenario.

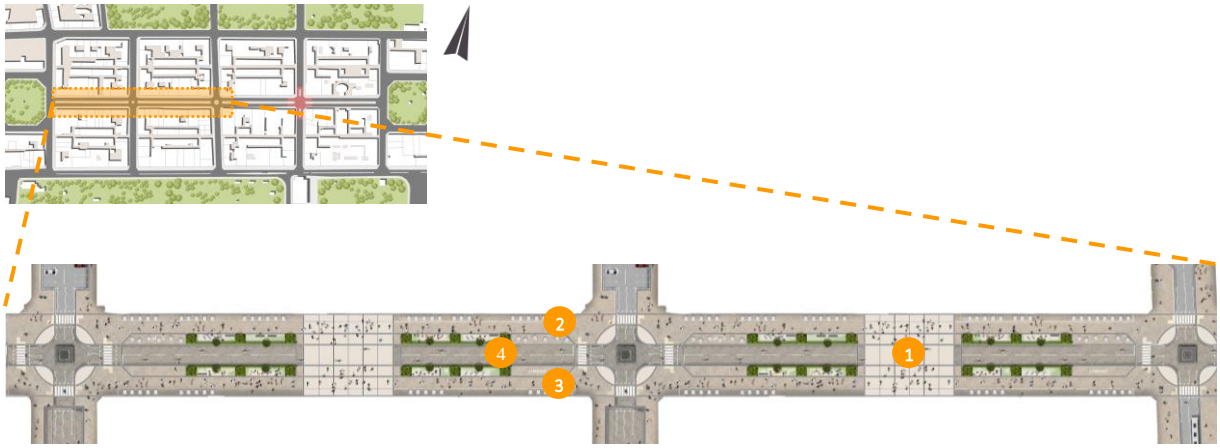

Figure 31 Points selected for further analysis (source: Own elaboration, 2022 and The City of Edinburgh Council et al., 2021)

5.2.2. Scenarios

All three scenarios (*Figures 32, 33, 34*) show how tourist thermal comfort can change based on climate-sensitive implementation. The *Cool Case* is focused more on the changes in thermic properties (albedo) due to the George Street area's maintenance and urban design project. The *Green Case* is restricted only to hedges and shrubs along the George Street axis and potted trees around the main roads. Both cases are conform with the design guidelines of the cultural heritage of New Town.

Figure 32 *Base Case* masterplan (source: Own elaboration, 2022)

Figure 33 *Cool Case* masterplan (source: Own elaboration, 2022)

Figure 34 *Green case* masterplan (source: Own elaboration, 2022)

All the parameters for each scenario were analysed for the worst conditions (hottest day) during four timesteps: 10am, 1pm, 4pm and 8pm, to determine the thermal comfort in the morning, during lunch as the George Street has many restaurants frequented by the tourists, and in the evening. The extra time step 4pm is analysed as it has the hottest temperature.

5.2.2.1. Potential Air Temperature - T_{Air}

In all the timeframe presented in *Figure 35*, the air temperature pattern between the *Base Case* and the *Green Case* does not change for the majority of the map, which is expected as the cases do not differ much. Regarding the *Cool Case*, the simulation shows a slightly different pattern, projecting the cooling effect of the new materials used. The areas mostly affected by the change are George Street and its perpendicular streets. It is important to stress that the difference in the T_{Air} is more significant in the areas exposed to solar radiation rather than the areas in the shadow most of the day. The difference between Base Case and Cool Case does not appear to fluctuate through the day for the same area but remains almost constant.

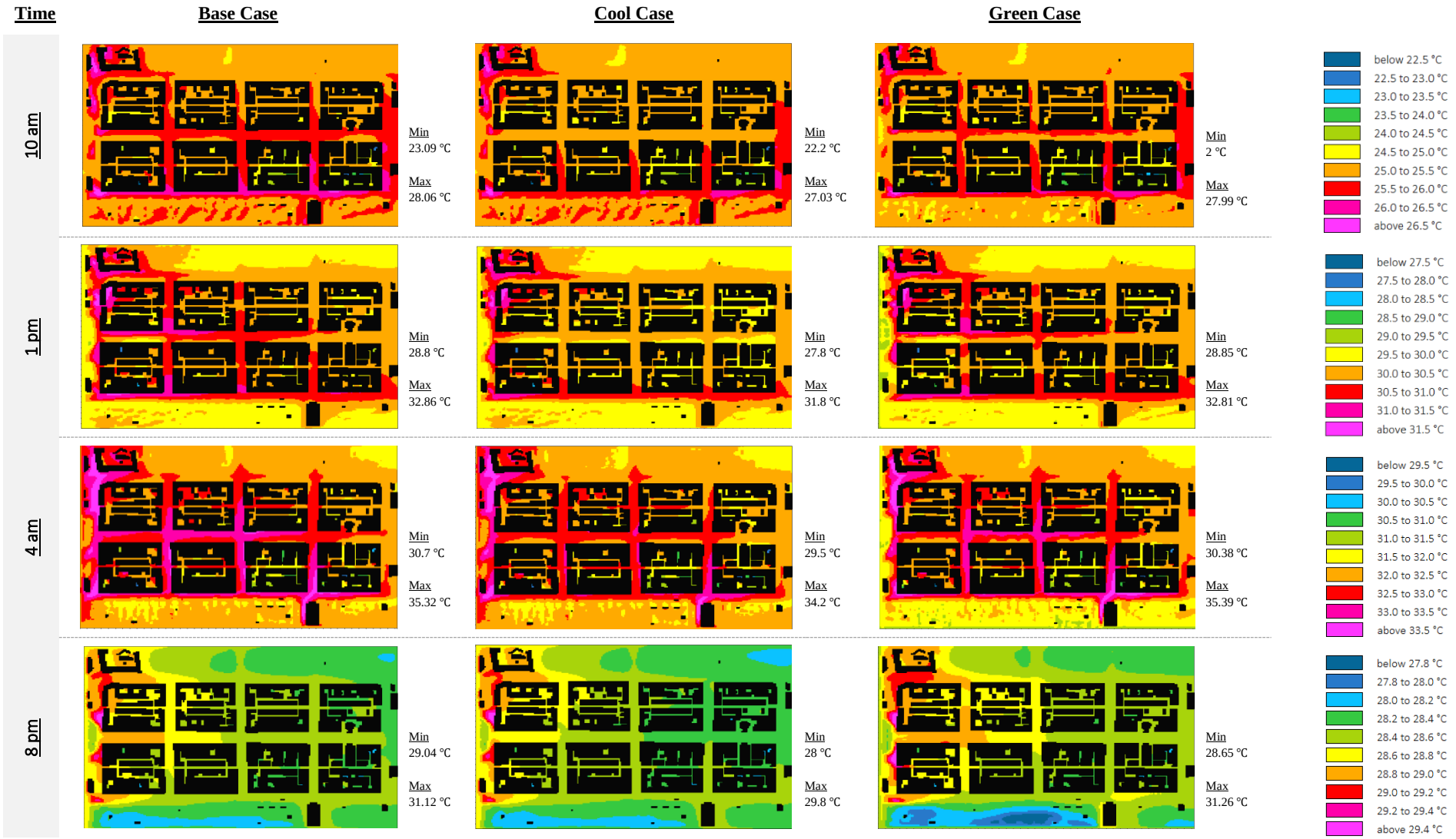

Figure 35 Simulated Potential Air Temperature during 18th July at 1.5m height (source: Own elaboration, 2022; software: ENVI-met®)

All the 4 points selected for further analysis have the same T_{Air} from the start of the day till 10 am and from 6 pm till the end of the day. R3 appears to be a cooler spot between 10am and 6pm, compared to R1, R2 and R4 (*Graph 15*). This happens since this point is in shadow during the day. R2 appears to be the hottest spot from 10 am to 6pm. All the points appear to have decreased in temperature in the *Cool Case (Graph 16)* and do not have much difference between them. In R1, R2 and R4, the cooling effect is more intensive than in R3, but this point remains the coolest. In the *Green Case (Graph 17)*, as expected only, R4 shows the difference in T_{Air} between 10am and 6pm, but R3 remains the least hot point.

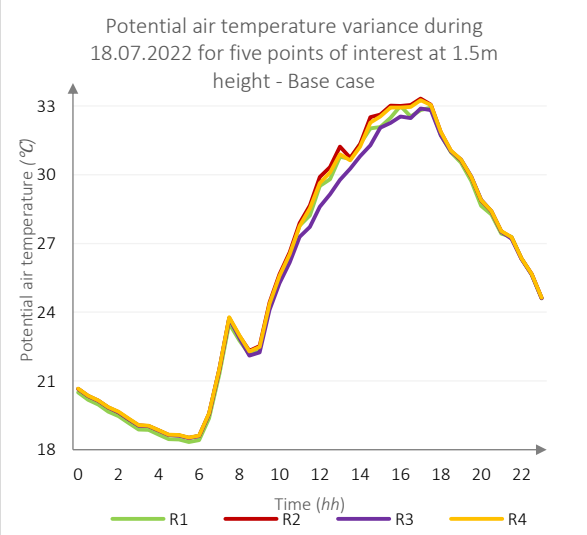

Graph 15 Potential air temperature variance during 18th of July for 5 points – Base case (source: Own elaboration, 2022; software: Excel)

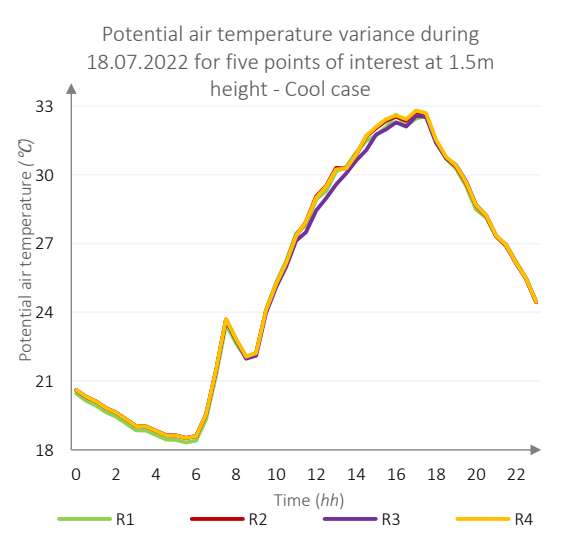

Graph 16 Potential air temperature variance during 18th of July for 5 points – Cool case (source: Own elaboration, 2022; software: Excel)

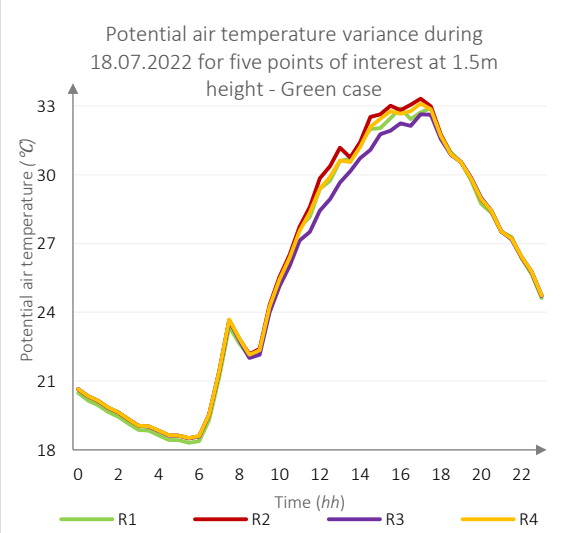

Graph 17 Potential air temperature variance during 18th of July for 5 points–Green case (source: Own elaboration, 2022; software: Excel)

The effects of climate-sensitive solutions adapted to the two scenarios compared to the *Base Case* have different intensities among the 4 points of interest (*Graphs 18, 19, 20 and 21*). As mentioned previously, the changes between scenarios start from 10am until 6 pm. The *Green Case* seems not to have impacted the T_{Air} in a considerable way, and the most impact is in R4 as it is located near the green area. Regarding the *Cool Case*, the intensity of changes is higher in R2, mainly because of the shade element positioned at that point. R3 has the most minor change intensity of T_{Air} from the beginning of the day till 6 pm, and the cooling effect seems to appear after 6 pm, contrary to the other points.

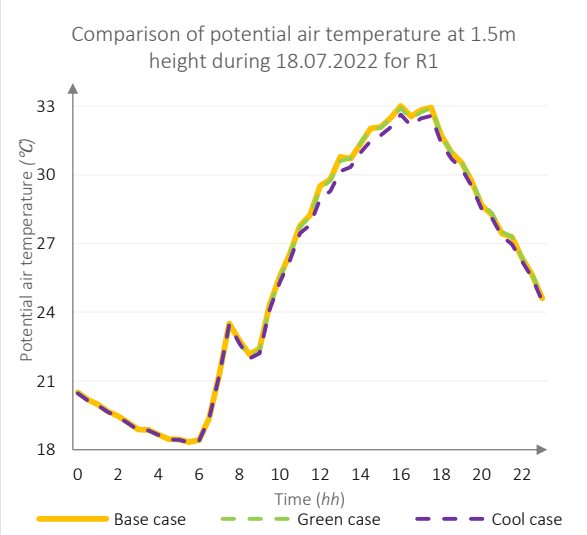

Graph 18 Potential air temperature comparison during 18th of July between scenarios at 1.5m height – R1 (source: Own elaboration, 2022; software: Excel)

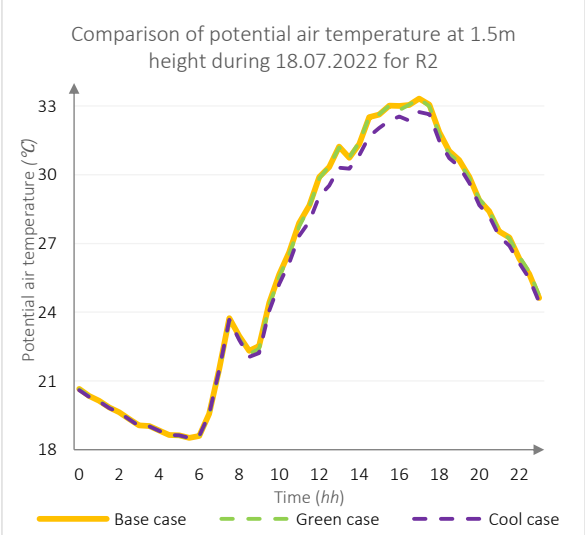

Graph 19 Potential air temperature comparison during 18th of July between scenarios at 1.5m heigh – R2 (source: Own elaboration, 2022; software: Excel)

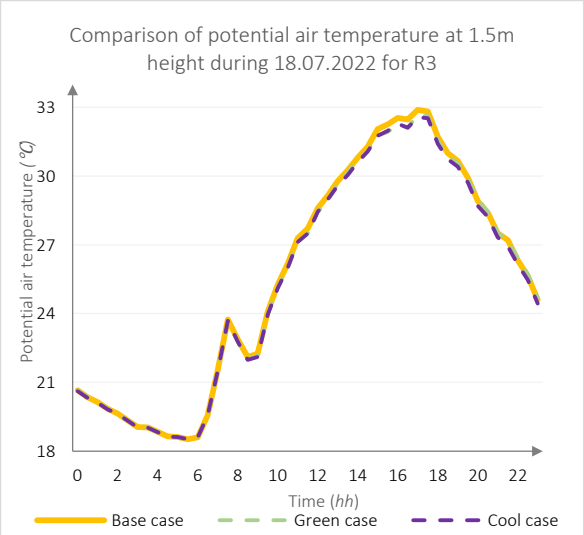

Graph 20 Potential air temperature comparison during 18th of July between scenarios at 1.5m height – R3 (source: Own elaboration, 2022; software: Excel)

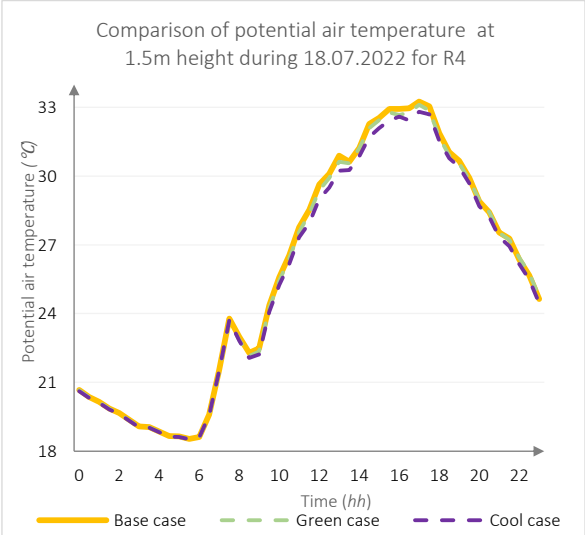

Graph 21 Potential air temperature comparison during 18th of July between scenarios at 1.5m height – R4 (source: Own elaboration, 2022; software: Excel)

5.2.2.2. Relative Humidity - Rh

Figure 36 shows the relative humidity patterns during the selected times. The *Cool Case* shows a slightly different pattern, similar to the one of T_{Air} among George Street and the perpendicular streets towards it, but the change is around 2-4%. The difference between Base Case and Cool Case does not appear to fluctuate through the day for the same area but remains almost constant. Regarding the *Green Case* with an increment of values near only George street, only on the southwest part.

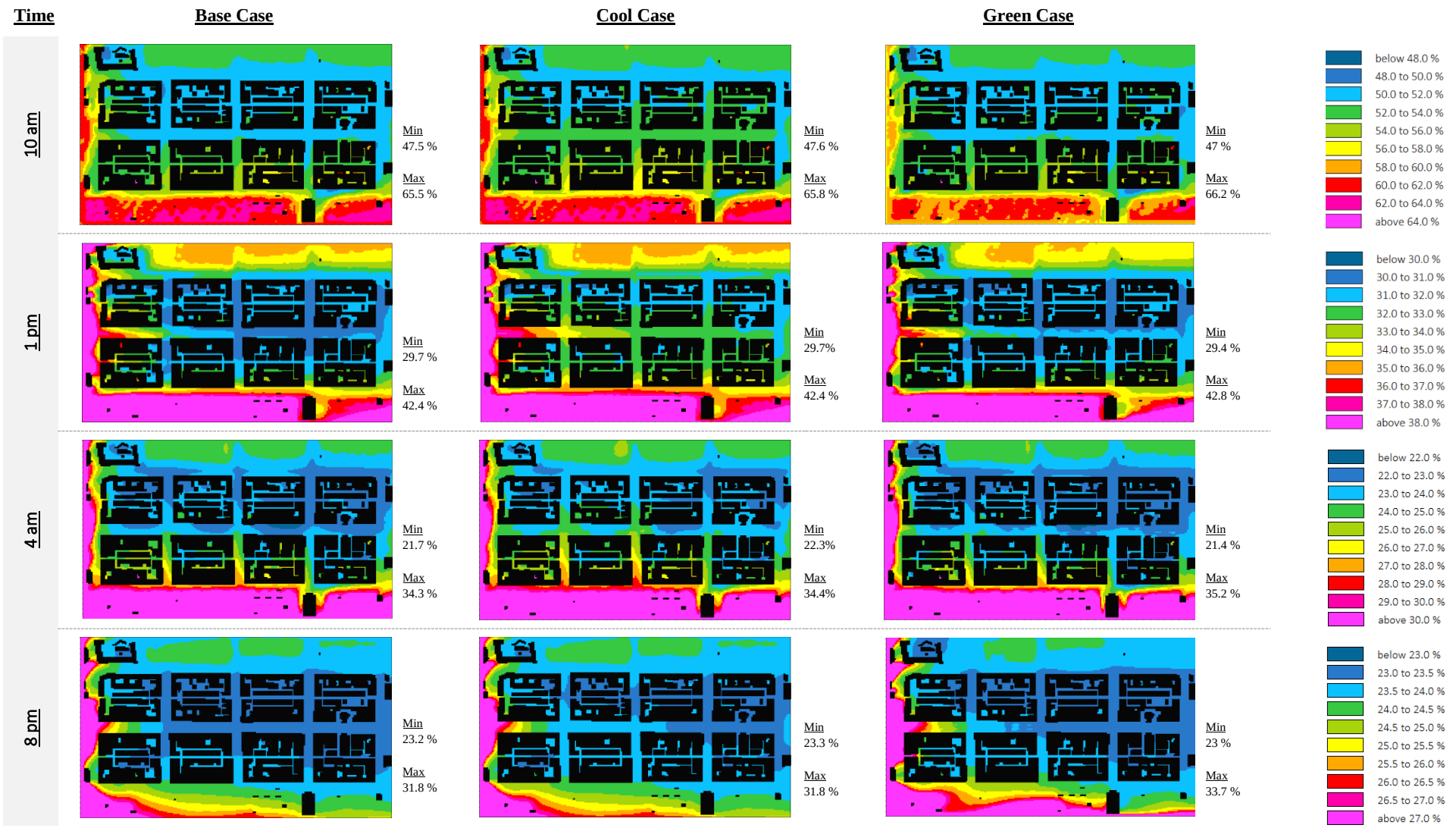

Figure 36 Simulated Relative Humidity during 18th July at 1.5m height (source: Own elaboration, 2022; software: ENVI-met®)

Points R2, R3 and R4, have the same relative humidity levels till 8 am, while R1 shows slightly higher values. While after 8 am till 6 pm, overall, the values start to drop for all points, and R3 is the point with the higher humidity (*Graph 22*). The lowest values are between 4 pm and 7 pm, and they start to rise. All the points' relative humidity values appear to have slightly increased in the *Cool Case (Graph 23)* from 8 am to 6 pm, and the change is more intensive for R2 and R4. Their value almost reaches the ones of R3. In the *Green Case (Graph 24,)* as expected, only R4 shows the difference in Rh between 10 am and 6 pm, but it does not surpass the values of R3. The values after that time are similar to the *Base Case*.

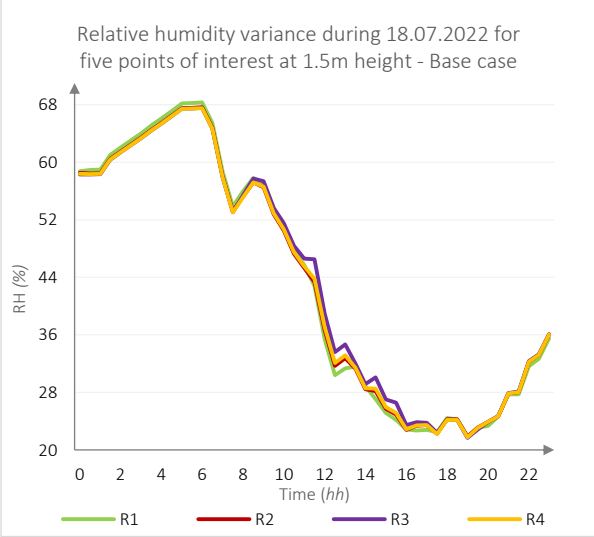

Graph 22 Relative humidity variance during 18th of July for 5 points at 1.5m height – Base case (source: Own elaboration, 2022; software: Excel)

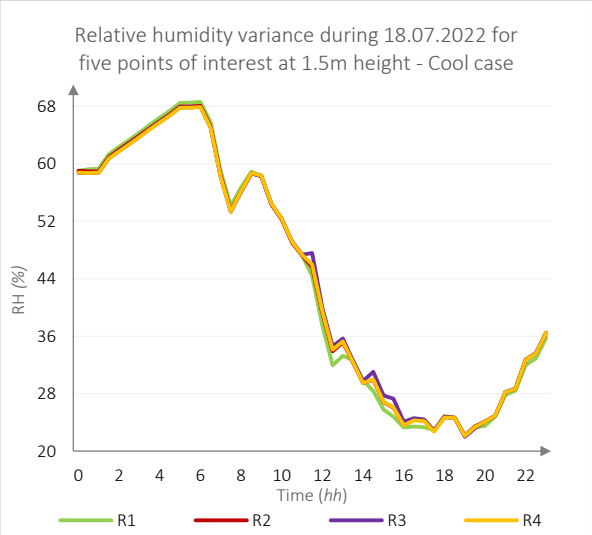

Graph 23 Relative humidity variance during 18th of July for 5 points at 1.5m height – Cool case (source: Own elaboration, 2022; software: Excel)

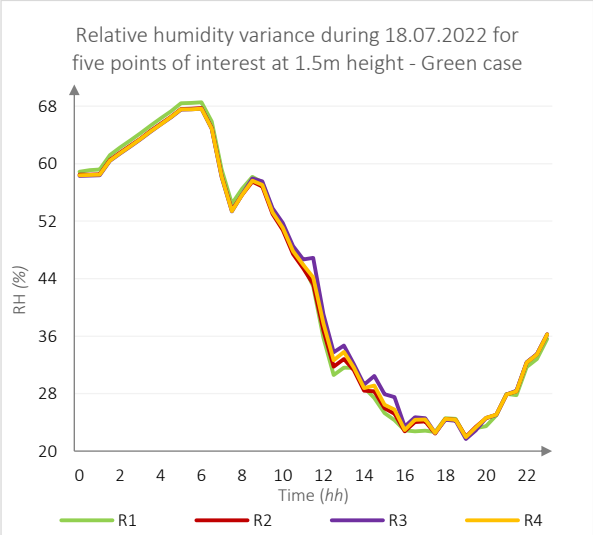

Graph 24 Relative humidity variance during 18th of July for 5 points at 1.5m height – Green case (source: Own elaboration, 2022; software: Excel)

Compared to the *Base Case*, the increment among the 4 points of interest is different (*Graphs 25, 26, 27 and 28*). As mentioned previously, the changes between scenarios start from 8am until 6 pm. *Green case* has impacted not much considerably only R4 as it is located near the green area. Regarding the *Cool Case*, all the points seem to have been affected as the Rh results are higher, but at R2, there is a major difference due to the cooling effect of the shade positioned. The slightest difference is at R3, as this point is mainly in the shadow during the entire day.

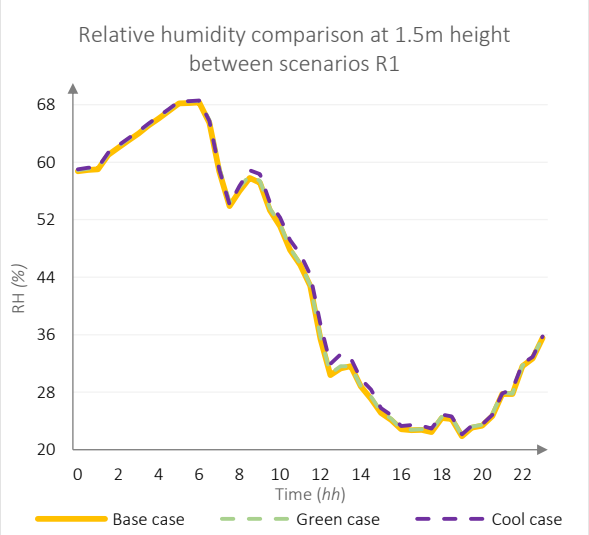

Graph 25 Relative humidity comparison during 18th of July between scenarios at 1.5m height – R3 (source: Own elaboration, 2022; software: Excel)

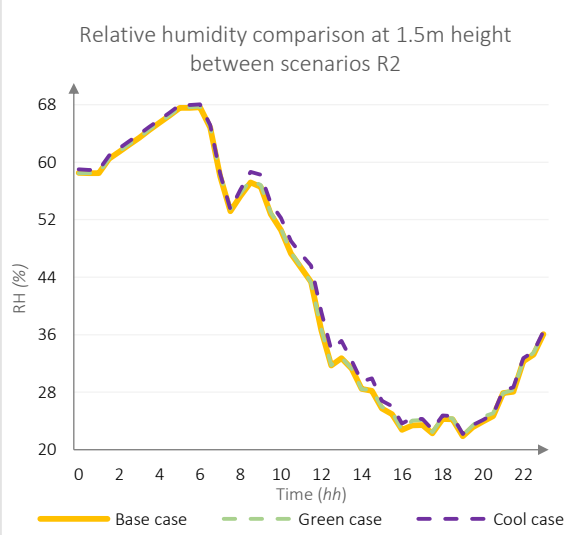

Graph 26 Relative humidity comparison during 18th of July between scenarios at 1.5m height – R3 (source: Own elaboration, 2022; software: Excel)

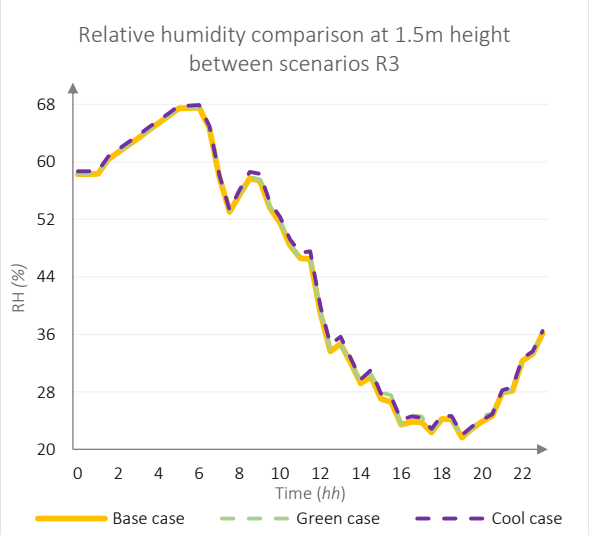

Graph 27 Relative humidity comparison during 18th of July between scenarios at 1.5m height – R3 (source: Own elaboration, 2022; software: Excel)

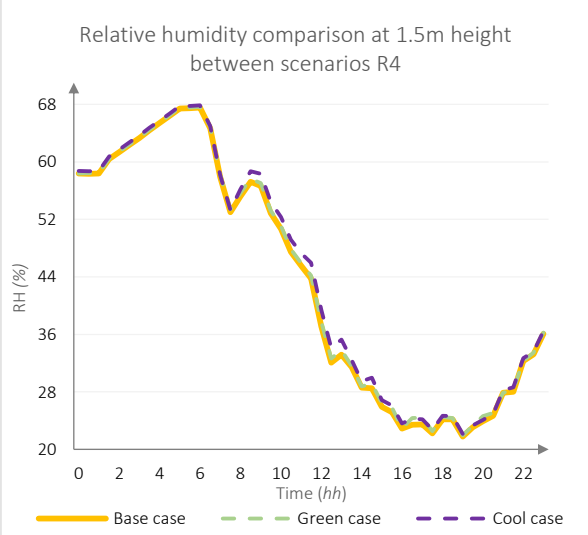

Graph 28 Relative humidity comparison during 18th of July between scenarios at 1.5m height – R3 (source: Own elaboration, 2022; software: Excel)

5.2.2.3. Mean Radian Temperature - T_{mrt}

The mean radian temperature patterns during the four timeframes (*Figure 37*), give an overview of the changes between the actual conditions of the site towards the *Green Case* and *Cool Case*. The difference is more notable between the *Base Case* and *Cool Case*. This difference is expected only along George Street and the perpendicular streets but not inside the eight blocks. However, in the *Green Case*, we can see considerable changes near the added green elements. The situations appear the same for the shade areas created in the *Cool Case*, which similar to the *Green Case*, the difference is reflected equally to the footprint of the interventions (shades and green elements), and the radius change does not exceed their footprint.

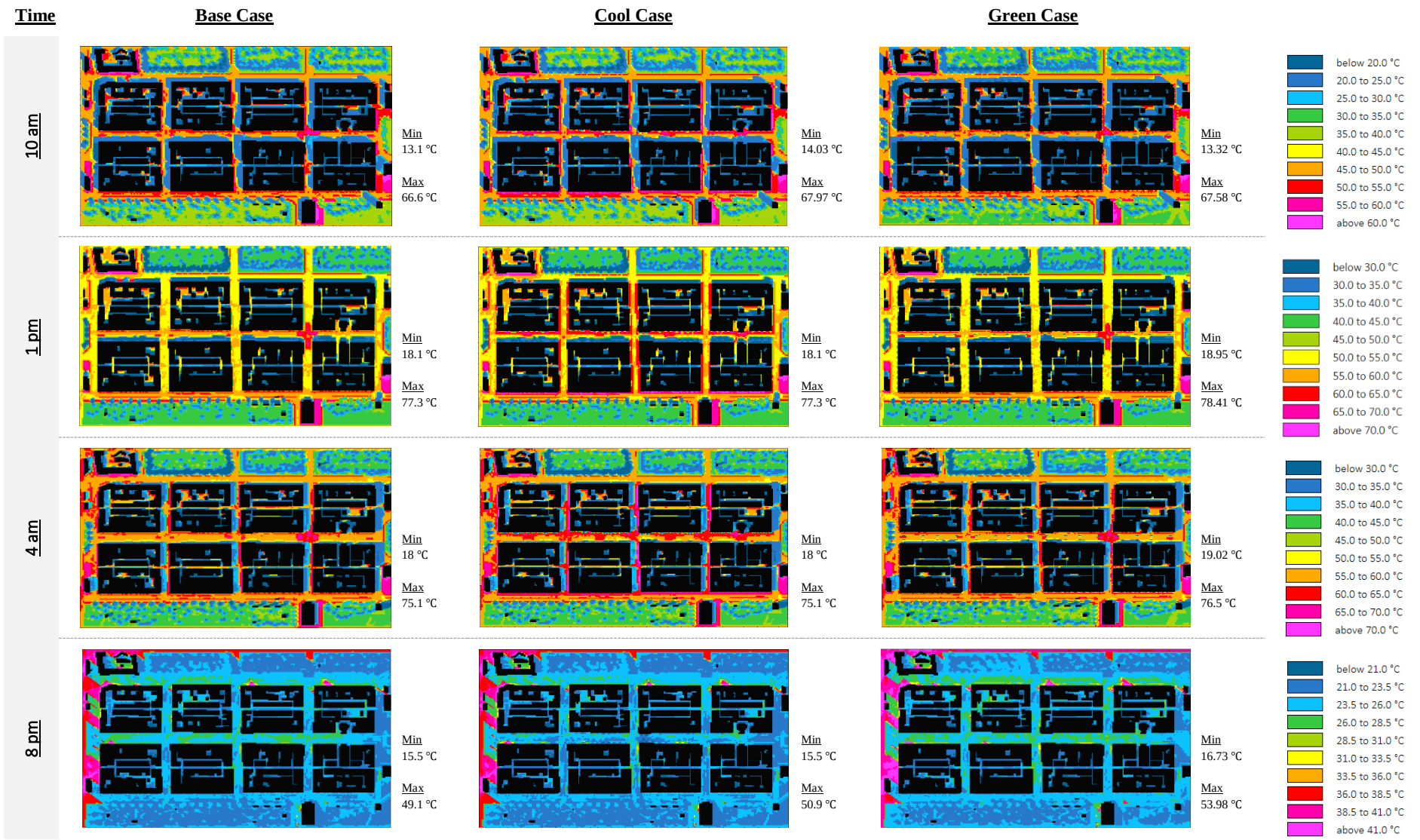

Figure 37 Simulated Mean Radiant Temperature during 18th July at 1.5m height (source: Own elaboration, 2022; software: ENVI-met®)

All the points have the same T_{mrt} till 6am (*Graph 29*). While after 6am till 8pm, the values start to rise and reach the maximum at 2pm till 4pm, and after that, the values start to drop. R3 is the point with the lowest T_{mrt} except from 6pm till 8pm. At 9.30am T_{mrt} value drops drastically for R1, a possible software error in calculation. T_{mrt} of R2 appears to have dropped drastically in the *Cool Case (Graph 30)* from 8am till 6pm. In the case of R1 and R4 T_{mrt} has increased, but for R1 the change is more considerable. In the *Green Case (Graph 31),* only R3 and R4 show lower values between 4pm and 8pm, and R3 is the colder spot.

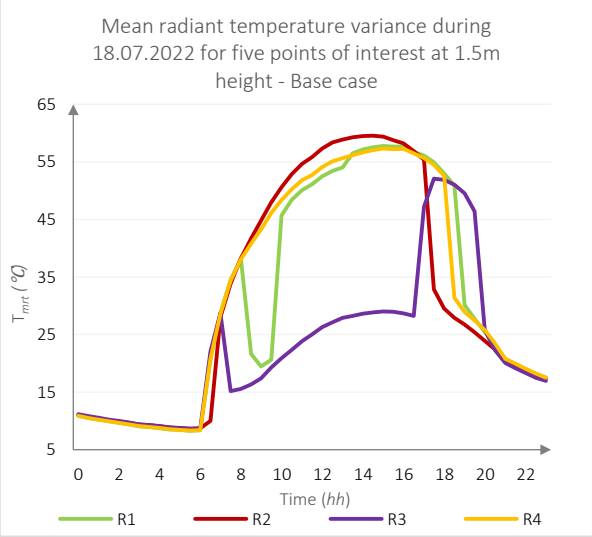

Graph 29 T_{mrt} variance during 18th of July for 5 points at 1.5m height – Base case (source: Own elaboration, 2022; software: Excel)

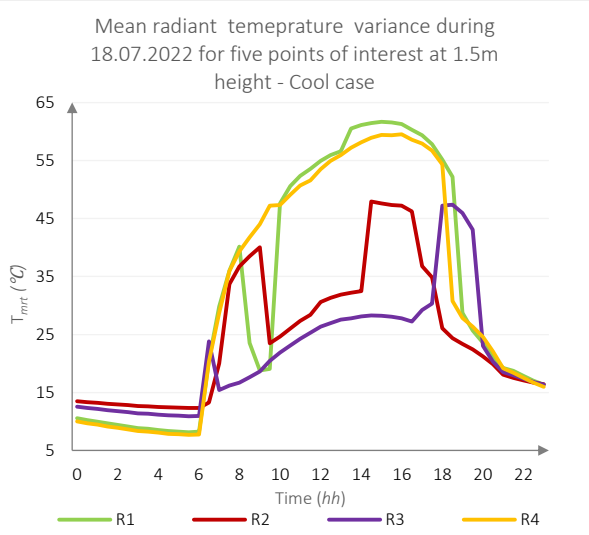

Graph 30 T_{mrt} variance during 18th of July for 5 points at 1.5m height – Cool case (source: Own elaboration, 2022; software: Excel)

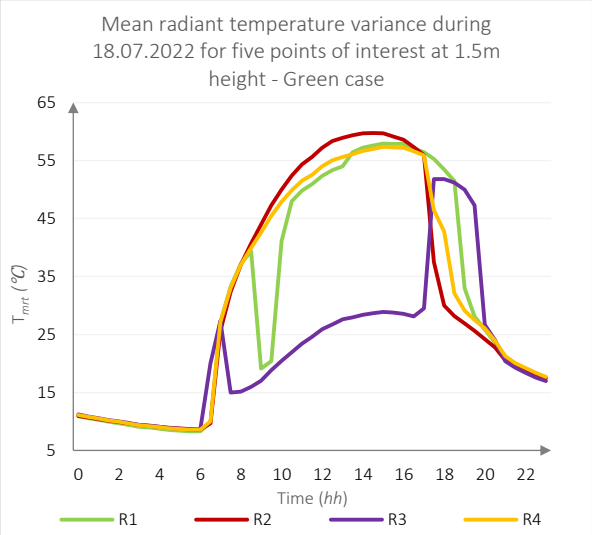

Graph 31 T_{mrt} variance during 18th of July for 5 points at 1.5m height – Green case (source: Own elaboration, 2022; software: Excel)

For R1 and R2 T_{mir} has increased in the *Cold Case* (*Graphs 32 and 35*), while for R2 and R3 T_{mir} has decreased. The effects of climate-sensitive solutions adapted into the two scenarios compared to the *Base Case* have different intensities among the 4 points of interest. As mentioned previously, the changes between scenarios start from 10am until 6 pm. *Green Case* seems not to have impacted the T_{Air} considerably, and the most impact is in R4 as it is located near the green area. Regarding the *Cool Case*, the intensity of changes is higher in R2; this is mainly because of the shade element positioned in that point. R3 has the least change intensity of T_{Air} from the beginning of the day till 6 pm and the cooling effect seems to appear after 6 pm, contrary to the other points.

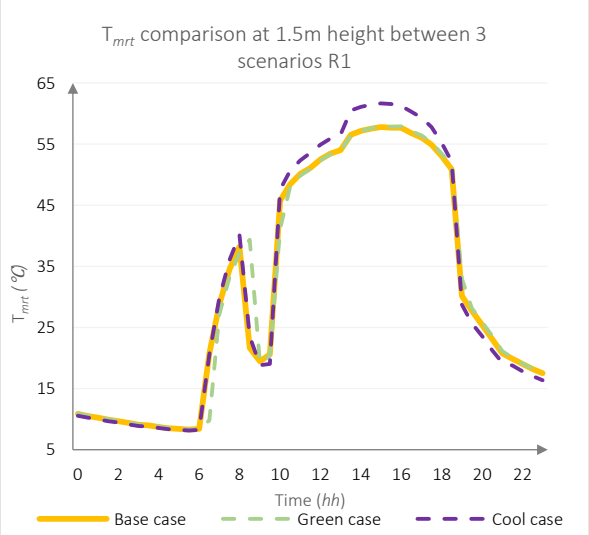

Graph 32 T_{mrt} comparison during 18th of July between scenarios – R1 (source: Own elaboration, 2022; software: Excel)

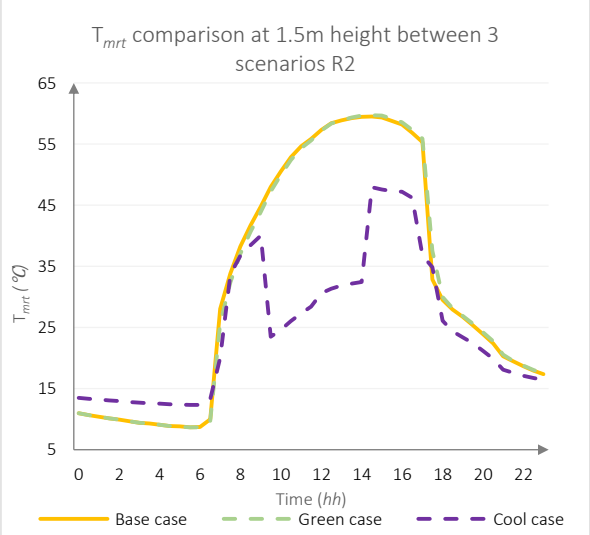

Graph 33 T_{mrt} comparison during 18th of July between scenarios – R2 (source: Own elaboration, 2022; software: Excel)

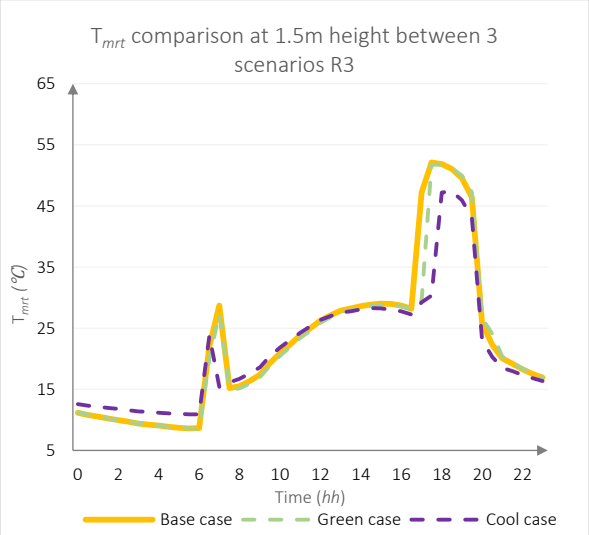

Graph 34 T_{mrt} comparison during 18th of July between scenarios at 1.5m height – R3 (source: Own elaboration, 2022; software: Excel)

Graph 35 T_{mrt} comparison during 18th of July between scenarios at 1.5m height – R4 (source: Own elaboration, 2022; software: Excel)

5.2.2.4. Physiological Equivalent Temperature - PET

In contrast to the above parameters, PET has a broader range of values throughout the site during the four time frames (*Figure 38*). There are changes between *Base Case* and *Green Case* even in areas with no new implementations. As all the input parameters are the same except for the green elements, these changes must be due to software errors. Similar to the case of T_{mrt}, the lowest PET is the footprint of shade areas in the *Cool Case* and green elements in the *Green Case*. At 8 pm there are no significant differences between scenarios.

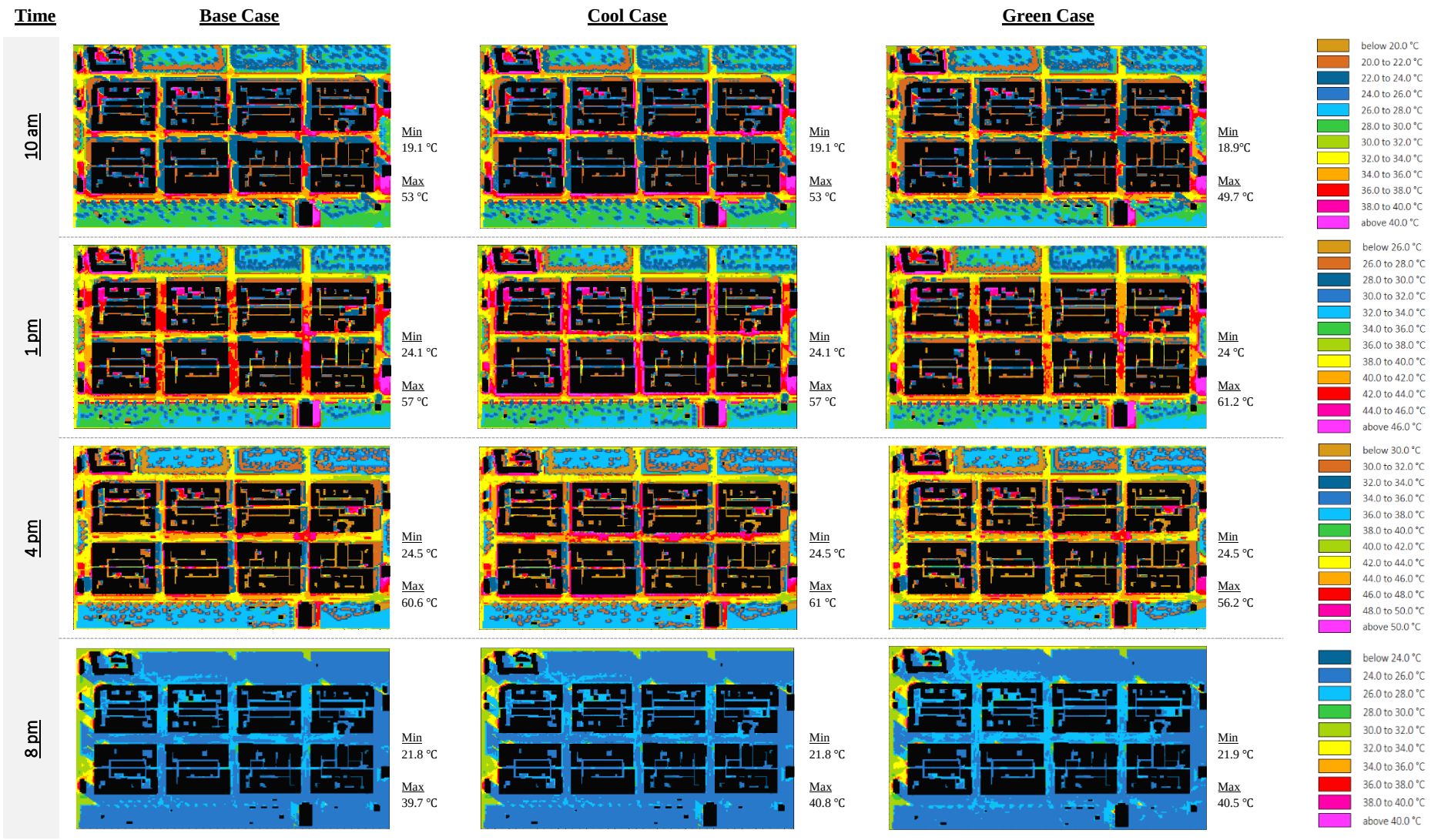

Figure 38 Simulated Physiological Equivalent Temperature during 18th July at 1.5m height (source: Own elaboration, 2022; software: ENVI-met®)

Similar to the MRT case, the results show different values of PET for each point. From the start of the day, till 7am, all the points have very similar values. The lowest PET value is at 6am (13℃). R2 shows the highest values during all day with a max of 44.2 ℃ at 4 pm; after then, R2 is the lowest (*Graph 36*). At 9.30 am PET value drops drastically for R1 due to the possibility of error in the calculation of T_{mrt}. R1 and R4 have similar PET along the day. R3 presents the lowest PET for most of the day, except from 5pm the values rise till R3 has the highest values. From 8pm till the end of the day, PET values drop for all the points and have very similar values.

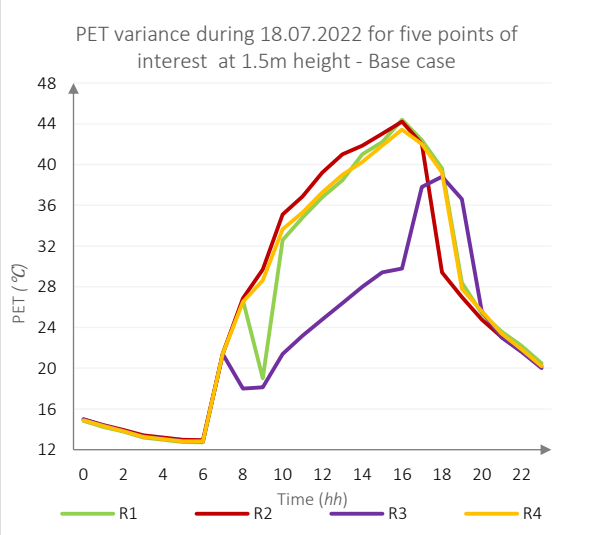

Graph 36 PET variance during 18th of July for 5 points – Base case (source: Own elaboration, 2022; software: Excel)

In the *Cool Case*, the points do not have any more approximately the same value from the start of the day till 7 am (*Graph 37*). R1 is the point with the highest increased PET and became the hottest among the points. R2 is the point with the most visible decrease of PET values from 8am to 6 pm, and the change is more considerable for R2 and R4. Their value almost reaches the ones of R3. In the Green Case (*Graph 38*), only R4 shows a slight decrease in PET. The same anomalies of R1 at 9.30 am are presented in both scenarios as in the *Base Case*. In all the cases, the highest PET reaches the maximum at 4pm, similar to the maximum air temperature recorded on the 18th of July in Edinburgh for R1, R2 and R4. The maximum for R3 is reached around 6 pm.

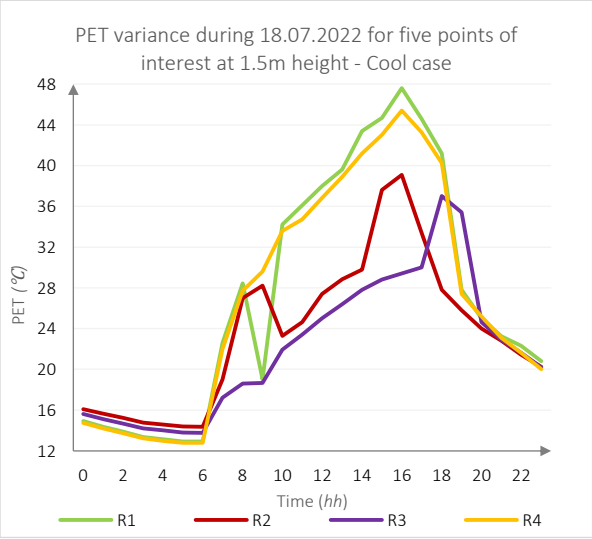

Graph 37 PET variance during 18th of July for 5 points at 1.5m height – Cool case (source: Own elaboration, 2022; software: Excel)

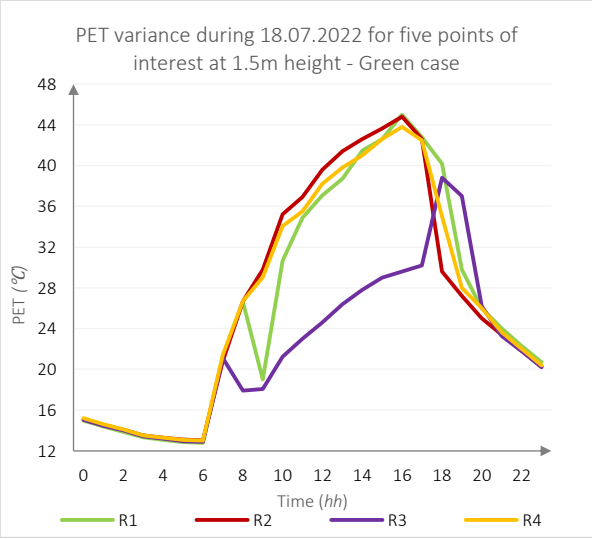

Graph 38 PET variance during 18th of July for 5 points at 1.5m height– Green case (source: Own elaboration, 2022; software: Excel)

The behaviour of PET after the interventions adapted into the two scenarios compared to the *Base Case* is different among the four points of interest (*Graphs 39, 40, 41 and 42*). For R2 and R3, PET changes start at the beginning of the day. *Green case* seems not to have impacted the PET, and changes consist of small increments in PET. Only at R3 between 4pm and 6pm, there is a considerable decrease in PET. Regarding the *Cool Case* for R1 and R4, the changes consist of an increment in PET, while in the case of R2 and R3; PET has decreased considerably for R2. The pattern of PET change for R2 does not seem to follow a similar trend as the other points during the day.

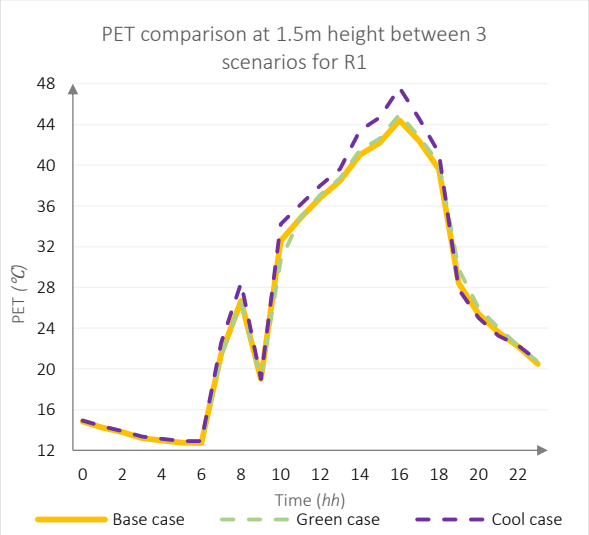

Graph 39 PET comparison during 18th of July between scenarios – R1 (source: Own elaboration, 2022; software: Excel)

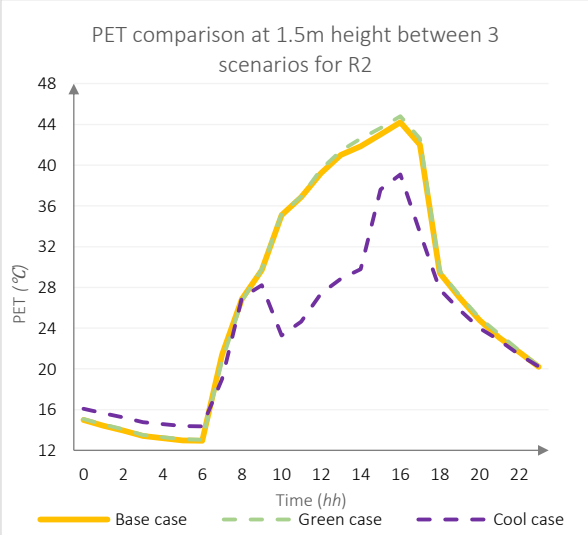

Graph 40 PET comparison during 18th of July between scenarios – R2 (source: Own elaboration, 2022; software: Excel)

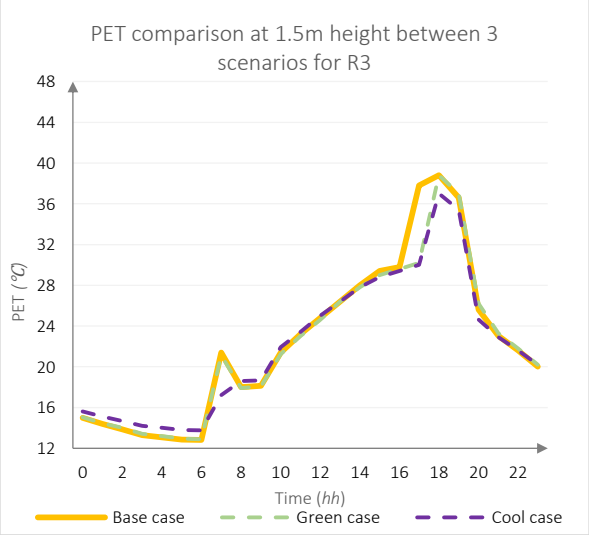

Graph 41 PET comparison at 1.5m height during 18th of July between scenarios – R3 (source: Own elaboration, 2022; software: Excel)

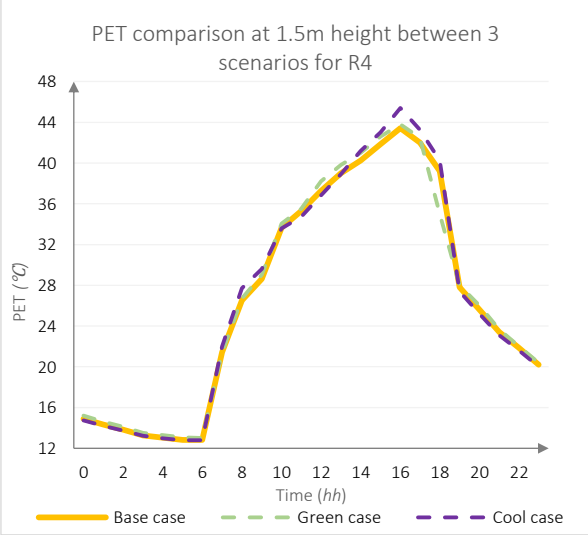

Graph 42 PET comparison at1.5m height during 18th of July between scenarios – R4 (source: Own elaboration, 2022; software: Excel)

CHAPTER 6: DISCUSSION

6.1. LCZ

The merit of LCZ scheme lies in its detailed classification of urban land-use type [Wang *et al.*, 2018]. The input data used come from remote sensing image analysis, the output quality is improved compared to the general classification through the basis method.

6.1.1. Morphological parameters

Morphological parameters help to define bias characteristics of urban settlements [Wicki and Parlow, 2017], are much easier to calculate and independent from sun position or surface materials, allowing a comparison between cities with different geographic locations. These two last characteristics can be evaluated through the thermic parameters, but need more accurate data and expertise. However, it is important to point out that also the morphological parameters can have different opinion on how to be calculated, as the results might be different [Wicki and Parlow, 2017]. Regarding the mean building height in fact there are different method of calculations, such as masking the ground pixels, therefore considering only the building pixels; or including the ground pixels and considering them 0. Steward and Oke [2012] consider the geometric average of building height. In this study the weighted average mean building, omitting the ground pixels was adapted, as it was connected to the further calculations of the other morphological parameters and due to the 15m aggregation resolution.

6.1.2. Combination of LULC and morphological parameters

A perfect fit for each build-up class through morphological parameters was not achieved. Some classes could fit in one LCZ through 4 parameters, while come other classes resulted to fit in more than one. To prevent the overlapping of the thresholds, and avoiding different LCZ classes affiliated with one LULC class, the LULC classification should represent more specific land use category. An example is the problem with I1 class, which include the *Industrial, commercial, public, military and private units* (*Annex 4*). These classes include also the mix use building and in sense of commercial units, there are throughout the city, especially in the Old Town and this is the area with the most ununiformed pattern. Some LULC classes as R1/ R2and R3 have been classified with unusual LCZ class. This is due to the fact that the LULC map was created in e different geographical projection system rather than British National Gird, and it is accompanied with errors while geographically transforming, compared to the high resolution of the data origin of the other parameters. However the LULC map used is only as an input factor in this case, but the use for future classification is very promising [Wilow and Parlow, 2017]. In creating a more detail LULC map, taking into consideration culture heritage aspect, might result need to new range values of thresholds for each LCZ class or new LCZ classes.

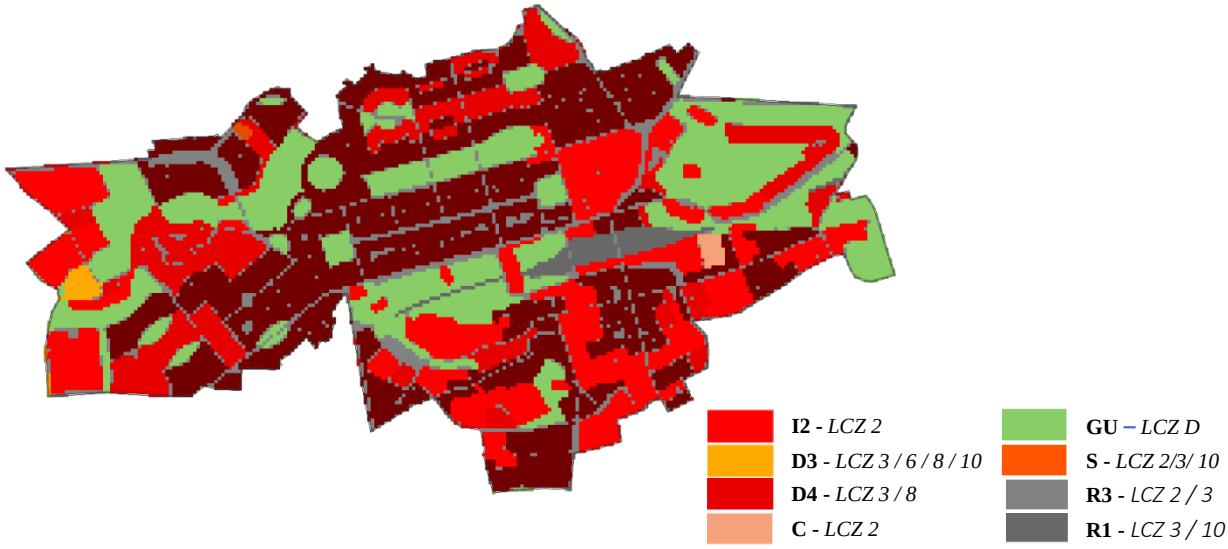

Figure 39 Close up of conceptual LCZ map in the area of the World Heritage property - New Town and Old Town (source: Own elaboration, 2022)

6.1.3. Potential aggregations in the future

The actual method allows for wide dynamicity in potential aggregation, which may consist of two aspects: LULC classification or method of data discretisation. The first one allows to capturing the heterogeneity of a city, which is useful in cases of European cities and can be tailored to specific conditions of the study area. Regarding historic urban towns, the classification of LULC can introduce classes representing cultural heritage elements. The representation can be in different scales and methods. One potential option is classifying based on the UNESCO Paris Convention of 1972 classification (*Table 24*). In this case, there is a level of standardisation and different historic towns LCZ can be compared with each other. However, nowadays, there are attempts to classify cultural heritage assets based on architectural and construction characteristics, including their location's climatic conditions energy performance. An example is following the classification proposed by the project Climate for Culture [Eibl, 2010] (*Figure 40*).

Table 24 Definition and classification of culture heritage based on the Paris Convention of 1972. (source: UNESCO – World Heritage Centre, 1972)

Monuments	architectural works, works of monumental sculpture and painting, elements or structures of an archaeological nature, inscriptions, cave dwellings and combinations of features, which are of outstanding universal value from the point of view of history, art or science;
Groups of buildings	groups of separate or connected buildings which, because of their architecture, their homogeneity or their place in the landscape, are of outstanding universal value from the point of view of history, art or science;
Sites	works of man or the combined works of nature and man, and areas including archaeological sites which are of outstanding universal value from the historical, aesthetic, ethnological or anthropological point of view.

Category	Use	Volume	Construction	
Church	sporadic	Huge	Heavy	
Museum	permanent	Small huge	Light heavy	
Palace	permanent seasonal	Huge	Heavy	
Residential	permanent seasonal	Small	Light heavy	
Outstanding	all	all	all	

a

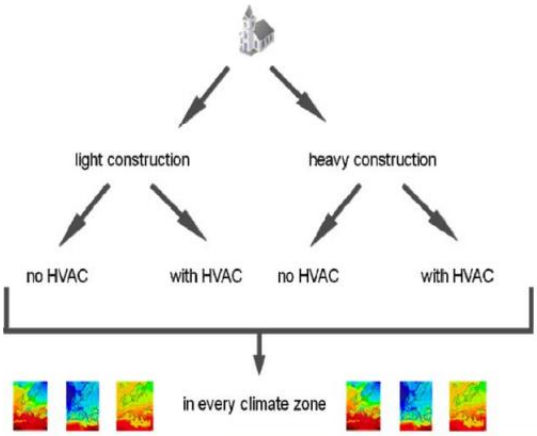

b

Figure 40 Example of simple classification of culture heritage assets proposed from Climate for Culture project. a) architectural and building structure; b) climatic condition and building structure energy performance (source: Eibl, 2010)

The second can influence the final results as it is connected with the calculation. Choosing between the five different methods: lot area polygon, urban block, regular grid (cell size is variable here), neighbourhood (*Figure 41*) and sensor unit area, can be for different reasons. For instance, choosing a regular grid of 100m size can help compare the final LCZ map between the GIS method and WUDAPT protocol to determine which one detects the city's heterogeneity more efficiently, similar to studies in high-density cities [Wang et al., 2018].

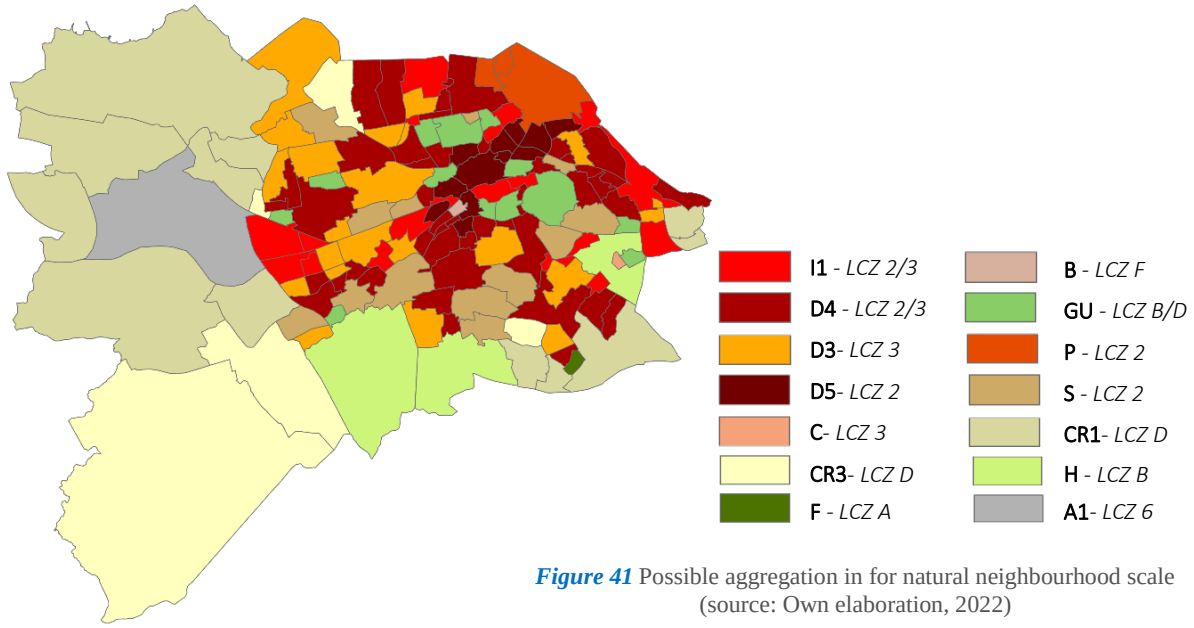

Figure 41 Possible aggregation in for natural neighbourhood scale (source: Own elaboration, 2022)

6.1.4. Limitations

Land Use/Land Cover (LULC) was a very part of the aggregation of LCZ. Due to a lack of time delivering this study, it was impossible to create an updated LULC map for Edinburgh through remote sensing. Meanwhile, the City of Edinburgh Council does not offer high-resolution versions. Finally, the LULC used, even though it is provided in GIS format, is created through remote sensing. This LULC classification did not contain any class related to cultural heritage. Developing the morphological parameters through GIS-method requires immense data, which datasets might not be available globally. The data used in this study combines GIS and remote sensing data such as the LIDAR data in cloud point format from

Scotland Service. The data with the highest probability of error is the vegetation layer, as LIDAR dataset available was unclassified. On the contrary of the DEM and DSM, retrieved from the same dataset, in which the comparison with other older versions of DEM and DSM could be conducted, the vegetation layer could only be compared and validated in only some areas, mainly urban parts. All the errors from this layer were transferred during the calculation of the Sky View Factor. However, this factor can be neglectable, as the focus was more on the urban cultural heritage area. Regarding the calculation of aspect ratio, the software had some limitations as could only calculate the street canyon H/W ratio, and it could not calculate the building height–spacing ratio for LCZs 8–10 and the tree height–spacing ratio for LCZs A–G. Due to the difficulty of calculating the terrain roughness parameter and the thermal, radiative, and metabolic parameters [Quan and Basal, 2021], the classification was based on only six morphological parameters. However, as the impervious surface fraction (IPS) was calculated in an indirect way, the probability of errors for impervious surface fraction is increased. This parameter and the pervious impervious surface fraction as were calculated from the LULC classification map, did not match perfectly the real situation, as the original geographic projection system this data is created is not the same with the British National grid and the geographic transformations reduces the accuracy.

6.2. Outdoor thermal comfort

6.2.1. Thermal sensation

Overall the difference in air temperature has change visibly only in the *Cool Case (Figure 42)* and the interventions in this scenario have reduced the T_{Air}. The effect is measurable in the areas which are exposed in direct radiation during the day, therefore we can see in the site differences up to 0.8℃ mainly building faces facing south during the day, as Edinburgh is located in the North hemisphere. This reduction is positive as usually East-West oriented street constantly exhibits higher air temperature than the streets perpendicular to them [Valdez, 2021]. Also, as the pick hour is 4pm, the faces building faces facing west – southwest will show a difference. In the centre the difference is bigger, as in this point not only the actual area has changed, but also the surrounding, bringing more change. It is important to point out that air temperature depends on wind speed and direction and the software applies these parameters from the border of the site.

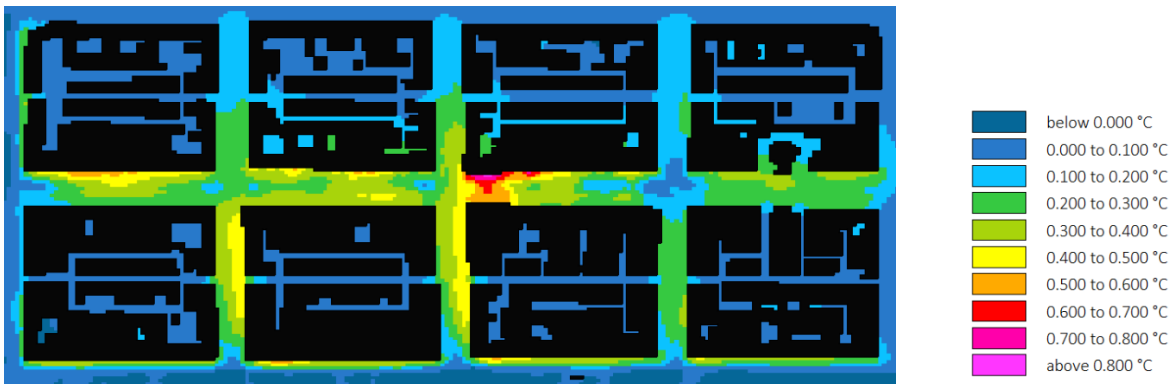

Figure 42 T_{Air} absolute difference between *Base Case* and *Cool Case* at 4pm 18th of July (source: Own elaboration)

The magnitude of change resulted different in each point of interest conducted as these points where chosen for their different characteristics, starting for location. R2 exposed to the direct sun all day overcomes up to a reduction till 3% up T_{Air}. This reduction is a result of both changes of material and shaded elements. R3 represents the least change but it is important to say that the changes are close to linear, 0.5 – 1% from 8am till the end of the year. Comparing R1 and R2, both exposed to direct solar radiation, we understand that the use of high albedo ground surface materials is more effective accompanied by shading. In case of the *Green Case*, there are times of the day, when the T_{Air} is actually increased.

Table 25 Summary of T_{Air} parameter change for 5 points (source: Own elaboration, 2022; software: Excel)

Scenario	*Base Case*	*Cool Case*	*Green Case*
Min T_{Air} (°C)	18.338	18.324	18.31
	18.519	18.521	18.504
	18.516	18.514	18.506
	18.536	18.518	18.516
Max T_{Air} (°C)	33.003	32.621	32.914
	33.319	32.737	33.325
	32.89	32.563	32.641
	33.257	32.807	33.11
Average T_{Air} (°C)	25.618	25.406	25.583
	25.815	25.516	25.784
	25.546	25.4	25.463
	25.779	25.532	25.697
Change of T_{Air} from *Base Case* at 4 pm (°C)	0	0.382	0.101
	0	0.466	0.179
	0	0.252	0.295
	0	0.334	0.254
	R1	R2	R3	R4

Graph 43 Change of T_{Air} between *Base Case* and *Cool Case* for 5 points of interest in % (source: Own elaboration, 2022; software: Excel)

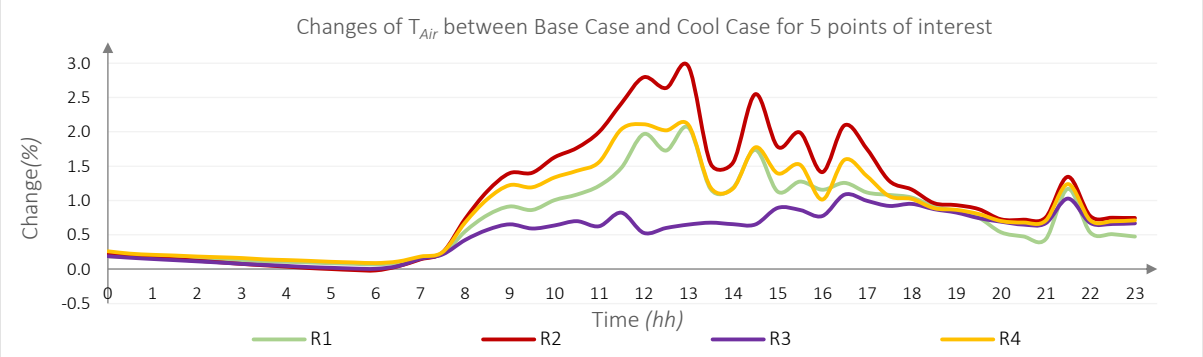

Graph 44 Change of T_{Air} between *Base Case* and *Cool Case* for 5 points of interest in % (source: Own elaboration, 2022; software: Excel)

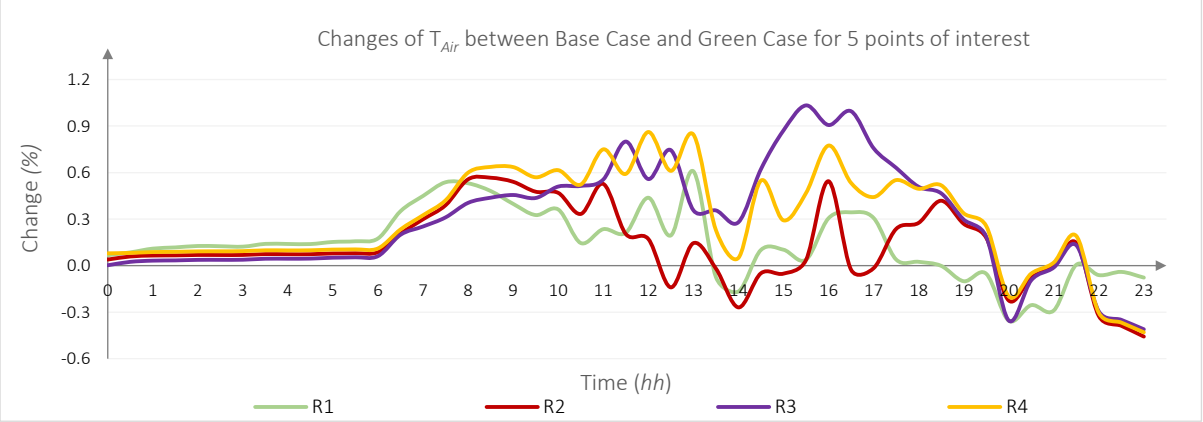

Relative humidity changes as expected are the opposite of the temperature trend. In both scenarios the relative humidity has increased. In *Cool Case* R2 reaches an increment till 7.5%. For all the points there is a drastic lack of change at 2pm as at that time the wind direction comes from the south and the buildings act as a barrier for the wind in George Street [Talhegani *et al.*, 2015]. In case of the *Green Case*, the small changes for R1, R2 and R3 might have come due to wind direction and speed change from the hedges and the large shrubs. These fluctuations, similar to the one of air temperature, matches the changes the wind trajectory, showing that the urban morphology plays an important role in wind patterns and consecutively to the climate parameters.

Table 26 Summary of Rh parameter change for 5 points (source: Own elaboration, 2022; software: Excel)

Scenario	*Base Case*	*Cool Case*	*Green Case*
Min Rh (%)	21.85	22.14	21.97
	21.85	22.19	22.02
	21.66	22.02	21.7
	21.78	22.12	21.95
Max Rh (%)	68.32	68.57	68.55
	67.63	68.03	67.72
	67.55	67.89	67.62
	67.53	67.84	67.64
Average Rh (%)	43.424	22.14	43.632
	43.352	22.19	43.529
	43.795	22.02	43.997
	43.387	22.12	43.688
Change of Rh from *Base Case* at 4 pm (%)	0	-0.47	-0.07
	0	-0.85	0.04
	0	-0.63	0
	0	-0.72	-0.07
	R1	R2	R3	R4

Graph 45 Change of Rh between *Base Case* and *Cool Case* for 5 points of interest in % (source: Own elaboration, 2022; software: Excel)

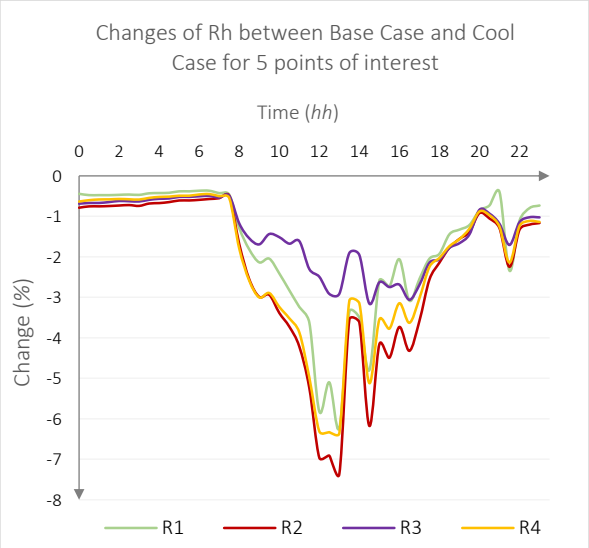

Graph 46 Change of Rh between *Base Case* and *Green Case* for 5 points of interest in % (source: Own elaboration, 2022; software: Excel)

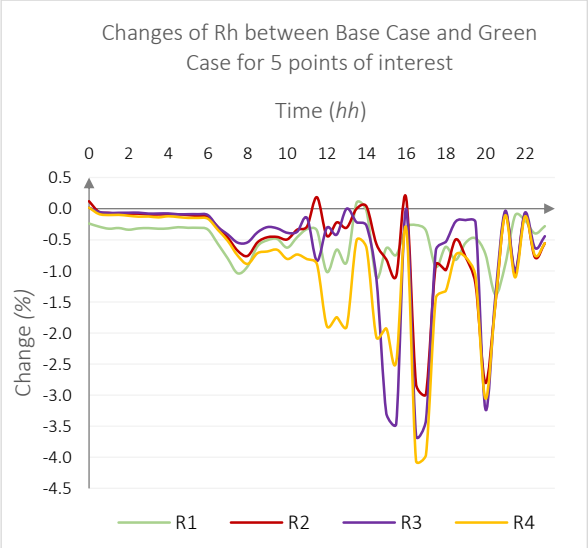

Mean radiant temperature (T_{mrt}) is play a vital role in human thermal comfort and during summertime is the driving parameter of the PET index. T_{mrt} is directly linked to the short- and longwave radiation exchange of a standard human, therefore thermic building properties tend to have an impact in T_{mrt} value ranges. In general, the change of material (*Cool Case*) has decreased the T_{mrt} only by 4℃ at 4pm, but in cases near the shaded areas the decrease is around 24 ℃. However, the shaded elements positioned near the northeast facades are not affecting the T_{mrt} at this time.

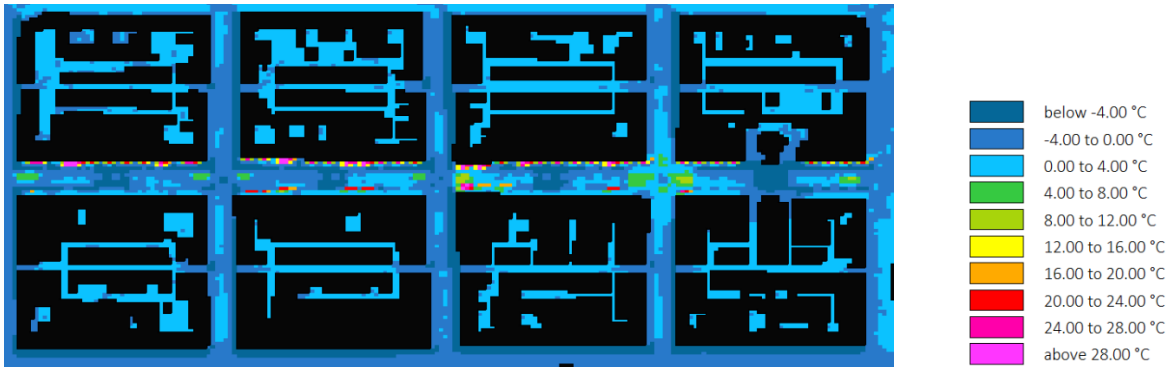

Figure 43 T_{mrt} absolute difference between *Base Case* and *Cool Case* at 4pm 18th of July (source: Own elaboration)

In *Cool Case* R2 is the most affected with decrease up to 45% of T_{mrt}, showing that the change in albedo and the shade have had a huge impact in the accumulated heat at that point. The opposite happens during the start of the day, T_{mrt} results higher then *Base Case*, as all the accumulated heat is released. R1 and R4 are points that are not affected also by the shade of the buildings during the day; therefore the change is more consistent during the day (around 5%). *Graph 47* shows that when the solar radiation angle is near 0 the R2 and R3 have similar trend line between them, but different from R1 and R4. Probably these points are affected by the thermal properties of the buildings. This result is expected as T_{mrt} is more affected by urban geometry [Taleghani *et al.*, 2015].

Table 27 Summary of T_{mrt} parameter change for 5 points (source: Own elaboration, 2022; software: Excel)

Scenario	*Base Case*	*Cool Case*	*Green Case*
Min T_{mrt} (°C)	8.29	8.13	8.3
	8.67	12.33	8.65
	8.6	10.91	8.58
	8.31	7.68	8.56
Max T_{mrt} (°C)	57.78	61.68	57.9
	59.54	47.96	59.76
	52.13	47.41	51.79
	57.32	59.54	57.38
Average T_{mrt} (°C)	31.454	32.31	31.543
	32.067	24.853	32.066
	22.814	21.782	22.338
	32.656	32.592	32.015
Change of T_{mrt} from *Base Case* at 4 pm (°C)	0	-3.58	-0.19
	0	11	-0.37
	0	0.93	0.14
	0	-2.28	0.05
R1	R2	R3	R4

Graph 47 Change of T_{mrt} between *Base Case* and *Cool Case* for 5 points of interest in % (source: Own elaboration, 2022; software: Excel)

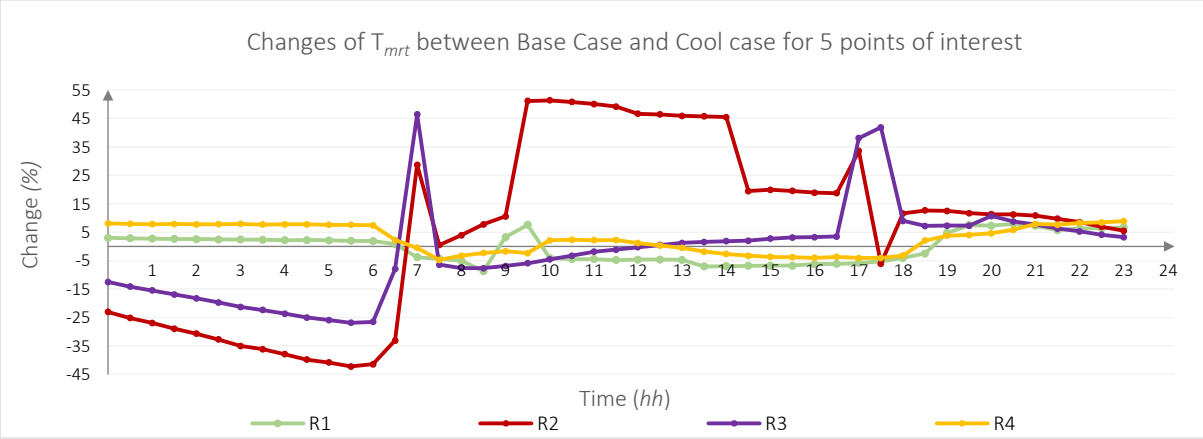

In the *Base Case* in the central axis PET reaches 44℃, which for a tourist walking would implicate an extreme heat stress, but in the actual case the axis is a vehicle road, not pedestrian path. However, in the George street proposal, PET is increased by almost 4℃ (*Figure 44*), as high albedo can lower air temperature but it can affect in a negative way the psychophysical wellbeing of the pedestrians [Salata *et al.*, 2015]. The opposite has resulted regarding the thermal comfort under the new shading elements near the southeast building facades, overgoing an improvement, as for example at 4pm PET was decreased by 13℃.

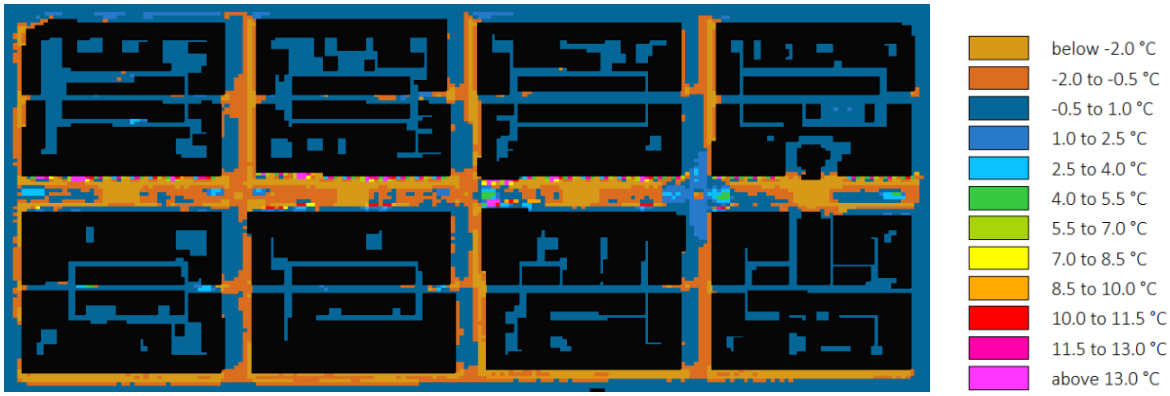

Figure 44 PET absolute difference between *Base Case* and *Cool Case* at 4pm 18th of July (source: Own elaboration)

In *Cool Case* R2 is the most affected with decrease up to 35% of PET and this is due to the change $T_{mrt.}$ At 7am and 5pm there are both R2 and R3 have unexpected difference compared to the *Base Case*, probably due to software error, or wind direction change. From 8am till 1pm the effects the changes have led to increase of PET, but the change is within 5%. R4 is the point with more linear change. In the *Green Case* R3 shows unexpected change at 5 pm (20%). In case of R4 which is near the new green elements, PET has mostly increased, apart from the one at 5pm. This is probably due to the fact that the green elements are not very high and cannot provide shade over the height of tourists.

Table 28 Summary of PET parameter change for 5 points (source: Own elaboration, 2022; software: Excel)

Scenario	*Base Case*	*Cool Case*	*Green Case*
Min PET (℃)	12.722	12.906	12.801
	12.934	14.356	13.037
	12.816	13.746	12.889
	12.805	12.778	13.02
Max PET (℃)	44.407	47.601	45.001
	44.201	39.094	44.801
	38.801	37.001	38.801
	43.429	45.4	43.802
Average PET (℃)	26.42	27.256	26.598
	26.802	23.558	27.003
	22.47	22.092	22.176
	26.765	27.009	26.938
Change of PET from *Base Case* at 4 pm (℃)	0	-3.194	-0.594
	0	5.107	-0.6
	0	0.398	0.2
	0	-1.971	-0.373
R1	R2	R3	R4

Referring back to the PET, the parameter increases during the start of the day and in the evening. Regarding the start of the day till 6am, the increase occurs due to the releasing of heat stored during the previous day (17.07.2022), and in the evening is due to the heat stored during the day (18.07.2022).

Graph 48 Change of PET between *Base Case* and *Cool Case* for 5 points of interest in % (source: Own elaboration, 2022; software: Excel)

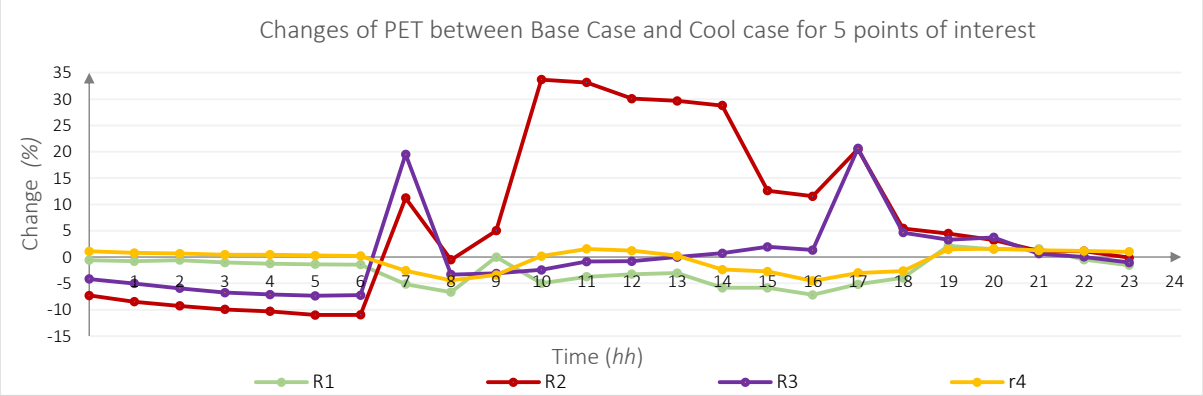

Graph 49 Change of PET between *Base Case* and *Green Case* for 5 points of interest in % (source: Own elaboration, 2022; software: Excel)

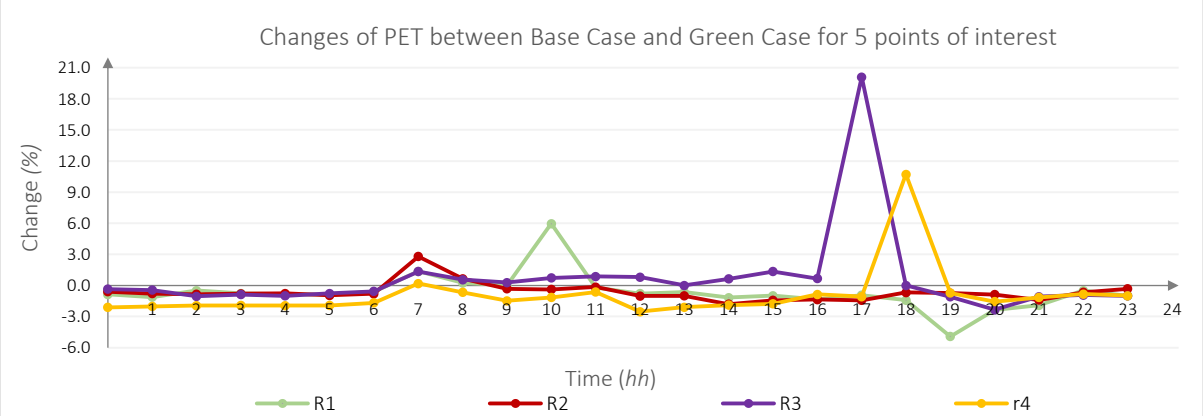

Different climates vary on the comfort ranges and this ranges also changes during seasons [Nasrollahi *et al.*, 2017]. Researchers have studied these indices in large geographical scale and in terms of daily, monthly and seasonal timeframes (*Figure 45*). The comparison with the results achieved from ENVI-met software is compared with previous studies of locations with the similar climate, as due to time it was impossible to organise a field questionnaire to investigate the tourists' thermal satisfaction on the local climate of the site. As Edinburgh has a temperate climate, the comparison of thermal sensation is made with case studies with similar climate like in countries in North and West of Europe.

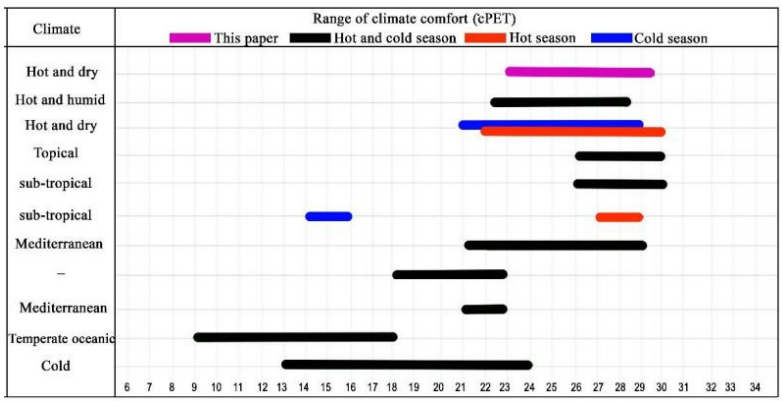

Figure 45 Thermal comfort range of PET in different studies (source: Nasrollahi *et al.*, 2017)

In *Base Case* only R3 is within desirable comfort range for most of the time, while in other points from 9am till 7pm tourists would be in seriously heat stress. In the *Cool Case* R2 reaches the desirable comfort range. In the Green Case there are not considerable changes and the R1, R2 and R4 are still locations where a tourist can experience seriously heat stress. In both cases in R1 where the space is designated for events, it is suggested that organisers avoid 10am till 6pm as it will not be comfortable for the audience. Visitors wanting to spend time in the sitting area, this time frame would not be very comfortable during hot sunny days.

Graph 50 Comparison between PET and comfort range - *Base Case* for 5 points of interest (source: Own elaboration, 2022)

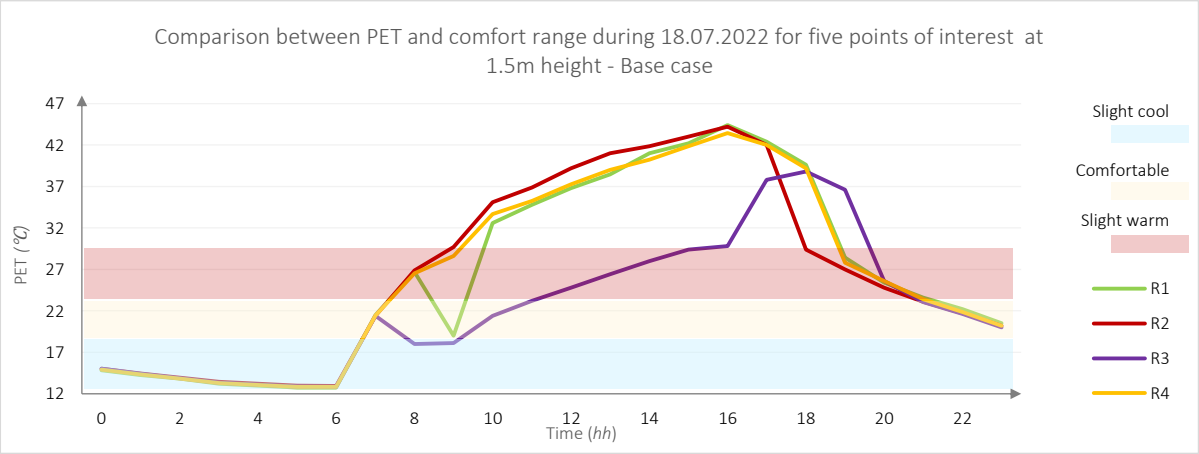

Graph 51 Comparison between PET and comfort range - *Cool Case* for 5 points of interest (source: Own elaboration, 2022)

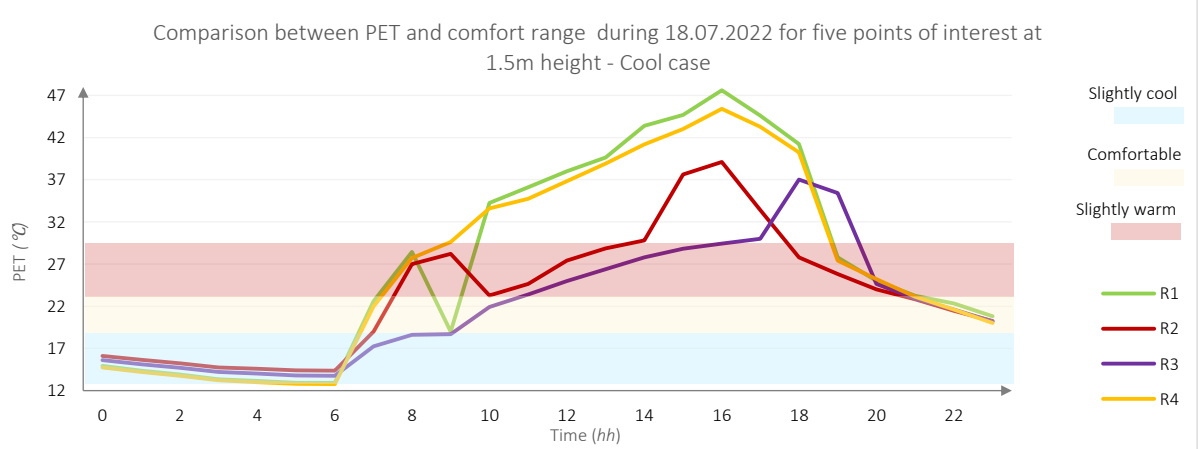

Graph 52 Comparison between PET and comfort range – *Green Case* for 5 points of interest (source: Own elaboration)

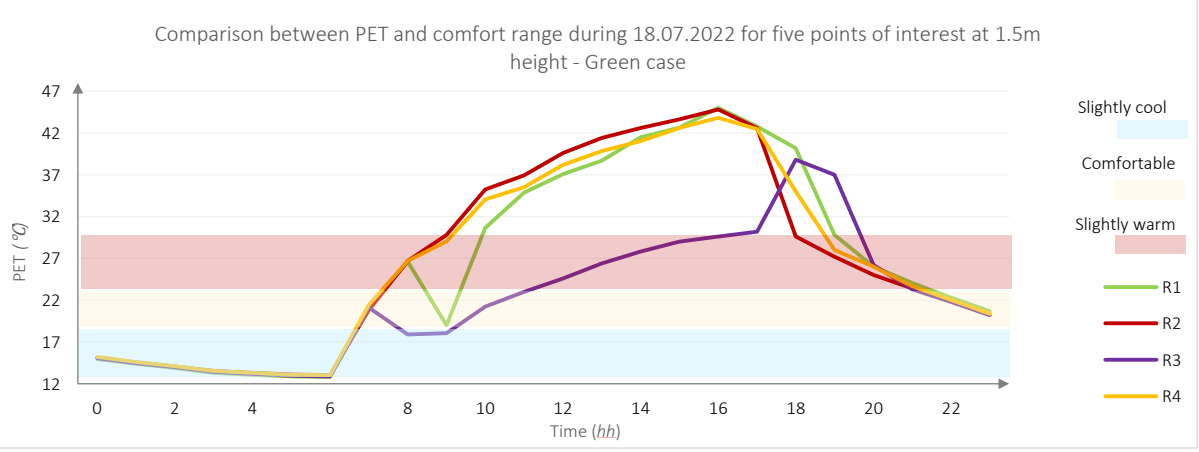

With the changes expected due to climate change, the thermal comfort of tourists or pedestrians in general will shift even more from the desirable range. Compared to the hottest day occurred in Edinburgh, the frequency of desirable comfort range does not exceed 50% mostly (*Graphs 53, 54 and 55*), and the discomfort is experienced during 10am and 6pm which is the most frequented period by visitors. The improvements proposed in the new project may improve the quality of spaces and reduce pollution by shifting from vehicle road to pedestrian one, but urban design choices can have negative impacts on thermal comfort.

Graph 53 PET frequency in comfort range – Base *Case* for 5 points of interest (source: Own elaboration, 2022)

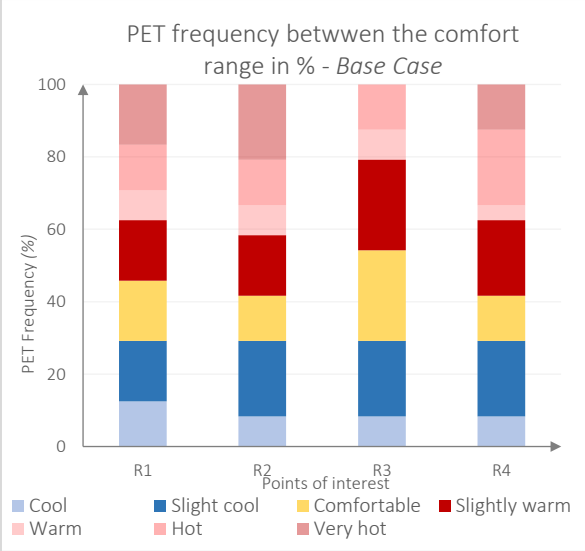

Graph 54 PET frequency in comfort range – *Green Case* for 5 points of interest (source: Own elaboration, 2022)

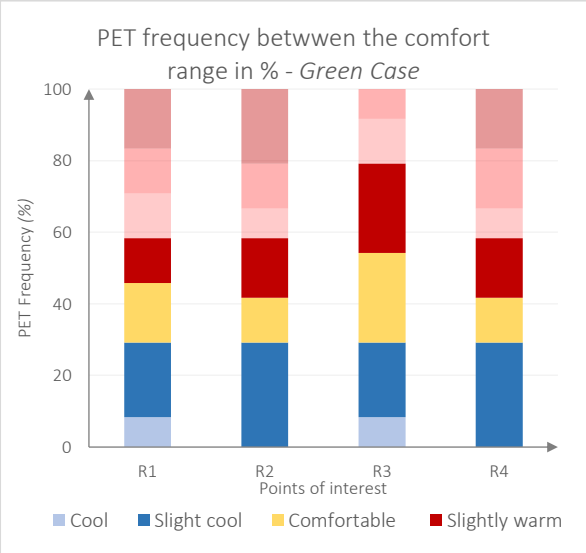

Graph 55 PET frequency in comfort range – *Cool Case* for 5 points of interest (source: Own elaboration, 2022)

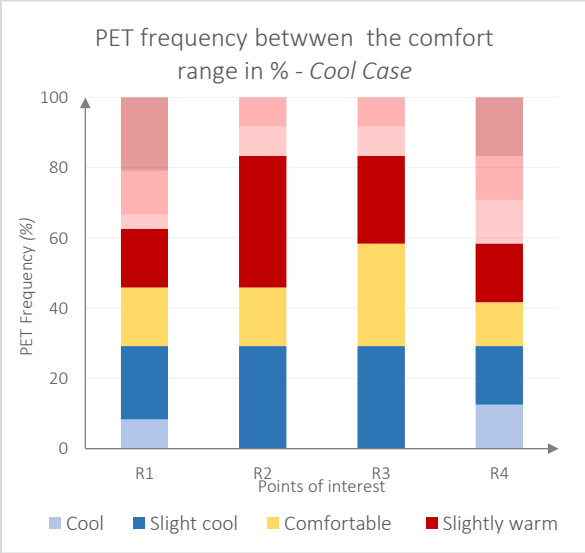

6.2.2. Recommendations for implementations

In cases of objects, blocks and urban areas put under protection due their culture heritage values, very often proven successful cases in improving the outdoor thermal comfort cannot be implemented as they might not be integrated in harmonisation with the historic urban landscape. However, culture heritage sites are best representation of adapting due to different conditions [Sedova, 2021]. The main interventions in improving the outdoor thermal comfort consist on using vegetated spaces, cooling materials and shading elements.

Maintenance

Maintenance leads to thermal properties changes, as albedo used in this research. Despite this, the maintenance of the buildings should be very careful and done with the appropriate

technique. Sandstone used to construct New Town is very sensitive towards erosion and wind over time [The Engine Shed, 2018], while physical and chemical cleaning can remove the patina, formed during the years and adding more values to the site [HS, 2007].

Materials

The study showed that using materials with higher albedo can decrease T*Air*, but can worsen the thermal comfort conditions [Taleghani *et al.*, 2015]. While these materials can be useful in winter, during the touristic seasonal period, the pavement used inside the blocks can be a more appropriate choice in this matter.

Figure 46 Pavement materials in one of alleys inside the blocks (source: Author, 2022)

Temporal interventions

These types of interventions can be suitable for the case study as they do not cause permanent changes or damages, so to historical sites. Studies have evaluated that temporary elements effects can have a major impact on T_{mrt} and PET than on T_{Air} [Saloma, 2021], due to the shading effect they provide [Nasrollahi *et al.*, 2017]. At the present, business in the area are using them for sitting areas (*Figure 47*), but a special need in using sustainable materials and appropriate one for improving the outdoor thermal comfort. In addition, temporal interventions can be changed due to time easily and can be very diverse / innovative.

Figure 47 Actual temporal structures by business owners used in George Street (source: Author, 2022)

Green elements

The low heat capacity of vegetation and the shade that can be provide for the pedestrians can create favourable conditions for the tourists [Taleghani *et al.*, 2015]. Their usage in this case can be considered as temporal interventions, if they are planted in pots and do not interfere with the visual axis of George Square that connect the two square gardens from East to West.

Figure 48 Photo of tourists and locals spending time in St Andrew Square Garden (source: Author, 2022)

6.2.3. Limitations

Urban historic towns consist on complex and very heterogeneous urban forms, with very unique architectural characteristics, thus the spatial discretisation that ENVI-met® results in site model far different from the reality. The time needed to simulate more detailed models is relatively higher; therefore, the model gird cell size was constrained to 4x3x3 m. Another important factor is the building materials properties. ENVI-met® offers a very narrow building materials catalogue, not considering their properties at ageing state. Ageing affects the building material properties, making the model more inaccurate. In this study the thermic properties were adapted from literature review with similar characteristics. The wind speed and directions are parameters that constantly change, despite using Full forcing mode (wind speed and direction input every 30 minutes), thereby leading to the deviation of expected air temperatures [Salata *et al.*, 2015]. At the same time the software leads to instability for wind speed less than 1 m/s at 10 m or changes in wind direction more than 90^{o}, contradicting the field measured data. The output from the simulation consists of Potential Air Temperature (θ) and calculates all the parameters at sea level pressure (1013hPA), not reflecting the real values at the actual site pressure level. Culture heritage assets cannot be fully adapted to achieve thermal comfort, due to the limited interventions allowed from the specific design guidelines and management plans in force. Therefore, the possible scenarios considered not contradicting the historic landscape and the identity of the site.

CHAPTER 7: CONCLUSION

7.1. Summary of findings

Local Climate Zine has become a standardised method to evaluate the impact of urban morphology on the local temperature. It can help examine the UHI phenomenon and can be compared between cities if generated following the same scheme. This study evaluates UHI using morphological parameters in conjunction with the LULC classification and LCZ scheme method. Urban details are more precisely captured using the GIS approach, allowing the use of different methods to assign LCZ classes. In the case of the Edinburgh LCZ process:

- These parameters were extracted from high–resolution data, and the values do not fluctuate substantially, but differences are visible and measurable.
- The combination of the LCZ thresholds [Steward and Oke, 2012] with the LULC classes allows having a view of the heterogeneity of European cities' urban forms.
- A fine resolution of 15m shows that one LULC class can be attributed to different LCZ classes through morphological parameters, as it depends on the way of LULC classification.
- In the case of Edinburgh, with the data available, the entire fitting combination of LULC and LCZ classes through the morphological parameters was not achieved, as one LULC class could fit in more than one LCZ class.
- The existing method can be adopted in different scales (resolution) or with different LULC classifications. However, some classes are not fitting to any LCZ classes based on expert knowledge, and further studies are required.

The historical layers of Edinburgh attract visitors from all around the world. Exploring the World Heritage site is unrelated to the local climate conditions and the effect of UHI, which consequently affect the thermal comfort that tourist experience. Analysing three scenarios with climate-sensitive implementations, we can conclude:

- The thermal conditions of the New Town at the actual state are more favourable from 8 am till 10 am and then after 8 pm overall.
- However, areas near the northwest building facades can have heavier fluxes of tourists as the thermal comfort during the day is within the desirable range.
- Due to the guidelines, the most effective climate-sensitive solutions cannot be implemented. Urban vegetation must not be invasive and create visual barriers, despite its role in the urban microclimate.

- Different pavement materials create different T_{mrt}. Even though high albedo materials can reduce the air temperature, they can worsen the comfort conditions of tourists in the hot season.

- Shade elements have a more beneficial impact than pavement material change. This impact is observed to have higher intensity on areas that are exposed to solar radiation throughout the day, as the accumulation of the heat stored.

7.2. Recommendations for future studies

Due to the lack of accuracy of the LULC, subsequent investigations are needed for the actual LULC classification. The methodology employed throughout the study can be modified to accommodate various LULC classifications and resolution scales, such as neighbourhood, residential, or the suggested 300 m, depending on the target group (urban planning, ecology, landscape, etc. studies) referring to the map and the scale of the case study. The conceptual LCZ map can be used to measure the degree of the UHI effect and conduct an additional study on the cultural heritage locations. Smaller regions can benefit from in-situ surveys and measurements that include the thermic characteristics to improve the classification's accuracy. The results of urban morphology can be used with great accuracy by local planners as a guide and to help designers work in the future to enhance outdoor thermal comfort.

The tourists' outdoor thermal comfort is directly related to the tourism industry, economy and employment opportunities. Extended observation time at cultural heritage assets, fitting the entire touristic season in Edinburgh, can be helpful in creating a proper thermal comfort calendar showing the most optimal time to visit the New Town area. Other critical conditions that need attention to evaluate, such as the coldest time, and the negative effects of new materials in the proposed project, might be beneficial in this case. Due to climate change, Edinburgh is expected to become warmer and wetter, which adds another critical situation to the site. An investigation of thermal comfort during rainy days would be useful to propose appropriate solutions. The impact of climate-sensitive solutions can prolong tourist stays and more revenue for the citizens. Comparing the PET with field surveys for a more accurate correlation with the thermal sensation of Edinburgh can be more useful if integrated and compared with Tourism Climate Comfort Index. Estimating the TCCI allows estimations with other cities and implements similar tourism development strategies.

REFERENCES

ABOUGENDIA, S. M., AYAD H. M. & EL-SAYAD, Z. T., 2020. Classification framework of Local Climate Zones using world urban database and access portal tools: Case study of Alexandria city, Egypt. *Sustainable Development and Planning.* [online]. **XI**, pp. 309-322. [viewed 22 May 2022]. Available from: https://doi.org/10.2495/sdp200251

AMBROSINI, D., GALLI, G., MANCINI, B., NARDI, I. & SFARRA, 2014. Evaluating Mitigation Effects of Urban Heat Islands in a Historical Small Center with the ENVI-Met® Climate Model. *Sustainability*. [online]. **6**(10), pp. 7013-7029. Basel, Switzerland: MDPI. [viewed 24 September 2021]. Available from: https://doi.org/10.3390/su6107013

ANĐELKOVIĆ G., PAVLOVIĆ S., ĐURĐIĆ S., BELIJ, STOJKOVIĆ S., 2016. "Tourism climate comfort index (TCCI) – An attempt to evaluate the climate comfort for tourism purposes: The example of Serbia", *Global NEST Journal*. [online]. **18**(3), pp 482-493. [viewed 14 March 2022]. Available from: doi.org/10.30955/gnj.001798

BARLOW, J. F., 2014. Progress in observing and modelling the urban boundary layer. *Urban Climate*. [online]. **10**(2), pp. 216-240. Netherland: Elsevier. [viewed 21 May 2022]. Available from: https://doi.org/10.1016/j.uclim.2014.03.011

BERDAHL, P. & BRETZ, S. E., 1997. Preliminary survey of the solar reflectance of cool roofing materials. *Energy and Buildings.* [online]. **25**(2), pp. 149-158. Netherland: Elsevier. [viewed 21 June 2022]. Available from: https://doi.org/10.1016/S0378-7788(96)01004-3

BERTOLIN, CH., 2019. Preservation of cultural heritage and resources threatened by climate change. *Geosciences.* [online]. **9**(6), pp. 250-261. Basel, Switzerland: MDPI. [viewed 21 May 2022]. Available from: https://doi.org/10.3390/geosciences9060250

BRUSE, M., 1999. The influences of local environmental design on microclimate, PhD Thesis, University of Bochum, Bochum, Germany (*in German*).

CARROLL, P. & AARREVAARA, E., 2018. Review of Potential Risk Factors of Cultural Heritage Sites and Initial Modelling for Adaptation to Climate Change. *Geosciences.* [online]. **8**(9), pp. 322 – 332. Basel, Switzerland: MDPI. [viewed 10 September 2021]. Available from: https://doi:10.3390/geosciences8090322

CARROLL, P. & AARREVAARA, E., 2021. The Awareness of and Input into Cultural Heritage Preservation by Urban Planners and Other Municipal Actors in Light of Climate Change. *Atmosphere*. [online]. **12**(6), pp. 726–742. Basel, Switzerland: MDPI. [viewed 9 September 2021]. Available from: https://doi.org/10.3390/atmos12060726

CARTER, T.R. & BLANTRAN DE ROZAN, M., 1993. Workbook Methods for Problem Definition and Scoping in Climate Impact Assessment. in UNEP-Canada Workshop on Impacts and Adaptation to Climate Variability and Change, Toronto, Canada, 29.11 – 3.12, 1993.

CASSAR, M., 2005. *Climate Change and the Historic Environment*. [online]. London: Centre for Sustainable Heritage, University College London. [viewed 08 September 2021]. Available from: http://discovery.ucl.ac.uk/2082/1/2082.pdf

CHEN, H., OOKA, R., HARAYAMA, K., KATO, S. & LI, X., 2004. Study on outdoor thermal environment of apartment block in Shenzhen, China with coupled simulation of convection, radiation and conduction. *Energy and Buildings.* [online]. **36**(12), pp. 1247-1258. [viewed 14 March 2022]. Available from: https://doi.org/10.1016/j.enbuild.2003.07.003

CHEN, Y., ZHENG, B. & HU, Y, 2020. Mapping local climate zones using ArcGIS-based method and exploring land surface temperature characteristics in Chenzhou, China. *Sustainability.* [online]. **12** (7), pp. 2974. Basel, Switzerland: MDPI. [viewed 12 June 2022]. Available from: https://doi.org/10.3390/su12072974

CHING, J., MILLS, G., BECHTEL, B., SEE, L., FEDDEMA, J., WANG, X., REN, C., BROUSSE, O., MARTILLI, A., NEOPHYTOU, M., MOUZOURIDES, P., STEWARD, I., HANNA, A., NG, E., FOLEY, M., ALEXANDER, P., ALIAGA, D., NIYOGI, D., SHREEVASTAVE, A., BHALACHNDRAN, P., MASSON, V., HIDALGO, J., FUNG, J., ANDREDE, M., BAKLANOV, A., DAI, W., MILCINSKI, G., DEMUZERE, M., BRUNSELL, N., PESARESI, M., MIAO, S., MU, Q., CHEN, F., & THEEUWES, N., 2018. WUDAPT: An Urban Weather, Climate, and Environmental Modeling Infrastructure for the Anthropocene. *Bulletin of the American Meteorological Society*. [online]. **99**(9), pp. 1907–1924. Boston: American Meteorological Society. [viewed 14 May 2022]. Available from: https://doi.org/10.1175/BAMS-D-16-0236.1

CLIMATE EMERGENCY RESPONSE GROUP, 2021. *Delivering on Scotland's response to the climate emergency - 12 immediate actions for the new Scottish Government in the year of COP26.* [online]. p 8. Scotland: Climate Emergency Response Group. [viewed 27 April 2022]. Available from: https://cerg.scot/wp-content/uploads/2021/09/CERG_Report_Final_Sept_2021.pdf

COLETTE, A. & CASSAR, M. 2007. *Climate change and world heritage: Report on predicting and managing the impacts of climate change on world heritage, and strategy to assist states parties to implement appropriate management responses*. [online]. Paris: UNESCO/WHC. [viewed 9 September 2021]. Available from: https://unesdoc.unesco.org/ark:/48223/pf0000160019

COUNCIL OF EUROPE, 2017. Recommendation of the Committee of Ministers to member States on the European Cultural Heritage Strategy for the 21st Century. In Proceedings of the 1278th meeting of the Ministers' Deputies. [online]. Strasbourg: Council of Europe. [viewed on 19 April 2022]. Available online: https://rm.coe.int/16806f6a03

CROSSLEY, J. AND JANSEN, D., 2021. Saunders' Research Onion: Explained Simply. [online] [viewed on 12 May 2022]. Available from: https://gradcoach.com/saunders-research-onion/

DASTGERDI A. S. & De Luca, G., 2019. Joining Historic Cities to the Global World: Feasibility or Fantasy? *Sustainability.* [online]. **11**, pp. 1–14. Basel, Switzerland: MDPI. [viewed 15 April 2022]. Available from: https://www.mdpi.com/2071-1050/11/9/2662/pdf

DASTGERDI A. S. & SARGOLINI, M., 2019. Vulnerability Assessment and Conservation of Heritage Sites in a Changing Climate. *International Journal of Landscape Architecture Research.* [online]. **3**(2), pp. 121-129. Oxford shire: Taylor & Francis. [viewed 17 April 2022]. Available from:

https://www.researchgate.net/publication/338254727_Vulnerability_Assessment_and_Conservation_of_Heritage_Sites_in_A_Changing_Climate

DeCarlo, M. 2018. *Scientific Inquiry in Social Work.* [online]. [viewed 14 March 2022]. Available from: https://scientificinquiryinsocialwork.pressbooks.com/chapter/6-3-inductive-and-deductive-reasoning/#:~:text=Deductive%20research%20approach%20is%20most,that%20emerge%20from%20those%20theories.

EIBL, M., 2010. *Simplified classification categories of historic buildings.* [online] pp. 10-14. Munich. [viewed 25 May 2022]. Available from: https://www.climateforculture.eu/index.php?inhalt=download&file=pages/user/downloads/project_results/D_02.1_final_publish.pdf

EMMANUEL, R., ROSENLUND, H. & JOHANSSON, E., 2007. Urban shading—a design option for the tropics? A study in Colombo, Sri Lanka. *International Journal of Climatology*. [online]. Special Issue: Urban Climatology ICUC6, **27**(14), pp. 1995-2004. [viewed 25 April 2022]. Available from: https://doi.org/10.1002/joc.1609

ENVI-MET, 2021. *ENVI_MET Unfolded Part 12: Spaces I.* [video] 7 January 2021 [viewed 28 April 2022]. Available from: https://www.youtube.com/watch?v=gcXn-eU_Oyg&t=113s

ERLANDSON, J. M., 2008. Racing a Rising Tide: Global Warming, Rising Seas, and the Erosion of Human History. *The Journal of Island and Coastal Archaeology*. [online] **3**(2), pp.167–169. London: Routledge [viewed 11 March 2022]. Available from: https://doi.org/10.1080/15564890802436766

ESPON, 2020. *Working Paper: Measuring economic impact of cultural heritage at territorial level Approaches and challenges.* [online]. Luxenberg: ESPON EGTC. [viewed 23 April 2022]. Available from: https://www.espon.eu/sites/default/files/attachments/Working%20Paper%2C%20Cultural%20heritage.pdf

FERGUSON, B., 2021. Former culture chief blames heritage status for Edinburgh becoming 'overwhelmed' with visitors. *The Scotsman.* [online]. 26 August 2021. [viewed 06 May 2022]. Available from: https://www.scotsman.com/whats-on/arts-and-entertainment/former-culture-chief-blames-heritage-status-for-edinburgh-becoming-overwhelmed-with-visitors-3359966

FITZPATRICK, S. M., TORBEN, C. R. & JON M. E., 2015. Recent Progress, Trends, and Developments in Island and Coastal Archaeology. *The Journal of Island and Coastal Archaeology*. [online]. **10** (1), pp. 3–27. London: Routledge [viewed on 5 March 2022]. Available from: https://doi.org/10.1080/15564894.2015.1013647

GÁLA, C. V. & KÁNTORBC, N., 2020. Modeling mean radiant temperature in outdoor spaces, A comparative numerical simulation and validation study. *Urban Climate*. [online]. **32** (1), pp. 100571. Netherland: Elsevier. [viewed on 22 March 2022]. Available from: https://doi.org/10.1016/j.uclim.2019.100571

GOBAKKEN, L., MATTSSON, J. AND ALFREDSEN, G., 2008. In-service performance of wood depends upon the critical in-situ conditions. Case studies, paper prepared for the 39th Annual Meeting of the International Research Group on Wood Protection, IRG/WP 09-20382, Istanbul, 25-29 May, IRG Secretariat, Stockholm.

HALFPENNY, 2021. Former culture chief blames heritage status for Edinburgh becoming 'overwhelmed' with visitors. *The Scotsman.* [online]. 26 August 2021. [viewed 06 May 2022]. Available from: https://www.scotsman.com/whats-on/arts-and-entertainment/former-culture-chief-blames-heritage-status-for-edinburgh-becoming-overwhelmed-with-visitors-3359966

HARVEY, D. & PERRY, J., 2015. *The Future of Heritage as Climates Change: Loss, Adaptation and Creativity*. New York: Routledge.

HAUGEN, A. & MATTSSON, J., 2011. Preparations for climate change's influences on cultural heritage. *International Journal of Climate Change Strategies and Management.* [online]. **3**(4), pp. 386-401. Bingley: Emerald Publishing. [viewed 02 September 2021]. Available from: http://dx.doi.org/10.1108/17568691111175678

HALL, C. M., BAIRD, T., MICHAEL, J. & RAM, Y., 2016. Climate change and cultural heritage: conservation and heritage tourism in the Anthropocene. *Heritage, Tourism and Climate Change. Guest Ed: C. Michael Hall.* [online]. **11**(1), pp. 10–204. London: Routledge. [viewed on 12 May 2022]. Available from: https://doi.org/10.1080/1743873X.2015.1082573

HÄGLUND, M., ISAKSSON, T. & THELANDERSSSON, S., 2010. Onset of mold growth – the effect on climate variability and different geographic locations. [online]. Paper prepared for the 41st Annual Meeting of the International Research Group on Wood Protection, IRG/WP 10-20446, Biarritz, 9-13 May, IRG Secretariat, Stockholm. [viewed on 22 May 2022]. Available from: https://www.cabdirect.org/cabdirect/abstract/20103342140

HEAD, L., 2010. Cultural ecology: Adaptation–retrofitting a concept? *Progress in Human Geography.* [online]. **34**(2), pp. 234–242. [viewed on 14 May 2022]. Available from: https://doi.org/10.1177/0309132509338978

HISTORIC ENVIRONMENT SCOTLAND. 2018. *Scotland's Historic Environment Audit 2018.* [online]. Edinburgh: Historic Environment Scotland. [viewed on 5 March 2022]. Available from: https://www.historicenvironment.scot/archives-and-research/publications/publication/?publicationId=7821f0c5-cf3f-4ecc-87e4-a9a601032e54

HISTORIC ENVIRONMENT SCOTLAND, 2019a. *A guide to climate change impacts – On Scotland's Historic Environment.* [online]. Edinburgh: Historic Environment Scotland. [viewed 15 April 2022]. Available from: https://www.historicenvironment.scot/archives-and-research/publications/publication/?publicationId=843d0c97-d3f4-4510-acd3-aadf0118bf82

HISTORIC ENVIRONMENT SCOTLAND, 2019b. T*he Old and New Towns of Edinburgh World Heritage Site: A short guide.* [online]. Edinburgh: Historic Environment Scotland. [viewed 16 May 2022]. Available from: https://pub-prod-sdk.azurewebsites.net/api/file/03527539-297e-44b7-9a0e-aa6301039f92

HISTORIC SCOTLAND, 2007. *Inform Guide: Cleaning Sandstone - Risks and Consequences.* [online]. Edinburgh: Historic Scotland. [viewed 23 June 2022]. Available from: https://app-hes-pubs-prod-neu-01.azurewebsites.net/api/file/8391e2d9-15d6-4cbe-917b-a6c000f556b0

ICOMOS, 1995. *Advisory Body Evaluation: Nomination on The Old and New Towns of Edinburgh.* [online]. **728.** Paris: ICOMOS, International Secretariat. [viewed on 6 May 2022]. Available from: https://whc.unesco.org/document/154125

ICOMOS, 2003. *Evaluations of cultural properties 2003* [online]. Paris: ICOMOS, International Secretariat. [viewed on 16 May 2022]. Available from: http://www.icomos.org/images/DOCUMENTS/World_Heritage/Volumes_Evaluation/EN_Volume_d%C3%A9valuation_2003_COMPLET.pdf

IPCC, 1992. *Preliminary Guidelines for Assessing Impacts of Climate Change*. [online]. IPCC: Geneva, Switzerland. [viewed 20 May 2022]. Available from: https://wedocs.unep.org/bitstream/handle/20.500.11822/30469/PreliminaryGuidelines.pdf?sequence=1&isAllowed=y

IPCC, 2001. Third Assessment Report: Climate Change. [online]. p. 398. PCC: Geneva, Switzerland. [viewed 15 April 2022]. Available from: https://aimlexchange.com/search/wiki/page/Talk:IPCC_Fourth_Assessment_Report/citation

IPCC, 2014a. *Fifth Assessment Report: Climate Change.* [online]. IPCC: Geneva, Switzerland. [viewed 15 April 2022]. Available from: https://www.ipcc.ch/assessment-report/ar5/

IPCC, 2014b. Climate Change 2014-Impacts, Adaptation and Vulnerability: Part A: Global and Sectoral Aspects. [online]. pp. 535-612. [viewed 15 April 2022]. Available from: http://dx.doi.org/10.1017/CBO9781107415379.013

IPCC, 2022. *"Summary for Policymakers" in Climate Change 2022: Impacts, Adaptation and Vulnerability. Contribution of Working Group II to the Third Assessment Report of the Intergovernmental Panel on Climate Change.* [online]. Cambridge UK: Cambridge University Press. [viewed 10 May 2022]. Available from: https://www.ipcc.ch/report/ar6/wg2/downloads/report/IPCC_AR6_WGII_SummaryForPolicymakers.pdf

JACOBS & THE CITY OF EDINBURGH, 2019. *Edinburgh, City Centre Transformation.* [online]. Edinburgh: City of Edinburgh Council. [viewed 24 May 2022]. Available from: https://indd.adobe.com/view/521e1afd-b20c-4332-a8a5-5bb0c3e352e9

JIGYASU, R., 2019. Managing cultural heritage in the face of climate change. *Journal of International Affairs*. [online]. **73**(1), pp. 87-100. New York: Journal of International Affairs Editorial Board. [viewed 01 May 2022]. Available from: https://www.jstor.org/stable/26872780

JIANGA, S., HUANGA, F., ZHANA, W., BECHTELC, B., LIUA, Z., DEMUZEREC, M., HUANGD Y., XUE, Y., MAF, L., XIAG, W., QUANH, J., HONGA, F., JIANGA, L, LAIA, J., WANGA, C., KONGA, F., DUA, H., MIAOA, S., CHENA, Y. & ZHANGA, X., 2021. Mapping Local Climate Zones: A Bibliometric Meta - Analysis and Systematic Review. *OSF*

Preprints. [online]. pp. 1–106. [viewed 01 May 2022]. Available from: doi:10.31219/osf.io/c2bez

KOTHARKAR, R. & BAGADE, A., 2018. Evaluating urban heat island in the critical local climate zones of an Indian city. *Landscape and Urban Planning*. [online]. **169**, pp. 92 - 104. Netherland: Elsevier. [viewed on 10 March 2022]. Available from: https://doi.org/10.1016/j.landurbplan.2017.08.009

LECHA, L. & SHACKLEFORD, P., 1997. Climate services for tourism and recreation. *WMO Bulletin*. [online]. **46**(1), pp. 46–47. [viewed 13 March 2022]. Available from: https://library.wmo.int/doc_num.php?explnum_id=6850

LEVERMORE, G., PARKINSONA, J., LEE, K., LAYCOCKA, P. & LINDLEYA, S., 2018. The increasing trend of the urban heat island intensity. *Urban Climate*. [online]. **24**, pp. 360–368. [viewed 01 May 2022]. Available from: https://doi.org/10.1016/j.uclim.2017.02.004

LIN, T. P., MATZARAKIS, A. & HWANG, R. L., 2010. Shading effect on long-term outdoor thermal comfort. *Building and Environment*. [online]. **45**(1), pp. 213–221. Netherland: Elsevier. [viewed 18 May 2022]. Available from: https://doi.org/10.1016/j.buildenv.2009.06.002

LINBERG, F., GRIMMOND, S., SHIHO ONOMURA, S. & JÄRVI, L., 2015. MEP - An integrated tool for urban climatology and climate-sensitive planning applications. *ICUC9-9th International Conference on Urban Climate jointly with 12th Symposium on the Urban Environment, Toulouse, France*. [online]. [viewed 22 May 2022]. Available from: tps://www.conftool.com/icuc9/index.php/TUKUP7_%28cont%29-3-3431366_a.pdf?page=downloadPaper&filename=TUKUP7_%28cont%29-3-3431366_a.pdf&form_id=343&form_version=final

LIU, W., ZHANG, Y. & DENG Q., 2015. The effects of urban microclimate on outdoor thermal sensation and neutral temperature in hot-summer and cold-winter climate. *Energy and Buildings*. [online]. **128**, pp. 190-197. Netherland: Elsevier. [viewed 18 May 2022]. Available from: https://doi.org/10.1016/j.enbuild.2016.06.086

LOULANSKI, T., 2006. Revising the concept for cultural heritage: The argument for a functional approach. *International Journal of Cultural Property*. [online]. **13**(2), pp. 207–233. Cambridge: International Cultural Property Society [viewed 13 May 2022]. Available from: https://doi.org/10.1017/S0940739106060085

LU, S., XIA, H., WEI, S., FANG, K.& QI, Y., 2016. Analysis of the differences in thermal comfort between locals and tourists and genders in semi-open spaces under natural ventilation on a tropical island. *Energy and Buildings*. [online]. **129**, pp. 264-273. Netherland: Elsevier. [viewed 08 March 2022]. Available from: doi.org/10.1016/j.enbuild.2016.08.002

MACDONALD, N., PHILLIPS, I. D. & THORPE, J., 2008. Reconstruction of long-term precipitation records for Edinburgh: an examination of the mechanisms responsible for temporal variability in precipitation. *Theoretical and Applied Climatology*. [online]. **92**(3), pp. 141–154. [viewed 13 March 2022]. Available from: https://doi.org/10.1007/s00704-007-0324-202

MAHAROOF, N., EMMANUEL, R., AND THOMSON, C. 2020. Compatibility of local climate zone parameters for climate sensitive street design: Influence of openness and surface properties on local climate. *Urban Climate*, **33** (100642), pp. 1-15. [viewed 25 May 2022]. Available from: https://doi.org/10.1016/j.uclim.2020.100642

MAHDJOUBI, L., HAWAS, S., FITTON, R., DEWIDAR, K., NAGY, G., ZAATREH, A.A., MARSHALL, A., ABDELHADY, E., 2017. *A guide for monitoring the effects of climate change on heritage building materials and elements.* [viewed 13 March 2022]. Available from: https://uwe-repository.worktribe.com/OutputFile/882592

MARKHAM, A. & WISER, J., 2015. A Heritage Coalition's Call to Action' on Climate Change and Cultural Heritage. *Forum Journal*. [online]. **29**(4), pp. 19–23. Washington D.C.: National Trust for Historic Preservation. [viewed on 5 March 2022]. Available from: http://muse.jhu.edu/journals/forum_journal/v029/29.4.markham.html

MARKHAM, A., OSIPOVA, E., LAFRENZ SAMUELS, K. & CALDAS, A., 2016. *World Heritage and Tourism in a Changing Climate.* [online]. Paris: United Nations Environment Programme, Nairobi, Kenya and United Nations Educational, Scientific and Cultural Organization. [viewed 13 April 2022]. Available from: https://whc.unesco.org/document/139944

MARZEION, B. & LEVERMANN, A., 2014. Loss of Cultural World Heritage and Currently Inhabited Places to Sea Level Rise. *Environmental Research Letters.* [online]. **9**(3), pp. 034001 – 034008. Bristol: IOP Publishing. https://iopscience.iop.org/article/10.1088/1748-9326/9/3/034001

MATCHETT, C., 2020. How Edinburgh compares to other world cities like Miami and Dubai in terms of tourist to resident ratios. *Edinburgh Evening News*. [online]. 02 January. [viewed 20 September 2021]. Available from: https://www.edinburghnews.scotsman.com/whats-on/arts-and-entertainment/how-edinburgh-compares-to-other-world-cities-like-miami-and-dubai-in-terms-of-tourist-to-resident-ratios-1353183

MATZARAKIS, A., 2006. Weather-and climate-related information for tourism. *Tourism and Hospitality Planning & Development*. [online]. **3**(2), pp. 99-115. [viewed 13 March 2022]. Available from: doi.org/10.1080/14790530600938279

MATZARAKIS, A., MAYER, H. & IZIOMON, M. G. 1999. Applications of a universal thermal index: physiological equivalent temperature. *International Journal of Biometeorology.* [online]. 4**3,** pp. pp. 76-84. Dordrecht: Springer. [viewed 24 June 2022]. Available from: https://doi.org/10.1007/s004840050119

MATZARAKIS, A., RUTZ, F. & MAYER, H., 2010. Modelling radiation fluxes in simple and complex environments: basics of the RayMan model. *International Journal of Biometeorology.* [online]. **54**(2), pp. 131-139. [viewed 24 May 2022]. Available from: https://doi.org/10.1007/s00484-009-0261-0

MET OFFICE, 2016. *Eastern Scotland: climate* [online]. pp. 1.-6. Devon: Met Office. [viewed 10 May 2022]. Available from: https://www.metoffice.gov.uk/binaries/content/assets/metofficegovuk/pdf/weather/learn-about/uk-past-events/regional-climates/eastern-scotland_-climate---met-office.pdf

MET OFFICE, 2018a. *UKCP18 Science Overview Report November 2018* (Updated March 2019), version 2.0. [online]. Devon: Met Office. [viewed 06 May 2022]. Available from: https://www.metoffice.gov.uk/pub/data/weather/uk/ukcp18/science-reports/UKCP18-Overview-report.pdf

MET OFFICE, 2018b. *UK Climate Projections User Interface*, version: 2.7.0 [online]. Devon: Met Office. [viewed 06 May 2022]. Available from: https://ukclimateprojections-ui.metoffice.gov.uk/products

MET OFFICE, 2018c. *UKCP18 Marine report.* [online]. Devon: Met Office. [viewed 08 May 2022]. Available from: https://www.metoffice.gov.uk/pub/data/weather/uk/ukcp18/science-reports/UKCP18-Marine-report.pdf

MET OFFICE, 2022a. *UK Met Office Climate Averages 1961-2020*. [online]. January 2020. [viewed 10 May 2022]. Available from: https://www.metoffice.gov.uk/research/climate/maps-and-data/uk-climate-averages/gcvwqum6h

MET OFFICE, 2022b. *UK and regional series*. [online]. May 2022. [viewed 10 May 2022]. Available from: https://www.metoffice.gov.uk/research/climate/maps-and-data/uk-and-regional-series

MIECZKOWSKI, Z. T., 1985. The Tourism Climatic Index: A Method of Evaluating World Climates for Tourism. *Canadian Geographer*. [online]. **29**(3), pp. 220-233. [viewed 13 March 2022]. Available from: https://doi.org/10.1111/j.1541-0064.1985.tb00365.x

MITCHELL, H., 2019. It's official: today is the hottest day in Edinburgh EVER after temperatures hit 31.2°C at 3pm. *Edinburgh Live*. [online]. 2f July. [viewed 17 July 2022]. Available from: https://www.edinburghlive.co.uk/news/edinburgh-news/its-official-today-hottest-day-16647441

NATIONAL OCEANIC AND ATMOSPHERIC ADMINISTRATION (NOAA), 2017. *Global and regional sea level rise scenarios for the United States.* [online]. **83**, p. 22. Maryland: Silver Spring. [viewed 04 May 2022]. Available from: https://tidesandcurrents.noaa.gov/publications/techrpt83_Global_and_Regional_SLR_Scenarios_for_the_US_final.pdf

NASROLLAHI, N., HATAMI Z. & TALEGHANI, M., 2017. Development of outdoor thermal comfort model for tourists in urban historical areas; A case study in Isfahan. *Building and Environment.* [online]. **125**, pp. 356–372. Netherland: Elsevier. [viewed on 09 March 2022]. Available from: doi.org/10.1016/j.buildenv.2017.09.006

NIKOLOPOULOU, M. AND LYKOUDIS, S., 2007. Use of outdoor spaces and microclimate in a Mediterranean urban area. *Building and Environment.* [online]. **42**(10), pp. 3691-3707. Netherland: Elsevier. [viewed on 12 May 2022]. Available from: https://doi.org/10.1016/j.buildenv.2006.09.008

OKE, T. R., 1976. The distinction between canopy and boundary- layer urban heat islands. *Atmosphere*. [online]. **14**(4), pp. 268-277 [viewed 12 May 2022]. Available from: https://doi.org/10.1080/00046973.1976.9648422

OKE, T. R., 1982. The energetic basis of the urban heat island. *Quarterly Journal of the Royal Meteorological Society*. [online]. **108**(455), pp. 1-24. [viewed 11 March 2022]. Available from: https://doi.org/10.1002/qj.49710845502

OKE, T. R., 1988. Street design and urban canopy layer climate. *Energy and Buildings*. [online]. **11**(1), pp. 103-113. Netherland: Elsevier. [viewed 21 May 2022]. Available from: https://doi.org/10.1016/0378-7788(88)90026-6

OKE, T. R., JOHNSON, G. T., STEYN, D. G. & WATSON, I. D., 1991. Simulation of surface urban heat island under ideal conditions at night–Part 2: Diagnosis and causation. *Boundary-Layer Meteorology*. [online]. **56**, pp. 339-358. [viewed 24 May 2022]. Available from: doi:10.1007/BF00119211

OKE, T. R., 1995. The heat island of the urban boundary layer: Characteristics, causes and effects. *Wind Climate in Cities*. [online]. NATO ASI Series, **277,** pp 81–107. Dordrecht: Springer. [viewed 14 May 2022]. Available from: https://doi.org/10.1007/978-94-017-3686-2_5

OKE, T. R., 2004. Initial guidance to obtain representative meteorological observations at urban sites. I*OM Rep. 81, WMO/TD*. [online]. **1250**, p. 47. [viewed 24 September 2021]. Available from: https://library.wmo.int/doc_num.php?explnum_id=9286

OKE, T. R., MILLS, G., CHRISTEN, A. & VOOGT, J. A., 2017. *Urban climates.* Cambridge: Cambridge University Press.

PARK, H.S., 1986. Features of the heat island in Seoul and its surrounding cities. Atmospheric Environment. [online]. **20**(10), pp. 1859-1866. Netherland: Elsevier. [viewed 11 April 2022]. Available from: https://doi.org/10.1016/0004-6981(86)90326-4

PARSAEE, M., JOYBARIB, M. M., MIRZAEIC, P. A. & HAGHIGHATB, F., 2019. Urban Heat Island, urban climate maps and urban development policies and action plans. *Environmental Technology and Innovation.* [online]. **14**, p. 16. Netherland: Elsevier. [viewed 11 March 2022]. Available from: https://doi.org/10.1016/j.eti.2019.100341

PATEL, S., 2015. The research paradigm – methodology, epistemology and ontology – explained in simple language. [online] [viewed 10 March 2022]. Available from: https://salmapatel.co.uk/academia/the-research-paradigm-methodology-epistemology-and-ontology-explained-in-simple-language/

PENDLEBURY, J., SHORT, M. & WHILE, A., 2009. Urban World Heritage Sites and the problem of authenticity. *Cities.* [online]. **26**(6), pp.349–358. Netherland: Elsevier [viewed 13 April 2022]. Available from: https://doi.org/10.1016/j.cities.2009.09.003

PEARSON, D. M., & GORMAN, J., 2010. Exploring the relevance of a landscape ecological paradigm for sustainable landscapes and livelihoods: A case-application from the Northern Territory Australia. *Landscape Ecology*. [online]. **25**(8), pp. 1169–1183. [viewed on 24 September 2021]. Available from: https://doi.org /10.1007/s10980-010-9498-6

PERON, F., & DE MARIA M. M., SPINAZZE, F. & MAZZALI, U., 2015. An Analysis of the Urban Heat Island of Venice Mainland. *Sustainable Cities and Society.* [online]. **19**, pp. 300 – 309. [viewed on 24 September 2021]. Available from: https://doi.org/10.1016/j.scs.2015.05.008

QUAN, J., 2019. Enhanced geographic information system-based mapping of local climate zones in Beijing, China. *Science China Technological Sciences*. [online]. **62**, pp. 2243–2260. Dordrecht: Springer. [viewed on 22 May 2022]. Available from: https://link.springer.com/article/10.1007/s11431-018-9417-6

QUAN, S. J & BANSALA, P., 2021. A systematic review of GIS-based local climate zone mapping studies. *Building and Environment.* [online].**196**, 107791. Netherland: Elsevier. [viewed on 12 May 2022]. Available from: https://doi.org/10.1016/j.buildenv.2021.107791

ROCKMAN, M., 2015. An NPS Framework for Addressing Climate Change with Cultural Resources. *The George Wright Forum.* [online]. **32**(1), pp. 37–50. [viewed on 5 March 2022]. Available from: https://www.jstor.org/stable/43598399

ROWLAND, M. J. 1992. Climate change, sea-level rise and the archaeological record. *Australian Archaeology*. [online]. **34**(1), pp. 29–33. [viewed 6 September 2021]. Available from: https://doi.org/10.1080/03122417.1992.11681449

ROWLAND, M. J., 1999. Accelerated climate change and Australia's cultural heritage. *Australian Journal of Environmental Management.* [online]. **6**(2), pp.109–118. [viewed 5 September 2021]. Available from: https://doi.org/10.1080/14486563.1999.10648457

ROWLAND, C., SCHOLEFIELD, P., O'NEIL, A. & MILLE, J., 2020. *Quantifying rates of urban creep in Scotland: results for Edinburgh between 1990, 2005 and 2015.* [online]. Aberdeen, Scotland: Centre of Expertise of Water. [viewed 14 June2022]. Available from: https://www.crew.ac.uk/sites/www.crew.ac.uk/files/sites/default/files/publication/Quantifying%20rates%20of%20urban%20creep%20for%20Scotland%20MAIN%20REPORT.pdf

SABBIONI, C., CASSAR, M., BRIMBLECOMBE, P. & LEFEVRE, R. A., 2008. Vulnerability of Cultural Heritage to Climate Change. *Pollution Atmospherique.* [online]. **202**, p. 157-169. Loos, France: Association pour la Prevention de la Pollution Atmospherique. [viewed 8 September 2021]. Available from: https://scholars.cityu.edu.hk/en/publications/vulnerability-of-cultural-heritage-to-climate-change(17a72197-a631-469f-ae72-096cce8c68bc).html

SALATA, F., GOLASI, I., VOLLARO A. L. & VOLLARO, R. L., 2015. How high albedo and traditional buildings' materials and vegetation affect the quality of urban microclimate. *Energy and Buildings.* [online]. **99**, pp. 32-49. Netherland: Elsevier. [viewed 11 May 2022]. Available from: https://doi.org/10.1016/j.enbuild.2015.04.010

SALOMA, M. G. P., 2021. The impact of Public Space's Temporary Interventions in Outdoor Thermal Comfort and Microclimate: Analysis of Lahti's Market Square during Spring. *MUrCS Proceedings 2021*. [online]. **2**, pp. 160–177. Lahti: LAB University [viewed 24 June 2022]. Available from: https://www.theseus.fi/bitstream/handle/10024/512333/LAB_2021_MUrCS.pdf?sequence=5&isAllowed=y

SANTAMOURIS, M., 2014a. On the energy impact of urban heat island and global warming on buildings. *Energy and Buildings.* [online]. **82**, pp. 100–113. Netherland: Elsevier. [viewed 11 March 2022]. Available from: https://doi.org/10.1016/j.enbuild.2014.07.022

SANTAMOURIS, M., 2014b. Cooling the cities—A review of reflective and green roof mitigation technologies to fight heat island and improve comfort in urban environments. *Solar Energy*. [online]. **103**, pp. 682–703. [viewed 11 March 2022]. Available from: https://doi.org/10.1016/j.solener.2012.07.003

SAUNDERS M., LEWIS, P. & THORNHILL, A., 2019. Research Methods for Business Students. 8th edition. Harlow: Pearson.

SCOTT D., GÖSSLING S. & DE FREITAS C.R., 2008. Preferred climates for tourism: case studies from Canada, New Zealand and Sweden. *Climate Research*. [online]. **38** (1), pp. 61–73. [viewed 31 March 2022]. Available from: doi.org/10.3354/cr00774

SCOTT, D., HALL, C. M. & GÖSSLING, S., 2016. A Report on the Paris Climate Change Agreement and Its Implications for Tourism: Why We Will Always Have Paris. *Journal of Sustainable Tourism.* [online]. **24**, pp. 933–948. London: Routledge. [viewed 31 March 2022]. Available from: doi.org/10.1080/09669582.2016.1187623

SEDOVA, A. 2021. Cultural heritage adaptation is sustainable! *IOP Conference Series: Earth and Environmental Science*. [online], **822,** pp. 012006. [viewed 15 July 2022]. Available from: https://iopscience.iop.org/article/10.1088/1755-1315/822/1/012006/pdf

SESANA, E., GAGNON, A. S., CIANTELLI, CH., CASSAR, J. & HUGHES, J. J., 2021. Climate Change Impacts on Cultural Heritage: A Literature Review. *WIREs Climate Change.* [online]. **12**(4), e710. New York: Wiley Periodicals LLC. [viewed 08 September 2021]. Available from: doi.org/10.1002/wcc.710

SHACKLEFORD, P. & OLSSON, L. E. 1995. Tourism, climate and weather. *WMO Bulletin*. [online]. **44**(3), pp. 239–242. [viewed 11 March 2022]. Available from: https://library.wmo.int/doc_num.php?explnum_id=6838

SIGLER, L., GILABERT, J. & VILLALBA,G., 2022. Exploring Methods for Developing Local Climate Zones to Support Climate Research. *Climate.* [online]. **10**(7), pp. 109-129. [viewed 12 August 2022]. Available from: https://doi.org/10.3390/cli10070109

SMITH. P. F., 2014. Climate change and cultural heritage: A race against time. Oxfordshire: Routledge.

STEWARD, I.D. AND OKE, T. R., 2012. Local Climate Zones for Urban Temperature Studies. *Bulletin of the American Meteorological Society*. [online] **93**(12), pp. 1879-1900. [viewed 24 May 2022]. Available from: 10.1175/BAMS-D-11-00019.1

THE ADAPTATION SCOTLAND, 2021. *Summary: Climate Projections for Scotland.* [online]. Edinburgh: The Adaptation Scotland. [viewed 17 March 2022]. Available from: https://www.adaptationscotland.org.uk/application/files/5716/1114/1258/Climate_projections_for_Scotland_summary_single_page_FINAL.pdf

THE CITY OF EDINBURGH COUNCIL, 2013a. *Resilient Edinburgh Climate Change Adaptation Framework 2014–2020.* [online]. Edinburgh: City of Edinburgh Council. [viewed 11 May

2022]. Available from: https://www.edinburgh.gov.uk/downloads/file/24708/resilient-edinburgh-climate-change-adaptation-framework-2014-to-2020

THE CITY OF EDINBURGH COUNCIL, 2013b. *Public and Accessible Transport Action Plan 2013 – 2020*. [online]. Edinburgh: City of Edinburgh Council. [viewed 13 May 2022]. Available from: https://www.edinburgh.gov.uk/downloads/file/26156/public-and-accessible-transport-action-plan

THE CITY OF EDINBURGH COUNCIL, 2016. *Edinburgh Adapts, Our Vision 2016-2050*. [online]. Edinburgh: Sustainable Development Partnership. [viewed 16 May 2022]. Available from: https://www.edinburgh.gov.uk/downloads/file/24705/edinburgh-adapts-our-vision-2016-to-2050

THE CITY OF EDINBURGH COUNCIL, 2016. *Edinburgh Adapts Climate Change Adaptation Action Plan 2016-2020*. [online]. Edinburgh: Sustainable Development Partnership. [viewed 16 May 2022]. Available from: https://www.adaptationscotland.org.uk/application/files/5514/7940/1819/Edinburgh_Adapts_Adaptation_Action_Plan_Final_For_Web.pdf

THE CITY OF EDINBURGH COUNCIL, 2020. *Edinburgh Design Guidance*. [online]. Edinburgh: The City of Edinburgh Council. [viewed on 10 May 2022]. Available from: https://www.edinburgh.gov.uk/downloads/file/29052/edinburgh-street-design

THE CITY OF EDINBURGH COUNCIL, 2021a. *2030 Climate Strategy: Delivering a Net Zero, Climate Ready Edinburgh*. [online]. Edinburgh: City of Edinburgh Council. [viewed 06 May 2022]. Available from: https://www.edinburgh.gov.uk/downloads/file/30783/2030-climate-strategy

THE CITY OF EDINBURGH COUNCIL, 2021b. *City Plan 2030 - Proposed plan*. [online]. Edinburgh: City of Edinburgh Council. [viewed 14 March 2022]. Available from: https://www.edinburgh.gov.uk/downloads/file/29997/proposed-plan-written-statement

THE CITY OF EDINBURGH COUNCIL, 2021c. *City Mobility Plan 2021-2030*. [online]. Edinburgh: City of Edinburgh Council. [viewed 14 March 2022]. Available from: https://www.edinburgh.gov.uk/downloads/file/29320/city-mobility-plan-2021-2030

THE CITY OF EDINBURGH, 2022. *Adopted Roads*. [online]. Edinburgh: City of Edinburgh Council. [viewed 15 June 2022]. Available from: https://data.edinburghcouncilmaps.info/datasets/cityofedinburgh::adopted-roads-1/about

THE CITY OF EDINBURGH COUNCIL, STRATEGY AND COMMUNICATIONS, 2021. *Edinburgh by Numbers 2021*. [online]. pp. 69–70. Edinburgh: City of Edinburgh Council. [viewed 17 March 2022]. Available from: https://www.edinburgh.gov.uk/downloads/file/30669/edinburgh-by-numbers-2021

THE CITY OF EDINBURGH COUNCIL, HISTORIC ENVIRONMENT SCOTLAND & EDINBURGH WORLD HERITAGE, 2016. *Old and New Towns of Edinburgh World Heritage Site – Management Plan 2017 – 2022*. [online]. Edinburgh: Historic Scotland. [viewed on 10 May 2022]. Available from: https://ewh.org.uk/plan/assets/Management-Plan-2018b.pdf?

THE CITY OF EDINBURGH COUNCIL, TRANSPORT SCOTLAND, SUSTRANS, PLACE FOR EVERYONE, STREETS-UK, FAITHFULL GOULD, ATKINS, LDA DESIGN & LUMA, 2021. *George Street and First New Town – Final Concept Design and Operational Plan Update* [online]. Edinburgh: City of Edinburgh Council. [viewed 21 May 2022]. Available from: https://www.edinburgh.gov.uk/georgestreet/about-1

THE COCKBURN ACCOSIOATION, 2021. *George Street – First New Town" Proposals*. [online]. 26 March. [viewed on 21 June 2022]. Available from: https://www.cockburnassociation.org.uk/planning-consultation-responses/george-street-first-new-town-proposals/

UNESCO, 1972. *17th session of World Heritage Committee World - Convention concerning the protection of the world cultural and natural heritage, Paris, France.* [online]. Paris: UNESCO/WHC. [viewed on 11 September 2022]. Available from: https://whc.unesco.org/archive/convention-en.pdf

UNESCO, 1976. *Recommendations Concerning the safeguarding and contemporary role of historic areas.* [online]. Paris: UNESCO/WHC. [viewed on 12 March 2022]. Available from: http://portal.unesco.org/en/ev.php-URL_ID=13133&URL_DO=DO_TOPIC&URL_SECTION=201.html

UNESCO, 1995. *19th session of World Heritage Committee World - Convention concerning the protection of the world cultural and natural heritage, Berlin, Germany.* [online]. Paris: UNESCO/WHC. [viewed on 5 May 2022]. Available from: https://whc.unesco.org/document/799

UNESCO, 2005. *Old and New Towns of Edinburgh – the World Heritage site and its conservation areas.* [online]. Paris: UNESCO/WHC. [viewed on 4 March 2022]. Available from: https://whc.unesco.org/document/104891

UNESCO, 2008. *32nd session of World Heritage Committee World - Convention concerning the protection of the world cultural and natural heritage, Quebec City, Canada.* [online]. Paris: UNESCO/WHC. [viewed on 12 May 2022]. Available from: https://whc.unesco.org/archive/2008/whc08-32com-7Be.pdf

UNESCO, 2015. *Operational Guidelines for the Implementation of the World Heritage Convention.* [online]. UNESCO: Paris, France. [viewed 28 February 2022]. Available from: https://whc.unesco.org/document/137843

UNIVERSITY OF EDINBURGH, 2019. *Culture and heritage.* [online]. 06 September 2019. [viewed 11 May 2022]. Available from: https://www.ed.ac.uk/visit/city/see-and-do/culture

URDANIZ, A.V. Z., 2018. Regional Heritage Dimensions vs. Management Boundaries: A comparative framework of European and Asian countries. *International Review for Spatial Planning and Sustainable Development*. [online]. **6**(2), pp. 64–81. Japan: International Community of Spatial Planning and Sustainable Development. [viewed 28 March 2022]. Available from: http://dx.doi.org/10.14246/irspsd.6.2_64

VILES, H. A. 2002. Implications of future climate change for stone deterioration. *Geological Society*, [online]. **205**(1), pp 407–418. London: Special Publications. [viewed 05 September 2021]. Available from: https://doi.org/10.1144/gsl.Sp.2002.205.01.29

YANA, C., GUOAB, Q., LI, H., LI, L. & QIUA, G. Y., 2019. Quantifying the cooling effect of urban vegetation by mobile traverse method: A local-scale urban heat island study in a subtropical megacity. *Building and Environment.* [online]. **169**. Netherland: Elsevier. [viewed 12 June 2022]. Available from: https://doi.org/10.1016/j.buildenv.2019.106541

VALDEZ, A. M. A., 2021. Urban morphology and streetscaping as an approach to mitigate Urban Heat Island in Glasgow City Centre. *MUrCS Proceedings 2021*. [online]. **2**, pp. 124–141. Lahti: LAB University [viewed 24 June 2022]. Available from: https://www.theseus.fi/bitstream/handle/10024/512333/LAB_2021_MUrCS.pdf?sequence=5&isAllowed=y

WANG, R., REN, C., XU, Y. & LAU, K., 2018. Mapping the local climates zones of urban areas by GIS-based and WUDAPT methods: A case study of Hong Kong. *Urban Climate*. [online]. 24, pp. 567-576. Netherland: Elsevier. [viewed 12 June 2022]. Available from: https://doi.org/10.1016/j.uclim.2017.10.001

WATSON, S. J., KRITHARAS, P. & HODGSON, G. J., 2015. Wind Speed Variability across the UK between 1957 and 2011. *Wind Energy*. [online]. **18**(1), pp. 21-42. [viewed 12 June 2022]. Available from: https://doi.org/10.1002/we.1679

WICKI, A. & PARLOW, E., 2017. Attribution of local climate zones using a multi-temporal land use/land cover classification scheme. *Journal of Applied Remote Sensing*. [online]. **11**(2), pp. 026001- 026017. Bellingham, Washington, United States: SPIE [viewed 12 May 2022]. Available from: doi: 10.1117/1.JRS.11.026001.

WEATHER UNDERGROUND, 2022. *Bannerman Way Weather Station - IEDINB74.* [online]. Weather underground, 2022. [viewed 07 July 2022]. Available from: https://www.wunderground.com/dashboard/pws/IEDINB74

WMO, 2021. *State of the Global Climate 2020*. [online].**1264**. Geneva: WMO. [viewed 10 May 2022]. Available from: https://library.wmo.int/index.php?lvl=notice_display&id=21880#.YH18CO8zZBw

ZACHARIAS, J., STATHOPOULOS, T. & WU, H., 2001.Microclimate and downtown open space activity. *Environment and Behavior*. [online]. **33**(2), pp. 296 – 315. [viewed 12 March 2022]. Available from: https://doi.org/10.1177/00139160121973007

ZALA, M, 2020. Vulnerability and Glasgow Greendex: A framework to optimise the impact of green infrastructure in improving socio-environmental vulnerability. *MUrCS Proceedings 2020.* [online]. **1**, pp. 89–110. Lahti: LAB University [viewed 22 March 2022]. Available from: https://www.theseus.fi/bitstream/handle/10024/346538/ZALA_MEGI_THESIS_LAB_.pdf?sequence=2&isAllowed=y

ZHANG, G., HE B., ZHU, Z. & DEWANCKER B. J., 2019. Impact of Morphological Characteristics of Green Roofs on Pedestrian Cooling in Subtropical Climates. *International Journal of Environmental Research and Public Health.* [online]. **16**(2), pp. 179–199. [viewed 21 May 2022]. Available from: https://doi.org/10.3390/ijerph16020179

ZHENG, Y., REN, C., XU, Y., WANG, R., HO, J., LAU, K. & NG, E., 2018. GIS-based mapping of Local Climate Zone in the high-density city of Hong Kong. *Urban Climate.* [online]. **24**, pp 419-448.[viewed 10 March 2022]. Available from: https://doi.org/10.1016/j.uclim.2017.05.008\

Appendix 1: PRINCIPAL CLIMATE CHANGE RISKS AND IMPACTS ON CULTURAL HERITAGE

source: Colette and Cassar, 2007, 25

Climate indicator	Climate change risk	Physical, social and cultural impacts on cultural heritage
Atmospheric moisture change	- Flooding (sea, river) - Intense rainfall - Changes in water-table levels - Changes in soil chemistry - Ground water changes - Changes in humidity cycles - Increase in time of wetness - Sea-salt chlorides	- pH changes to buried archaeological evidence - Loss of stratigraphic integrity due to cracking and heaving from changes in sediment moisture - Data loss preserved in waterlogged / anaerobic / anoxic conditions - Eutrophication accelerating microbial decomposition of organics - Physical changes to porous building materials and finishes due to rising damp - Damage due to faulty or inadequate water disposal systems; historic rainwater goods not capable of handling heavy rain and often difficult to access, maintain, and adjust - Crystallisation and dissolution of salts caused by wetting and drying affecting standing structures, archaeology, wall paintings, frescos and other decorated surfaces - Erosion of inorganic and organic materials due to flood waters - Biological attack of organic materials by insects, moulds, fungi, invasive species such as termites - Subsoil instability, ground heave and subsidence - Relative humidity cycles/shock causing splitting, cracking, flaking and dusting of materials and surfaces - Corrosion of metals - Other combined effects eg. increase in moisture combined with fertilisers and pesticides
Temperature change	- Diurnal, seasonal, extreme events (heat waves, snow loading) - Changes in freeze-thaw and ice storms, and increase in wet frost	- Deterioration of facades due to thermal stress - Freeze-thaw/frost damage - Damage inside brick, stone, ceramics that has got wet and frozen within material before drying - Biochemical deterioration - Changes in 'fitness for purpose' of some structures. For example overheating of the interior of buildings can lead to inappropriate alterations to the historic fabric due to the introduction of engineering solutions - Inappropriate adaptation to allow structures to remain in use
Sea level rises	- Coastal flooding - Sea water incursion	- Coastal erosion/loss - Intermittent introduction of large masses of 'strange' water to the site, which may disturb the metastable equilibrium between artefacts and soil - Permanent submersion of low-lying areas - Population migration - Disruption of communities - Loss of rituals and breakdown of social interactions
Wind	- Wind-driven rain - Wind-transported salt - Wind-driven sand - Winds, gusts and changes in direction	- Penetrative moisture into porous cultural heritage materials - Static and dynamic loading of historic or archaeological structures - Structural damage and collapse - Deterioration of surfaces due to erosion

Climate indicator	Climate change risk	Physical, social and cultural impacts on cultural heritage
Desertification	- Drought - Heat waves - Fall in water table	- Erosion - Salt weathering - Impact on health of population - Abandonment and collapse - Loss of cultural memory
Climate and pollution acting together	- pH precipitation - Changes in deposition of pollutants	- Stone recession by dissolution of carbonates - Blackening of materials - Corrosion of metals - Influence of bio-colonialisation
Climate and biological effects	- Proliferation of invasive species - Spread of existing and new species of insects (eg. termites) - Increase in mould growth - Changes in lichen colonies on buildings Decline of original plant materials	- Collapse of structural timber and timber finishes - Reduction in availability of native species for repair and maintenance of buildings - Changes in the natural heritage values of cultural heritage sites - Changes in appearance of landscapes - Transformation of communities - Changes in the livelihood of traditional settlements - Changes in family structures as sources of livelihoods become more dispersed and distant

Appendix 2: SUMMARISES OF INDICES USED IN URBAN AREAS EVALUATING THE THERMAL IMPACT ON TOURISTS

source: Nasrollahi *et al.*, 2017

Index	Usage	Description	Expressed	Indication
Apparent Temperature	Outdoors	AT = T + 0.33e – 0.7|U| -4 T = dry bulb temperature e= vapour pressure derived from dew point |U| = Wind speed	Temperature Degrees Celsius	Comparable thermal sensation indication
Predicted Mean Vote (PMV)	Indoors	Meteorological Variables: air temperature, humidity, wind speed, mean radiant temp + clothing and activity	Scale between -3 to +3	Quantifies Discomfort
Standard Predicted Mean Vote (SPMV)	Outdoors	Adjusted PMV to include more extreme humidity	Scale between -3 to +3, where 0 is neutral	Quantifies Discomfort
Physiologically Equivalent Temperature (PET)	Outdoors	Four meteorological variables. Standardized clothing and activity for indoor activity	Temperature Degrees Celsius	Air temperature required to reproduce a comfortable indoor setting
*Standard Effective Temperature (SET**	Indoors	Air Temp, wind speed, mean radiant temp. Assumes 50% humidity. Standard clothing and activity	Temperature Degrees Celsius	Compares individual physiological comfort to a reference environment.
Outdoor Standard Effective Temperature (OUT_SET)*	Outdoors	Derived from SET with simplified mean radiant temperature. Assumes activity and clothing value for outdoor uses.	Temperature Degrees Celsius	As with SET*
Thermal Sensation Index (TSI)	Outdoors	Air temperature, Solar radiation and Wind Speed	Scale between 1 – 7, where 4 is neutral	Quantifies discomfort
Universal Thermal Climate Index (UTCI)	Outdoors	Air temperature, mean temperature wind speed, water vapour pressure or relative humidity. Can be coupled with clothing model.	Temperature Degrees Celsius	Indication of physiological thermal stress under a wide range of conditions and climates.

Appendix 3: **GEORGE STREET-NEW TOWN PROJECT, FULL STUDY AREA**

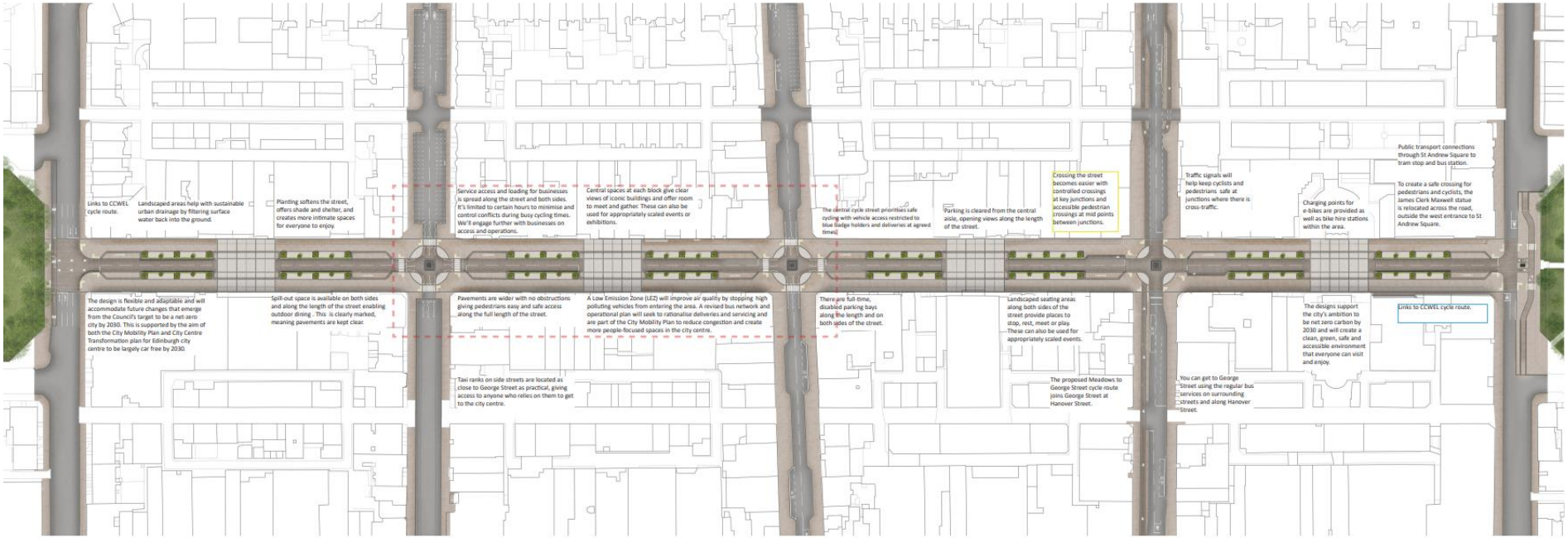

Figure 49 George Street - New Town project

Sustainability is central to the design and the proposals support our ambition to be a net-zero carbon city by 2030. Significantly reducing vehicle access will encourage more people to choose sustainable transport instead of the car. While introducing a variety of suitable shrubs and hedging will help to increase local biodiversity. Investment in well-planned improvements to the outdoor space, including landscaped seating areas is shown to attract more people to visit and spend time in the area.

Figure 50 3D renders of George Street - New Town project

Appendix 4: LAND USE CLASSES AND THEIR CODES

Source: Copernicus Land Monitoring Service at the European Environment Agency, 2018.

https://land.copernicus.eu/user-corner/technical-library/urban_atlas_2012_2018_mapping_guide

Class	CODE	Description
Discontinuous very low-density urban fabric (S.L.: < 10%)	D1	Average degree of soil sealing: <10 % Residential buildings, roads and other artificially surfaced areas. The vegetated areas are predominant, but the land is not dedicated to forestry or agriculture. Example: exclusive residential areas with large gardens.
Discontinuous low-density urban fabric (S.L.: 10% -30%)	D2	Average degree of soil sealing: 10 - 30% Residential buildings, roads and other artificially surfaced areas. The vegetated areas are predominant, but the land is not dedicated to forestry or agriculture.
Discontinuous medium density urban fabric (S.L.: 30% -50%)	D3	Average degree of soil sealing: > 30 - 50% Residential buildings, roads and other artificially surfaced areas. The vegetated areas are predominant, but the land is not dedicated to forestry or agriculture.
Discontinuous dense urban fabric (S.L.: 50% - 80%)	D4	Average degree of soil sealing: > 50 - 80% Residential buildings, roads and other artificially surfaced areas.
Continuous urban fabric (S.L.: > 80%)	D5	*Land Cover:* Average degree of soil sealing: > 80% Built-up areas and their associated land, if these areas are not suitable to be mapped separately with regard to the minimum mapping unit size. Buildings, roads and sealed areas cover most of the area; non-linear areas of vegetation and bare soil are exceptional. *Land Use:* Predominant residential use: areas with a high degree of soil sealing, independent of their housing scheme (single family houses or high-rise dwellings, city centre or suburb). Included are downtown areas and city centres, and Central Business Districts (CBD) as long as there is partial residential use.
Green urban areas	GU	Public green areas for predominantly recreational use such as gardens, playgrounds, zoos, parks, castle parks and cemeteries. Suburban natural areas that have become and are managed as urban parks. Forests or green areas extending from the surroundings into urban areas are mapped as green urban areas when at least two sides are bordered by urban areas and structures, and traces of recreational use are visible.
Railways and associated land	R1	Railway facilities including stations, cargo stations and service areas.

Class	CODE	Description
Fast transit roads and associated land	R2	Roads defined as “motorways” in the navigation data, including motorway rest, service areas, tolls, parking areas, only accessible from the motorways. Areas surrounded by highway or railway junctions have to be included in the corresponding network. Motorways that are not included in the navigation data are to be mapped by the service provider.
Other roads and associated land	R3	Roads, crossings, intersections and parking areas, including roundabouts and sealed areas with “road surface”.
Sports and leisure facilities	S	All sports and leisure facilities including associated land, whether public or commercially managed, public arenas for any kind of sports including associated green areas, parking places, etc.: • Golf courses; • Sports fields (also outside the settlement area); • Camp grounds; • Leisure parks; • Riding grounds; • Racecourses; • Amusement parks; • Swimming resorts etc.; • Holiday villages (“Club Med”); • Allotment gardens • Glider or sports airports, aerodromes without sealed runway; • Marinas.
Industrial, commercial, public, military and private units	I1	*Land cover:* Artificial structures (e.g. buildings) or artificial surfaces (e.g. concrete, asphalt, tar, macadam, tarmac or otherwise stabilised surface, e.g. compacted soil, devoid of vegetation), occupy most of the surface. Included are associated areas, such as roads, sealed areas and vegetated areas, if these areas are not suitable to be mapped separately with regard to the MMU size. *Land use:* Industrial, commercial, public, military or private units. The administrative boundaries of the production or service unit are mapped, including associated features larger than the MMU (e.g. sports areas or transport structures). Also included are: • Bare soil and/or grassland potentially used for storage of material or as enclosures for livestock. • Compounds with significant amounts of green or natural areas but with industrial, commercial, military or public use. Example: communication tower, antennas or wind motors and their associated land.

Class	CODE	Description
		This class contains: *a) Industrial uses and related areas* • Sites of industrial activities, including their related areas such as storage areas; • Production sites; • Energy plants: nuclear, solar, hydroelectric, thermal, electric and wind farms; • Sewage treatment plants; • Farming industries (farms with large buildings and / or greenhouses) • Antennas, even with predominant vegetated areas. The vegetated areas may be predominant, but the land is not dedicated to forestry or agriculture; • Water treatment plants; • Sewage plants; • Seawater desalination plants. The industrial units can be distinguished from residential built-up areas by the type of buildings, their access to transport features and the surroundings: • Buildings with large surface areas (inside, not all rooms need daylight, as in dwelling houses); • Good access to roads and parking for customers; • Industrial areas are often outside the historical city centre. *b) Commercial uses, retail parks and related areas* • Surfaces purely occupied by commercial activities, including their related areas (e.g. parking areas even larger than the MMU); • High-rise office buildings; • Petrol and service stations within built-up areas. • The commercial units can be distinguished from residential built-up areas by the type of large buildings, their access to transport features and the surroundings: • Buildings with large surface areas (inside, not all rooms need daylight, as in dwelling houses); • Good access to roads and parking for customers; • Pure commercial areas are often outside the historical city centre. Not included are: Petrol stations along fast transit and main roads with access only from these roads. They are mapped together with the road transport system. *c) Public, military and private services not related to the transport system* Surfaces purely occupied by general government, public or private administrations including their related areas (access ways, lawns, military training areas, parking areas). Included are: • Schools and universities;

Class	CODE	Description
		• Hospitals and other health services or buildings; • Places of worship (churches / cathedrals / religious buildings); • Archaeological sites and museums; • Administration buildings, ministries; • Penitentiaries; • Military areas including bases and ports; • Military exercise areas fenced and under current use; • Castles, etc. not primarily used for residential purposes (building management, gardeners, etc. living there is not residential use in this sense); • Private storage areas without a residential component, such as compounds of garages. d) *Civil protection and supply infrastructure* • Dams, dikes, irrigation and drainage canals and ponds and other technical public infrastructure, to be mapped with the roads, embankments and associated land included; • Includes also breakwaters, piers and jetties, sea walls and flood defences; • (Ancient) city walls, other protecting walls, bunkers; • Avalanche barriers. Not included are: • Noise barriers; • Water courses (within e.g. diked canals) if the water area is wider than 10 m; • Reservoirs along natural water courses
Construction sites	C	Spaces under construction or development, soil or bedrock excavations for construction purposes or other earthworks visible in the image. Clear evidence of actual construction needs to be identifiable in the data, such as actual excavations and machinery on site, or ongoing construction of any stage, land under development, etc.
Isolated structures	I2	Isolated artificially structures with a residential component, such as (small) individual farm houses and related buildings. The mapping unit will never be surrounded by any urban class other than transportation network. The mapping unit is no larger than 2 ha. Exception: border blocks / polygons in housing developments (they may be adjacent to roads and non-urban classes).
Land without current use	B	Areas in the vicinity of artificial surfaces still waiting to be used or re-used. The area is obviously in a transitional position, “waiting to be used”. Waste land, removed former industry areas, (“brown fields”) gaps in between new construction areas or leftover land in the urban context (“green fields”). No actual agricultural or recreational use. No construction is visible, without maintenance, but no undisturbed fully natural or semi-natural vegetation (secondary ruderal vegetation). Also areas where the street network is already finished, but actual erection of buildings is still not visible.

Class	CODE	Description
Mineral extraction and dump sites	M	• Open pit extraction sites (sand, quarries) including water surface, if • MMU, open-cast mines, inland salinas, oil and gas fields; • Their protecting dikes and / or vegetation belts and associated land such as service areas, storage depots; • Public, industrial or mine dump sites, raw or liquid wastes, legal or illegal, their protecting dikes and / or vegetation belts and associated land such as service areas.
Open spaces with little or no vegetation (beaches, dunes, bare rocks, glaciers)	GR	Beaches, dunes, sand: • < 10% vegetation cover; • Beaches, dunes and sand plains, (coastal or inland location), gravel along rivers; • Seasonal rivers, if water is characteristic for a shorter part of the year (< 2 months). b) Bare rocks: • > 90% of the land surface of bare rocks, (i.e. < 10% vegetation); • Rocks, gravel fields, landslides; • Scree (fragments resulting from mechanical and chemical erosion. Weathering rocks forming heaps of coarse debris at the foot of steep slopes), cliffs, rocks. c) Sparsely vegetated areas: • Steppes, tundra, badlands, scattered high altitude vegetation. Bare soils inside military training areas. Vegetation cover 10 - 50%. d) Burnt areas: • Recently burnt forest or shrubs (but not natural grassland), still mainly black on EO data. e) Snow and ice: • Glacier and perpetual snow.
Port areas	P	Administrative area of inland harbours and sea ports. Infrastructure of port areas, including quays, dockyards, transport and storage areas and associated areas.
Airports	A1	Administrative area of airports, mostly fenced. Included are all airport installations: runways, buildings and associated land. Military airports are also included.
Arable land (annual crops)	CR1	• Fields under rotation system. Can be non-irrigated or permanently irrigated. Also includes rice fields; • Fields laid in fallow are included
Complex and mixed cultivation patterns	CR2	• Annual crops associated with permanent crops such as orchards; • Complex cultivation patterns; • Land principally occupied by agriculture, with significant areas of natural vegetation; • Agro-forestry areas.

Class	CODE	Description
Pastures	CR3	Pasture and meadow under agricultural use, grazed or mechanically harvested; Wooded meadows, pastures with scattered trees.
Forests	F	• Broad leaved forest, coniferous forest and mixed forest; • Transitional woodland and shrub (clear cut, new plantations and regeneration, or damage forest); • With ground coverage of tree canopy > 30%, tree height > 5 m, including bushes and shrubs at the fringe of the forest; • Included tree nurseries, Populus plantations, Christmas tree plantations; • Forest regeneration / re-colonisation: clear cuts, new forest plantations
Herbaceous vegetation associations (natural grassland, moors...)	H	• Vegetation cover more than 50%, ground coverage of trees with height >5 m: <30%, areas with minor / without artificial or agricultural influence; • Sclerophyllous vegetation; • Bushy sclerophyllous vegetation (e.g. maquis, garrigue); • Abandoned arable land with bushes; • Woodland degradation: storm, snow, insects or air pollution; • Areas under power transmission lines inside forest; • Fire breaks; • Steep bushy slopes of eroded areas; • Abandoned vineyards or orchards, arable land and pastures under natural colonisation; • Dehesas with bush proliferation indicating no agricultural or farming use for a rather long time; • Bushy areas along creeks. • Bushes, shrubs and herbaceous plants, dwarf forest in alpine or coastal regions (Pinus Mugo forests). Height is maximum 3 m in climax stage. Natural grassland
Wetlands	WL	Inland wetlands: • Areas flooded or liable to flooding during a large part of the year by fresh, brackish or standing water with specific vegetation coverage made of low shrub, semi-ligneous or herbaceous species; • Water fringe vegetation, reed beds of lakes, rivers and brooks. Sedge and fen-sedge beds, swamps; • Peat bogs, with or without peat extracting areas; • Shallow water areas covered with reed; • Seasonal rivers, if water course is not visible in the EO data. Coastal wetlands: • Areas, flooded or liable to flooding during a large part of the year by brackish or saline water, susceptible to flooding by sea water. Often in the process of fi in and gradually being colonised by halophytic plants;

Class	CODE	Description
		• Specific vegetation coverage made of low shrub, semi-ligneous or herbaceous species; • Alluvial planes, marshes and intertidal flats • Salinas (salt production sites by evaporation).
Water	W	The visible water surface area on the EO data is delineated. EO data should be considered as a primary (guiding) data source. • Sea; • Lakes; • Fish ponds (natural, artificial) • Rivers, including channelled rivers; Canals.

Appendix 5: METEOROLOGICAL DATA ON 07.07.2020

Date	Time	SW dir	SW dif	LW	TA	RH	Wind speed	Wind Direction	Precipitation
06.07.2022	18:00:00	0	0	0	290.45	70	4.28	286	0
06.07.2022	18:30:00	0	0	0	290.45	70	2.86	308.5	0
06.07.2022	19:00:00	0	0	0	289.45	73	3.64	308.5	0
06.07.2022	19:30:00	0	0	0	289.25	72	2.86	308.5	0
06.07.2022	20:00:00	0	0	0	289.15	73	3.64	308.5	0
06.07.2022	20:30:00	0	0	0	288.45	76	3.22	286	0
06.07.2022	21:00:00	0	0	0	287.85	77	3.08	308.5	0
06.07.2022	21:30:00	0	0	0	287.15	80	3.33	308.5	0
06.07.2022	22:00:00	0	0	0	286.95	80	2.92	286	0
06.07.2022	22:30:00	0	0	0	286.85	80	3.39	286	0
06.07.2022	23:00:00	0	0	0	286.85	80	3.75	308.5	0
06.07.2022	23:30:00	0	0	0	286.85	80	2.64	286	0
07.07.2022	00:00:00	0	0	0	286.75	81	2.53	308.5	0
07.07.2022	00:30:00	0	0	0	286.75	81	2.97	308.5	0
07.07.2022	01:00:00	0	0	0	286.65	82	2.36	308.5	0
07.07.2022	01:30:00	0	0	0	286.65	82	2.56	308.5	0
07.07.2022	02:00:00	0	0	0	286.45	82	3.06	286	0
07.07.2022	02:30:00	0	0	0	286.35	83	2.28	308.5	0
07.07.2022	03:00:00	0	0	0	286.35	83	2.11	308.5	0
07.07.2022	03:30:00	0	0	0	286.35	83	2.31	286	0
07.07.2022	04:00:00	0	0	0	286.25	83	2.31	286	0
07.07.2022	04:30:00	0	0	0	286.15	83	2.17	308.5	0
07.07.2022	05:00:00	0	0	0	285.95	84	1.44	308.5	0
07.07.2022	05:30:00	0	0	0	285.85	84	1.89	286	0
07.07.2022	06:00:00	0	0	0	285.95	83	1.69	308.5	0
07.07.2022	06:30:00	0	0	0	286.35	81	2.17	308.5	0
07.07.2022	07:00:00	0	0	0	286.85	79	1.89	308.5	0
07.07.2022	07:30:00	0	0	0	287.35	78	2.14	308.5	0
07.07.2022	08:00:00	0	0	0	288.15	76	1.94	286	0
07.07.2022	08:30:00	0	0	0	288.25	75	2.67	286	0

Date	Time	SW dir	SW dif	LW	TA	RH	Wind speed	Wind Direction	Precipitation
07.07.2022	09:00:00	0	0	0	288.65	74	2.11	308.5	0
07.07.2022	09:30:00	0	0	0	289.35	72	2.53	308.5	0
07.07.2022	10:00:00	0	0	0	289.65	69	2.72	286	0
07.07.2022	10:30:00	0	0	0	290.45	66	1.94	308.5	0
07.07.2022	11:00:00	0	0	0	291.05	66	2.5	286	0
07.07.2022	11:30:00	0	0	0	291.85	61	2.47	308.5	0
07.07.2022	12:00:00	0	0	0	292.95	58	2.42	308.5	0
07.07.2022	12:30:00	0	0	0	293.25	60	2.75	286	0
07.07.2022	13:00:00	0	0	0	293.85	56	2.86	286	0
07.07.2022	13:30:00	0	0	0	294.05	57	3.44	308.5	0
07.07.2022	14:00:00	0	0	0	294.45	56	3.69	286	0
07.07.2022	14:30:00	0	0	0	294.65	56	2.94	286	0
07.07.2022	15:00:00	0	0	0	294.55	57	3.53	286	0
07.07.2022	15:30:00	0	0	0	294.55	60	3.42	308.5	0
07.07.2022	16:00:00	0	0	0	294.45	61	4	286	0
07.07.2022	16:30:00	0	0	0	294.45	60	3.75	286	0
07.07.2022	17:00:00	0	0	0	294.25	62	3.19	308.5	0
07.07.2022	17:30:00	0	0	0	293.65	63	2.97	286	0
07.07.2022	18:00:00	0	0	0	294.45	62	3.17	308.5	0
07.07.2022	18:30:00	0	0	0	294.05	63	3.64	286	0
07.07.2022	19:00:00	0	0	0	293.75	63	2.56	308.5	0
07.07.2022	19:30:00	0	0	0	293.05	66	4.03	308.5	0
07.07.2022	20:00:00	0	0	0	291.95	70	2.72	286	0
07.07.2022	20:30:00	0	0	0	291.55	72	2.67	286	0
07.07.2022	21:00:00	0	0	0	291.15	73	2.55	286	0
07.07.2022	21:30:00	0	0	0	290.55	77	3.03	286	0
07.07.2022	22:00:00	0	0	0	289.55	81	2.67	286	0
07.07.2022	22:30:00	0	0	0	289.45	79	2.06	286	0
07.07.2022	23:00:00	0	0	0	289.35	78	2.86	286	0
07.07.2022	23:30:00	0	0	0	289.15	78	1.5	286	0
08.07.2022	00:00:00	0	0	0	289.15	78	2.53	308.5	0

Appendix 6: MATERIAL ASSIGNMENT OF PAVEMENTS FOR THE SIMULATION

Type of material	Area (m^2)	Percentage (%)
Antiskid Dressing	1450	0.34%
Block Paving	8860	2.09%
Concrete	5290	1.25%
Concrete Flags	96155	22.68%
Hard Landscaping	450	0.11%
HRA	161055	37.99%
HRA - Red Chippings	4580	1.08%
Setts	105210	24.82%
SMA	1702	0.40%
Stone Flags or Imitation	20578	4.85%
Surface Dressing	180	0.04%
Unknown	18425	4.35%

Type of surface	Area (m2)	Percentage (%)
Antiskid Dressing	269025	63.45%
Block Paving	136350	32.15%
Unknown	19085	4.5%

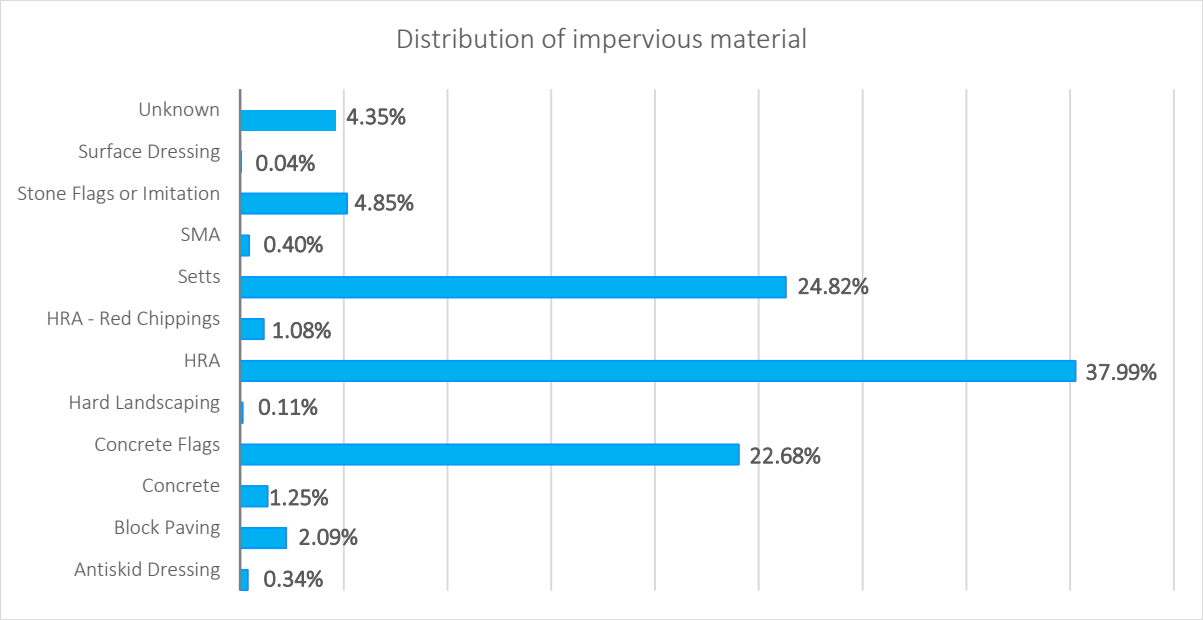

Assignment in ENVI-met

Type of material	ENVI- met input
Antiskid Dressing	Concrete Pavement grey
Block Paving	Red flags
Concrete	Concrete Pavement grey
Concrete Flags	Concrete Pavement grey
HRA	Asphalt
HRA - Red Chippings	Asphalt road with red coating
Setts	Red flags
SMA	Asphalt road with red coating
Stone Flags or Imitation	Red flags
Surface Dressing	Asphalt road with red coating
Unknown	Red flags

Appendix 7: METEOROLOGICAL DATA ON 17 – 18.07.2022

Date	Time	SW dir	SW dif	LW	TA	RH	Wind speed	Wind Direction	Precipitation
17.07.2022	18:00:00	0	0	0	297.25	50	3.97	218.5	0
17.07.2022	18:30:00	0	0	0	297.15	49	3.56	218.5	0
17.07.2022	19:00:00	0	0	0	297.05	50	3.31	218.5	0
17.07.2022	19:30:00	0	0	0	296.55	50	3.08	241	0
17.07.2022	20:00:00	0	0	0	296.05	51	2.78	218.5	0
17.07.2022	20:30:00	0	0	0	295.75	53	2.81	218.5	0
17.07.2022	21:00:00	0	0	0	295.85	55	2.36	218.5	0
17.07.2022	21:30:00	0	0	0	295.15	55	2.36	218.5	0
17.07.2022	22:00:00	0	0	0	294.95	56	2.25	286	0
17.07.2022	22:30:00	0	0	0	294.55	58	0.39	308.5	0
17.07.2022	23:00:00	0	0	0	293.85	62	0.42	286	0
17.07.2022	23:30:00	0	0	0	293.65	64	0.64	241	0
18.07.2022	00:00:00	0	0	0	293.05	67	1.17	218.5	0
18.07.2022	00:30:00	0	0	0	292.75	67	0.89	218.5	0
18.07.2022	01:00:00	0	0	0	292.55	67	0.25	218.5	0
18.07.2022	01:30:00	0	0	0	292.25	69	0	218.5	0
18.07.2022	02:00:00	0	0	0	292.05	70	1.11	218.5	0
18.07.2022	02:30:00	0	0	0	291.75	71	0.17	218.5	0
18.07.2022	03:00:00	0	0	0	291.45	72	0	218.5	0
18.07.2022	03:30:00	0	0	0	291.45	73	0.75	218.5	0
18.07.2022	04:00:00	0	0	0	291.25	74	0	218.5	0
18.07.2022	04:30:00	0	0	0	291.05	75	0	218.5	0
18.07.2022	05:00:00	0	0	0	291.05	76	0.25	218.5	0
18.07.2022	05:30:00	0	0	0	290.95	76	0	218.5	0
18.07.2022	06:00:00	0	0	0	291.05	76	0.56	218.5	0
18.07.2022	06:30:00	0	0	0	292.05	73	0	218.5	0
18.07.2022	07:00:00	0	0	0	294.05	66	0	218.5	0
18.07.2022	07:30:00	0	0	0	296.35	61	0	218.5	0
18.07.2022	08:00:00	0	0	0	295.25	64	1.33	83.5	0
18.07.2022	08:30:00	0	0	0	294.25	67	1.47	83.5	0

Date	Time	SW dir	SW dif	LW	TA	RH	Wind speed	Wind Direction	Precipitation
18.07.2022	09:00:00	0	0	0	294.25	67	0.86	38.5	0
18.07.2022	09:30:00	0	0	0	296.15	63	0.28	38.5	0
18.07.2022	10:00:00	0	0	0	297.25	61	0.97	61	0
18.07.2022	10:30:00	0	0	0	298.05	58	0.61	83.5	0
18.07.2022	11:00:00	0	0	0	299.15	56	2.72	218.5	0
18.07.2022	11:30:00	0	0	0	299.55	54	3.75	263.5	0
18.07.2022	12:00:00	0	0	0	300.65	46	3.06	241	0
18.07.2022	12:30:00	0	0	0	300.95	41	2.33	241	0
18.07.2022	13:00:00	0	0	0	301.65	42	3.36	241	0
18.07.2022	13:30:00	0	0	0	301.75	42	3.03	218.5	0
18.07.2022	14:00:00	0	0	0	302.25	39	3.44	218.5	0
18.07.2022	14:30:00	0	0	0	302.65	38	3.19	241	0
18.07.2022	15:00:00	0	0	0	303.15	36	2.78	263.5	0
18.07.2022	15:30:00	0	0	0	303.35	35	3.58	263.5	0
18.07.2022	16:00:00	0	0	0	303.55	33	2.83	218.5	0
18.07.2022	16:30:00	0	0	0	303.35	33	3.33	241	0
18.07.2022	17:00:00	0	0	0	303.85	33	2.89	241	0
18.07.2022	17:30:00	0	0	0	303.95	32	3.83	218.5	0
18.07.2022	18:00:00	0	0	0	302.85	34	4.25	218.5	0
18.07.2022	18:30:00	0	0	0	302.25	34	3.61	218.5	0
18.07.2022	19:00:00	0	0	0	302.05	31	3.89	218.5	0
18.07.2022	19:30:00	0	0	0	301.45	32	4.22	218.5	0
18.07.2022	20:00:00	0	0	0	300.75	33	2.64	241	0
18.07.2022	20:30:00	0	0	0	300.35	34	2.5	218.5	0
18.07.2022	21:00:00	0	0	0	299.55	37	0.47	218.5	0
18.07.2022	21:30:00	0	0	0	299.35	37	2.08	196	0
18.07.2022	22:00:00	0	0	0	298.55	41	0.11	218.5	0
18.07.2022	22:30:00	0	0	0	297.85	42	0.53	218.5	0
18.07.2022	23:00:00	0	0	0	296.75	45	0.94	218.5	0
18.07.2022	23:30:00	0	0	0	296.45	48	1.03	263.5	0
19.07.2022	00:00:00	0	0	0	295.95	49	0.33	218.5	0

Appendix 8: REPLACEMENT OF NEW PAVEMENT MATERIALS

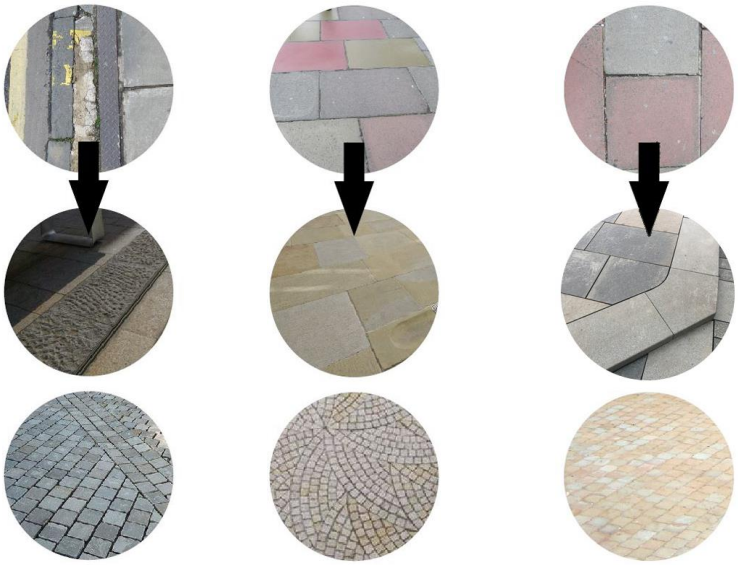

Figure 51 Actual pavement surfaces along George street and their replacement after proposal (source: The City of Edinburgh Council et al., 2021)

Appendix 9: ENVI-met SIMULATION SETTING

Envi-met Model Parameter		Case		
		Base case	Cold case	Green case
Model	Model dimension	222 x 171 x 32		
	Cell size	4 x 3 x 3 m		
	Method of vertical grid deneration	Equidistant, dz of lowest gridbox is split into 5 subcells		
	Model rotation out of grid North	-16		
	Nesting grid	3		
Meteorological Parameters	Meteorological forcing	Full Forcing		
	Temperature	Every 30 minutes *see Annex 7*		
	Relative humidity			
	Wind speed			
	Wind direction			
	Roughness Length	0.03 m		
Simulation time	Starting date	17 July 2022		
	Starting time	18:00		
	Simulation time	30 hours		
Materials	Buildings	White sandstone (before maintenance) See *Table 15*	White sandstone (after maintenance) PVC shade elements	White sandstone (before maintenance) See *Table 15*
	Roofs	Tiled roofs (before maintenance) See *Table 15*	Tiled roofs (after maintenance)	Tiled roofs (before maintenance) See *Table 15*
	Pavements	See *Table 16*	Yellow brick Smashed brick	See *Table 16*
Vegetation	Green spaces	-	-	64 Hedges dense 2m (4x3 m each)
	Trees			128 - Tamarix Gallica (French Tamarisk) 218 - Hornbeam young (Carpinus betulus)
Soil	Upper layer (0-20cm)	Rh – 53% / T - 22 ℃		
	Middle layer (20-50cm)	Rh – 53% / T - 21 ℃		
	Deep layer (50-200cm)	Rh – 53% / T - 20 ℃		
	Bedrock layer (below 200cm)	Rh – 53% / T - 19 ℃		

Appendix 10: **DISTRIBUTION OF MORPHOLOGICAL PARAMETERS FOR EACH LULC CLASS**

Mean building height

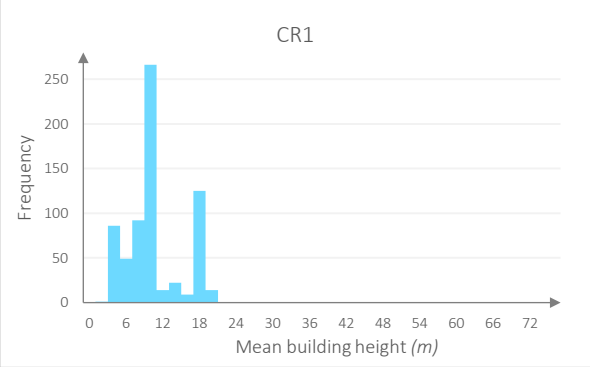

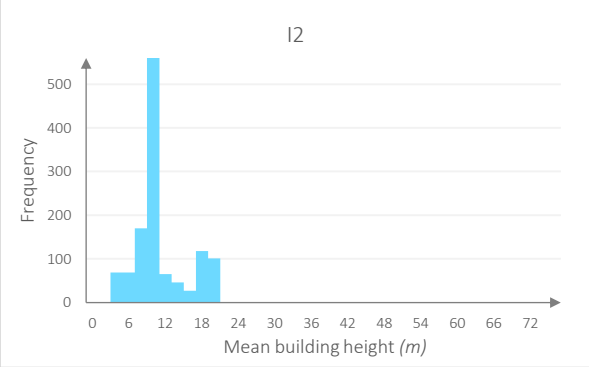

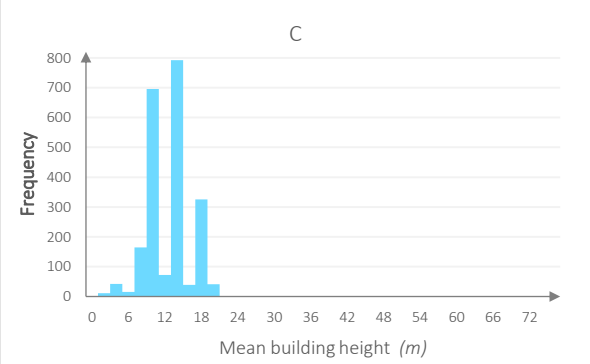

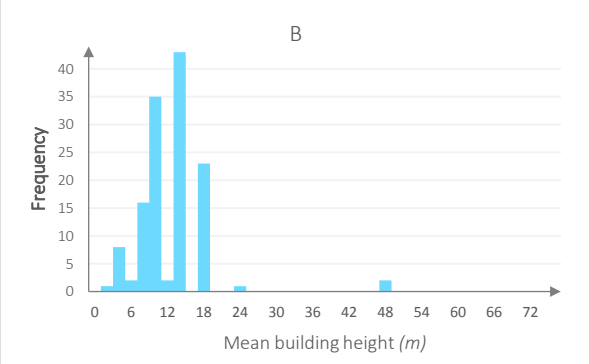

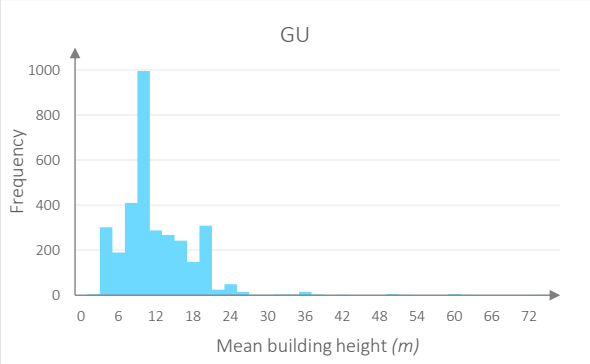

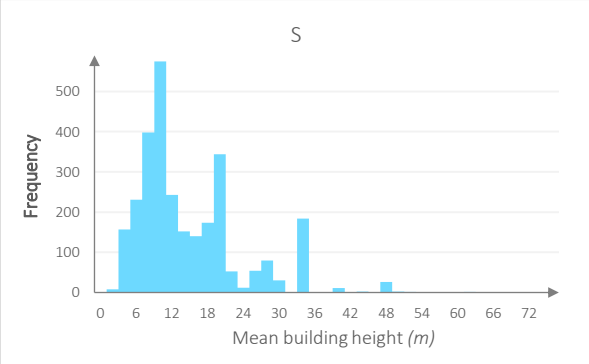

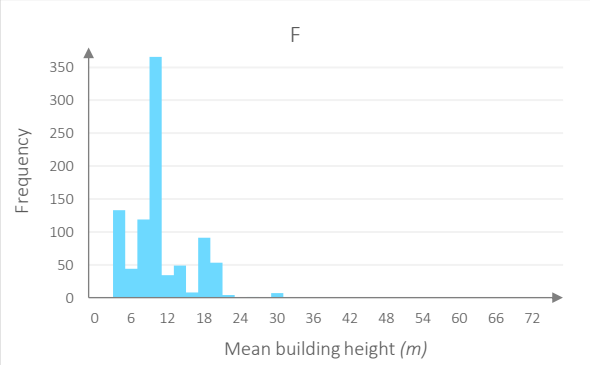

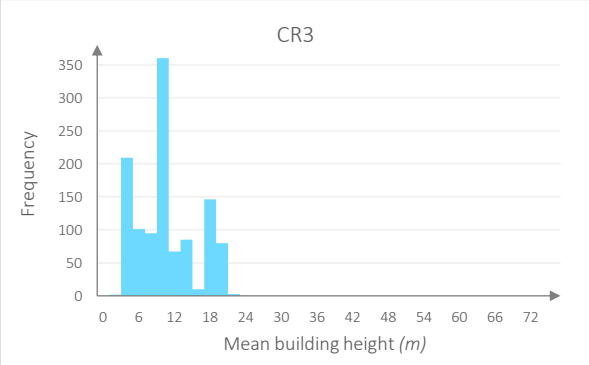

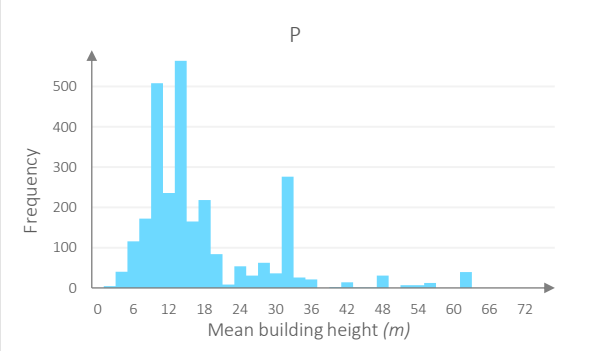
P
Frequency
0
100
200
300
400
500
0 6 12 18 24 30 36 42 48 54 60 66 72
Mean building height (m)

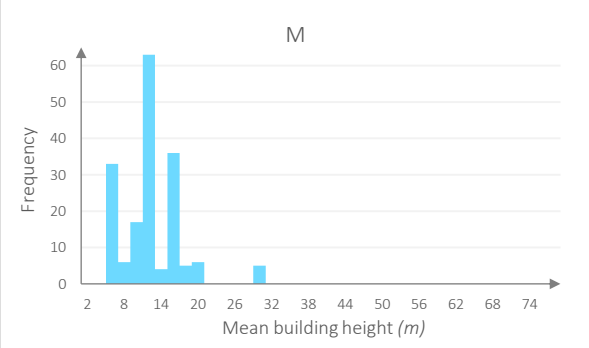
M
Frequency
0
10
20
30
40
50
60
2 8 14 20 26 32 38 44 50 56 62 68 74
Mean building height (m)

CR2
Frequency
0
0.5
1
1.5
2
2.5
3
3.5
4
0 6 12 18 24 30 36 42 48 54 60 66 72
Mean building height (m)

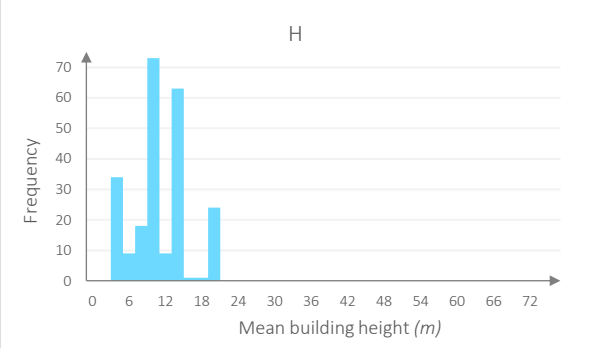
H
Frequency
0
10
20
30
40
50
60
70
0 6 12 18 24 30 36 42 48 54 60 66 72
Mean building height (m)

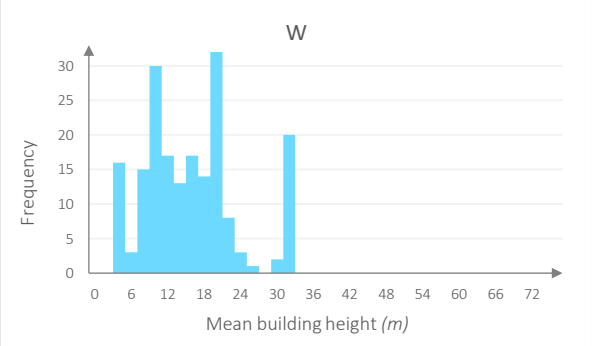
W
Frequency
0
5
10
15
20
25
30
0 6 12 18 24 30 36 42 48 54 60 66 72
Mean building height (m)

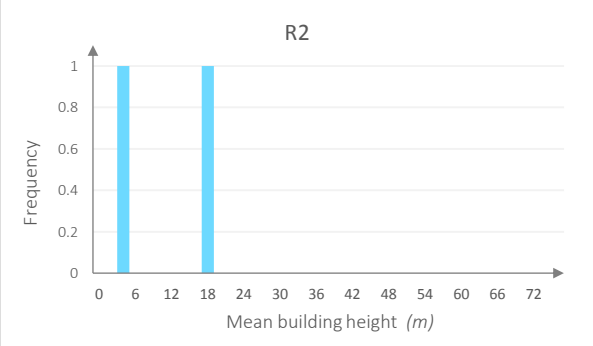
R2
Frequency
0
0.2
0.4
0.6
0.8
1
0 6 12 18 24 30 36 42 48 54 60 66 72
Mean building height (m)

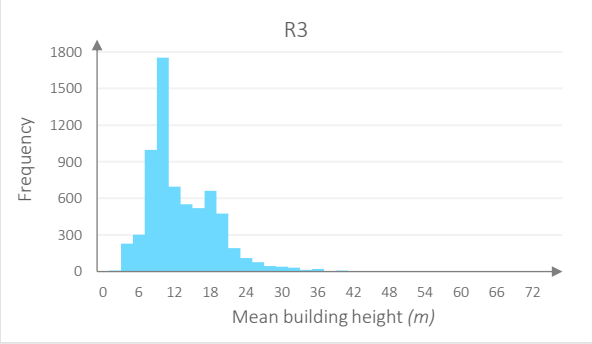
R3
Frequency
0
300
600
900
1200
1500
1800
0 6 12 18 24 30 36 42 48 54 60 66 72
Mean building height (m)

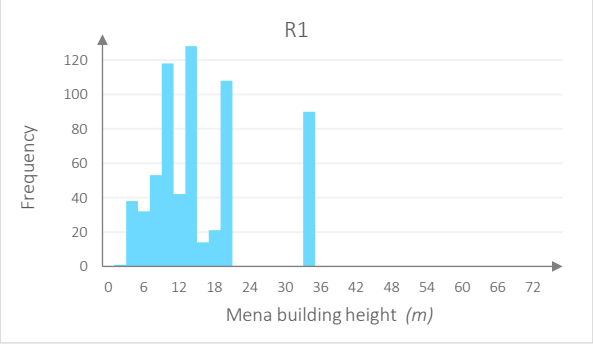
R1
Frequency
0
20
40
60
80
100
120
0 6 12 18 24 30 36 42 48 54 60 66 72
Mena building height (m)

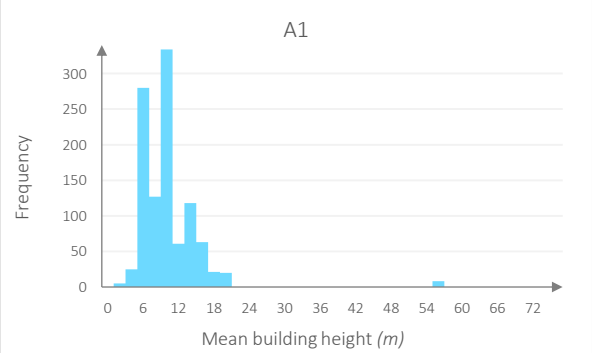
A1
Frequency
0
50
100
150
200
250
300
0 6 12 18 24 30 36 42 48 54 60 66 72
Mean building height (m)

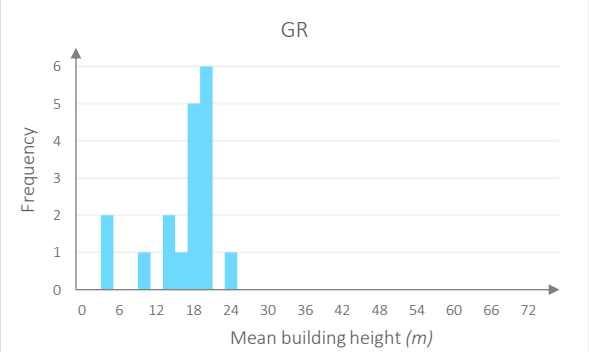
GR
Frequency
0
1
2
3
4
5
6
0 6 12 18 24 30 36 42 48 54 60 66 72
Mean building height (m)

Sky view factor

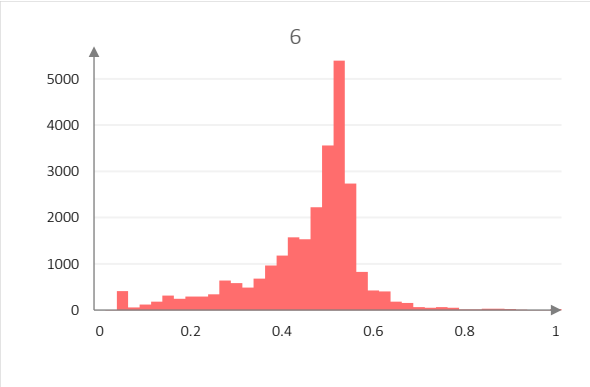

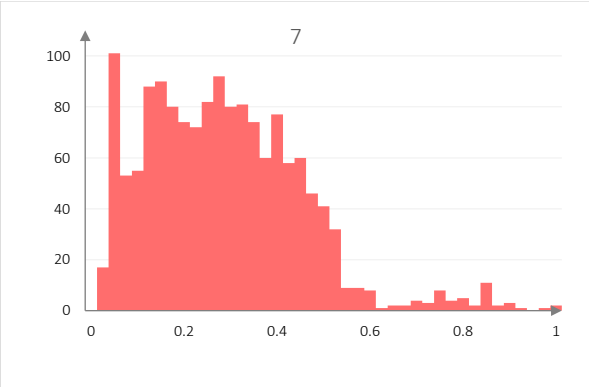

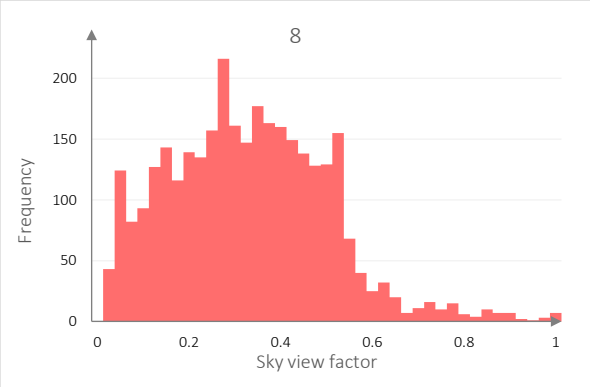

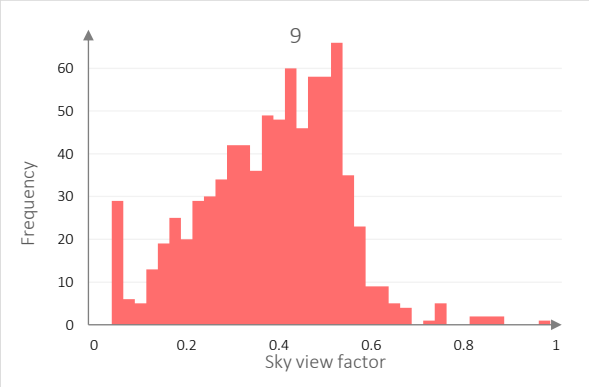

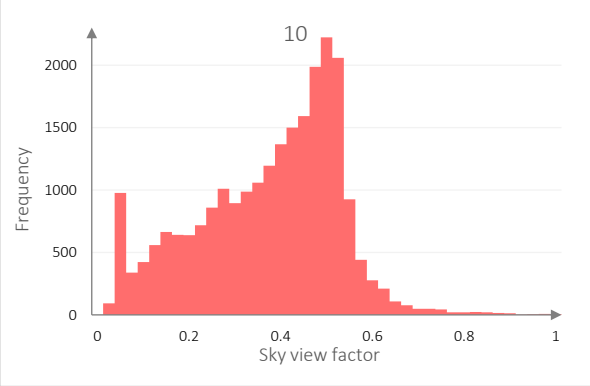

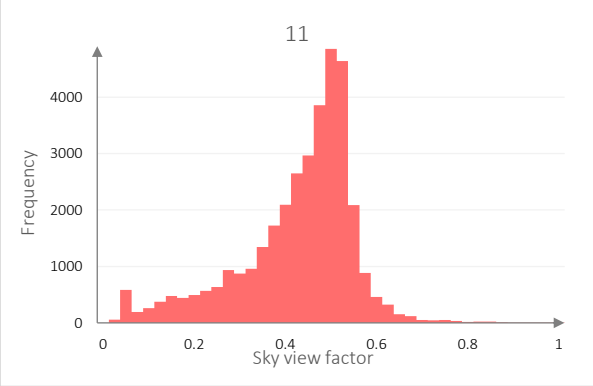

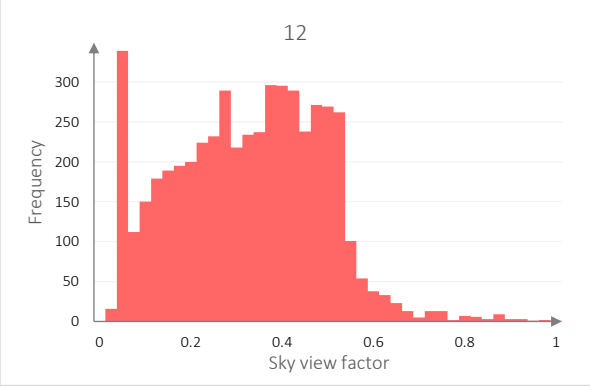

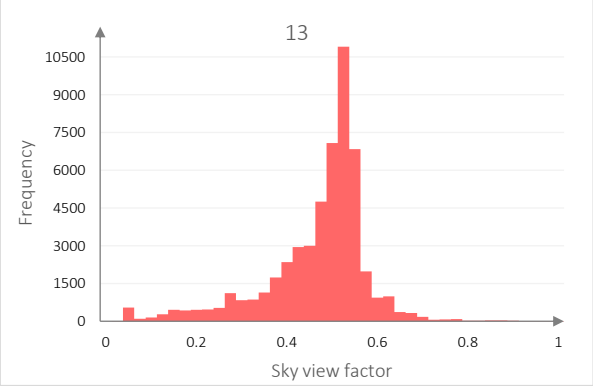

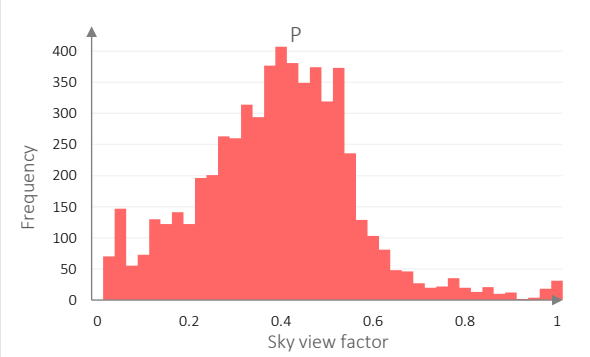
P
Frequency
Sky view factor

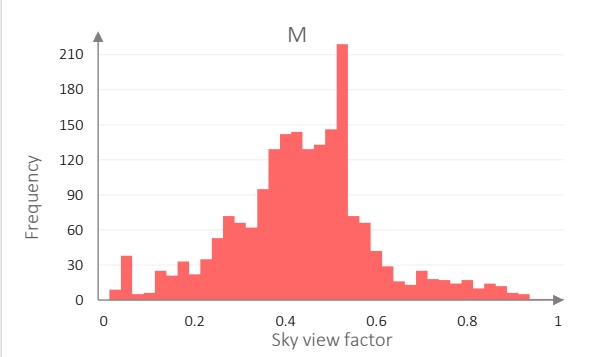
M
Frequency
Sky view factor

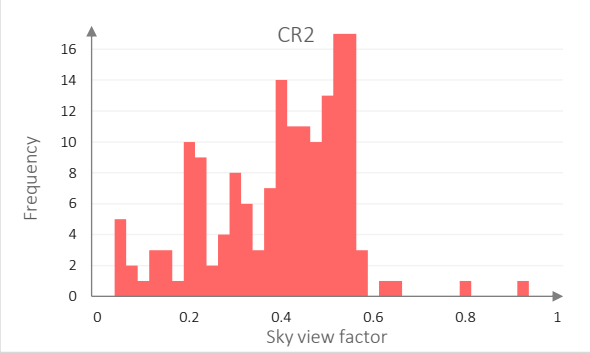
CR2
Frequency
Sky view factor

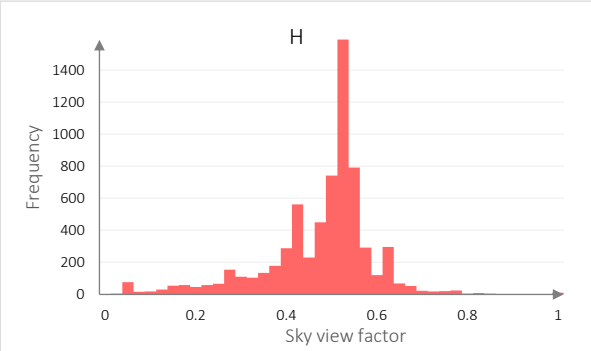
H
Frequency
Sky view factor

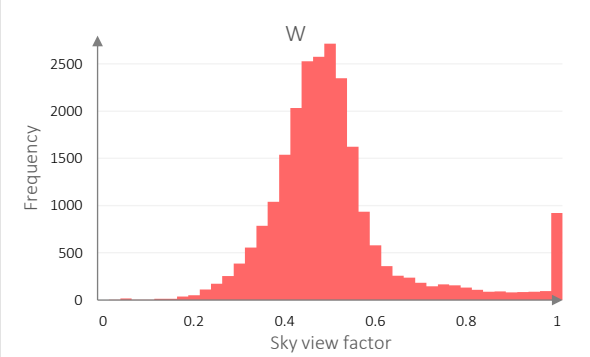
W
Frequency
Sky view factor

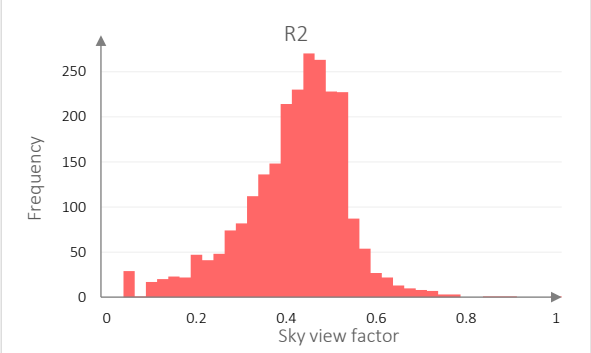
R2
Frequency
Sky view factor

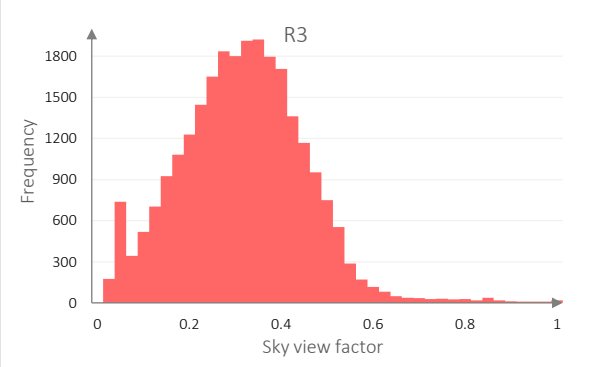
R3
Frequency
Sky view factor

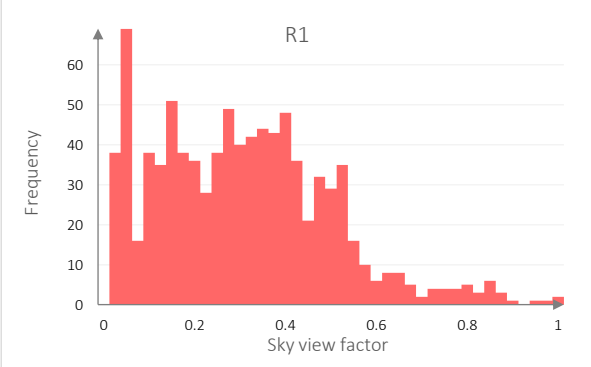
R1
Frequency
Sky view factor

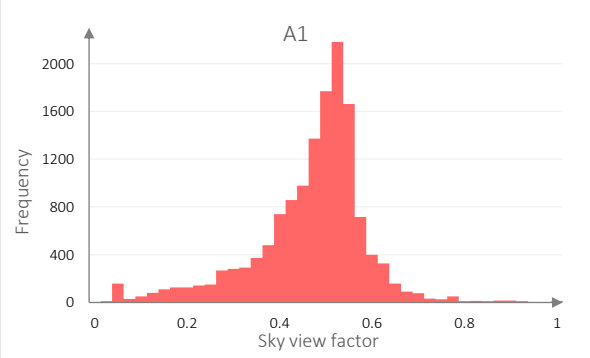
A1
Frequency
Sky view factor

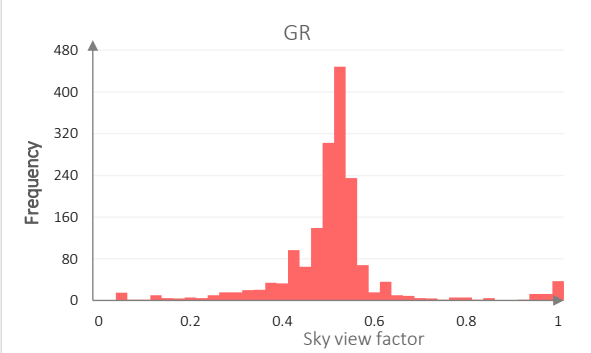
GR
Frequency
Sky view factor

Road aspect ratio

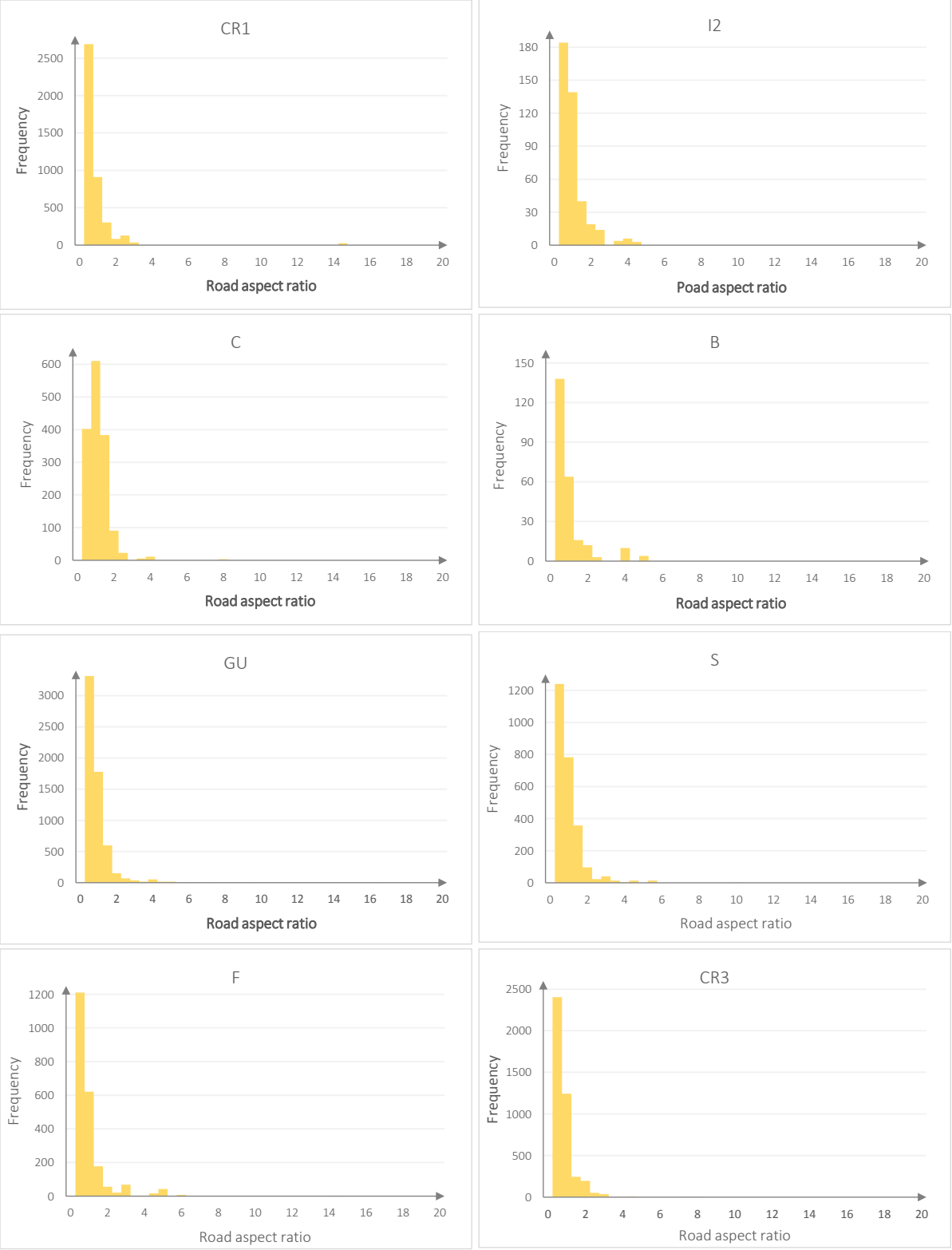

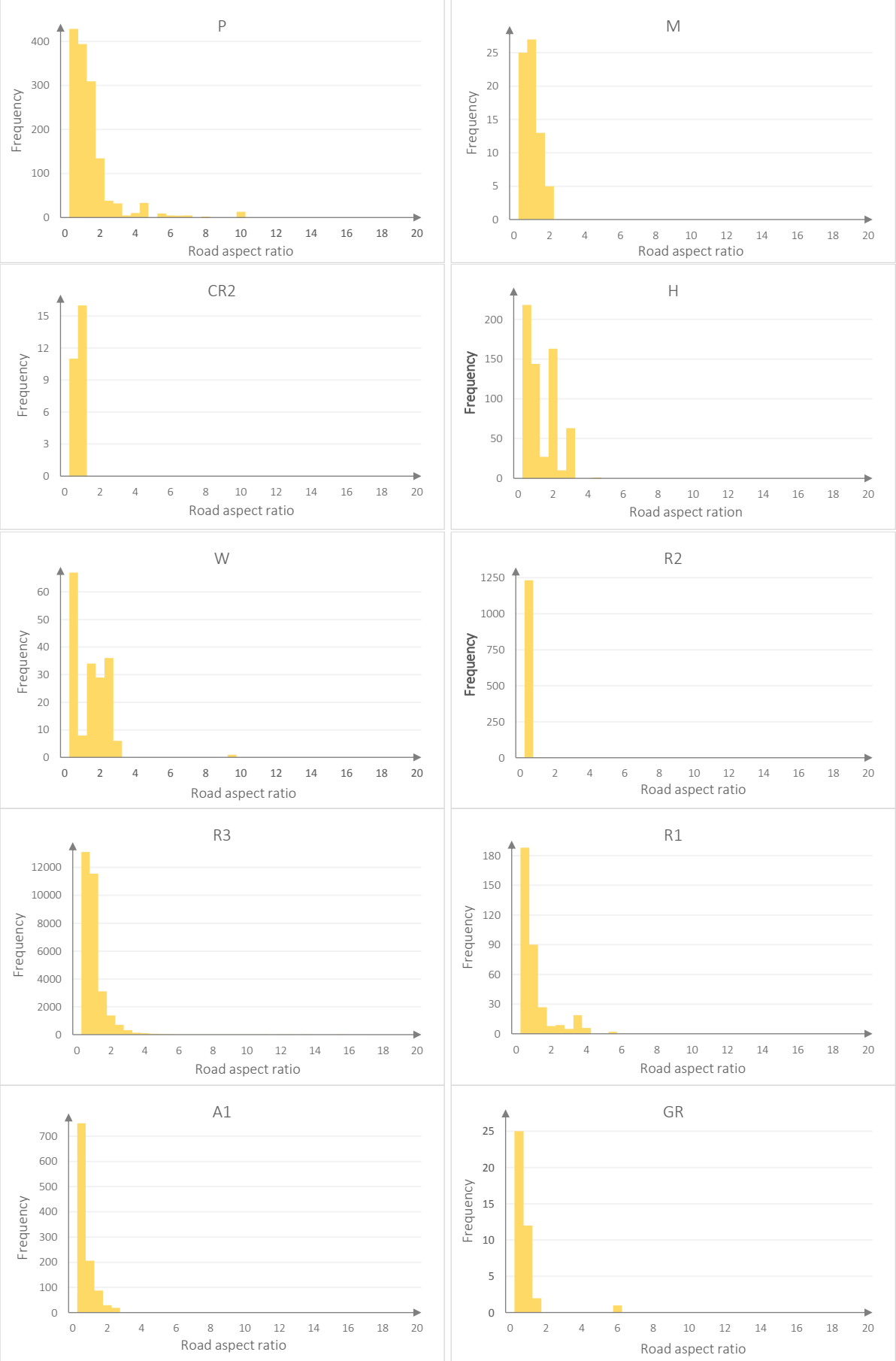
P
Frequency
Road aspect ratio
M
Frequency
Road aspect ratio
CR2
Frequency
Road aspect ratio
H
Frequency
Road aspect ration
W
Frequency
Road aspect ratio
R2
Frequency
Road aspect ratio
R3
Frequency
Road aspect ratio
R1
Frequency
Road aspect ratio
A1
Frequency
Road aspect ratio
GR
Frequency
Road aspect ratio